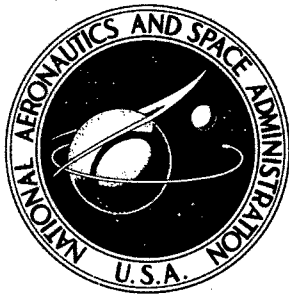


NASA CR-316

NASA CONTRACTOR
REPORT



P
002589

NASA CR-316

fnl

AMPTIAC

THERMAL INTEGRATION OF ELECTRICAL POWER AND LIFE SUPPORT SYSTEMS FOR MANNED SPACE STATIONS

by K. L. Hanson

Prepared under Contract No. NAS 3-2799 by
GENERAL ELECTRIC COMPANY
Valley Forge Space Technology Center
Philadelphia, Pa.
for

DISTRIBUTION STATEMENT A
Approved for Public Release
Distribution Unlimited

20020319 113

NATIONAL AERONAUTICS AND SPACE ADMINISTRATION - WASHINGTON, D. C. - NOVEMBER 1965

NASA CR-316

**THERMAL INTEGRATION OF ELECTRICAL POWER AND LIFE
SUPPORT SYSTEMS FOR MANNED SPACE STATIONS**

By K. L. Hanson

Distribution of this report is provided in the interest of information exchange. Responsibility for the contents resides in the author or organization that prepared it.

Prepared under Contract No. NAS 3-2799 by
GENERAL ELECTRIC COMPANY
Valley Forge Space Technology Center
Philadelphia, Pa.

for

NATIONAL AERONAUTICS AND SPACE ADMINISTRATION

For sale by the Clearinghouse for Federal Scientific and Technical Information
Springfield, Virginia 22151 - Price \$7.00

FOREWORD

This study was conducted under the management of Mr. Lloyd W. Ream, NASA-Lewis Research Center. The study was performed at the General Electric Company Space Technology Center, Valley Forge, Pennsylvania under the technical direction of Mr. K. L. Hanson, Manager, Space Power Sub-Systems Engineering.

Six auxiliary space power systems were designed to meet the requirements of a six-man orbiting space station. A life support system, including regenerative processes, was also designed to meet the same space station requirements. The endothermic processes of the life support system were identified, and the electrical power generating systems redesigned to incorporate furnishing the life support system endothermic processes from the power systems heat sources. The systems were evaluated to determine which integrated system offered the best advantage as the result of thermal integration. The selected system, the Isotope Brayton Integrated System, was then compared to a non-integrated Photovoltaic system.

The study identified areas of significant reduction in electrical power requirements for Life Support processes with a corresponding reduction in power plant size.

TABLE OF CONTENTS

<u>Section</u>		<u>Page</u>
1	INTRODUCTION	1
	1.1 Purpose	1
	1.2 Scope	1
	1.3 Approach	2
	1.4 References	5
2	SUMMARY OF RESULTS	7
	2.1 Introduction	7
	2.2 Non-integrated Systems	8
	2.3 Integrated Systems	11
	2.4 Conclusions	15
3	DESIGN REQUIREMENTS AND SYSTEM COMPARISONS	25
	3.1 Introduction	25
	3.2 Design Guidelines	26
	3.3 Method of Comparison.	29
	3.4 Systems Comparison	30
4	LIFE SUPPORT SYSTEM ANALYSIS	39
	4.1 General Requirements.	39
	4.2 Specific Requirements.	40
	4.3 Life Support Subsystems Design	40
	4.4 Subsystem Design Layout.	69
	4.5 Non-integrated Life Support System	71
	4.6 Integrated Life Support System	78
5	STIRLING SYSTEM ANALYSIS	93
	5.1 Description of Non-integrated System and Design.	93
	5.2 Non-integrated Solar Stirling System.	109
	5.3 Description of Integrated Solar Stirling System and Design . . .	113
	5.4 Non-integrated Isotope Stirling Cycle Power System Anlysis . .	118
	5.5 Integrated Power and Life Support Systems.	139
	5.6 Discussion of Integrated Power and Life Support Systems . . .	146
	5.7 References	147

TABLE OF CONTENTS (Cont)

<u>Section</u>		<u>Page</u>
6	BRAYTON SYSTEM ANALYSIS	149
6.1	Non-integrated System	149
6.2	Integrated Brayton Power Plant and Life Support System	206
6.3	References	222
7	SOLAR MERCURY RANKINE SYSTEM ANALYSIS	223
7.1	Introduction	223
7.2	Non-integrated System	223
7.3	Integrated Systems	230
7.4	Integrated System Parameters	237
7.5	References	239
8	PHOTOVOLTAIC POWER SYSTEM ANALYSIS	241
8.1	Introduction	241
8.2	Description of System and Design	243
8.3	Discussion of Power System	250
8.4	References	252
APPENDIX A.	ANALYSIS OF PEAK LOAD EFFECTS	253
A.1	Summary and Conclusions	253
A.2	Discussion and Background Information	253
A.3	Analysis	253
APPENDIX B.	SOLAR COLLECTOR DESIGN	255
B.1	Introduction	255
B.2	Design Values	255
B.3	Background and Analysis	255
APPENDIX C.	RADIATOR, ABSORBER AND HEAT EXCHANGER DESIGN	261
C.1	Radiator Design	261
C.2	Absorber Design	271
C.3	Heat Exchanger Design	296
C.4	References	304
APPENDIX D.	CABIN PRESSURIZATION	307
D.1	Power Available for Emergency Pressurization	307
D.2	Cabin Pressurization, Non-integrated Systems	309
D.3	Cabin Pressurization, Integrated Systems	310

SECTION 1

INTRODUCTION

1.1 PURPOSE

For long duration manned space missions the weight of material consumed by the life support function can become significant. For example, a paper by Mayo (Ref 1) states that the Apollo life support system consumes material at the rate of approximately 21 pounds per man day. Systems for reusing the water, oxygen, and eventually, the food consumed by the crew are being investigated for the purpose of reducing the material requirements for life support. References 2 and 3 describe regenerative life support processes, some of which utilize endothermic processes. Electrical heating is a straightforward method of obtaining the required process heat, though the resulting increase in the electrical power requirements increases the size of the power system and reduces the benefits of reusing life support material. Since the process is little affected by the source of the heat, the use of heat from the power system for the endothermic life support processes is a concept for improving the performance of the total system. The results of a preliminary study of the potential advantage of thermally integrating life support processes with electric power systems are given in Reference 4.

The purpose of this study was to evaluate the effects of thermal integration of the life support and electrical power systems of a six man space station. The thermal power and temperature requirements of specified life support systems were analyzed and the possible sources of thermal power from selected electric power systems were investigated. The intent of the study was to obtain maximum utilization of the waste energy available from the power generating system. Preliminary designs of thermally integrated electrical power/life support systems were evaluated and a selected system was compared with a photovoltaic power generation/life support system.

1.2 SCOPE

The following systems were considered in the study:

1.2.1 POWER SYSTEMS

- a. Solar Dynamic
 - 1. Stirling Cycle Power System
 - 2. Mercury Rankine Power System
 - 3. Brayton Cycle Power System
- b. Radioisotope Dynamic
 - 1. Stirling Cycle Power System
 - 2. Brayton Cycle Power System
- c. Solar Static
 - 1. Photovoltaic Power System

1.2.2 LIFE SUPPORT SYSTEMS

- a. CO₂ Regeneration by the Sabatier Method
- b. Urine Treatment by Distillation and Pyrolysis

- c. Waste Water Distillation
- d. Food Preparation
- e. Solid Waste Management

The scope of the study was limited to investigation of these life support and electric power systems. The life support systems identified are of current interest and, for the most waste products. The power systems are typical of those currently being studied and developed for manned space applications. Comparative analyses were to take into account at least the following factors:

- a. Reduction in electrical power requirements.
- b. Reduction in heat required by the power system.
- c. Reduction in radiator size and weight.
- d. Reduction in collector size and weight for the solar dynamics system.
- e. Reduction in isotope quantity.
- f. Hazards and safety considerations.
- g. Effects of integration on the operation of the power system and life support subsystems (e.g. complexity, reliability, effects of individual component failure.)
- h. Control problems and requirements.
- i. Component problems.
- j. Maintainability

The following items were specifically excluded from detailed consideration in this study:

- a. Cost
- b. Power conditioning and distribution
- c. Vibration and stress analysis
- d. Attitude control penalties for solar collector orientation
- e. Atmospheric drag
- f. Effect of the deployed power system on station ferry vehicle docking
- g. Isotope refueling
- h. Reliability analyses.

It was directed that a reasonable estimate of the state of the art for a six-man, earth-orbiting space station with a launch date of about 1970 be employed as the basis of system performance, specifically drawing on studies related to the Manned Orbiting Research Laboratory as the basic source of data for station configuration and constraints. Information from current and completed development programs in power and life support was to be used when applicable. The design effort emphasized system design with component design effort limited to obtaining preliminary size and weight data when such information was not available. System optimization was not studied in depth as the intent was to obtain maximum utilization of thermal integration.

1.3 APPROACH

The study was carried out in two phases. In the first phase the life support and electric power systems were designed on a non-integrated basis. Electrical heating was used for the life support processes for the six-man crew and the power systems designed to

supply the total station electrical load. As a result of this phase the endothermic requirements of the life support processes were identified, as were temperature levels at which thermal power should be available from the electric power systems. In the second phase the life support and electric power systems were thermally integrated to best take advantage of the sources of heat in the power systems. The total systems (life support plus electric power) were then compared in order to select a thermally integrated system for comparison with a state of the art photovoltaic powered space station. The goal was to study thermal integration and did not include the generation of concepts to advance the state of the art of life support and power systems and components.

A key problem in this type of study is to assure that equivalent systems are compared. The systems studied are in various stages of development and it was important that a consistent approach be used in establishing the state of the art that could be achieved when the space station becomes operational. Some of the system characteristics are quite different (e.g., the solar powered systems require orientation that is not required for the isotope powered systems). These differences would have led to different optimized station configurations but since the primary purpose here was the evaluation of thermal integration, the station concept was fixed. For design consistency, a set of guidelines identifying station requirements and constraints was prepared and is included in this report. The guidelines provide constraints sufficient to maintain design consistency but not so detailed as to penalize the different systems considered. Some important general guidelines were:

- a. Station Configuration - See Figure 1-1
- b. Six-man crew
- c. One year mission with resupply at 180 day intervals; Orbit--250 n. miles altitude, circular, 28.7 degrees inclination.
- d. Station Power Requirements (non-integrated)--6 kw continuous with 3 kw additional for one hour per day.
- e. Cabin Atmosphere--Total pressure of 10 psia; oxygen partial pressure of 160 mm of Hg; carbon dioxide partial pressure 3.8 mm Hg; and nitrogen diluent.

The design of components common to more than one system was coordinated to maintain consistency. The same design philosophy was used for all radiators and the performance of solar collectors was standardized for all solar powered systems. This approach eliminated many of the inconsistencies that are present when the results of independent studies are compared.

It was expected that system selection would be difficult because the comparison study was to include a number of performance areas. With such diverse areas as weight and maintainability included it was anticipated that no single system would be best in all respects so that some method of reducing system performance in different areas to a common denominator was needed. The technique selected was to derive a comparative Figure of

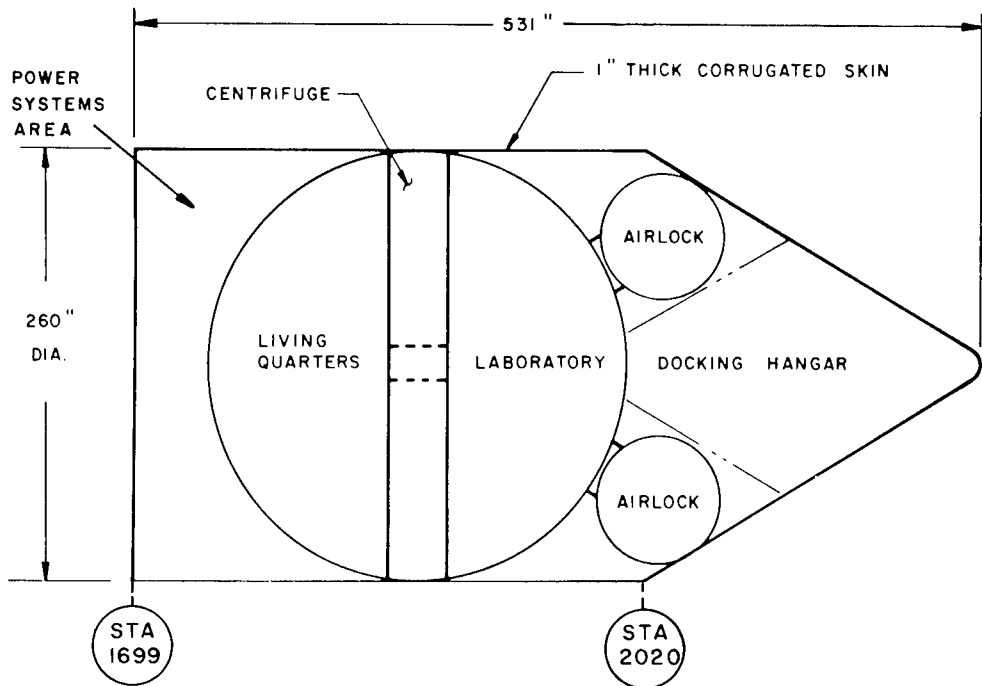


Figure 1-1. Basic Station Configuration

Merit for each system by summing the product of its relative performance in important performance areas by a weighting factor which represents the relative importance of the performance area. System comparison involves a comparison of the Figures of Merit since they represent the synthesis of the available information.

In applying the Figure of Merit technique it was assumed that all systems were capable of meeting the minimum mission requirements. If, for example, one of the systems had failed to meet one of the essential mission requirements that system would not have been competitive and need not have been considered further, no matter how desirable its other characteristics may have been. Since the Figure of Merit analysis includes all available performance data in the areas of performance deemed significant for the study, it provides a rational means of selection even when the differences between the derived Figures of Merit are very small. Even though the method provides a "best estimate" answer to the system selection problem it should be recognized that the correctness of the selection depends upon the adequacy of the list of performance areas, the performance data, and the weighting of the performance areas. The magnitude of the difference of the Figures of Merit of any two systems is both a measure of the difference in total performance and the level of confidence in the selection of one system over another.

The results of this study are influenced by engineering judgement in the selection of guidelines, in assumptions for interactions in areas that were beyond the scope of the study, in the interpretation of analysis, and in the estimation of certain system characteristics.

The Design Guidelines and the comparative Figure of Merit analysis provide the reader with a means of clearly identifying the rationale for the system selection. Additional areas of performance, and revised weighting factors or relative performances can be incorporated by the reader should he consider it necessary.

1.4 REFERENCES

1. Mayo, A. M.; Thompson, A. B.; and Whisenhunt, G. B.; "Design Criteria for a Manned Space-Laboratory Environmental Control System," *Journal of Spacecraft and Rockets*, 296-302, (1964).
2. Mason, J. L.; and Burris, W. L.; "Problems and Progress with Long-Duration Life-Support Systems," *AIAA-NASA 2nd Manned Space Flight Symposium* (American Institute of Astronautics and Aeronautics, New York, 1963), pp 329-340.
3. "Analytical Methods for Space Vehicle Atmosphere Control Processes," Technical Report No. ASD-TR-61-162, Part II, November 1962, Flight Accessories Laboratory, Wright-Patterson Air Force Base, Ohio.
4. Hanson, K. L., "A Preliminary Study of the Thermal Integration of Electrical Power and Life Support Systems For Manned Space Vehicles," *Third Biennial Aerospace Power Systems Conference*, (AIAA/SAE/ASME/IAPG/Electron Devices Group IEEE), September 1-4, 1964, Philadelphia, Pa. AIAA Paper No. 64-622.

SECTION 2 SUMMARY OF RESULTS

2.1 INTRODUCTION

The power requirements for both the non-integrated and the thermally integrated systems are tabulated in Table 2-1. The total electrical power for the non-integrated station is not considered sufficient for a six man station because the life support requirement leaves too little power for operation of a station of this size. This circumstance was caused by initially specifying the total power requirement on the basis of data from other studies and then defining the life support system power requirements in this study. The life support requirements were greater than had been expected. It was not considered necessary to redesign the power systems to provide an increased power requirement to achieve the primary purpose of the study which was to evaluate thermal integration of the electrical power and life support systems.

The system designs generated in the study are shown in Figures 2-1 through 2-8. A summary tabulation of the sizes and weights of the systems is given in Table 2-2 and 2-3. The Performance Areas selected as pertinent for this study and the relative weights assigned to them are shown in Table 2-4. It is considered that this list of Performance Areas and weighting factors is not universally applicable. For other missions different relative weights could apply and the list of Performance Areas could be modified. For this study the list is sufficient to include the important factors, is broken down into enough detail to provide a measure of the inherent differences in the systems, but is not detailed to the point of providing undue emphasis to minor differences in the systems, and provides reasonably independent areas for evaluation so that interactions between the various areas do not significantly complicate the assignment of degrees of performance or change the effective weight factors.

2.2 NON-INTEGRATED SYSTEMS

The Relative Figures of Merit for the Non-Integrated Systems are presented in Table 2-4. The results group into three categories which can be identified as solar dynamic, isotope dynamic, and solar photovoltaic. It should be noted that the requirement for solar orientation was considered a definite disadvantage though the significance of the penalty is mission-dependent. If the major mission of the station is to provide a zero "g" laboratory, the need for solar orientation may impose a small penalty as the time rate of change in direction to maintain solar orientation is low, and an orientation system of some type would be a station requirement. However, for most missions the lack of a solar orientation requirement for the isotope powered systems is a significant advantage.

The Non-Integrated Life Support Subsystem power requirements are tabulated in Table 2-5.

TABLE 2-1. SUMMARY OF POWER REQUIREMENTS (KW)

	SOLAR STIRLING	ISOTOPE STIRLING	SOLAR BRAYTON	ISOTOPE BRAYTON	SOLAR MERCURY-RANKINE	PHOTO-VOLTAIC
a. NON-INTEGRATED STATION						
1. POWER SYSTEM ELECTRICAL OUTPUT	6.24	6.24	6.24	6.24	6.51	6.21
2. POWER CONDITIONING PENALTY ⁽¹⁾	0	0	0	0	0.27	0.21
3. BATTERY CHARGING ⁽²⁾	0.24	0.24	0.24	0.24	0.24	0
4. LIFE SUPPORT PROCESSES	4.43	4.43	4.43	4.43	4.43	4.43
5. LIFE SUPPORT THERMAL LOSSES	0.14	0.14	0.14	0.14	0.14	0.14
6. OTHER ELECTRICAL POWER	1.43	1.43	1.43	1.43	1.43	1.43
b. INTEGRATED STATION						
1. POWER SYSTEM OUTPUT (ELECTRICAL)	3.27	3.27	3.27	3.27	3.41	6.21
2. POWER SYSTEM OUTPUT (THERMAL)	3.41	3.41	4.46	4.46	3.41	0
3. POWER CONDITIONING PENALTY ⁽¹⁾	0	0	0	0	0.14	0.21
4. BATTERY CHARGING ⁽²⁾	0.24	0.24	0.24	0.24	0.24	0
5. LIFE SUPPORT THERMAL LOSSES	0.51	0.51	0.35	0.35	0.51	0.14
6. LIFE SUPPORT PROCESS POWER SUPPLIED AS THERMAL POWER	2.90	2.90	4.11	4.11	2.90	0
7. LIFE SUPPORT POWER SUPPLIED ELECTRICALLY	1.60	1.60	1.60	1.60	1.60	4.43
8. OTHER ELECTRICAL POWER	1.43	1.43	1.43	1.43	1.43	1.43

(1) Power Conditioning penalties were imposed to account for the different types of power produced by the systems. The objective was to size the systems to supply equivalent amounts of power to the station.

(2) The battery charging requirement is for the battery package to supply the peak power requirement. There is no equivalent requirement for the photovoltaic system as the battery charging requirement is accounted for in the system design.

TABLE 2-2. NON-INTEGRATED SYSTEM - SUMMARY OF CHARACTERISTICS

DESIGN PARAMETER	SOLAR STIRLING	ISOTOPE STIRLING	SOLAR BRAYTON	ISOTOPE BRAYTON	SOLAR MERCURY RANKINE	PHOTO-VOLTAIC
POWER SYSTEM WEIGHT (LB)	2317	2286	3464	4684	2379	4323
LIFE SUPPORT SYSTEM WEIGHT (LB)	622	622	622	622	622	622
TOTAL SYSTEM WEIGHT (LB)	2939	2908	4086	5306	3001	4945
INTEGRAL RADIATOR SURFACE AREA (FT ²)	----	625	----	615	164	----
NON-INTEGRAL RADIATOR PROJECTED AREA (FT ²)	108	----	210	----	----	----
POWER SYSTEM STOWED VOLUME (FT ³)	980	75	1400*	95	1025*	830
COLLECTOR DIAMETER (FT)	23.9	----	24.6	----	34.2	----
GROSS SOLAR ARRAY AREA (FT ²)	----	----	----	----	----	1655
ISOTOPE POWER REQUIREMENT (KW _T)	----	32.0	----	30.0	----	----

TABLE 2-3. INTEGRATED SYSTEM - SUMMARY OF CHARACTERISTICS

DESIGN PARAMETER	SOLAR STIRLING	ISOTOPE STIRLING	SOLAR BRAYTON	ISOTOPE BRAYTON	SOLAR MERCURY RANKINE	PHOTO-VOLTAIC
POWER SYSTEM WEIGHT (LB)	1695	1849	2229	3008	1940	4323
LIFE SUPPORT SYSTEM WEIGHT (LB)	678	678	780	780	678	622
TOTAL SYSTEM WEIGHT (LB)	2373	2527	3009	3788	2318	4945
INTEGRAL RADIATOR SURFACE AREA (FT ²)	----	310	----	310	100	----
NON-INTEGRAL RADIATOR PROJECTED AREA (FT ²)	69	----	158	----	----	----
POWER SYSTEM STOWED VOLUME (FT ³)	790	65	1150*	89	1025*	830
COLLECTOR DIAMETER (FT)	20.5	----	19.0	----	27.8	----
GROSS SOLAR ARRAY AREA (FT ²)	----	----	----	----	----	1655
ISOTOPE POWER REQUIREMENT (KW _T)	----	20.0	----	18.0	----	----

*Includes Volume of lengthened vehicle caused by Power System exceeding Guidelines envelope.

TABLE 2-4. RESULTS OF NON-INTEGRATED SYSTEMS COMPARISON

PERFORMANCE AREA	WEIGHT FACTOR	SOLAR STIRLING		ISOTOPE STIRLING		SOLAR BRAYTON		ISOTOPE BRAYTON		SOLAR MERCURY RANKINE		PHOTO-VOLTAIC	
		DOP	PI	DOP	PI	DOP	PI	DOP	PI	DOP	PI	DOP	PI
1 WEIGHT	3	8	24	8	24	4	12	0	0	8	24	1	3
2 VOLUME	4	2	8	10	40	-2	-8	9	36	1	4	3	12
3 AREA	5	8	40	10	50	7	35	10	50	5	25	1	5
4 HAZARDS	5	7	35	2	10	9	45	3	15	7	35	10	50
5 LAUNCH, STARTUP, AND RE-START CONSIDERATIONS	3	4	12	10	30	3	9	9	27	2	6	6	18
6 MAINTENANCE REQUIREMENTS	3	6	18	6	18	8	24	8	24	8	24	10	30
7 COMPLEXITY AND RELIABILITY	5	2	10	8	40	4	20	9	45	4	20	10	50
8 CONTROL REQUIREMENTS	1	6	6	8	8	6	6	8	8	6	6	10	10
9 DEVELOPMENT REQUIRED	1	2	2	3	3	4	4	5	5	6	6	10	10
10 RISKS & UNCERTAINTIES IN DEVELOPMENT SCHEDULE	1	2	2	4	4	4	5	5	5	2	2	10	10
11 STATION INTEGRATION	3	6	18	10	30	3	9	10	30	5	15	8	24
12 VEHICLE ATTITUDE RESTRAINTS	3	2	6	10	30	2	6	10	30	2	6	2	6
13 ISOTOPE REQUIREMENT	3	10	30	-5	-15	10	30	-4	-12	10	30	10	30
14 ADAPTABILITY	3	7	21	8	24	8	24	9	27	5	15	10	30
FIGURE OF MERIT			232		296		220		290		218		288

DOP - Degree of Performance - Ranges from -5 to 10
 PI - Performance Index

Weight Factors range from 1 to 5

TABLE 2-5

NON-INTEGRATED LIFE SUPPORT SUBSYSTEMS POWER REQUIREMENTS

	PROCESS POWER (WATTS)	SUPPORT POWER (WATTS)
C0 ₂ RECOVERY CANISTERS	1,867	40
ELECTROLYSIS CELLS	1,000	-
PYROLYZATION UNIT	130	-
C0 ₂ ACCUMULATOR PUMP	-	100
URINE WATER RECOVERY	303	7
SOLID WASTE TREATMENT	320	7
WASTE WATER RECOVERY	442	7
FOOD MANAGEMENT	69	-
COOLING SYSTEM	-	130
HEAT LEAKAGE (LUMPED)	-	137
MISCELLANEOUS HARDWARE	-	7
	<u>4,131</u>	<u>435</u>

TOTAL ELECTRICAL POWER REQUIREMENT = 4,566 WATTS

2.3 INTEGRATED SYSTEMS

Relative Figures of Merit were derived for the thermally integrated systems and the results are given in Table 2-6. The Solar Photovoltaic system was included in this evaluation for comparison and to serve as the basis for correlating the Non-integrated results with the Integrated results. The non-integrated systems were compared as a group independently of the integrated systems. The Figures of Merit so derived are relative and valid for the systems included in each comparison. With the Photovoltaic system as a standard, comparisons of the two sets of data can be made, since the Photovoltaic system Figure of Merit was the same for both evaluations.

The Life Support Subsystem Process and Temperature requirements are given in Table 2-7. The integrated Life Support Subsystem Power Requirements are given in Table 2-8.

TABLE 2-6. RESULTS OF THERMALLY INTEGRATED SYSTEMS COMPARISON

PERFORMANCE AREA	WEIGHT FACTOR	SOLAR STIRLING		ISOTOPE STIRLING		SOLAR BRAYTON		ISOTOPE BRAYTON		SOLAR MERCURY RANKINE		PHOTO-VOLTAIC	
		DOP	PI	DOP	PI	DOP	PI	DOP	PI	DOP	PI	DOP	PI
1 WEIGHT	3	10	30	8	27	8	24	5	15	9	27	1	3
2 VOLUME	4	4	16	10	40	0	0	9	36	1	4	3	12
3 AREA	5	9	45	10	50	8	40	10	50	7	35	1	5
4 HAZARDS	5	6	30	1	5	9	45	2	10	6	30	10	50
5 LAUNCH, STARTUP, AND RESTART CONSIDERATIONS	3	4	12	9	27	3	9	8	24	1	3	6	18
6 MAINTENANCE REQUIREMENTS	3	6	18	6	18	8	24	8	24	8	24	10	30
7 COMPLEXITY AND RELIABILITY	5	1	5	7	35	3	15	8	40	3	15	10	50
8 CONTROL REQUIREMENTS	1	5	5	7	7	5	5	7	7	5	5	10	10
9 DEVELOPMENT REQUIRED	1	1	1	2	2	3	3	4	4	4	5	5	10
10 RISKS & UNCERTAINTIES IN DEVELOPMENT SCHEDULE	1	1	1	4	4	3	3	5	5	2	2	10	10
11 STATION INTEGRATION	3	6	18	10	30	4	12	10	30	5	15	8	24
12 VEHICLE ATTITUDE RESTRAINTS	3	2	6	10	30	2	6	10	30	2	6	2	6
13 ISOTOPE REQUIREMENT	3	10	30	1	3	10	30	2	6	10	30	10	30
14 ADAPTABILITY	3	6	18	7	21	7	21	8	24	4	12	10	30
FIGURE OF MERIT			235		299		237		305		213		288

DOP - Degree of Performance - Ranges from 0 to 10

PI - Performance Index

Weight Factors range from 1 to 5

TABLE 2-7. LIFE SUPPORT SUBSYSTEMS ENDOTHERMIC PROCESS TEMPERATURE
AND POWER REQUIREMENTS (kW)

PROCESS	OPERATION	1800° F T _o 2200° F	600° F	170° F T _Q 180° F	155° F
OXYGEN RECOVERY	DESICCANT DESORBING	-	1.225	-	-
	PYROLYZATION OF METHANE	.130	-	-	-
	SIEVE DESORBING	-	.642	-	-
	EVAPORATION	-	-	-	.243
WATER RECOVERY	PYROLYSIS	.060	-	-	-
	EVAPORATION	-	-	-	-
	EVAPORATOR	-	-	-	.442
	SLUDGE DEHYDRATION	-	.012	-	.293
WASTE WATER RECOVERY	WASTE DISINFECTION	-	.015	-	-
	FOOD PREPARATION	-	-	.027	-
	BAKING	-	-	.009	-
	CLEANING	-	-	.025	-
FOOD PREPARATION	STERILIZATION	-	.008	-	-
	SUBTOTALS:	.190	1.887	.076	.978
TOTAL KILOWATTS:				3.131	

TABLE 2-8. INTEGRATED LIFE SUPPORT SUBSYSTEM POWER REQUIREMENTS

ELECTRICAL POWER REQUIREMENT	SOLAR STIRLING ISOTOPE STIRLING SOLAR MERCURY RANKINE	SOLAR BRAYTON ISOTOPE BRAYTON
	1.60	1.60
ENDOTHERMIC POWER AT 600° F*	1.87	----
ENDOTHERMIC POWER AT 400° F*	----	2.55
ENDOTHERMIC POWER AT 155° F	1.03	1.03
TOTAL THERMAL LOSSES	0.51	0.53
TOTAL KW	5.01	5.71

*Note that more endothermic power is required at 400° F than at 600° F.

2.4 CONCLUSIONS

Significant advantages in performance can be achieved by Thermal Integration. The net reduction of 2.97 KW in the life support electrical power requirement makes it possible to reduce the size of the power system or makes additional electrical power available for other functions. As indicated previously the electrical power available for the non-integrated station is not considered sufficient and it is likely that the second approach would be taken. Since the size of some of the rotating equipment is in the region where size effects are significant, the second approach does not penalize the system efficiency. Quantitatively, the net benefit of thermal integration is a function of the tradeoff between the increase in equipment, control requirements, and system interactions and the improved performance that results from replacing electrical power with relatively "low-cost" thermal power. The benefits are considered to outweigh the disadvantages. The additional equipment added to the station in the form of piping, pumps, valves, heat exchangers, and temperature controls is similar to equipment needed for other station functions so that extensive development of new types of components or advances in the state of the art would not be required. It had been expected that the different power systems would thermally integrate differently because of the different operating temperatures. The study results show that the power systems integrate to the same degree in reducing the electrical power required for the life support system.

However, no one system was shown to be clearly superior to all others in all respects and system selection is dependent upon the criteria of selection. Based upon the ground rules for this study the Isotope Stirling system is considered to be the best non-integrated system. The differences between the systems are not sufficient to reach this conclusion with complete confidence. Small changes in the degree of performance could affect the relative ranking of the systems. It should be noted that the criteria of selection were not derived for a state of the art, very-near-future flight program. For such a program greater emphasis would be placed on utilization of flight qualified hardware, cost, and the minimization of development and schedule risks.

The sources of heat for thermal integration from the Mercury Rankine and the Stirling systems were readily determined as soon as the process thermal requirements were known. The temperature of heat rejection from the Rankine cycle was such that heat was available for all life support processes within the temperature range of the system. The heat rejection temperature of the Stirling cycle was so low that high temperature heat from the source was required for some of the life support processes that could be thermally integrated. A tradeoff was necessary for the Brayton system to determine that it was best to utilize heat being rejected from the power system even though its temperature was below the optimum for the life support processes so that the amount increased. The removal of heat at a higher temperature from the power system penalized total system performance.

One of the most important benefits of thermal integration is the reduction in size of the heat source. The penalties associated with a folding mirror are significant for this station configuration. A single piece mirror that exceeds the diameter of the vehicle is out of the question. The consequence of a folding mirror is to increase the volume necessary for packaging the system and is likely to be very expensive in terms of structural design, particularly if the overall length of the vehicle on the launch stand is increased. Thus, the solar powered systems are likely to be designed with the mirror sized by the diameter of the vehicle and thermal integration would be used to reduce the electrical power requirement to the level compatible with the mirror size and/or to make more electrical power available for the station. With the isotope systems the approach to thermal integration depends upon a tradeoff between the benefits of additional electrical power to the station and the gains achieved by reducing the size of the power system and hence the amount of isotope fuel required.

Thermal integration of the isotope powered systems is more easily accomplished than the solar powered systems. The heat is available near the cabin where it is utilized. By comparison the solar heat source is remote from the cabin since the absorber must be located at the focal point of the mirror. A detailed investigation of the method of transporting heat from the absorber to the cabin area was not carried out. To accommodate deployment, this heat transfer loop requires a method of providing flexibility in the piping system with zero leakage of the working fluid. Since elevated temperatures are involved, this may be a difficult requirement. For the purposes of this study such a heat transfer loop was assumed feasible, probably by exothermic brazing, and was used for both integrated and non-integrated systems as needed.

The thermally integrated systems were compared by the same method used for the non-integrated systems. The selected system, the Isotope Brayton, is considered superior to the other systems for this mission on the basis of the available information. As discussed previously there is uncertainty in the system selection because the difference in the Figures of Merit for the systems is relatively small. It is recognized that more detailed optimization of the power systems could result in improvements in performance particularly for the Brayton systems where the use of a liquid filled radiator and liquid cooled heat source would be expected to result in a significant weight reduction.

The benefits that can be derived from the thermal integration concept are not restricted to the items discussed in this report. Though the waste heat that can be derived from a conventional photovoltaic system is at such a low temperature as to be of little interest, auxiliary sources of heat could be provided with a photovoltaic system for use in the life support processes. Thus it should be possible to reduce the size of photovoltaic systems in the same proportion as the thermal to electric power systems. Additional concepts include the use of thermal integration in maintaining the temperature environment of the station and the use of the excess water from the life support system heated with power system heat to provide impulse for attitude control and station keeping.

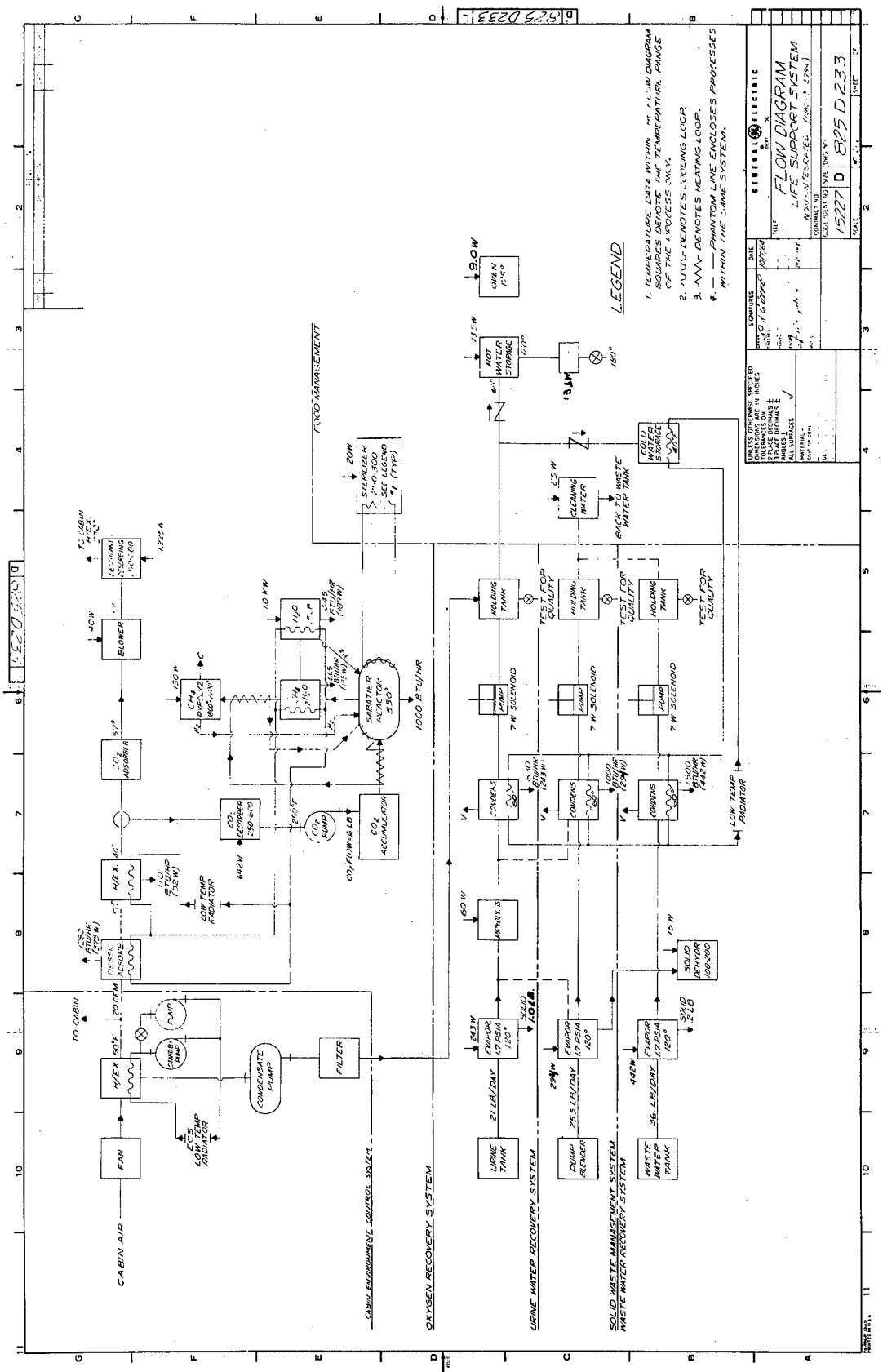


Figure 2-1. System Layout for Non-Integrated Life Support System

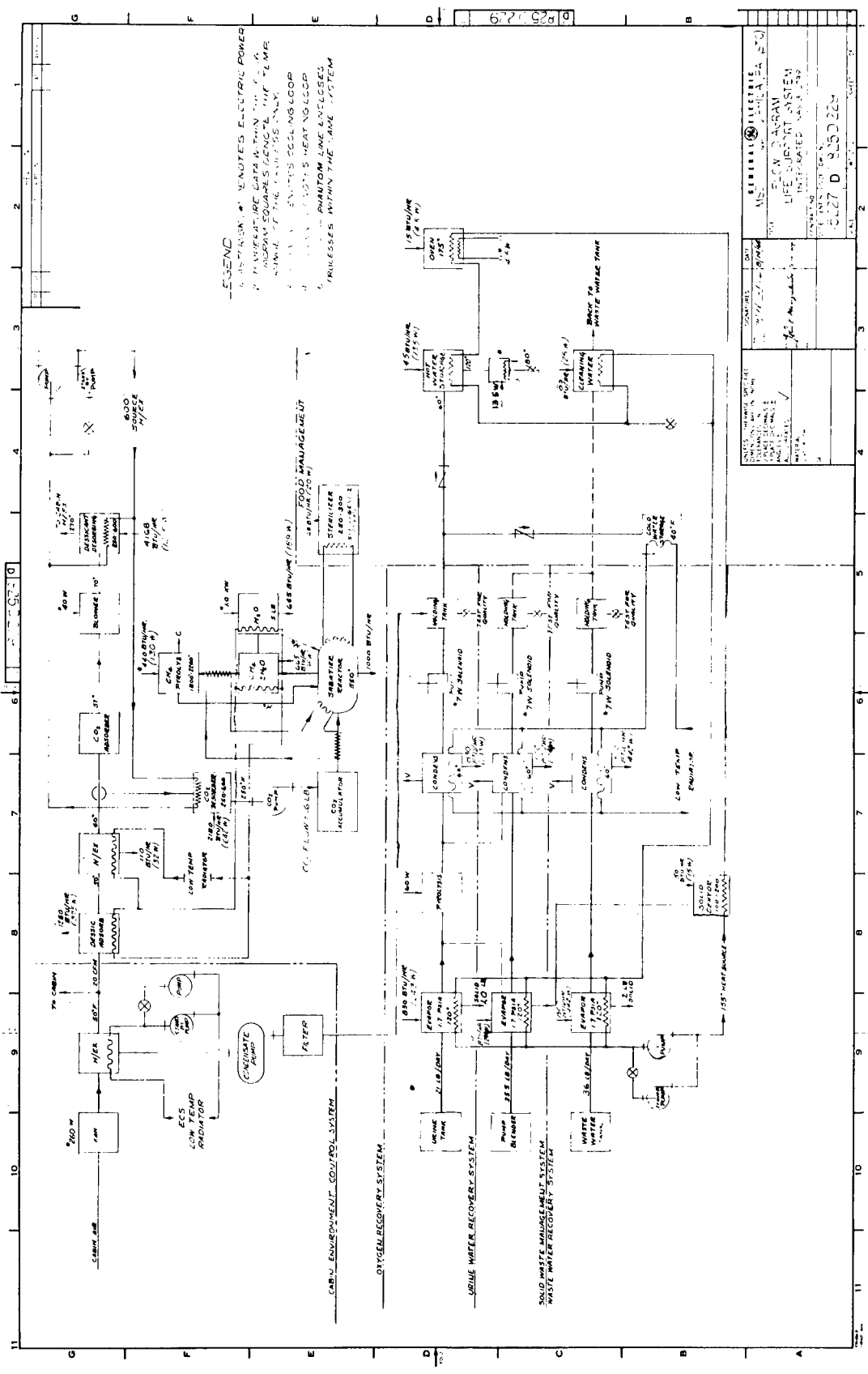


Figure 2-2. System Layout for Thermally-Integrated Life Support System

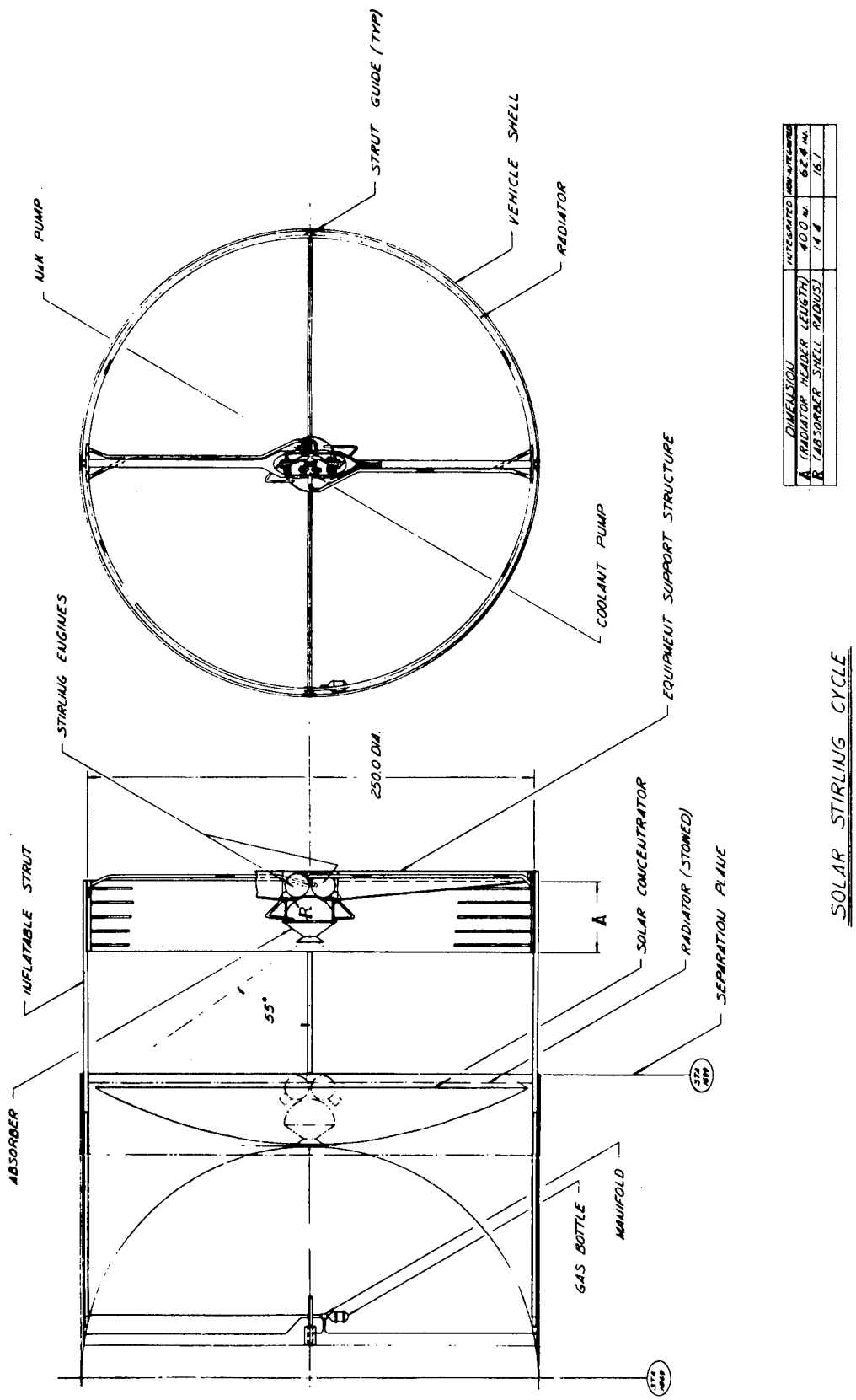


Figure 2-3. System Layout for Solar Stirling Power System

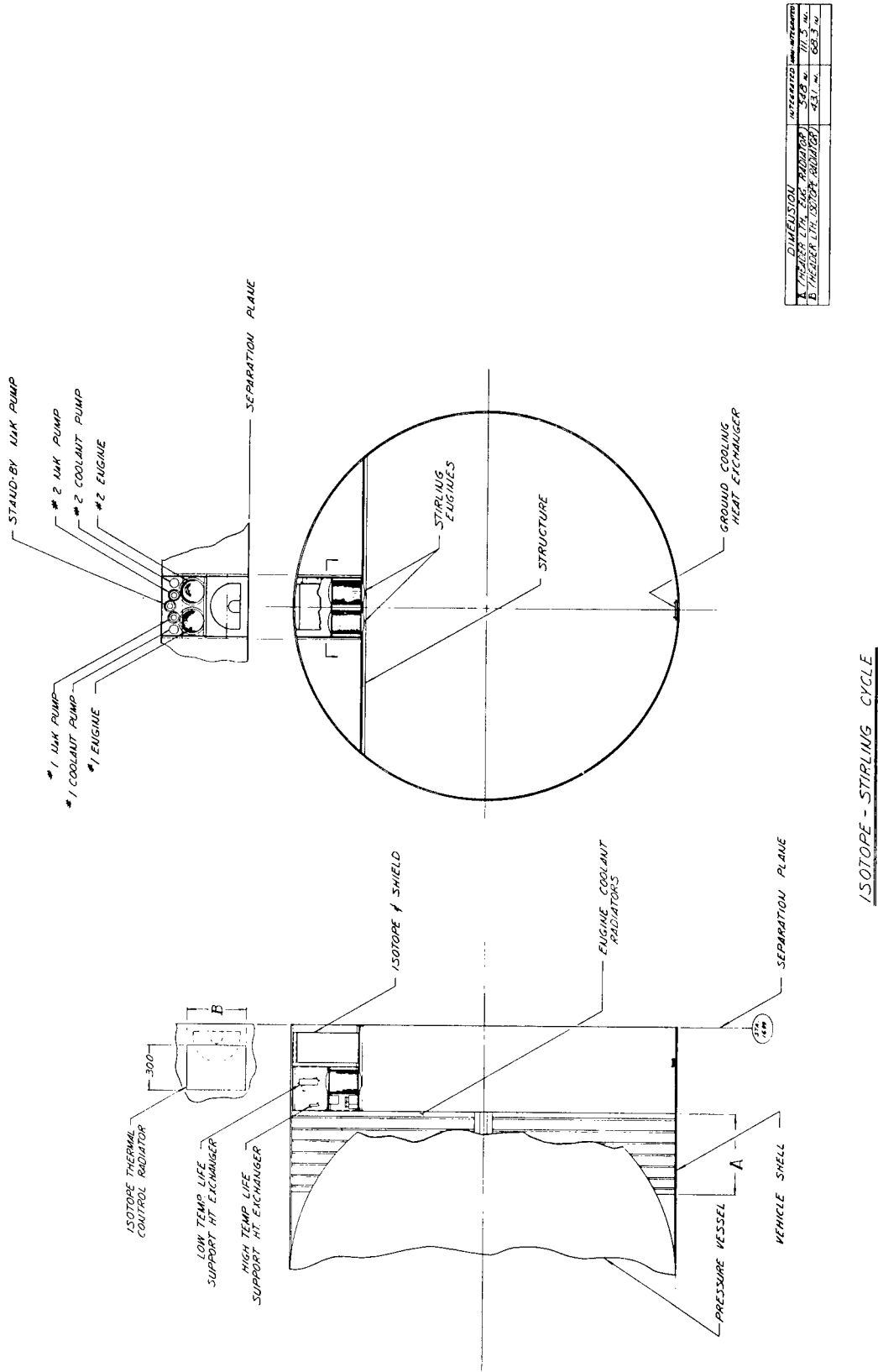


Figure 2-4. System Layout for Isotope Stirling Power System

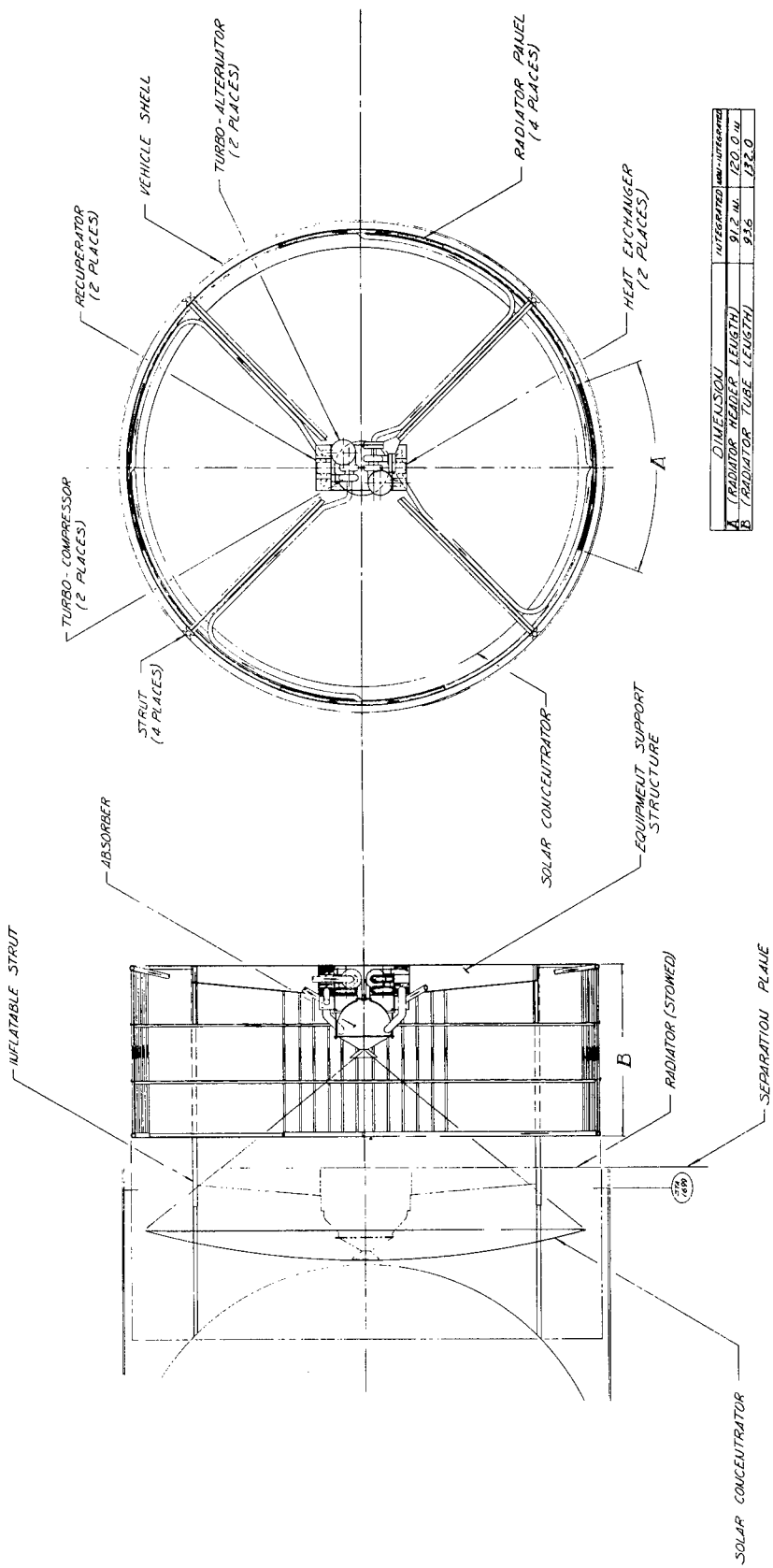


Figure 2-5. System Layout for Solar Brayton Power System

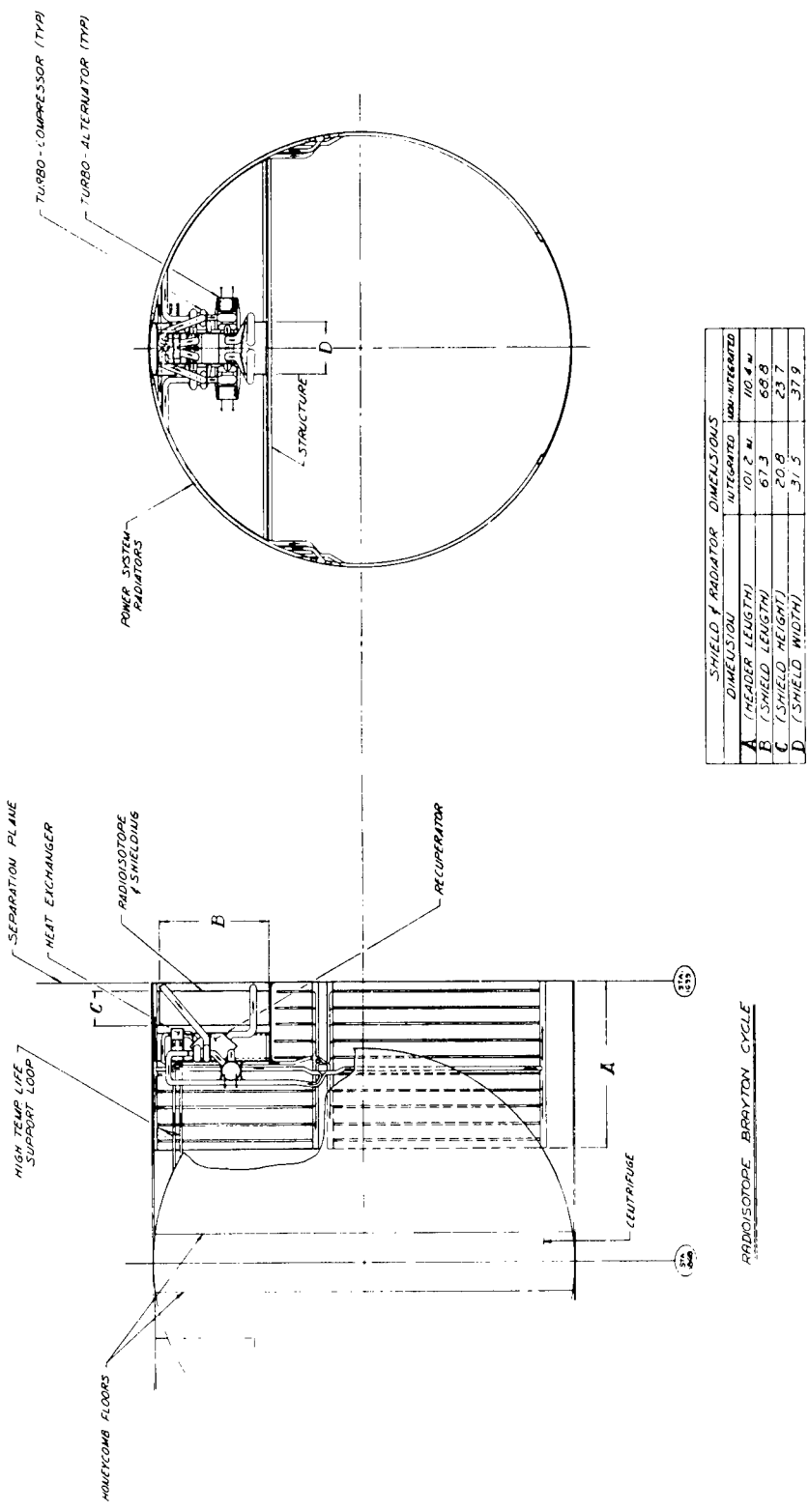


Figure 2-6. System Layout for Isotope Brayton Power System

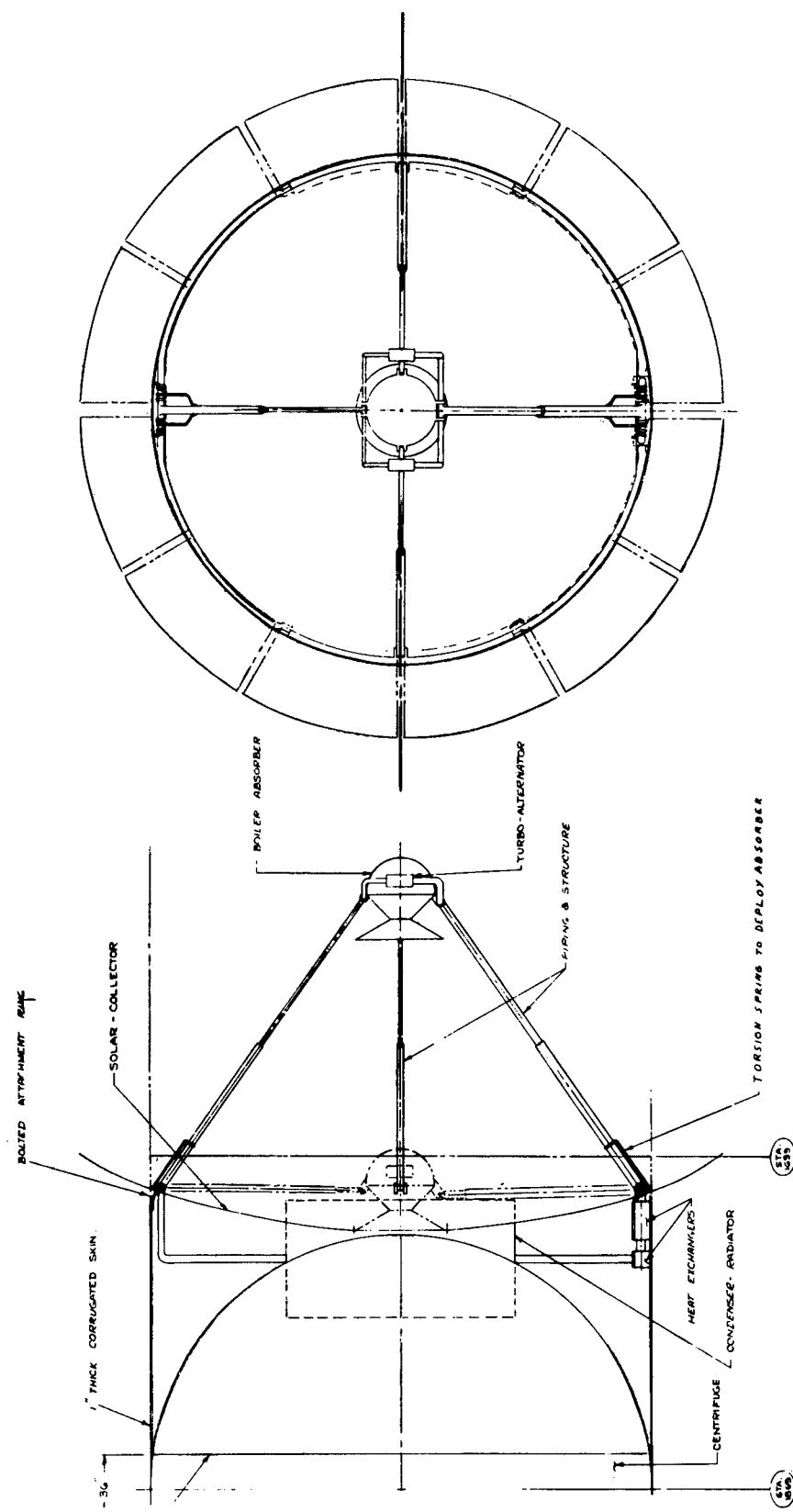


Figure 2-7. System Layout for Solar Mercury Rankine Power System

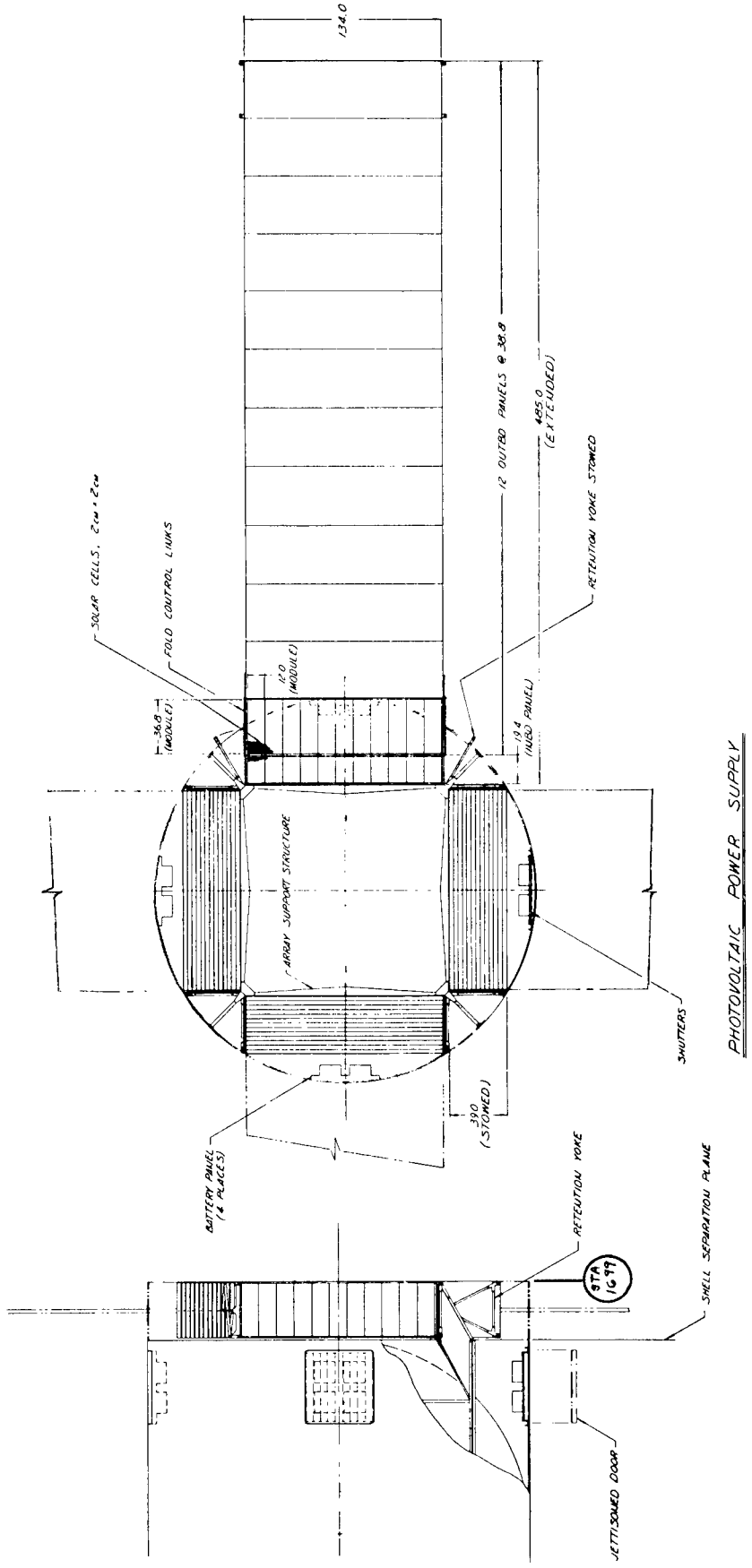


Figure 2-8. System Layout for Photovoltaic Power System

SECTION 3 DESIGN REQUIREMENTS AND SYSTEMS COMPARISONS

3.1 INTRODUCTION

Two important requirements for the study were to design the systems on a consistent basis so that no system was unduly penalized by the system specifications and to compare the systems on the basis of their total performance so that the selected systems best met the mission requirements. In order to meet these requirements a set of guidelines was derived to serve as system design requirements, and a method for obtaining a comparative Figure of Merit was developed for system evaluation and selection. This study was directed at thermal integration of the life support and electrical power systems using conservative designs that are representative of the achievable state of the art in the near future. It was a study goal to take advantage of the available information on the various types of power and life support systems when possible and to generate new design data only when necessary. Therefore, development test results were used as the first choice; results from and goals for funded development programs were second choice; and analytical results were the third choice for design data.

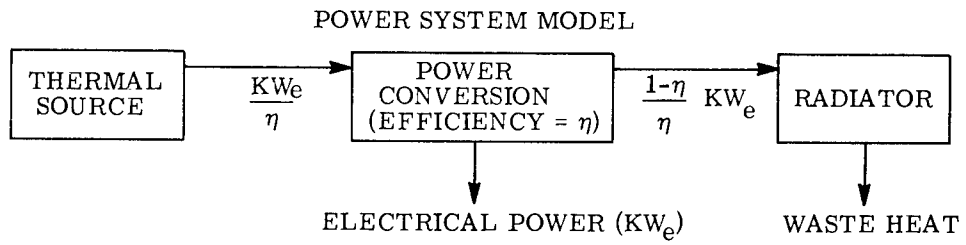
The concept of the thermal integration of the electrical power and life support systems is straightforward. For long duration manned space missions significant weight savings can be achieved by recovering water and oxygen from the waste products from the crew.

Many of the recovery processes are endothermic. The process thermal power can be supplied with electrical power from the station electrical power system, but it is evident that electrical power is expensive from the sources competitive for this application.

Any technique for using thermal power directly from the power system that reduces the total electrical power requirement is likely to improve over-all system performance.

Since the thermal to electrical power systems must reject heat, it appears to be desirable to utilize this waste heat in the life support system before rejecting this heat from the system. Gross consideration of the effects of utilizing heat from various locations in the space station is shown in Figure 3-1. The power system with over-all efficiency of η is represented as three elements: thermal source, power conversion, and radiator.

The amounts of power from the source and radiator are KW_e/η and $[(1-\eta)/\eta] KW_e$ where KW_e is the electrical output of the system. Three sources of life support process heat are postulated; the thermal source, exothermic processes in the life support system or other external sources such as on board electronic components and waste heat from the radiator. For each percent that the total electrical power requirement is reduced by thermal integration, the element size is reduced by the percent indicated in the figure. As anticipated, it is most desirable to utilize waste heat from the radiator and least desirable to utilize heat directly from the thermal source. However, for achievable values of over-all system efficiency the differences are small to improve system performance. The amount of heat that can be used is more important than the source of this heat.



SOURCE OF LIFE SUPPORT PROCESS HEAT	% REDUCTION IN ELEMENT SIZE PER % REDUCTION IN ELECTRICAL POWER REQUIREMENT		
	Thermal Source	Power Conversion	Radiator
Thermal Source	1-η	1	1
Life Support Exothermic or other External	1	1	1
Radiator	1	1	$1 + \frac{\eta}{1-\eta}$

Figure 3-1. Effects of Source of Life Support Heat

3.2 DESIGN GUIDELINES

Since the purpose of this study was to evaluate the relative merits of thermal integration of various power systems with the life support system, it was necessary to establish a consistent set of ground rules. For concreteness, this study has utilized the design objectives and physical constraints which are compatible with the Manned Orbital Research Laboratory (MORL) activities being sponsored by NASA and being led by the Langley Research Center. This six-man space station would consist of a nearly spherical cabin in a 260-inch diameter vehicle. The vehicle would be launched unmanned and would rendezvous with one or more manned vehicles. They would dock, transfer the crew and remain attached to the station. It is assumed that the vehicle will be launched with the primary power supply inoperative.

The station would function in a 250 n.m. orbit and would receive a re-supply vehicle every 180 days. A maximum re-supply weight of 20,000 lbs. is postulated. The station would be oriented towards the sun and would be expected to operate for one year. Sources of data included reports prepared by Douglas Aircraft on MORL* and NASA-supplied data on work done by General Dynamics/Astronautics in the life support area.

*E. W. Bonnett, "Report on a System Comparison and Selection Study of a Manned Orbital Research Laboratory": Douglas Report SM-44607, September 1963, Contract Number NAS 1-2974.

3.2.1 DESIGN GUIDELINES - DEFINITIONS

3.2.1.1 Orbit Definition

Altitude:	250 n. miles circular
Inclination:	28.7 degrees
Period:	94 minutes
Time in Dark: (Penumbra)	36 min. (maximum) 28.2 min. (minimum)

The rate of precession of the orbit plane due to the oblate earth is such that the period of the variation in eclipse time is estimated to be about 60 days.

3.2.1.2 External Environment

Atmosphere:	Extended ARDC, 1959
Solar Constant:	Nominal 130 watts/ft. ²
Effective Space Sink Temperature:	400°R
Micrometeoroids:	$N (> M) = \alpha M^{-\beta}$
where:	
	$N (> M)$ = number of particles impacting per unit time of mass M and larger.
	α = 5.3×10^{-11} particles/ft. ² -day
	β = 1.34
	M = meteoroid mass, grams
Ionizing Radiation:	Negligible for this orbit (insofar as this study is concerned)

3.2.1.3 Station Configuration

See Figure 1-1. The MORL configuration was to be used and the envelope to be maintained if possible.

3.2.1.4 Vehicle Orientation

Vehicle oriented with respect to the sun.

Solar collector/absorber and photovoltaic performance based on a time average mis-orientation with respect to the sun of 0.1 degree. (Time average of absolute value of orientation error.)

3.2.1.5 Power Requirements

Average Load:	6.24 KW _e (electrical power to station bus which includes .24 KW to charge batteries to supply peak loads)
Minimum Emergency Power:	1.4 KW _e
Peak Power Requirement:	9.0 KW _e . Up to one hour in any 24-hour period. Time between peak demand assumed to be at least five times the duration of the peak load.

Power Conditioning Requirements: 50% as 28 VDC
 50% as 110/220 VAC 400 cps
 Power Conditioning Penalties: dc-to-ac, efficiency = 87%
 ac-to-de, efficiency = 92%
 frequency change, efficiency = 91%

3.2.1.6 Crew Size and Duty Schedule

Six-man crew

Each astronaut is assumed to spend the following percentages of time in the various occupations.

Sleeping	33%
Recreation	18%
Duty	47%
Inside Maintenance	1.4%
Outside Maintenance	0.2%
Rendezvous Operations	0.4%

3.2.1.7 Life Support Requirements

Cabin Atmosphere

Total Pressure	10.0 psia
O ₂ Partial Pressure	160 mm Hg
CO ₂ Partial Pressure	3.8 mm Hg
N ₂ Partial Pressure	Diluent
Relative Humidity	50%
Nominal Dry Bulb Temperature	72°F
Ventilation Rate	35 cfm/man.
Cabin Atmosphere Volume	3470 ft. ³
Air Lock Atmosphere Volume	90 ft. ³ (total)

3.2.1.8 Redundancy Design Philosophy

Crew safety considerations are an important design factor. The power supply will be modularized to provide power in the event of failure of a unit. For critical components, a minimum of two units capable of independent operation will be provided. Both will operate during normal conditions. The smallest size unit that will be considered will have sufficient capacity to provide 1.4 KW_e, the minimum emergency power requirement. By definition the following components will not be redundant:

- Mirror-absorber
- Isotope heat source (except for cooling circuits)
- Radiator (except when loss of radiator cooling will effect cooling of isotope heat source)

3.2.1.9 Isotope Heat Source

The isotope heat source shall be Pu-238. Detailed consideration of safety considerations and cooling before system startup are beyond the scope of the study. Sufficient shielding will be provided to assure that a 30 rem per year whole body dose will not be exceeded.

3.3 METHOD OF COMPARISON

3.3.1 PURPOSE OF THE PROCEDURE

The purpose of the evaluation procedure was to provide a method evaluating, comparing and selecting power systems and life support systems for an orbiting space station application. It was intended to compare a number of different systems, each designed to meet the same criteria on a basis that was rational, accurate, consistent, and included all pertinent factors. Only systems that met minimum mission requirements would be included in the comparison and it was expected that different systems would excel in the various areas of composition. It was considered improbable that the "best" system, over-all, would be obvious. Since system selection from a number of nearly equal systems was to be made on the basis of a variety of performance areas, it was considered desirable to reduce performance in the various areas to a numerical value. It was considered necessary that the system be flexible enough to accommodate new information — either in or out of the scope of the present study. Finally the method of evaluation should provide guidance for system design.

3.3.2 DESCRIPTION OF THE PROCEDURE

It was considered that a Figure of Merit (F. O. M.) made up of a linear combination of performance indices best met the requirement of the evaluation procedure. The pertinent Performance Areas were defined and listed. It was intended that these be independent of each other. Their relative importance for this study was evaluated by comparing them with each other and a weight factor assigned to each Performance Area. A range of 0 to 5 was used and the Performance Areas and their Weight Factors are shown in Table 2-4.* The value of the Weight Factor increases with increasing importance of the Performance Area. The characteristics of each system to be evaluated were compared with each other in each Performance Area to establish a Degree of Performance. A range of -5 to 10 was used for Degree of Performance with the value increasing with better performance.** Performance Indices were formed by multiplying the Degree of Performance by the Weight Factor. The Performance Indices for each system were summed to obtain its Figure of Merit.

This evaluation and comparison technique was an orderly process for system selection but did not eliminate the need for engineering judgement. Some of the Performance

*Performance Areas with a Weight Factor of zero do not influence the evaluation and were not listed in the table. An obvious one is Cost which was outside the scope of the study.

**Since Degrees of Performance are relative, negative values have no particular significance. Though a range of 0 to 10 was sufficient for most cases it was necessary to extend the range to maintain a relation between the Figures of Merit for both the Integrated and the Non-Integrated systems.

Areas are qualitative in that performance could not be reduced to a numerical value within the scope of the study. Judgement was used to evaluate them and to eliminate, insofar as possible, the effects of overlapping Performance Areas. The Figures of Merit in this report represent the considered judgements of the individuals participating in the study and reviewing its results. The tabulated Performance Indices show the detailed evaluations and comparisons and make it possible for the reader to study the selection process in detail, if he desires.

The Figures of Merit derived in this report are relative since no absolute standard of performance was available. Comparison of these results with other evaluations must be done very carefully.

3.4 SYSTEMS COMPARISON

3.4.1 INTRODUCTION

The Performance Areas and Degrees of Performance tabulated in Tables 2-4 and 2-6 are discussed in the following paragraphs. The Power/Life Support Systems, grouped as integrated and non-integrated, were compared in order to select the system with the "best" performance, all pertinent factors considered. The photovoltaic system was not affected by thermal integration so its Figure of Merit was made the same for both comparisons. With it as a reference it was possible to maintain a relation between the integrated and non-integrated Figures of Merit. The range of Degrees of Performance was selected in order to account for system differences in a consistent manner. The use of negative values of Degree of Performance was merely a convenient method of extending the scale as the values are relative and only differences between numbers were significant.

3.4.2 NON-INTEGRATED SYSTEMS COMPARISON

3.4.2.1 Weight (Weight Factor = 3)

The total weight of the electrical power and life support system was evaluated. Weight was considered of intermediate importance as an evaluation criteria. Performance was assigned on the basis of comparing the tabulated weights which included supporting structure, interconnecting piping, heat exchangers, and controls. No penalty was assessed to those systems that violated the design guideline envelope.

3.4.2.2 Volume (Weight Factor = 4)

Volume is defined as the volume of the space station pre-empted by the electrical power and life support systems equipment in the launch configuration. Volume requirement was considered a more important criteria for selection than weight. Degrees of performance were assigned on the basis of the tabulated equipment volumes. To maintain consistency a negative value was assigned to the Solar Brayton system.

3.4.2.3 Area (Weight Factor = 5)

Area was evaluated by considering the projected area of the station in its orbiting configuration. A penalty would have been added if the utilization of the surface of the station for radiators exceeded the available surface. A high weight factor was applied because of the penalties associated with orbit maintenance to compensate for atmospheric drag and attitude disturbance torques. Numerical values of area were available from the design data for determining the Degrees of Performance. The systems which used the surface of the station for radiator area have a performance advantage. This was easily accomplished with the isotope powered systems but not with the solar powered systems.

The Solar Brayton and Stirling systems have the radiators located adjacent to the absorber and have an area penalty. The Solar Mercury Rankine system utilized telescoping lines to transport fluid to and from a radiator mounted on the station surface. This resulted in a reduction in projected area but increased the development required and the risks in the schedule as there was no proven method of providing leakproof telescoping lines that was considered state of the art.

3.4.2.4 Hazards (Weight Factor = 5)

This Performance Area represented the risks to crew safety associated with each system. Consequently a high Weight Factor was assigned. A quantitative evaluation of risk was not available so the Degrees of Performance were determined on a qualitative basis. Hazards included the problems that could result from failure of the rotating equipment, radiation from the isotopes, contamination of the cabin with injurious materials such as mercury vapor, and the consequences of a catastrophic battery failure.

The photovoltaic system was considered to offer the smallest potential hazard to the crew and station. There were batteries present in all of the systems and the increased size of the photovoltaic battery package was not considered to significantly increase the risk. The isotope powered systems introduced a radiation source not present in the solar powered systems. The risk due to mechanical failure of rotating equipment was considered essentially equal for all of the dynamic systems. The inert working fluid of the Brayton systems was considered less hazardous than the fluids used in the Stirling and Rankine systems. These considerations resulted in the tabulated Degrees of Performance.

3.4.2.5 Launch, Start-up, and Restart (Weight Factor = 3)

This Performance Area included the requirements of the launch phase, the initial start-up and activation of the station, and the problems associated with restarting the system in space in the event it became necessary.

Detailed consideration of the launch phase was outside the scope of the study. This phase was considered to include the final portions of the countdown sequence, launch and injection into orbit, and orbiting flight prior to power plant startup and station occupancy. None of the systems operate during this phase. Final confidence tests such as electrical continuity checks and plumbing leak tests would be completed. Isotope fuel capsules would be installed and possibly working fluid would be loaded into the heat exchanger loops. Cooling, as required, would be provided after installation of isotope heat sources. Based on the philosophy that flight equipment design is primarily determined by flight requirements rather than by ground support equipment limitations or complexity, launch phase considerations were not a major factor in establishing Degrees of Performance.

The isotope powered systems were considered relatively easy to start in orbit. Heat is available at any time compared to the solar powered systems which must be oriented during station daylight to provide heat. In addition the solar powered systems require an absorber erection sequence and mirror unfolding in some cases. The Stirling engine which uses an electric motor start was considered to have an advantage over the Brayton and Rankine systems which had turbine starts. Startup of the photovoltaic system required solar orientation plus an array erection sequence. Though this system did not require the achievement of a thermal balance associated with the other systems the complexity of the array erection sequence was considered sufficient to rank this system between the solar dynamic and isotope dynamic systems.

Restart considerations for the dynamic systems were considered similar to those just described for startup. Restart was not required for the photovoltaic system.

3.4.2.6 Maintenance Requirements (Weight Factor = 3)

The design guidelines specified an operational life of one year and all systems were designed to meet this requirement without planned replacement of any component. Therefore this Area of Performance was primarily concerned with the routine of monitoring system operation and minor maintenance. The photovoltaic system was considered to require the least maintenance. In addition it was noted that its maintenance requirements can be satisfied with a minimum of "crisis conditions" because it is modularized to the point that a failure in one section can be accommodated for a considerable period of time with only minor adjustments in station routine. The Brayton systems were considered to require the least maintenance of the dynamic systems partly because their working fluid is inert and was the only fluid in the system. The Stirling engine systems were considered to require the most maintenance because of the possible wearout of rings, seals and other mechanical parts. The range of Degrees of Performance was reduced because of the opinion that differences in performance in the area are relatively small.

3.4.2.7 Complexity and Reliability (Weight Factor = 5)

Reliability was considered of prime importance in the evaluation of the systems and a high value of Weight Factor was assigned. However, detailed reliability analyses were beyond the scope of this study and, in fact, definitive reliability predictions are not possible for conceptual designs of advanced systems as generated for this study. Complexity was used as one measure of reliability and was considered a penalty as it affected the potential for malfunctions and failures. The number of parts was not the only measure of complexity because they can be interconnected in modules to reduce the effect of failures, e.g., the solar array.

The photovoltaic system was considered most reliable. This system requires solar orientation for operation so that a failure in the attitude control system will result in a loss of power. However the system can tolerate more degradation in attitude control system performance than the solar dynamic systems. It is also modularized so that more than one section could fail and station operation could continue on a reduced basis. The isotope systems were considered more reliable than the solar dynamic systems with the turbine equipment superior to the Stirling engine. These considerations resulted in the Degrees of Performance tabulated.

3.4.2.8 Control Requirements (Weight Factor = 1)

Several aspects of control requirements such as weight, complexity and reliability, and interaction with other subsystems were included in other Areas of Performance. This Area served to evaluate the remaining aspects of control requirements and was assigned a low weight factor. The photovoltaic system was considered to have the least control requirement. Satisfactory control of the elements in the solar cell power system has been demonstrated in orbit, though on a smaller scale than required for this application. The control requirements of all dynamic systems were considered to be similar. Control of solar absorber operation was rated more difficult than isotope heat exchanger control.

3.4.2.9 Development Required (Weight Factor = 1)

The scope of the development program required to provide a flight system and the difficulty of the anticipated development problems were evaluated in this Performance Area. A low Weight Factor was assigned to this area because system development programs are expected for this manned space station, an advanced concept with a launch date quite far in the future. A system was not to be heavily penalized if a development program was required to achieve an improved performance capability.

Though not yet demonstrated in this size of system the photovoltaic system was considered to be an extension of existing technology compared to the programs required

to provide dynamic systems. Because of the extensive development completed on the Mercury Rankine system it was considered to require less development than the other dynamic systems. Closed cycle Brayton systems were evaluated to be closer to state of the art than Stirling engines for one year operation. It was not meant to minimize the development required to "man-rate" isotope systems but this heat source was considered to rate better than the solar heat sources because of the development required for the large solar collectors. Isotope availability is more a matter of cost and policy than a development problem. Consideration was given to the programs completed and underway to evaluate and solve the safety problem associated with orbiting isotope heat sources.

3.4.2.10 Risks and Uncertainties in Development Schedules (Weight Factor = 1)

It was the intent of this Performance Area to assess the relative risks and uncertainties in system development schedules staying compatible with a flight date after the program starts. The systems that can be programmed with confidence to meet a launch date are better than systems that may become the pacing item of the total program. Since the launch period was quite far in the future there was time for solution of most of the unanticipated problems that would occur (assuming an early start on the development program) with all of the systems and this Area was assigned a low Weight Factor.

Development of the photovoltaic system requires primarily extension of present capability and this system has the least risk. Though isotope inventory is limited and costly, the lead time is such that there could be less risk with this heat source than with the large collectors required for solar powered systems. The boiling and condensing in zero "g" requirement of the Rankine system was evaluated to be an area of risk as were seals and lubrication of the Stirling engine. Sealing of the telescoping lines in space by an endothermic brazing process is considered feasible, but as yet is not proven for space application. This method was used for the Solar Mercury Rankine system, which is penalized slightly for that risk in this Performance Area.

3.4.2.11 Station Integration (Weight Factor = 3)

This Performance Area included the interaction of the power and life support systems with the other systems in the station. Included were restraints that are imposed upon the operation of the other systems such as the solar orientation accuracy requirement, the compatibility with guideline interfaces, installation, and similar items. This is an important Area in a hardware development program, particularly if a new system were to be installed in a completely designed station. For this evaluation it was assumed that the design status of the station was still preliminary and that changes in station system interfaces would not create serious problems. Therefore an intermediate Weight Factor was used. Violations of the guideline envelope were considered a significant disadvantage.

In evaluating system performance the isotope systems were rated higher than the others. Their equipment was compact and relatively easy to place in the station. (The radiation characteristic was accounted for in Weight and other Areas.) The battery package provides for temporary overload conditions and there was a minimum of interaction with other systems. The photovoltaic system was rated better than the solar dynamic systems. The Solar Mercury Rankine and the Solar Brayton systems were penalized for extending the guideline station envelope.

3.4.2.12 Vehicle Attitude Restraints (Weight Factor = 3)

This Performance Area considered restraints imposed upon the mission capabilities of the station by the power and life support systems. The major problem was the requirement for solar orientation of the station for astronomy, meteorology, and similar missions. There was a significant difference between the isotope and solar powered systems. Insofar as this area was concerned the difference in the orientation requirements of the photovoltaic and the solar dynamic systems was not considered significant.

3.4.2.13 Isotope Requirement (Weight Factor = 3)

Analysis of the isotope requirement was included in the evaluation because of cost and limited supply. Degrees of Performance were assigned on the basis of the isotope inventory and negative values were used for the Isotope Stirling and Brayton systems to maintain consistency with the integrated systems.

3.4.2.14 Adaptability (Weight Factor = 3)

This area was included to account for the flexibility inherent in some systems. In a program with the scope of a manned orbiting space station it was considered that development would be initiated before all requirements were known in detail. Some variation in electrical power requirements usually occurs during such a program and power system design requirements change with time. Systems that can proceed with development with a minimum of redesign rate higher than those which cannot. The capability for limited growth was also included in this Area.

The photovoltaic system was considered most adaptable. The design has sufficient modularization that changes in size can be accomplished by the addition (or deletion) of a module unit. Development of standard modules could proceed with confidence that progress was being made on the final flight design. The Brayton system was considered to be the most flexible dynamic system as changes in load could be accommodated by varying the pressure in the system. To a lesser degree the same approach could be used with the Stirling engine system. Growth capability can be incorporated into the isotope package design to provide adaptability that is not possible with the design and fabrication of large solar collectors.

3.4.3 INTEGRATED SYSTEMS COMPARISON

3.4.3.1 Weight (Weight Factor = 3)

Degree of Performance factors were assigned by comparing the total system weights.

3.4.3.2 Volume (Weight Factor = 4)

Degree of Performance factors were assigned by comparing the total system volumes in the launch configuration. Life Support System volume was essentially equal for all systems.

3.4.3.3 Area (Weight Factor = 5)

Degree of Performance factors were assigned by comparing the projected areas of the stations in orbiting configuration.

3.4.3.4 Hazards (Weight Factor = 5)

Thermal integration introduced a risk of leakage of the high temperature heat exchanger fluid used to provide heat to the life support processes. Therefore Degrees of Performance were decreased in relation to the non-integrated systems. The decrease in the amount of the isotope inventory was not considered to affect the radiation hazard sufficiently to change the relative ranking of the systems.

3.4.3.5 Launch, Startup, and Restart Considerations (Weight Factor = 3)

Thermal integration increased the complexity of the startup procedure because additional heat exchanger loops were involved. The time to achieve thermal balance will be increased. The mirror unfold sequence was no longer required for startup of the Solar Stirling and Brayton systems. Degrees of Performance were shifted relative to the value for the photovoltaic system to account for these changes.

3.4.3.6 Maintenance Requirements (Weight Factor = 3)

The addition of the thermal integration equipment slightly increased the need for maintenance and monitoring performance. Relative to other factors, the difference between integrated and non-integrated systems was not considered significant and the Degrees of Performance were made equal.

3.4.3.7 Complexity and Reliability (Weight Factor = 5)

The equipment needed for thermal integration was similar for all dynamic systems and the additional potential dynamic systems failure modes were considered of the same consequence. The Degrees of Performance were uniformly decreased from their non-integrated values to account for a decrease in reliability.

3.4.3.8 Control Requirements (Weight Factor = 1)

Thermal integration increases the interaction between the power and life support systems which increases the control requirements. The degree of interaction was evaluated to be such that a uniform decrease in the non-integrated Degrees of Performance was necessary to represent differences in performance in this Area.

3.4.3.9 Development Required (Weight Factor = 1)

The development required for thermal integration was considered to be straightforward. Development of each system can proceed independently as the interface can be defined with relative ease for use in individual system design and testing. Additional testing will be required at the combined system level to demonstrate compatibility. The Degrees of Performance were reduced from their non-integrated values to account for the additional scope of the development program.

3.4.3.10 Risks and Uncertainties in Development Schedule (Weight Factor = 1)

So far as could be determined most risks in the development schedule resulted from the power and the life support system individually and not with thermal integration. The equipment needed for thermal integration, with one exception, is conventional and of the type needed for other uses in the station. The exception was the requirement for a method of transporting heat from the absorber to the life support equipment for the solar dynamic systems. The method must allow for deployment of the absorber with near zero leakage to avoid degradation of reliability. The conceptual design was a telescoping tube with the joints to be sealed by an exothermic brazing process after deployment. This technique has not been demonstrated in space and is a development risk. Thermal integration was considered to involve no additional development risk for the isotope powered systems but some additional risk for the Solar Stirling and Brayton systems where heat transport from the absorber to the cabin was required. Degrees of Performance were assigned accordingly.

3.4.3.11 Station Integration (Weight Factor = 3)

Thermal integration primarily affected the interaction between the power and life support systems and was not considered to change the relative performance of the systems in this Performance Area. The one exception is that the change in station length needed to contain the Solar Brayton system is less for the integrated than for the non-integrated configuration. The length added to the station to contain the Solar Mercury Rankine system was the same for both the integrated and non-integrated configurations. Although the Rankine absorber extends only slightly into the instrumentation area aft of station 1699 and could probably be designed so that it would not lengthen the vehicle, the consistent assumption was made that the vehicle length would increase by the amount of the intrusion of the absorber.

3.4.3.12 Vehicle Attitude Restraints (Weight Factor = 3)

This Area of Performance was not affected by thermal integration and the Degrees of Performance are the same for both the integrated and the non-integrated systems.

3.4.3.13 Isotope Requirement (Weight Factor = 3)

The isotope inventory was significantly affected by thermal integration and the Degrees of Performance were determined by comparing the sizes of the required inventories.

3.4.3.14 Adaptability (Weight Factor = 3)

The size of either the life support or the power system could change a reasonable amount without upsetting the thermal balance between them. This provides a system design flexibility in the event of changing requirements. However, the thermal integration equipment itself (heat exchangers and pumps) does not readily provide a range in performance. Thus, a change in requirements would result in a change in component design. The relative performance of the integrated dynamic systems was considered to be the same as the non-integrated dynamic systems but a small penalty was imposed to account for the lack of capability to accommodate a change in requirement.

SECTION 4.
LIFE SUPPORT SYSTEM ANALYSIS

4.1 GENERAL REQUIREMENTS

The study is related to a six-man, earth-orbiting laboratory. The laboratory is a 260-inch diameter sphere divided into three basic compartments: crew quarters, laboratory quarters, and a centrifuge section as for the Manned Orbital Research Laboratory shown in Figure 4-1. The station is expected to remain in orbit for one year and would receive a resupply vehicle every 180 days.

Life Support System design parameters were set as follows:

Cabin Atmosphere

Total Pressure	= 10 psia
O ₂ Partial Pressure	= 160 mm Hg
CO ₂ Partial Pressure	< 3.8 mm Hg
N ₂ Partial Pressure	= Diluent
Relative Humidity	= 50%
Nominal Dry Bulb Temperature	= 72° F
Ventilation Rate	= 35 CFM/man
Cabin Atmosphere Volume	= 3470 Ft. ³

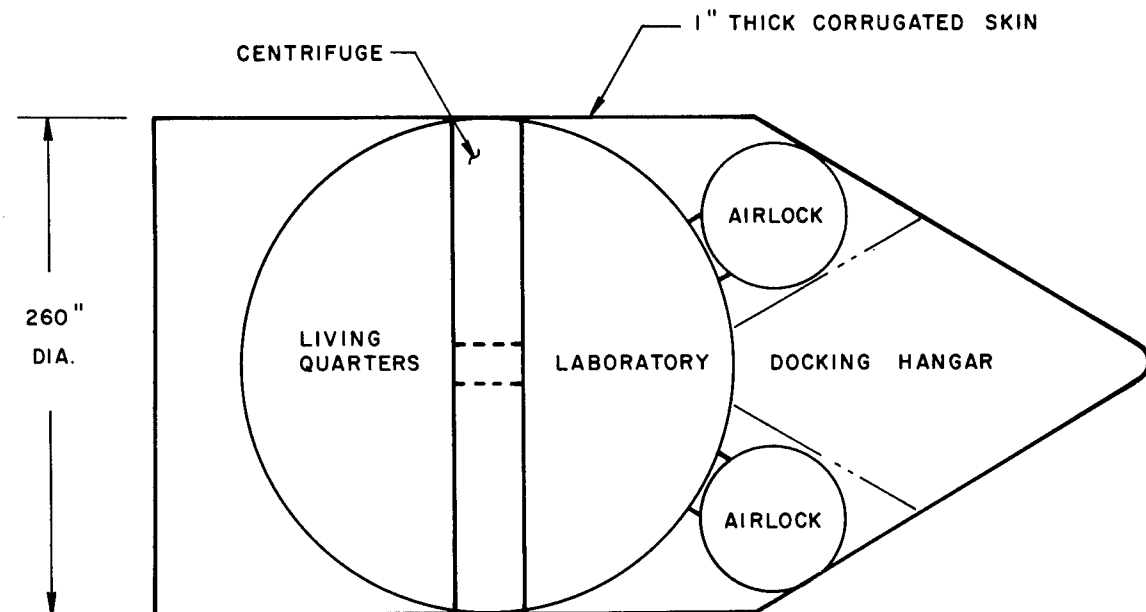


Figure 4-1. Basic Station Configuration

Metabolic Data

Oxygen Consumption	= 1.87 Lb/Man-day *
Water Allowance	= 7.72 Lb/Man-day
Food (dry)	= 1.38
CO ₂ Output	= 2.32 Lb/Man-Day *
Urine Water	= 3.30 Lb/Man-Day
Fecal Water	= 0.25 Lb/Man-Day
Urine and Fecal Solids	= 0.22 Lb/Man-Day
Evaporative Water Loss (Respiration and Perspiration)	= 5.90 Lb/Man-Day
Metabolic Water	= 0.72 Lb/Man-Day
Latent and Sensible Heat	= 11,112 BTU/Man-Day
Wash Water	= 6.0 Lb/Man-Day

4.2 SPECIFIC REQUIREMENTS

The life support subsystems used in this study include and have been limited to the following:

- a. CO₂ regeneration by the Sabatier Method
- b. Urine treatment by distillation and pyrolysis
- c. Waste water distillation
- d. Food preparation
- e. Solid waste management

The detail requirements of the study were:

- a. The non-integrated life support subsystem shall be designed for a six-man rating. The subsystems shall be evaluated analytically to determine electrical power requirements for normal and emergency operations.
- b. The endothermic areas of the life support subsystems, the required temperature levels and the rate of heat input shall be determined. The amount of non-electrical power which could be used should be established for each different power system.

4.3 LIFE SUPPORT SUBSYSTEMS DESIGN

The life support subsystems described in this section were designed using information from the MORL and other studies. Particular attention was given to the endothermic processes since they represented the areas for thermal integration with the electric power systems.

*Note the oxygen consumption and CO₂ outputs are not metabolically balanced. Maximum values are listed. The design value of CO₂ output is 2.25 Lb/man-day.

4.3.1 SABATIER METHOD FOR OXYGEN RECOVERY FROM CARBON DIOXIDE

4.3.1.1 Summary

The Sabatier method for oxygen recovery from carbon dioxide is a complex process involving both exothermic and endothermic reactions and processes.

Since this thermal integration report is concerned with the endothermic processes, a summary of these processes is presented for easy reference. Note that the figures presented are based on a six-man crew for extended missions. The power requirements listed are those required strictly for the process and do not include thermal losses in the equipment.

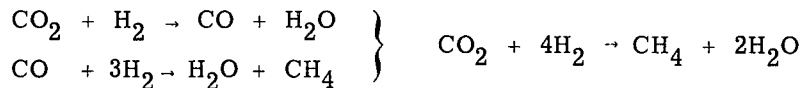
ITEM	OPERATING TEMPERATURE RANGE	ENDOTHERMIC POWER REQUIREMENT
Carbon Dioxide Collection	(Total for six-man crew)	
Desiccant Desorbing	250-600°F	1255 watts @ 250°F
Sieve Desorbing	250-600°F	642 watts @ 250°F
Pryolysis of Methane	1800-2200°F	<u>130 watts</u>
	TOTAL	1997 Watts

4.3.1.2 Introduction

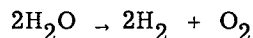
Oxygen recovery from carbon dioxide is a complicated but logically necessary process for extended mission space vehicles with large crews. Oxygen recovery is accomplished in four distinct phases:

1. Removal and Collection of Carbon Dioxide from the Cabin Atmosphere

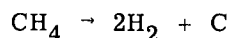
2. Sabatier Reaction



3. Water Electrolysis



4. Catalytic Pyrolyzation of Methane



4.3.1.2.1 Carbon Dioxide Collection

The carbon dioxide generated by the crew must be separated from the cabin atmosphere and collected prior to insertion into the Sabatier Reactor. Several collection methods have been or are being developed. Prominent among these is a regenerable adsorption process which is presently designed to jettison the carbon dioxide to space. Modifications to this "state of the art" system will permit collection of the carbon dioxide for use in the Sabatier Reaction. Figure 4-2 presents a schematic flow diagram of the CO₂ concentration process. A small

by-pass flow of cooled and dehumidified atmosphere gas from the cabin environmental control system is further dried by a desiccant and then is drawn through a carbon dioxide adsorbing material. The water vapor is initially removed from the gas flow since the carbon dioxide adsorbing material has a preferential affinity for water vapor. The dried and purified atmosphere gas flow leaving the desiccant and adsorber is then utilized to regenerate a second desiccant canister which is heated to increase the desorption rate. The second carbon dioxide adsorbing canister is also regenerated by heat and low pressure. The low pressure is induced by a gas pump which delivers carbon dioxide to the Sabatier Reactor. A special series of valves alternately switch one of the two desiccant canisters and one of the two carbon dioxide adsorbing canisters into the system while the other pair is being regenerated; thus constant system operation is provided.

4.3.1.3 System Description

After the main cabin atmosphere gas flow is cooled and dehumidified (considered saturated at 50°F) in the cabin environmental control system, a small by-pass flow in the order of 20 CFM at an assumed pressure of 1/2 atmosphere is drawn through the carbon dioxide collection system.* The six men will produce $\frac{2.25 \text{ lb. CO}_2/\text{man-day} \times 6 \text{ men}}{1440 \text{ min./day}}$

0.0094 lb. CO₂/min., thus for a 20 CFM cabin atmospheric gas flow, approximately

$$\frac{0.0094 \text{ lb. CO}_2/\text{min.}}{20 \text{ Ft.}^3 \text{ Gas/min.}} \times \frac{1}{0.04 \text{ lbs./ft}^3 \text{ density}}$$

or 0.0118 lb. CO₂ are contained in each pound of atmospheric gas. Comparing pound moles of the gases,

$$\frac{0.0118 \text{ lb. CO}_2}{1 \text{ Lb. O}_2 + \text{N}_2} \times \frac{30 \text{ M.W. O}_2 + \text{N}_2}{44 \text{ N.W. CO}_2} = 0.00805$$

or 0.805% CO₂ × 360 mm Hg total pressure equals 2.9 mm Hg CO₂ partial pressure maintained in the cabin. The flow is alternately valved through one of two desiccant canisters while the other is being regenerated. The desiccant removes approximately 0.71 pounds of water per hour from the flow stream. The specific volume of the vapor at saturation temperature is 1703.2 ft.³/lb. @ 9.2 mm Hg partial pressure. (Reference 1)

$$\frac{1 \text{ lb. Water}}{1703.2 \text{ ft.}^3} \times \frac{20 \text{ ft.}^3}{\text{Min.}} \times \frac{60 \text{ Min.}}{\text{Hr.}} = 0.707 \text{ lbs. water/hr.}$$

Molecular sieve type 13X is a good desiccant for this application because of its high capacity at reduced water vapor partial pressures and because of the low gas dew points of -70°F

*Boeing (2) utilized a gas flow of 10 CFM for a three man system. Studies previously completed by the General Electric Company, and a four-week test involving three "terranauts" provided data to support the decision to base the Life Support System design for this study on a cabin pressure of 7.5 psia rather than 10 psia, and on a CO₂ rate of 2.25 rather than 2.32 Lb/Man-day. The effects of a change in pressure on thermal integration are considered negligible.

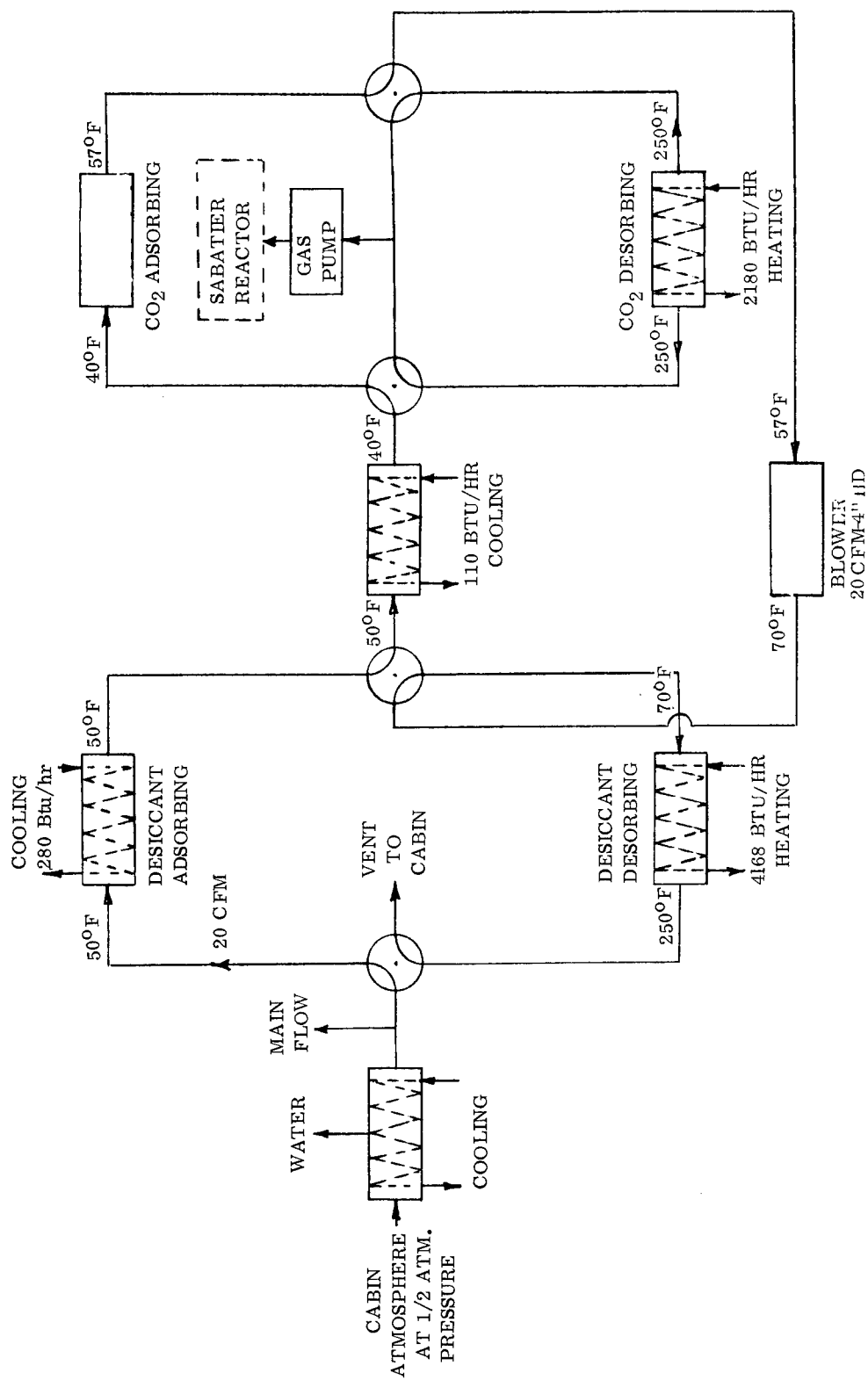


Figure 4-2. Carbon Dioxide Collection

which are attainable.* This maximum water vapor adsorption for the sieve at the above conditions is approximately 29% by weight as shown in Figure 4-3. The desiccant will liberate approximately 1280 BTU per hour for the above conditions.

$$0.71 \text{ lb. water/hr.} \times \frac{1800 \text{ BTU (7)}}{\text{Lb. Water}} = 1280 \text{ BTU/hr.}$$

If the canister were adiabatic, the temperature of the air flow would raise approximately 116.0°F .

$$\begin{aligned} Q &= \frac{wc}{\rho} \Delta t \\ 1280 \text{ BTU/Hr.} &= \frac{20 \text{ Ft.}^3}{\text{Min.}} \times \frac{60 \text{ Min.}}{\text{Hr.}} \times \frac{0.04 \text{ Lbs.}}{\text{Ft.}^3} \\ &\times \frac{0.23 \text{ BTU}}{\text{Lbs.}^{\circ}\text{F}} \times \Delta t \quad \therefore \Delta t = 116.0^{\circ}\text{F} \end{aligned}$$

Obviously, this cannot be tolerated since the adsorption capacity of the desiccant would decrease rapidly as shown in Figure 4-3. Consequently, a cooling coil of glycol is added to this canister to remove the heat of adsorption. A glycol flow of 0.5 GPM will exhibit an approximate temperature rise of 5.84°F to maintain a constant gas flow inlet and outlet temperature.

$$\begin{aligned} 1280 \text{ BTU/hr.} &= \frac{0.5 \text{ gal.}}{\text{Min.}} \times \frac{60 \text{ Min.}}{\text{Hr.}} \times \frac{8.6 \text{ Lbs.}}{\text{Gal.}} \\ &\times \frac{0.85 \text{ BTU}}{\text{Lbs.}^{\circ}\text{F}} \times \Delta t \quad \therefore \Delta t = 5.84^{\circ}\text{F} \end{aligned}$$

The dried atmospheric gas flow is further cooled to 40°F by an after-cooler to assure optimum operation in the carbon dioxide removal canister. The flow is alternately valved through one of the two carbon dioxide adsorption canisters which removes approximately 0.6 pounds of carbon dioxide per hour from the cabin atmosphere to maintain a carbon dioxide partial pressure below 3.8 mm Hg. A previous calculation shows that CO_2 partial pressure of 2.9 mm Hg is attainable.

$$\frac{2.25 \text{ Lbs. CO}_2}{\text{Day}} \times \frac{6 \text{ Men}}{1} \times \frac{\text{Day}}{24 \text{ Hours}} \times 0.562 \text{ lbs. CO}_2 \text{ produced per hour}$$

Two grades of Linde Molecular Sieve (Type 4A and 5A) exhibit high capacities and relatively

*Silica gel is also a good desiccant with a lower heat of adsorption (1100-1300 BTU/hr) however, the capacity is lower and the resulting gas dew point is higher than that of type 13X molecular sieve. Hamilton Standard and General Electric have utilized silica gel in present and past carbon dioxide removal systems; however, Boeing⁽²⁾ is utilizing type 13X sieve and have obtained good operational data. Also, Linde⁽⁴⁾ recommends the sieve adsorbent. An analysis showed essentially no difference in process heat requirements.

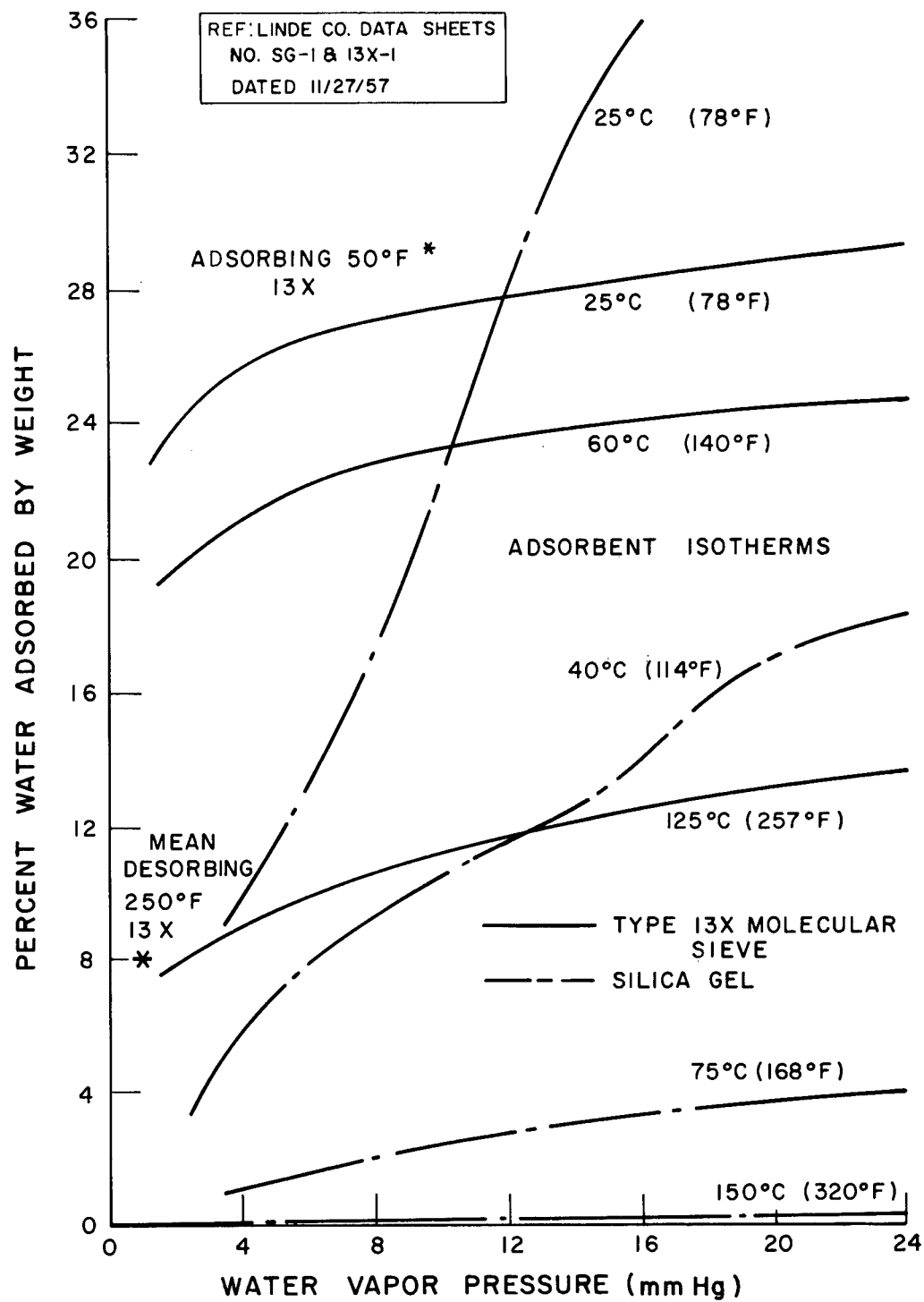


Figure 4-3. Water Vapor Adsorbent Characteristics

low heat of exothermic adsorption. Figure 4-4 illustrates the type 5A sieve* will adsorb approximately 10% carbon dioxide by weight. The sieve will liberate approximately 180 BTU per hour for the above CO₂ adsorption rate.**

$$\frac{0.6 \text{ lb. CO}_2}{\text{Hr.}} \times \frac{300 \text{ BTU}^{(3)}}{\text{Lb. CO}_2} = 180 \text{ BTU/Hr}$$

If the canister were adiabatic, the atmospheric gas flow will increase in temperature by approximately 17°F.

$$Q = w c_p \Delta t$$

$$180 \text{ BTU/Hr.} = \frac{20 \text{ ft.}^3}{\text{Min.}} \times \frac{60 \text{ Min.}}{\text{Hr.}} \times \frac{0.04 \text{ Lb.}}{\text{Ft.}^3} \times \frac{0.23 \text{ BTU}}{\text{Lbs.}^{\circ}\text{F}} \times \Delta t$$

$$\therefore \Delta t = 16.3^{\circ}\text{F}$$

This is not a significant rise, however with a highly conductive and finned canister exterior, the temperature increase of the atmospheric gas flow may be decreased to approximately 10°F. The atmospheric gas flow is then drawn through a blower and passed through the heated second desiccant canister such that the water is removed from the desiccant bed and is returned to the cabin. The temperature rise of the atmospheric gas flow through the compressor aids the desorption process of the desiccant. A compressor(6) rated at 20 CFM against 4 inches head of water at 1/2 atmosphere pressure will reject on the order of 40 watts or 135 BTU/HR to the atmosphere flow for a temperature rise of approximately 13°F through the compressor.

$$Q = W c_p \Delta t$$

$$135 \text{ BTU/HR} = \frac{20 \text{ Ft.}^3}{\text{Min.}} \times \frac{60 \text{ Min.}}{\text{Hr.}} \times \frac{0.04 \text{ Lb.}}{\text{Ft.}^3} \times \frac{0.23 \text{ BTU}}{\text{Lbs.}^{\circ}\text{F}} \times \Delta t$$

$$\Delta t = 12.2^{\circ}\text{F}$$

To effectively desorb the desiccant to a low residual water content, the bed is brought to a temperature of 250°F (considering 1/2 atmosphere) as shown in Figure 4-3. The 250°F gas flow effectively has an infinite water vapor capacity at 29.825 psia saturation. Consequently, a logarithmic decrease in desiccant water content is assumed with a mean desorption level at 8 percent. The higher the temperature of the heat source, not to exceed 600°F, the faster the desorption rate. Approximately 4168 BTU/HR is required to raise the atmospheric gas flow temperature and the desiccant bed temperature and to heat the bed for desorption.

*Boeing⁽²⁾ utilized type 4A sieve for their system however Linde⁽⁴⁾ recommends type 5A sieve. Since the adsorption characteristics are similar, the Linde recommendation was followed.

**Note that the CO₂ adsorption rate was rounded to 0.6 Lb/hr.

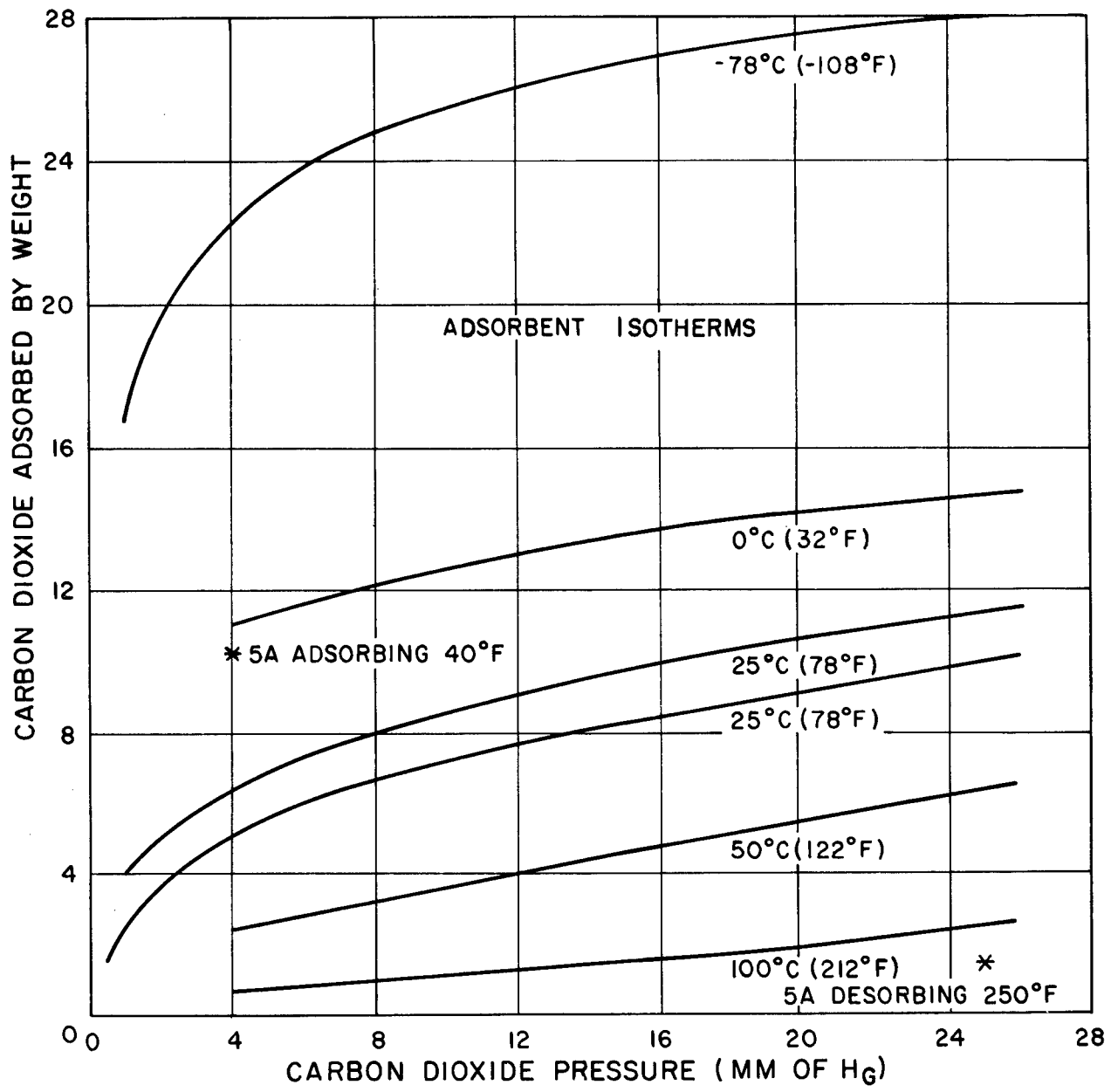


Figure 4-4. Carbon Dioxide Adsorbent Characteristics

Atmosphere

$$Q = \frac{20 \text{ ft.}^3}{\text{Min.}} \times \frac{60 \text{ Min.}}{\text{Hr.}} \times \frac{0.04 \text{ Lb.}}{\text{Ft.}^3} \times \frac{0.23 \text{ BTU}^{(5)}}{\text{Lbs.}^{\circ}\text{F}}$$

$$\times 180^{\circ}\text{F} = 1988 \text{ BTU/HR}$$

13X Sieve (Assumed canister size of 20 pounds)

$$Q = 20 \text{ Lbs.} \times \frac{0.25 \text{ BTU}^{(3)}}{\text{Lbs.}^{\circ}\text{F}} \times 180^{\circ}\text{F} = 900 \text{ BTU/HR}$$

Desorption

$$Q = \frac{0.71 \text{ Lb. Water}}{\text{Hr.}} \times \frac{1800 \text{ BTU}^{(7)}}{\text{Lb. Water}} = 1280 \text{ BTU/HR}$$

$$\text{TOTAL} \quad 4168 \text{ BTU/HR}$$

While the two desiccant canisters are alternately adsorbing and desorbing water vapor, the two carbon dioxide removal canisters are also alternately adsorbing and desorbing carbon dioxide. Desorbing of the carbon dioxide from molecular sieves is normally accomplished by merely venting the room temperature sieve to low pressure spatial vacuum. However, since the carbon dioxide is to be recovered, a gas pump is utilized to provide a low pressure and heating is required to separate the carbon dioxide from the sieve. The gas pump will maintain the carbon dioxide partial pressure at 25 mm Hg, consequently the sieve will desorb to approximately 1 percent as shown in Figure 4-4. The carbon dioxide recovered from the sieve is then pumped to the Sabatier Reactor. Heating the sieve to 250° F will desorb sufficient carbon dioxide to provide an efficient system and will require an influx of approximately 2180 BTU/HR. The higher the heat source temperature, up to approximately 600° F, the faster the desorption rate. Also the high temperature desorption may eliminate the need for gas pumping since a sufficiently high desorption gas pressure may be obtained by the high temperature to supply the carbon dioxide to the Sabatier Reactor.

Sieve (Assumed canister size of 40 pounds)

$$Q = 40 \text{ lbs.} \times \frac{0.25 \text{ BTU}^{(3)}}{\text{Lb.}^{\circ}\text{F}} \times 200^{\circ}\text{F} = 2000 \text{ BTU/HR}$$

Desorption

$$Q = \frac{0.6 \text{ lb. CO}_2}{\text{Hr.}} \times \frac{300 \text{ BTU}^{(3)}}{\text{Lb. CO}_2} = 180 \text{ BTU/HR}$$

$$\text{TOTAL} \quad 2180 \text{ BTU/HR}$$

There are several problem areas associated with an adsorption type carbon dioxide collection system. First the desiccant adsorbs carbon dioxide as well as water. Consequently, as the desiccant becomes saturated with water vapor, the carbon dioxide is displaced such that the carbon dioxide flow rate to the adsorbing canister will be greater than that contained in the inlet atmospheric gas flow. Secondly, some of the carbon dioxide remains entrained in the desiccant and is vented to the cabin during desiccant regeneration. Consequently, the overall system efficiency is decreased.

Thirdly, there may be a gradual build-up of water vapor concentration in the type 5A sieve used for carbon dioxide adsorption. Since this sieve is regenerated by heating the canister to 250°F and subjecting it to 25 mm Hg absolute pressure, the entrained water vapor may not be removed. Consequently, the sieve will be "poisoned" such that carbon dioxide adsorption will be greatly reduced.

This situation may be remedied by periodically heating the sieve to 600°F and removing the evolved gas.

4.3.1.4 Alternate Adsorption System

The MRD Division of the General American Transport Corporation is presently developing (under NASA contract) a non-moisture sensitive carbon dioxide adsorber which is regenerable. This will greatly decrease the complexity of carbon dioxide collection by eliminating the need for desiccant canisters and associated equipment. However, sufficient data had not been released to evaluate this carbon dioxide adsorption material in this study.

4.3.1.5 Alternate Collection System

4.3.1.5.1 Permeable Membranes

Permeable selective membranes which permit carbon dioxide to pass through at a faster rate than some other gases are a well known method for increasing carbon dioxide concentration and for separation of carbon dioxide from the cabin atmosphere. Conceivably a cascade series of these membranes will facilitate sufficient concentration of carbon dioxide gas for injection into the Sabatier Reaction. However, permeation rates for water vapor are of the same order of magnitude or greater than carbon dioxide for several polymeric films. Consequently, water vapor/carbon dioxide separation is again a problem in this concept, which requires further research and development of system requirements and operational parameters.

4.3.1.5.2 Freeze-Out

In vehicles where cryogenic heat sinks are available a freeze-out method of carbon dioxide collection may be utilized. CO₂ freezes at -109°F at one atmosphere pressure. A higher temperature sink is used for initial water vapor separation. However, the MORL vehicle probably will not have a heat sink of the required size since long term storage of cryogenics is not optimized as yet. The heat of liquification of carbon dioxide is 246.6 BTU/LB. For the system requirements, approximately 144 BTU/HR for the carbon dioxide and approximately 710 BTU/HR for the water vapor would be rejected to the cryogenic heat sink. This

will vaporize approximately 9.3 pounds of cryogenic oxygen per hour. This is considerably larger than that required from storage since most of the oxygen is recovered for reuse. Also, a space radiator may be used to provide the low temperature heat sink. However, since the heat rejection rate is a function of the fourth power absolute temperature difference between the radiator and the spatial heat sink, a prohibitively large radiator size is required to provide low temperature heat sink.

4.3.1.5.3 Sabatier Reaction

The collected carbon dioxide is compressed into a storage and surge tank to provide a continuous metered flow to the Sabatier Reactor.

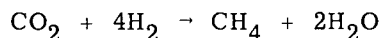
The Sabatier reaction mechanism takes place in two steps. First the carbon dioxide is hydrogenated to form carbon monoxide and water:



Secondly, the carbon monoxide is hydrogenated to form methane and water:



Combining the steps given the total reaction:



A thermodynamic analysis of the reaction shows it to be exothermic:

	HEAT OF FORMATION ⁽¹⁾		
	BTU/GRAM MOLE	NO. OF MOLES	TOTAL
Carbon Dioxide	(-373.0)	1	+373.0
Hydrogen	---	4	---
Methane	-71.0	1	-71.0
Water (Gaseous)	-229.2	2	<u>-458.4</u>
		TOTAL	-156.4

Therefore, for each gram mole of carbon dioxide consumed in the reactor, 156.4 BTU/HR are evolved or 1610 BTU/LB. of CO₂. Thus for a continuously operating reactor processing 0.6 pound of CO₂ per hour, approximately 1000 BTU/HR must be removed from the reactor.

$$\frac{1610 \text{ BTU}}{\text{Lb. CO}_2} \times \frac{0.6 \text{ Lb. CO}_2}{\text{Hr.}} = 966 \text{ BTU/HR.}$$

The reaction will take place at approximately 15 psia in the presence of a catalyst. The catalyst material and reaction chamber temperature are critical. A nickel catalyst at a 550° F chamber temperature has proven to have good operational parameters for the reaction, however, others are listed below:⁽³⁾

CATALYST	TEMPERATURE	RESULTS
Ruthenium	302° F	Complete reaction
Thoria Promoted Nickel	650-670° F	Complete reaction
Nickel on Kieselguhr	650° F	70% conversion
Nickel on Kieselguhr	230° F	Not given
Nickel on Gamma Alumina	---	Less active than on Kieselguhr

The weight of nickel catalyst required for the reaction is a function of operating temperature and carbon dioxide flow rate. For the previously described system approximately 1.72 pounds of catalyst are required. Also the catalyst is consumed at a rate of approximately 0.027 pound per day, consequently a method of replacing the catalyst or a large catalyst bed must be provided for extended missions. The resulting heated gases (methane and water) which exit from the reaction can be in heat exchanger contact with the cooler incoming carbon dioxide. Consequently, heat is exchanged and the reaction is self-supporting.

Initial start-up of the system requires a heater to boost the incoming gas temperature to begin the reaction. See Figure 4-6 for a block diagram. The methane and water gases are separated by condensation of the water. Each compound is then ready for further processing, electrolysis of water and pyrolyzation of methane. However, one problem with the separation process must be brought to light at this point. A small amount of methane will dissolve in the liquid water which may contaminate the water electrolysis unit or eventually contaminate the cabin atmosphere. By comparing the gram molecular weights of the two gases, the partial pressure of the methane may be determined for one atmosphere total pressure:

$$\frac{\text{one mole methane}}{\text{one mole methane} + \text{two moles water}} = \frac{1}{3} \times 1 \text{ atm.} = 0.33 \text{ atm. methane partial pressure}$$

At 50° F, the assumed water condensing temperature, the solubility proportionality constant is 2.97×10^4 atm. of solute pressure per unit concentration. (1)

$$\text{Thus, } \frac{0.33 \text{ atm. CH}_4}{2.97 \times 10^4 \text{ atm. CH}_4} \times \frac{0.0000111 \text{ mole CH}_4}{\text{mole H}_2\text{O}} = X$$

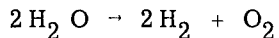
$$\text{Thus, by } \frac{X}{1-X} \frac{\text{M. W. CH}_4}{\text{M. W. H}_2\text{O}} = \frac{\text{Lbs. CH}_4}{\text{Lbs. H}_2\text{O}} \quad (1)$$

$$\frac{0.0000111}{1-0.0000111} \times \frac{16}{18} = 0.00001 \text{ lb. CH}_4 \text{ dissolved}$$

in each pound of water. Obviously this is a small amount for consideration as a cabin contaminant since methods of methane removal from human flatus must already be present in the cabin contaminant management system. However, the contamination of the electrolysis cell membrane may prove to be a serious problem which merits further investigation. Also liquid-gas contaminant separation requires additional study.

4.3.1.5.4 Water Electrolysis

Water electrolysis may be accomplished by a reverse fuel-cell process currently under development by General Electric for an oxygen recovery system (Bosch type).



The heat of dissociation of liquid water into gaseous hydrogen and oxygen is endothermic and amounts to 271.5 BTU/gram mole (liquid). ⁽¹⁾ The 6.2 gram moles of carbon dioxide which enters the Sabatier reactor per hour produce 12.4 gram moles or approximately 0.5 pound of water per hour. The electrolysis cell will thus theoretically consume 271.5 BTU/gram mole x 12.4 gram moles/hr. or 3365 BTU/HR or nearly 1 kilowatt of electrical power. Only electrical power may be utilized for this process. The electrolysis unit is further exemplified by the relationship between the standard free energy ΔF , standard heat of reaction ΔH (given above) and a term $T \Delta S$ representing the irreversibility of the system.

$$\Delta F = \Delta H - T \Delta S \quad \text{where } T = \text{absolute temperature}$$
$$\Delta S = \text{standard entropy change}$$

For the reversible, isothermal dissociation of water, the $T \Delta S$ term represents a potential cooling capacity. However, in practice, the electrolysis cell losses more than cancel this cooling effect.

The GE-MSD ion-exchange membrane type electrolysis cell unit operating at 1.75 volts per cell will dissociate 0.5 pounds of water per hour at an expenditure of approximately 1000 watts of electrical power (ΔH). The free energy of reaction (ΔF) will be approximately 1190 watts, thus the difference ($T \Delta S$) of 190 watts (645 BTU/HR) is the amount of cooling required.

A functional schematic of a single electrolysis cell is shown in Figure 4-5. A multi-cell stack of the cells will be required to provide the desired flow characteristics. The water supplied from the condenser is stored in an accumulator with a liquid electrolyte (sulfuric acid). The resulting solution is maintained in the chamber between two membrane electrodes. When electrical power is applied to the ion-exchange membrane, the water in solution is dissociated such that oxygen ions collect at the positive membrane/electrode and hydrogen ions collect at the negative membrane/electrode. The pure gases are thus formed on the far side of the membrane where the oxygen is vented to the cabin atmosphere and the hydrogen is returned to the Sabatier reactor. The electrolyte does not permeate the membrane or enter into a dissociation, thus the concentration is not affected.

The most important characteristics of the electrolysis unit are its high efficiency and the inherent capability to separate the gases from the liquid even in zero gravity. Of the 0.5 pound of water dissociated, approximately 0.44 pound of oxygen and 0.06 pound of hydrogen are produced per hour.

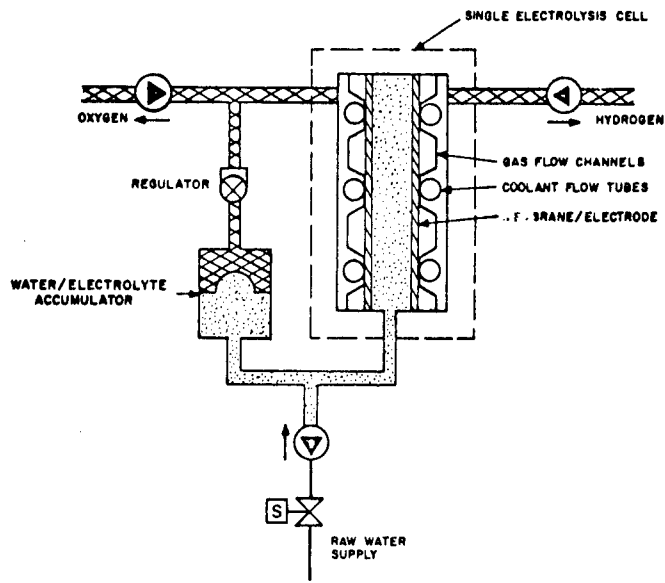
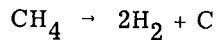


Figure 4-5. Functional Schematic of a Single Electrolysis Cell

4.3.1.5.5 Catalytic Pyrolyzation of Methane

The methane that is separated from the water vapor after the Sabatier reaction must be decomposed to recover sufficient hydrogen to close the cycle. The carbon is stored or jettisoned to space.



This is the most difficult process in the oxygen recovery system. Consequently, the penalties of recovering the hydrogen versus merely jettisoning the methane must be traded off for various mission lengths. Jettisoning of the methane would require storage of 0.06 pound of hydrogen (same as recovered from water) for each hour of operation of the Sabatier Reactor. This amounts to 1.44 pounds per day or approximately 526 pounds per year. An alternate approach is discussed later in this section.

The main problems ⁽⁸⁾ with the pyrolyzation of methane are the high temperatures of operation ($1800-2200^{\circ}\text{F}$ without a catalyst and $1500-1800^{\circ}\text{F}$ with a catalyst), and the removal of the carbon from the reactor and from the catalyst if used. The higher reactor temperature presents a problem of construction materials. Scraping or an equivalent method is required to remove the hard carbon scales from the walls. This amounts to 0.1635 pound of carbon produced per hour or 1432 pounds per year. Similar problems are encountered when a catalyst is utilized since the carbon inactivates the catalyst by reducing surface area or possibly even combining with the catalytic material. Consequently, the catalyst must periodically be replaced.

The heat of dissociation of methane is endothermic 71 BTU/mole⁽¹⁾ or 2010 BTU/LB. This amounts to 440 BTU/HR for the process flow rate of 6.2 moles per hour.

Alternate

An alternate approach is to pass the methane through a high energy plasma arc similar to that developed by General Electric⁽⁹⁾ for the reduction of carbon dioxide. The electric arc causes two reactions:

1. $\text{CH}_4 \rightarrow \text{C} + 2\text{H}_2$
2. $\text{CH}_4 \rightarrow \frac{1}{2} \text{C}_2 \text{H}_2 + \frac{1}{2} \text{H}_2$

The first reaction produces a light and fluffy carbon deposit which is more easily removed.

In the second reaction, the acetylene and hydrogen are separated by a heated palladium-silver membrane and then the acetylene is jettisoned. As a result 3/4 of the hydrogen is recovered for reuse in the Sabatier reactor.

Further catalytic pyrolyzation of the acetylene will produce carbon and hydrogen with all the carbon removal problems previously mentioned in preceding paragraphs.

Total System

The four integrated phases of the total system for oxygen recovery from carbon dioxide are illustrated in Figure 4-6 along with the cabin environmental control system.

4.3.2 WATER RECOVERY FROM URINE BY DISTILLATION AND PYROLYSIS

4.3.2.1 Summary

Potable water recovery from urine by distillation and pyrolysis is a proven method of obtaining high quality water. The method utilizes both endothermic and exothermic processes; however, since the study is concerned only with utilization of waste thermal energy, only the endothermic processes are listed in the following summary. Note the figures are for a six man crew and that system thermal losses are not computed except for the Pyrolysis Unit.

ITEM	OPERATING TEMPERATURE RANGE	ENDOTHERMIC POWER REQUIREMENT
Evaporator	100-120°F	243 Watts
Pyrolysis	1800°F	60 Watts
TOTAL		303 Watts

4.3.2.2 Introduction

The recovery of potable water from urine represents one of the major methods of reducing storage material which thus reduces vehicle launch weight and resupply logistics. A possible daily water balance for each crew member is given in Figure 4-7. Considering that all the respiration and perspiration water collected by the vehicle environmental control system is recovered, an additional source of 2.0 pounds of water per man day must

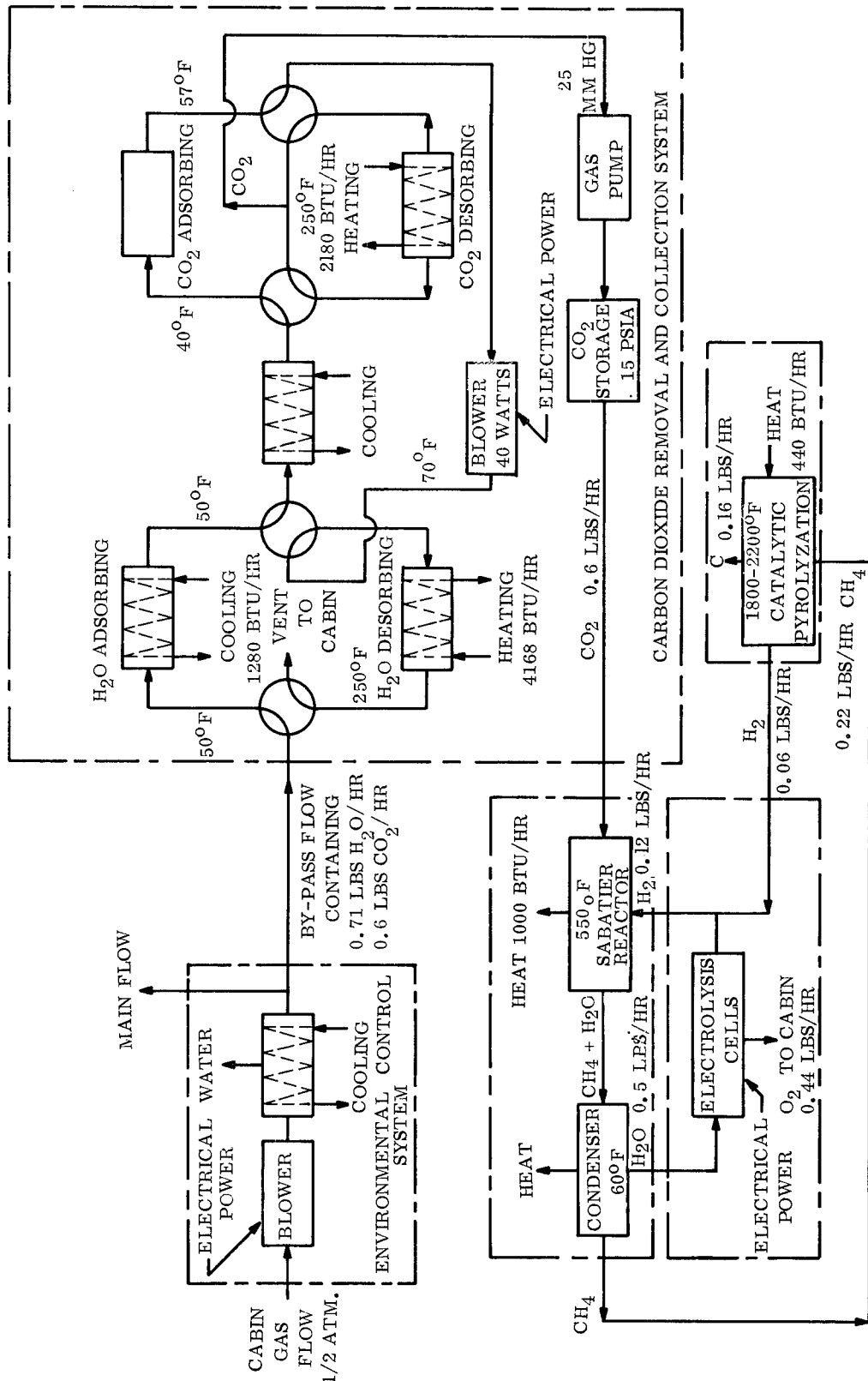


Figure 4-6. Total System for Oxygen Recovery from Carbon Dioxide (six-man system)

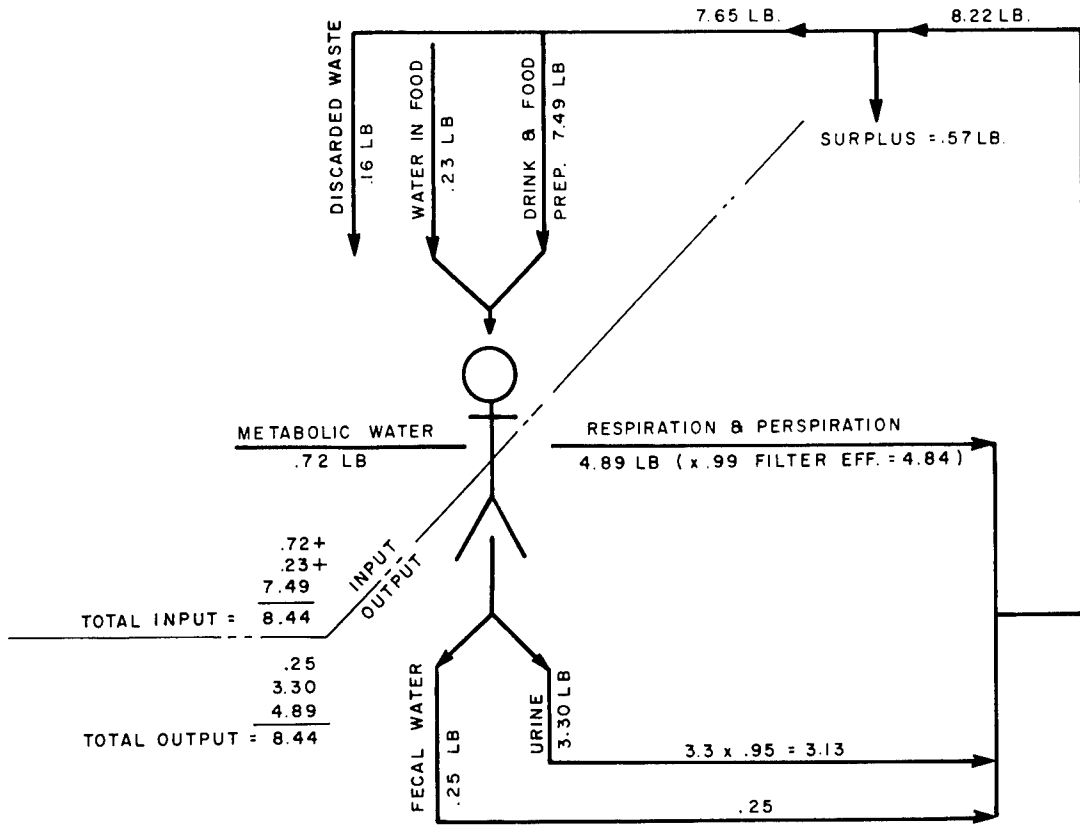


Figure 4-7. Daily Water Balance

be supplied for drinking and food preparation. This would amount to 4380 pounds of water for a 6 man-one year mission if the requirement were to be fulfilled from a stored source. Obviously, the launch weight and resupply logistics for this type of an open system cannot be tolerated.

4.3.2.3 System Description

The 3.3 pounds of water in the urine represents a source of potable water which along with the recovered respiration and perspiration water will more than fulfill the needs for drinking and food preparation water. In fact an excess of water is shown (see Figure 4-7.) since the water stored in the food adds to the system balance and the metabolic water produced by the men more than equals the water losses in waste solids, cabin leakage and system vacuum vents.

Vacuum distillation and pyrolysis has proven to be an efficient and reliable method of recovering high quality potable water from urine.

The quality of the water utilized for drinking and food preparation is of prime importance since the same water may be ingested several hundred times during the mission.

The high quality of the water reclaimed by the pyrolysis process is shown in Table 4-1. This water was recovered from a month old fecal-urine slurry accumulation as part of the Hydro-John* program and was analyzed by an independent laboratory. The points analyzed were adjudged to be well within the chemical standards established by the U.S. Public Health Service. Also bacteriological tests for members of the Coliform Group and Streptococcus were negative.

TABLE 4-1. WATER ANALYSIS OF PYROLYZEDWATER
FROM METABOLIC WASTES†

Ammonia as N, ppm	2.0
Phenolphthalein	
Alkalinity as CaCO_3 , ppm	0.0
Methyl Orange	
Alkalinity as CaCO_3 , ppm	6.0
pH	6.7
Specific Conductance	17.0
Micromhos @ 18C	
Specific Conductance	2.5
Micromhos @ 18C (corrected)	
Nitrite as N, ppm	0.19
Nitrate as N, ppm	0.0
Odor	None
Phenol, ppb	0.0

The distillation and pyrolysis system requires no chemical additives or filtering processes (and thus has few expendables) as illustrated in Figure 4-3. Therefore for a given crew size, the system weight penalty for water reclamation does not increase appreciably as the mission length increases.

Urine is added to an evaporator either directly from the source or from an intermediate storage container. The 21 pounds of urine per day will contain approximately 20 pounds of water.

After an initial batch of waste liquid enters the evaporator, the internal pressure of the evaporator is reduced to approximately 1.7 psia and sufficient thermal energy is transferred to the liquid from a hot fluid heat transport medium (waste heat) source to cause boiling at approximately 120°F. An average boiling rate of 0.80 pounds of water per hour will require approximately 830 BTU/HR waste heat transferred to the evaporator. The water vapor is then passed through a vapor pyrolysis unit which heats the vapor to 1800°F

*A waste management system developed by General Electric for NASA.

†Betz Laboratories, Inc., April 20, 1964, sample standards established by the United States Public Health Service.

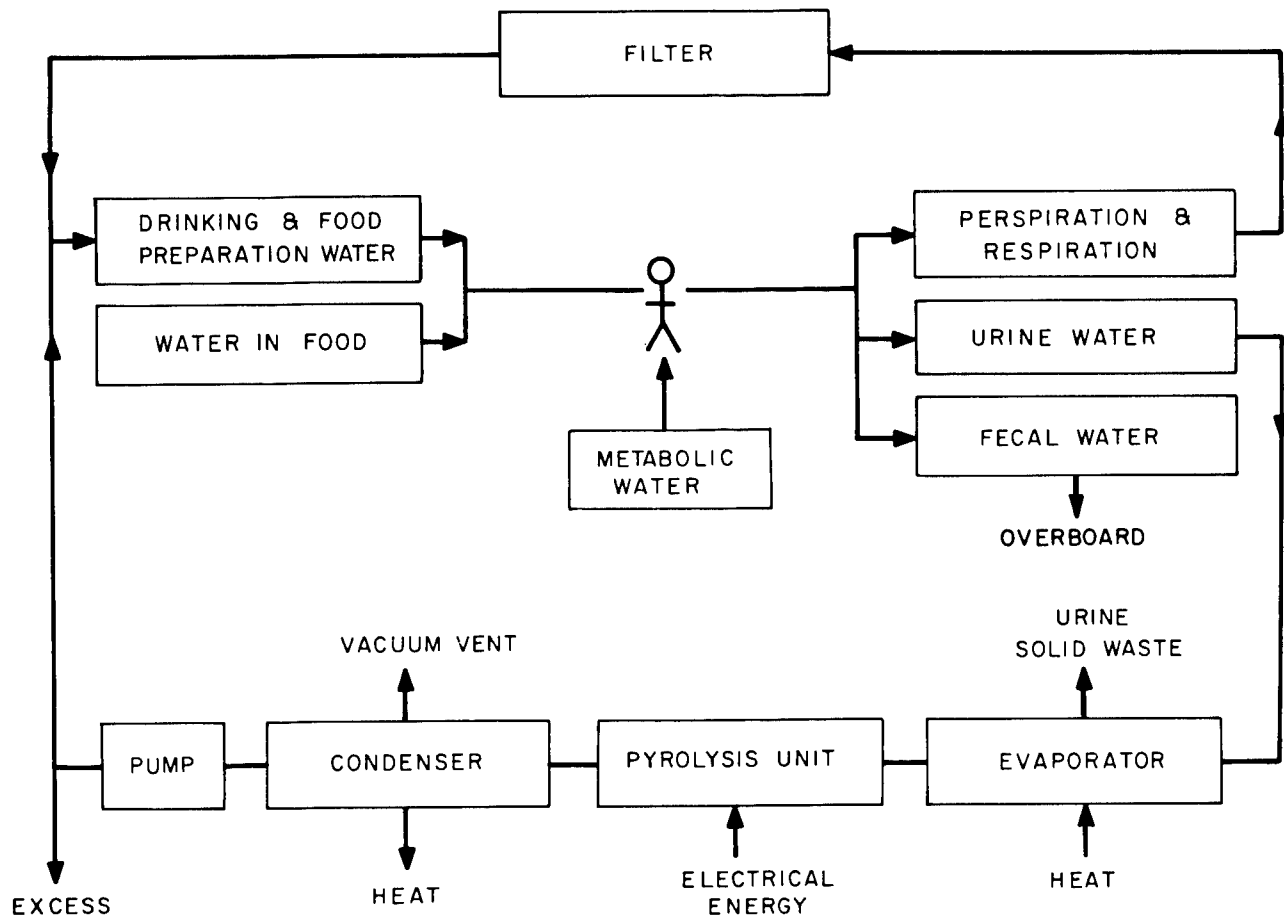


Figure 4-8. Closed-Loop Human Waste Water Process

and oxidizes the water vapor impurities in the presence of a catalyst. The oxygen which combines with the impurities is bled into the evaporator at a rate of approximately 6 atmospheric cubic centimeters per minute. The pyrolysis unit contains a counterflow heat exchanger and is jacketed with superinsulation to minimize heat losses.

Consequently, the overall energy requirements for the pyrolysis process is 80 watt-hours per pound of water recovered or 60 watts continuous. The pyrolyzed vapor is then liquified in a condenser while the gaseous non-condensables (impurities) are vented to space vacuum. A cold fluid liquid heat transport medium provides the sink to remove approximately 830 BTU/HR for condensation. A pump periodically removes the potable condensate to storage.

The only expendables of the system are the gases lost through the vacuum vent pressure control.

The oxygen (6 atm cc/min) supplied for catalytic oxidization of impurities in the pyrolysis unit will be vented through the condenser and lost to space vacuum. This will amount to 10 pounds for a one year mission.

$$\frac{6 \text{ cc}}{\text{min.}} \times \frac{525,000 \text{ min.}}{\text{mission}} \times \frac{\text{ft.}^3}{28,300 \text{ cc}} \times \frac{0.09 \text{ lbs.}}{\text{ft.}^3} = \frac{10.0 \text{ lbs.}}{\text{mission}}$$

The vented gases are also saturated with water vapor at a specific volume of $1205.7 \text{ ft.}^3/\text{lb}$. The oxygen will expand $\frac{14.7}{0.26} = 56.6$ times to give 56.6×6 or 339.6 cc/min vented gas at the low condenser pressure. Therefore, only 5.22 pounds of water are lost to spatial vacuum during normal venting in one year mission.

$$\frac{339.6 \text{ cc}}{\text{min.}} \times \frac{525,000 \text{ min.}}{\text{mission}} \times \frac{\text{ft.}^3}{28,300 \text{ cc}} \times \frac{\text{lb.}}{1206.7 \text{ ft.}^3} = \frac{5.22 \text{ lbs.}}{\text{mission}}$$

Also the residual gas used from the evaporator's solids expulsion mechanism is lost to space at each mechanism actuation. However, since this occurs only once a day the losses will be only 1.9 pounds of atmosphere gas for a one year mission. Calculated for an evaporator free volume of 200 in.³ at 0.5 atmosphere pressure and one actuation per day:

$$\frac{200 \text{ in.}^3}{\text{cleaning}} \times \frac{\text{ft.}^3}{1728 \text{ in.}^3} \times \frac{365 \text{ cleanings}}{\text{mission}} \times \frac{0.09 \text{ lbs.}}{\text{atmosphere}} \times \frac{\text{atmosphere}}{2} = \frac{1.9 \text{ lbs.}}{\text{mission}}$$

4.3.3 WASTE WATER RECOVERY BY DISTILLATION

4.3.3.1 Summary

Water recovery from waste water by distillation provides a non-potable water source which is of sufficient purity for washing. The described system utilizes both endothermic and exothermic processes; however, since this report deals with only utilization of waste

thermal energy, only the endothermic process is listed in the following summary. Note the figures are for a six man crew, and that system thermal losses are not computed.

ITEM	OPERATING TEMPERATURE RANGE	ENDOTHERMIC POWER REQUIREMENTS
Evaporator	100-120°F	442 Watts

4.3.3.2 Introduction

Waste water is considered to be the water which has been used to cleanse the bodies of the crew members (showers, washing , etc.), washing of clothing and eating utensiles and food preparation surface areas. The resulting liquid will contain many of the impurities commonly found in urine, although at decreased concentrations. Table 4-2 enumerates the impurities commonly found in wash water and urine. It is considered that benzalkonium chloride, a washing compound, will be mixed with the water prior to use.

An assumed break-down of the water required is given below:

WASH WATER REQUIREMENTS

Hand and face washing	1 lb/man day
Showering	3 lbs/man day accumulated over 3 days
Eating utensils cleansing	1 lb/man day
Washing of clothing	1 lb/man day accumulated over 6 days
TOTAL	6 lbs/man day

Based on the above table the men will shower once every three days and will wash their clothing once every 6 days. These water requirements may be reduced by the use of wash-dry cleansing pads and expendable clothing. However, since a system must be provided for the recovery of shower water, no appreciable advantage is seen by the use of expendable cleansing pads and clothing. Also, the weight of expendable clothing is quite high over a year long mission (see Table 4-3).

4.3.3.3 System Description

The system for distillation of waste water is very similar to the system utilized for distillation and pyrolysis of urine except pyrolyzation of the vapor may not be required. The solids in the wash water are separated from the liquid when the liquid is evaporated. However, as shown in Table 4-2, the waste wash water contains many of the impurities found in urine, consequently, the impurities which evaporate with the water and dissolve in the recovered water may accumulate over a long period to an intolerable level. Thus pre or post treatment of the liquid may be required or a portion or all the distilled waste water vapor may be pyrolyzed. Commensurate with the philosophy of maintaining expendable materials to a minimum and obtaining optimum utilization of equipment already existing in the system, the pyrolysis unit of the water recovery unit is utilized to maintain the wash water at an acceptable purity level by purifying only a small portion of the vapor flow.

Also the wash water is distilled at reduced pressures and 100-120°F temperatures to minimize volatile gas generation such as ammonia and organics. The system is thus illustrated in Figure 4-9.

TABLE 4-2. CHEMICAL COMPOSITION OF URINE AND WASH WATER

	URINE EXCRETION GRAMS/MAN-DAY	WASH WATER GRAMS/MAN-DAY
Solids	60.0	---
Urea	30.0	0.350
Hippuric acid	0.7	---
Uric acid	0.7	0.007
Creatinine	1.2	0.020
Indican (idoxyl potassium sulfate)	0.01	---
Oxalic acid	0.02	---
Allantoin	0.04	---
Amino-acid nitrogen	0.2	0.034
Purine basis	0.01	---
Phenols	0.2	---
Chlorine as NaCl	12.0	0.800
Sodium	4.0	0.800
Potassium	2.0	0.300
Calcium	0.2	0.010
Magnesium	0.15	0.001
Sulfur, total as S	1.0	---
Inorganic Sulfate as S	0.8	---
Neutral Sulfur as S	0.12	---
Conjugated Sulfates as S	0.08	---
Phosphate as P	1.1	---
Ammonia	0.7	---
Free fatty acids	--	0.420
Cholesterol	--	0.075
Squalene and paraffins	--	0.019
Triglycerides	--	0.050
Waxes	--	0.022
Lactic acid	--	0.250
Glucose	--	0.050
Benzalkonium chloride (washing compound)	--	0.566

TABLE 4-3. WEIGHT OF EXPENDABLE CLOTHING⁽¹⁾

ITEM	WEIGHT	ITEMS REQ'D. PER MISSION	TOTAL ITEM WEIGHT (LBS.)
Shirt	0.22	104	22.88
Trousers	0.59	104	61.36
Shorts	0.15	104	15.60
Socks	0.04	104	4.16
Cap	0.04	52	2.08
Shoes (Pair)	0.55	12	6.60
		TOTAL WEIGHT	112.68 LBS.

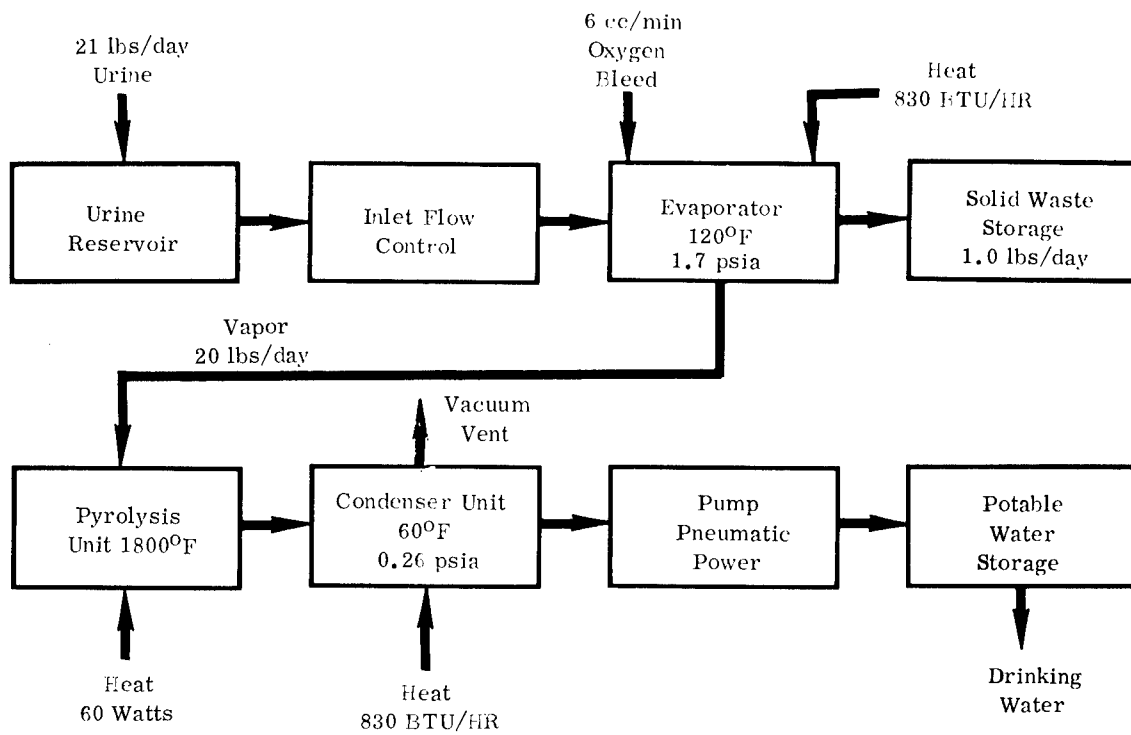


Figure 4-9. System Block Diagram

The waste water is added to the evaporator either directly from the source or from an intermediate storage container. The approximately 36 pounds of wash water which enter the system per day contains from 0.25 to 1% solids. After the initial batch of waste liquid enters the evaporator, the internal pressure of the evaporator is reduced to 1.7 psia and sufficient thermal energy is transferred to the liquid from a hot fluid heat transport medium (waste heat) source to cause boiling at 120°F . An average boiling rate of 1.5 pounds of water per hour requires approximately 1500 BTU/HR waste heat transferred to the evaporator. The waste solid residue is periodically expelled from the evaporator to maintain a high heat transfer coefficient or the evaporator heat exchange surface. The water vapor flow from the evaporator is divided such that a small amount is diverted to the pyrolysis unit of the urine - water recovery system. See Section 4.3. for details of the pyrolysis process. The major portion of the vapor flow is liquified in a condenser. A cold fluid heat transport medium provides the heat sink to remove approximately 1500 BTU/HR for condensation. A pump periodically removes the condensate to the wash water storage vessel where it is mixed with the small diverted liquid flow from the potable water recovery system. The purity of the stored wash water is thus determined by the amount of water by-passed to and purified by the pyrolysis unit, and then returned to wash water storage. Experimental data will establish the desired wash water purity, and thus the required by-pass flow rate; however, this will not significantly affect the total endothermic power requirements.

4.3.4 SOLID WASTE MANAGEMENT

4.3.4.1 Summary

Solid waste management is provided for fecal as well as all other waste materials. The described system utilized both endothermic and exothermic processes; however, since this report deals only with utilization of waste thermal energy, only the endothermic processes are listed in the following summary. Note the figures are for a six man crew and that system thermal losses are not computed.

These endothermic power requirements are as follows:

<u>ITEM</u>	<u>TEMPERATURE</u>	<u>ENDOTHERMIC POWER</u>
Evaporator	120°F	1000 BTU/HR (294 watts)
Sludge Dehydration	100-200°F	50 BTU/HR (14.7 watts)
Waste Disinfection	250°F	40 BTU/HR (12 watts)

4.3.4.2 Introduction

One of the most difficult problems of extended mission space flights is the management of waste solids. Included in this category are human excreta, food container refuse, urine solids, waste water solids, worn-out clothing, hair clippings, skin tissue, toe and finger-nail clippings, waste paper, hand tissues, expended air filters, etc. In obeisance to the philosophy of non-contamination of space, the vehicle must then become a veritable garbage truck in the collection and storage of the solid waste product.

The "state of the art" has not progressed sufficiently to utilize solid waste products to close the ecological cycle of the man in space.

4.3.4.3 System Description

Human excreta is of prime concern because of the high concentration of bacteria found in feces. Consequently, the fecal solid waste management must be completely sanitary in the manner of collection, transportation, and storage. Also the system must be psychologically acceptable to the crew over the entire mission duration.

Three basic methods are available for collection and transportation of the fecal stool:

1. Collect the stool in a plastic bag and hand carry the bag to a storage area.
2. Liquefy the stool with heat and pump the resulting slurry to storage.
3. Mix the stool with water and pump the resulting slurry to storage. (This method was utilized in Project Hydro-John, a complete waste management system developed by GE for NASA.)

The bag technique has a definite psychological disadvantage of handling the bagged feces, and the liquefaction by heat still requires a weight penalty for water to sanitize and clean the heating areas and pump. Mixing of the stool with water provides self-cleaning features

plus the fact that the water may be initially utilized to cleanse the rectal area after defecation. The use of toilet tissue is eliminated. The water utilized for flushing and cleansing is separated from the solid waste by distillation and is condensed for re-use as flush water. The solid sludge is periodically removed from the evaporator, thus minimizing the production of ammonia and organic gases. The solid wastes are stored in large porous bags and are vacuum dried to inhibit bacterial growth. Also a small amount of ammonia is generated in the fecal slurry and is dissolved in the condensed water. This ammonia is sufficient to sanitize the unit during flushing but is of sufficiently low concentration so as not to irritate the human skin.

Approximately 0.25 pounds of feces is excreted per man day and approximately 4 pounds of water per flush is required to cleanse the rectal area and to sanitize the unit. A possible fecal solid waste management system is shown in Figure 4-10.

The excreted stool is blended with 4 pounds of water and is pumped to the evaporator. The pressure of the evaporator is lowered to approximately 1.7 psia and sufficient thermal energy is transferred from a waste heat source to boil the water at 120°F. Low temperature boiling minimizes the volatile gases generated during the distillation process and thus maintains a higher purity level in the condensate. Approximately 1000 BTU/HR or 294 watts of waste heat is required by this process which vaporizes approximately 1 pound of water per hour. A small portion of the vapor flow is by-passed through the pyrolysis unit of the water recovery from the urine system while the major portion is liquefied in a condenser. The by-pass flow is thus purified of ammonia and organics and utilized to dilute the flush water to an acceptable purity level in the storage reservoir. In this manner pre or post treatment of the flush water is eliminated and expendable filters are not required. The condenser heat sink is a liquid heat transport medium which removes approximately 1000 BTU/HR or 294 watts to condense the water vapor. A small amount of ammonia and organics are also carried over to the condensate. The ammonia acts as a disinfectant such that the flush water also sanitizes the system.

The evaporator and heat exchanger surface is periodically cleaned when the fecal sludge is expelled. This assures a high heat transfer coefficient throughout the mission duration. The expelled fecal sludge is forced into a porous bag and the bag is subjected to low pressure and heating from a radiative waste heat source to cause drying. The 1.5 lbs. of fecal sludge collected per day contains approximately 1.2 lbs. of water. As shown in Figure 4-7, there is an excess of water in the system. This excess is produced by men at a rate of 4.2 pounds per day and is contained in the food at a rate of 3.0 pounds per day. Thus, even if the 1.2 pounds of fecal water is jettisoned to space, 6.0 pounds of excess water is produced per day. This excess will more than make up for system inefficiencies and losses due to cabin leakage.

The entrained water is removed from the fecal sludge by heating at a rate of 50 BTU/HR or 14.7 watts. The sludge is thus dried so that bacterial growth is inhibited. The 0.3 pound of dried feces will still have a volume approximately the same as the fecal sludge.

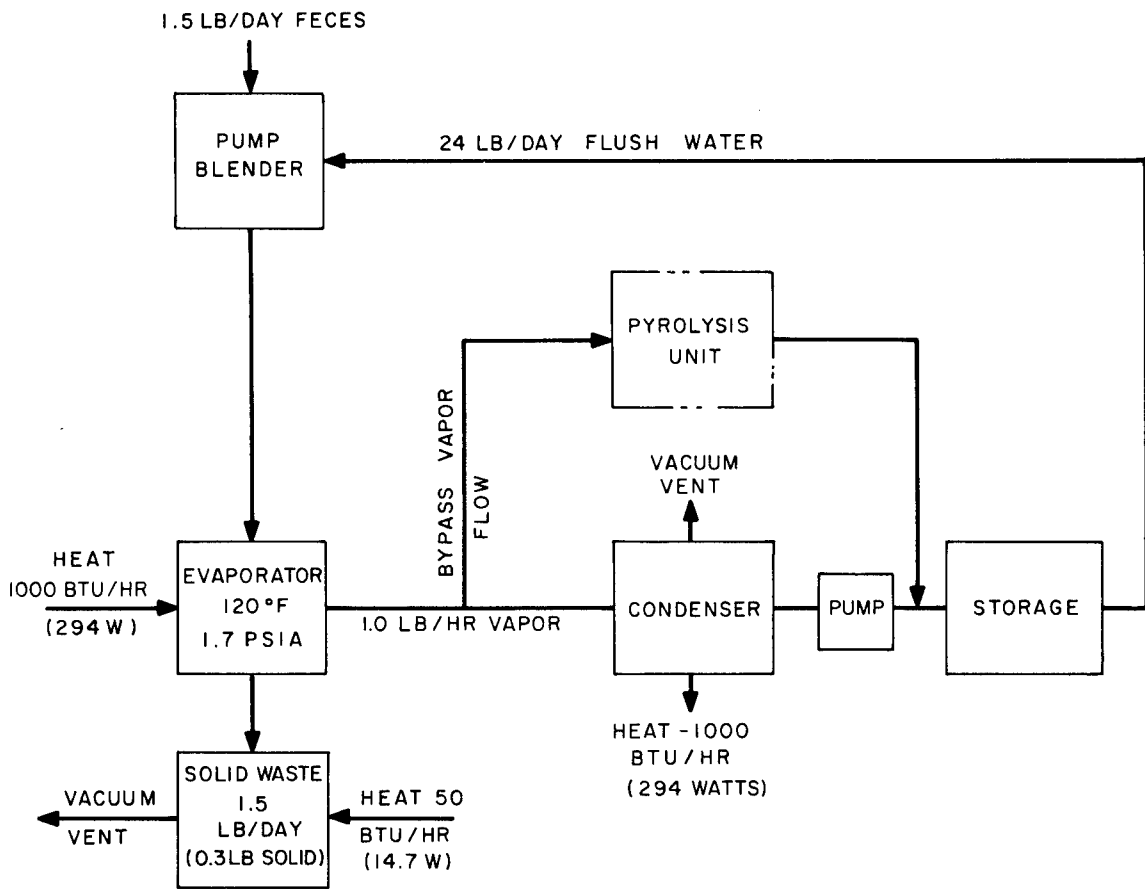


Figure 4-10. Fecal Solid Waste Management System

This amounts to nearly a 9 cubic foot volume per year. The dried feces may be compressed to the density of water, minimizing the storage volume to approximately 1.75 cubic foot per year.

4.3.4.4 Alternate Methods

An alternate method of fecal disposal is to incinerate the solid wastes and either store or jettison the ashes. However, this requires oxygen in an approximate amount equal to the weight of feces to be incinerated plus a high energy source to start the process. The recovery of the oxygen presents a problem of greater magnitude than oxygen recovery from carbon dioxide, consequently further discussion is not presented.

Microbial digestion of solid wastes is difficult to control in the small apparatus required for presently conceived space vehicles. Also oxygen is consumed in the digestion process, consequently the recovery of the oxygen is again a formidable problem. As space flight missions increase, microbial digestion of solid wastes will probably contribute to closing man's ecological cycle. However, a great deal of research is still required in this area.

Lyophilization or freeze distillation of the fecal sludge is accomplished by merely venting the sludge to a low pressure such that sensible heat is removed from the sludge to provide latent heat of vaporization. Consequently, the sludge freezes and bacterial growth is inhibited. The problem is then to store the frozen residue. If the frozen sludge is retained at the low pressure, the ice will sublime and the result will be much the same as the vacuum drying system previously described.

4.3.4.5 Other Solid Wastes Management Systems

Refuse disposal is a major problem of any manned space vehicle which cannot jettison refuse in order to avoid contamination of space. Since most of the refuse is thermoplastic material, it is expected that refusal will be heated to 250°F-300°F and molded into minimum volume for storage. Unavailability of sufficient data on the type and quantity of refusal material prevents any estimate of heat flow requirements for this purpose.

The urine solids and waste water solids are handled in a similar manner as fecal solids. Thus, they are vacuum dried and stored. It is considered that such items as skin tissue, hair clippings, toe and fingernail clippings are all part of waste water solids.

Such items as expended food containers, worn out clothing, waste paper, hand tissues, air filters, etc., will be compressed and bailed in a pneumatically operated press, disinfected, and sealed in plastic bags.

Disinfecting the materials is accomplished by heating them in excess of 250°F for several hours. This will also provide a minimum size bundle since most of the material will be thermoplastic, thus they will exude into most of the voids in the bail.

4.3.5 FOOD PREPARATION

4.3.5.1 Summary

Various diets have been proposed and laboratory tested for a life support system for Space Flight of extended time periods. Reconstituted dehydrated food, such as used in the General Electric 30 day 4-men simulated space mission of October, 1963, has been found to be acceptable both for its nutrient qualities and psychological factors of providing appealing and rewarding meals. Even though some fresh or frozen food may be used in future space flights, it has been assumed that all food is of the dehydrated type. The endothermic power requirements are as follows:

ITEM	OPERATING TEMPERATURE	AV. ENDOTHERMIC POWER REQ'T.
Food Preparation	180°F	90 BTU/HR.
Food Baking	175°F	30 BTU/HR.
Cleaning	170°F	83 BTU/HR.
Sterilization	250°-300°F	25 BTU/HR.

4.3.5.2 Introduction

Adequate nutrition must possess the quantity and quality of ingredients to maintain the body and mind of the human biological machine in its best operating conditions.

The essential nutrients in food, such as vitamins, aminoacids and minerals, can be supplied in the form of tablets, liquids, purees, etc., to satisfy the basic physical requirements. Special low residue diets have been studied to reduce some of the normal body functions, thus simplifying, at least apparently, the problem of supporting man's life during prolonged space flight. However, studies conducted at the General Electric Company and other major aerospace industry firms indicate that in addition to the nutritive qualities, food must be palatable, and equally important, it must look like real food. The importance of this requirement becomes more obvious when we consider the variety of unusual stresses imposed on men living in a space station, and the role of food as a reward in an otherwise routine environment.

Fresh or frozen food, although highly desirable, would pose enormous problems because of additional storage requirements, need for refrigeration equipment to prevent spoilage, and decreased payload capability. The problem is greatly minimized by the use of dehydrated food, in which the original water content has been reduced to less than 5%. Payload savings realized are at least 2.5 lb/man-day. The food itself when reconstituted with 180°F water recovers the texture, flavor, color and palatability of fresh food. Tests, such as the 30 day four-man simulated space flight conducted at General Electric MSD during October, 1963, showed that the dehydrated food was highly acceptable and rewarding.

4.3.5.3 Description

The average solid food requirements per man day has been set at approximately 4 pounds. Assuming that all food is of the dehydrated type, the four pounds would be made up from 1.0 lb. of dehydrated solid and 3.0 lbs. of hot water at 180°F. After absorption of the water, helped by kneading, the food must be held at 175°F for approximately five minutes. All food would be precooked and stored in expandable plastic containers capable of receiving the additional weight of reconstituting water.

An additional 2.3 lbs./man-day of water and .35 lbs./man-day of dehydrated solid are required for beverages. Food and beverage requirements defined for this study are shown in Figure 4-11.

The heat input required for the rehydration of the food is then:

$$\frac{3 \text{ lb. Water}}{\text{Man-day}} \times 6 \text{ Men} \times \frac{\text{Day}}{24 \text{ Hrs.}} \times \frac{1 \text{ BTU}}{\text{Lb. } ^\circ\text{F.}} \times 120^\circ\text{F} = 90 \text{ BTU/HR.}$$

The additional power for bringing the food mixture up to 175°F after mixing the dried solids at an assumed cabin storage temperature of 70°F with the 180°F water should be:

$$\frac{3.75 \text{ Lb. food}}{\text{Man-Day}} \times \frac{.9 \text{ BTU}}{\text{Lb. } ^\circ\text{F.}} \times 6 \text{ Men} \times \frac{\text{Day}}{24 \text{ Hrs.}} \times (175 - 168^\circ\text{F}) = 6 \text{ BTU/HR.}$$

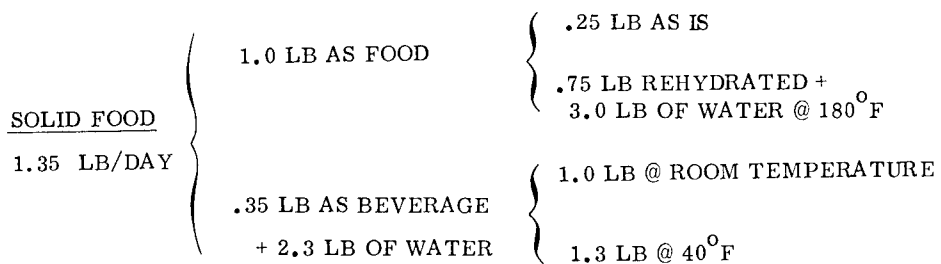


Figure 4-11. Food Requirements

Where 168°F is the calculated mixture temperature based on an average specific heat of .5 BTU/LB. $^{\circ}\text{F}$ for dehydrated foodstuff and .9 BTU/LB. $^{\circ}\text{F}$ is the assumed average specific heat of the food mixture. This amount is negligible.

The amount required to keep the food at 175° for a few minutes should also be negligible. It would be equivalent to the insulation losses of the oven. Taking these losses into account, a realistic average power requirement would be 30 BTU/HR.

In estimating peak power requirements it must be considered that man does not like to eat alone and that most likely two of the six men will be together on a "work shift." Assuming that the largest meal may be half of the daily ration and that the heating is done in 10 minutes, the peak power requirements would be:

$$P = \frac{2 \text{ Lb. Food}}{\text{Man}} \times \frac{2 \text{ Men}}{\text{Meal}} \times \frac{.9 \text{ BTU}}{\text{Lb. } ^{\circ}\text{F}} \times \frac{27^{\circ}\text{F}}{10 \text{ Min.}} \times \frac{60 \text{ Min.}}{\text{Hr.}} = \frac{584 \text{ BTU}}{\text{Hr. - Meal}}$$

or 171 watts/meal

Requirements for providing water at 40°F for cold beverages are not discussed due to the confinement of this discussion to endothermic power applications.

4.3.5.4 Sterilization of Utensils

In order to provide the true feeling of a good meal the man in a space cabin can use earth type "silverware" slightly magnetized to stay on a tray when not in use. Special

"sticky" sauces such as developed by Libby Food Scientists and successfully used during the GE 30-day 4-man simulated space flight, can hold the food to the tray or dish so that meals would be as natural as possible. This, of course, complicates the cleaning and sterilizing of eating utensils. Some of the dishes, especially when sticky sauces are used, could be made from edible material similar to the "bread sheets" used by the early Romans and some modern nomadic people, and consumed at the end of the meal. This would insure complete consumption of the prepared calories and reduce waste storage.

One pound per man-day of non-potable, clean, hot water is sufficient for cleaning personal eating utensils. The water with some cleaning additives would be contained in plastic bags together with the utensils to be cleaned. The hot water would be coming from the same reservoir which supplied hot water for personal hygiene. It is estimated that an additional 5 lbs/man-day is needed for personal hygiene and clothes (See Section 4.3.3). The total hot water requirements would then be 6 lbs./man-day. In order to utilize the same heating system as for the potable water only half of the amount would be heated and then mixed.

The average heat input to bring 3 lbs. of water to 170⁰F is 83 BTU/HR.

Sterilization of eating utensils can be done with 240⁰F superheated steam. A continuous operating sterilizer would require approximately 25 BTU/HR.

Another possible means of sterilizing is by using germicidal ultraviolet lamps. Two lamps of 5 watts each used intermittently a few times a day would provide good sterilization at a lower power input than required by the hot steam concept. In addition, the same lamps could be used to sterilize the cabin air if connected to the cabin environmental control system. The disadvantage of this system is that it requires electrical power rather than the available waste heat that this study is considering to utilize.

4.3.6 TABULATION OF ENDOTHERMIC REQUIREMENTS

Table 4-4 presents a summary of the endothermic power requirements identified in the previous sections. It must be noted that the resulting total power is not the total power required for the Life Support system since it only identifies energy which could be supplied from thermodynamic process. Energy requirements which must be supplied by electrical power, such as the 1.0 KW for electrolysis, and energy requirements to compensate for system losses or auxiliary equipment are not included.

4.4 SUBSYSTEM DESIGN LAYOUT

The general size and configuration of the principal system components are shown in isometric drawings illustrating the equipment layout within the living quarters. Most components require relatively little additional development, in one case (solid waste management) the entire subsystem has been designed, built and successfully operated.

Location of the equipment within the space cabin has been made according to the MORL cabin layout.

TABLE 4-4. LIFE SUPPORT SYSTEM - ENDOOTHERMIC POWER REQUIREMENT

Item	Subsystem	Operation	°F Range	Watts Endothermic Power	Average Continuous Endothermic Power In Watts		
					1800° - 2200°F	250° - 600°F	180° - 170°F
1	Oxygen Recovery	Desiccant Desorbing	250 - 600	1,225	1,225	642	
		Sieve Desorbing	250 - 600	642			
		Pyrolyzation of Methane	1800 - 2200	130			
2	Water Recovery	Evaporator	120	243	130	60	243
		Pyrolysis	1800	60			
3	Waste Water Recovery	Evaporator	120	442			442
4	Solid Waste Management	Evaporator	120	293	12	15	293
		Sludge Dehydration	100 - 200	15			
		Waste Disinfection	250	12			
5	Food Preparation	Food Preparation	180	27			27
		Baking	175	9			9
		Cleaning	170				25
		Sterilization	250 - 300	8		8	
		TOTAL	3,131	190	1,887	76	978

All the mechanical components, except the equipment related to human waste management, are located in the central console.

The dehydrated food which requires a considerable storage volume, approximately 71 Ft.³, for a ninety days resupply schedule, has been equally distributed and occupies most of the available space under each sleeping bunk. This should allow for a minimum amount of intrusion or disturbance within each man's personal area. A general cabin configuration layout is shown in Figure 4-12. Layouts of the individual systems are shown separately.

The oxygen recovery system, due to its relative complexity is shown first in an expanded view, Figure 4-13, then installed in the central console, Figure 4-14. The solid waste management is shown in a configuration similar to the GE Hydro-John in Figure 4-15. This drawing also includes, by logical necessity, the urinal and urine treatment equipment, with the exception of the recovered potable water which is stored and dispensed, for hygienical and psychological reasons, in the central console as shown in Figure 4-16. Waste water, mainly from washing and food preparations, is shown in the same drawing (i.e., Figure 4-16).

4.5 NON-INTEGRATED LIFE SUPPORT SYSTEM

4.5.1 GENERAL

The non-integrated life support system derives all of its energy requirements from the space station power generator.

The only other possible source of energy is the oxygen recovery system itself, with the exothermic reaction of the Sabatier reactor and the cooling lines of the CO₂ collection canister.

However, the Sabatier reactor's energy is not sufficient to sustain any of the remaining major systems' endothermic requirements. The lesser requirements in the food preparation area are relatively insignificant but of an intermittent nature, a factor which might upset the thermal balance of the reactor.

It is conceivable that some of the evaporative processes of the life support system could be supported by the fluid cooling the hot desiccant and desorbing CO₂ collection canisters. In this case, the cycling nature of the cooling process would make the system somewhat complicated and above all a non-critical failure of one of the other systems would affect the critical performance of the oxygen recovery system.

In view of the above reasons, no integration of energy requirements has been made within the Life Support system itself. The integration has been limited to the auxiliary equipment only as shown in the life support system flow diagram, Figure 4-17. A 30% glycol-70% water solution is used to remove heat from the system. Two separate cooling circuits are shown in the diagram even though both circuits would most probably go to the same radiator.

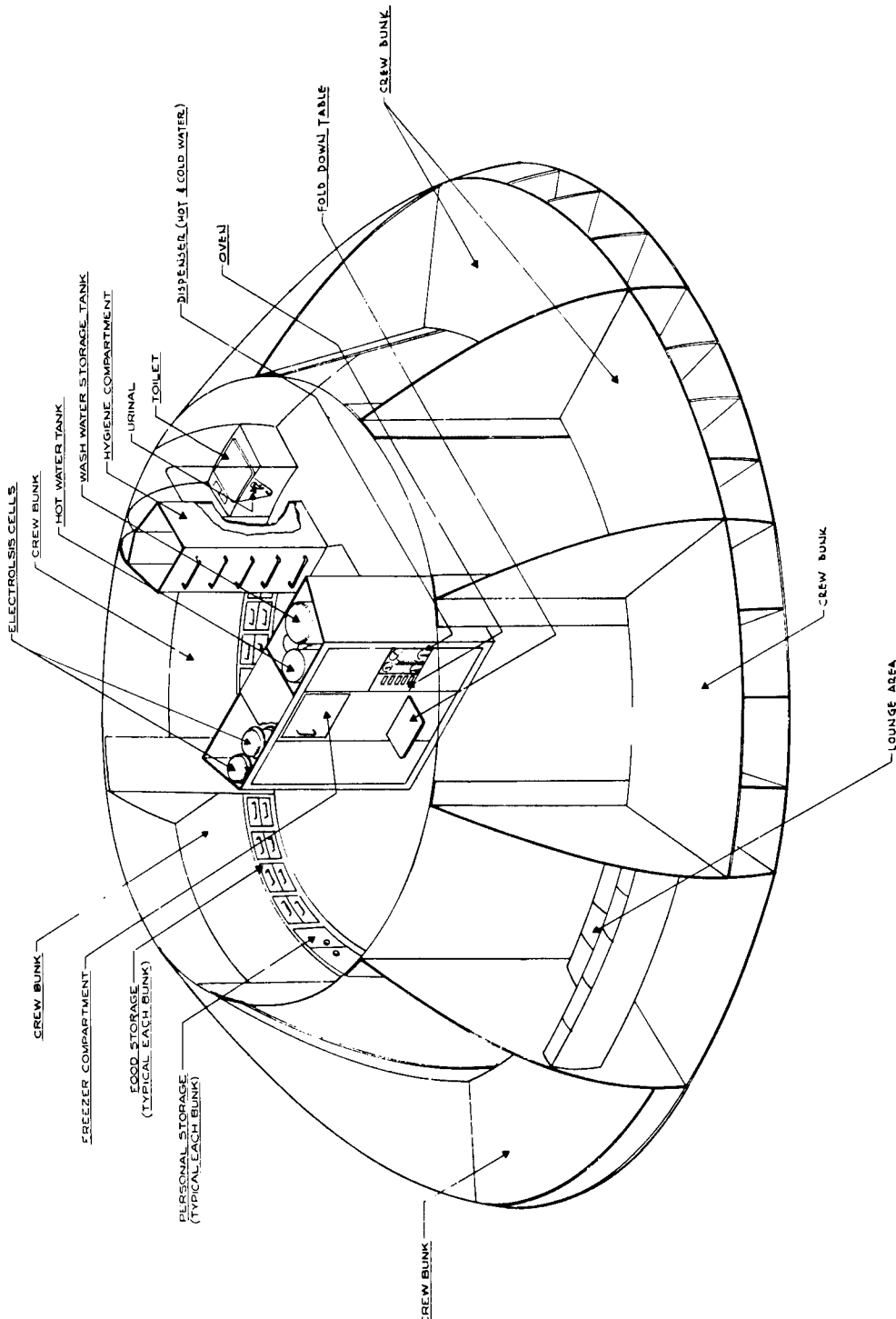


Figure 4-12. Life Support System Equipment Layout

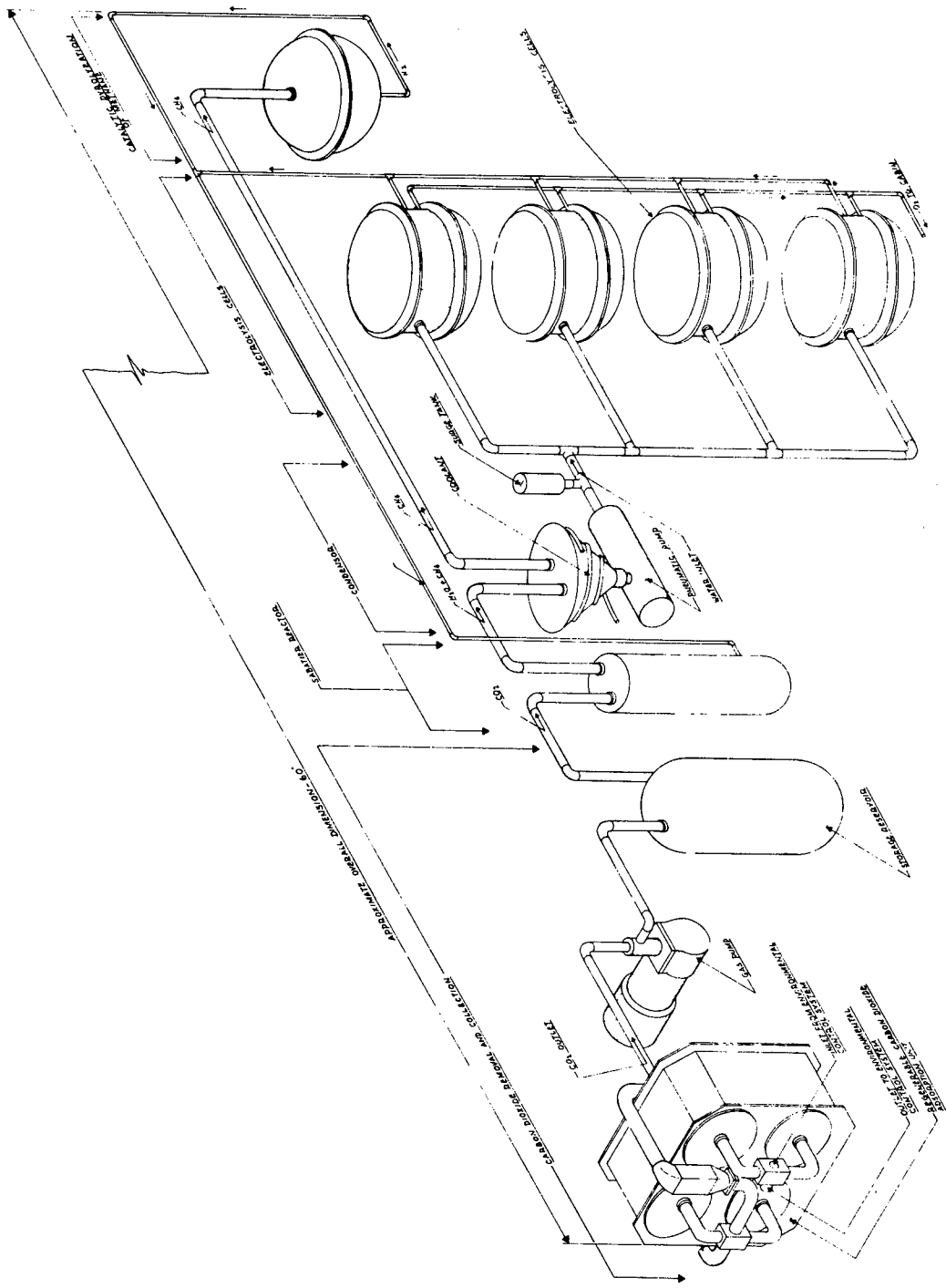


Figure 4-13. Sabatier Method for Oxygen Recovery from Carbon Dioxide

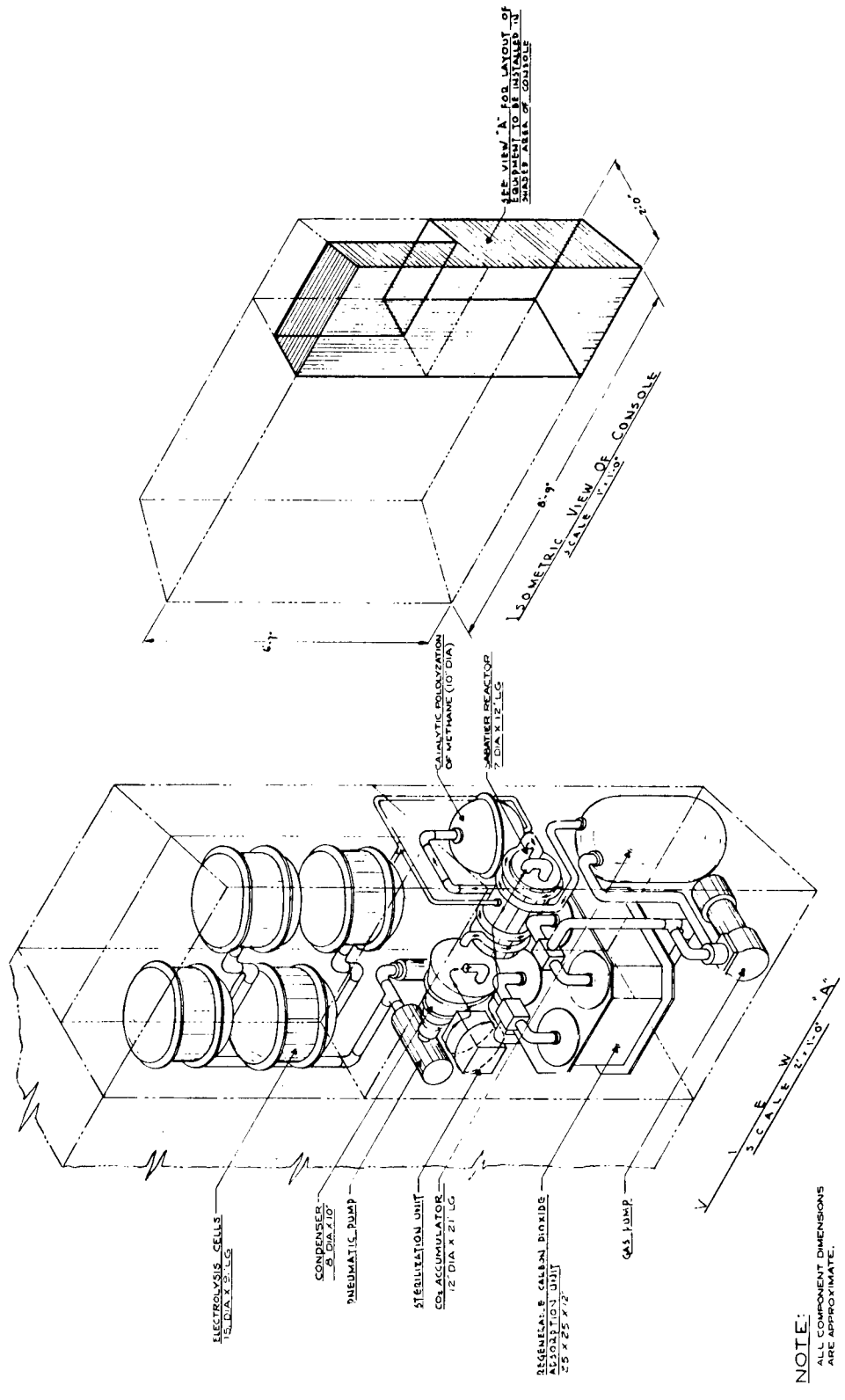


Figure 4-14. Oxygen Recovery from Carbon Dioxide - Equipment Layout

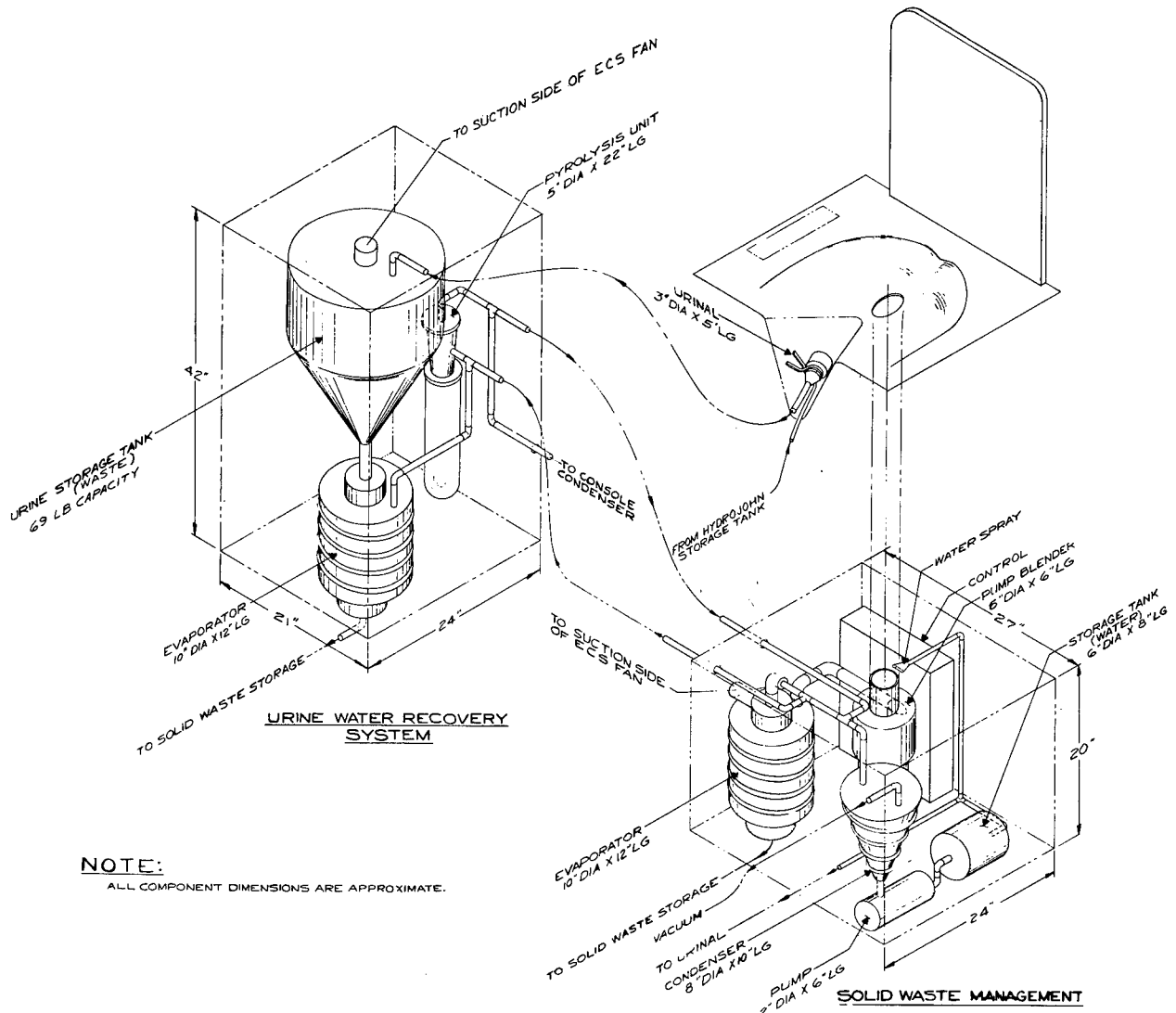


Figure 4-15. Waste Management

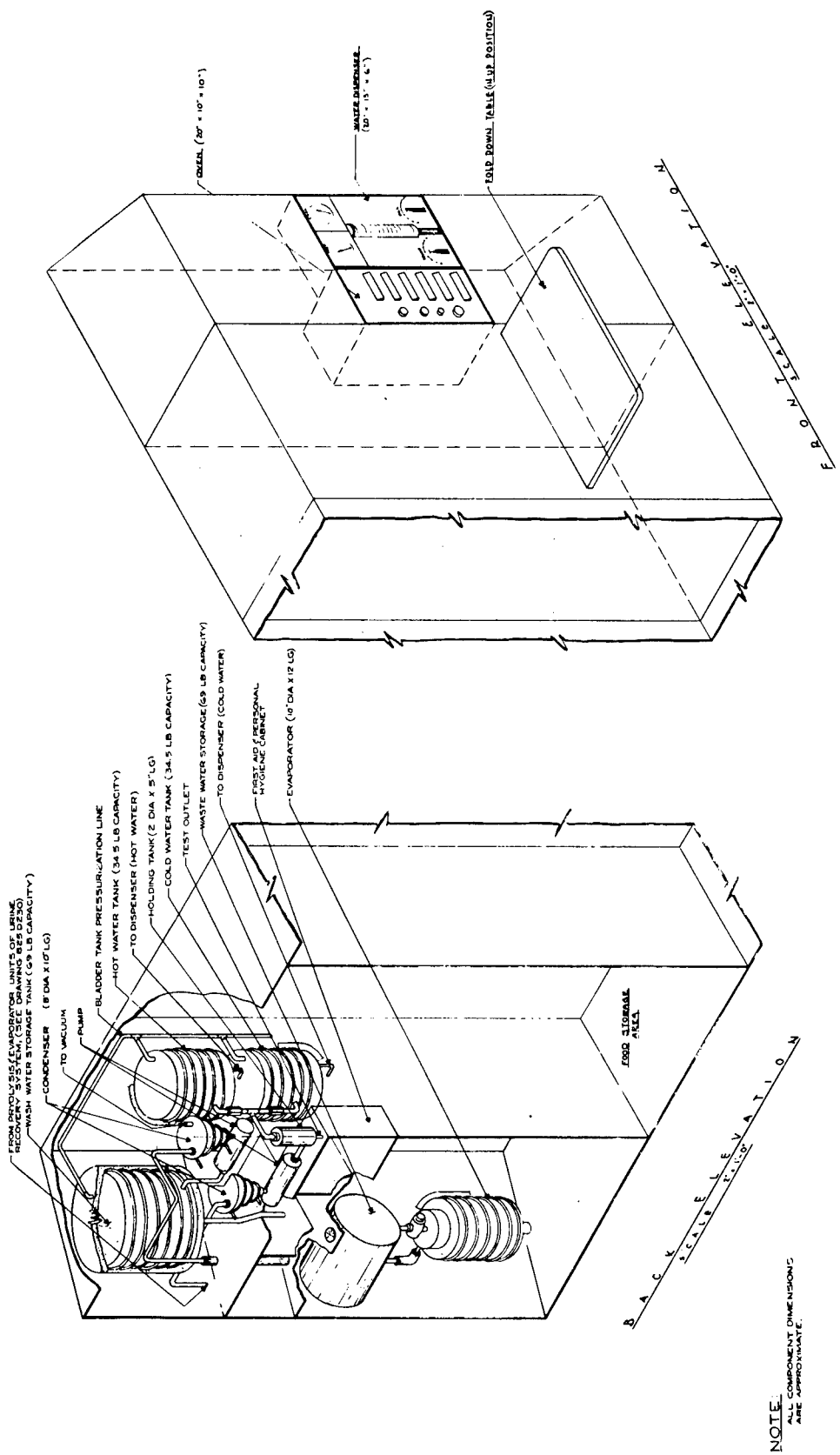


Figure 4-16. Water Recovery and Dispensing Equipment Layout

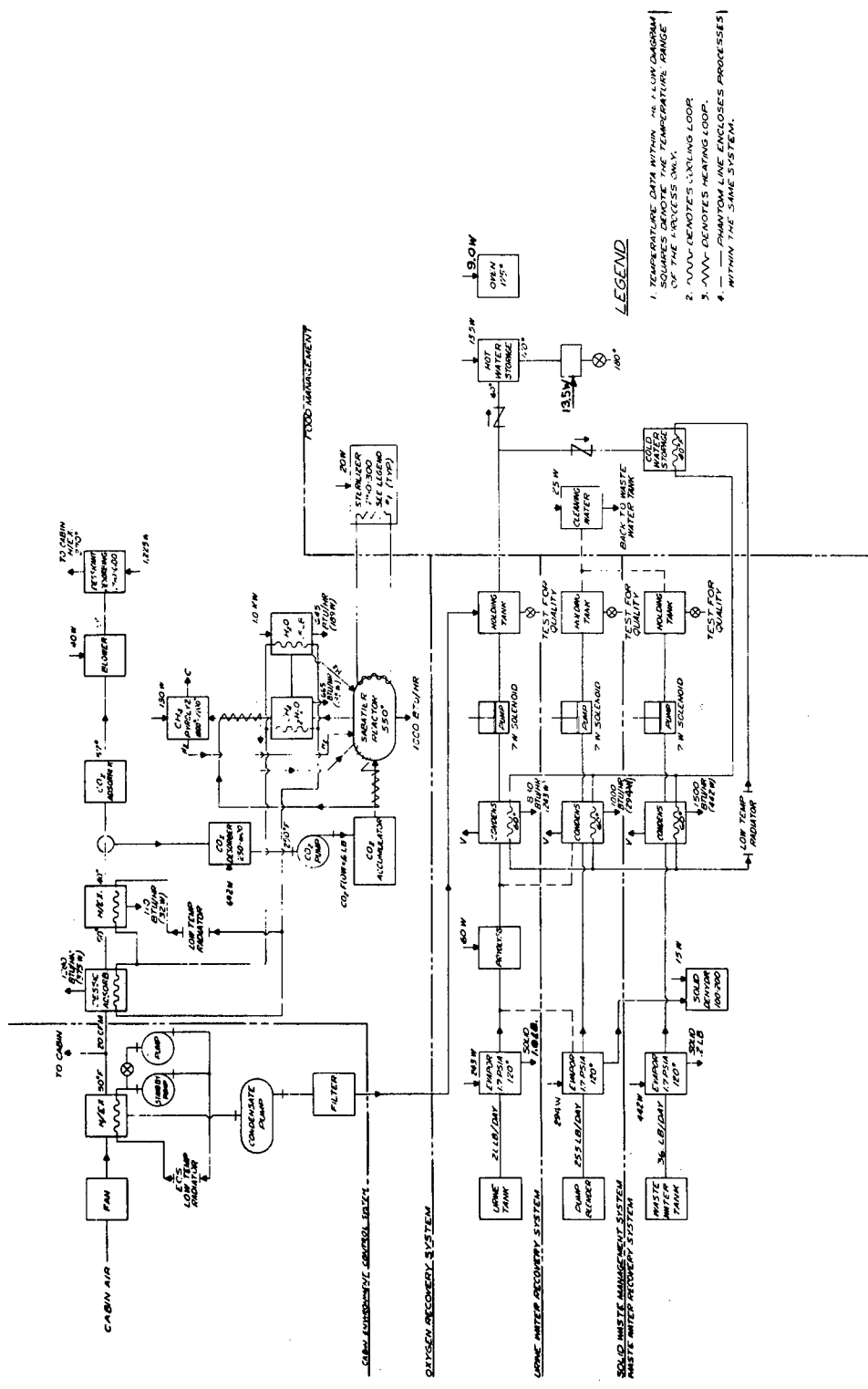


Figure 4-17. Flow Diagram - Life Support System - Non-Integrated

4.5.2 POWER REQUIREMENTS

The power needed to operate the non-integrated life support system is given by the sum of the endothermic process requirements listed in Table 4-4, plus the power required to operate the electrolysis unit and all pumps, solenoids, blowers, etc., for the subsystems support equipment. Table 4-5 gives the total power requirements. The process power identified in Table 4-4 has been listed separately from the auxiliary power in order to simplify the correlation of data.

4.5.3 WEIGHT REQUIREMENTS

The weight estimates for the non-integrated life support system are restricted to the operating equipment only and do not include initially stored items such as food and water or the storage containers. The storage of the food supplies above would amount to 1,035 lbs. for a ninety days resupply schedule. This weight above is by far greater than that of the life support equipment which is listed in Table 4-5.

TABLE 4-5. POWER REQUIREMENTS AND WEIGHTS ESTIMATE FOR
NON-INTEGRATED LIFE SUPPORT SYSTEM

SYSTEM	WEIGHT LBS.	PROCESS POWER WATTS	SUPPORT POWER WATTS
1. Oxygen Recovery			
CO ₂ Recovery Canisters	120	1,867	40
Electrolysis Cells	100	1,000	
Pyrolyzation Unit	20	130	
CO ₂ Accumulator Pump	7		100
Accumulator, Reactor, Condenser	26		
System Cooling	100		70
Heat Leakage			42
Misc. Hardware	12		7
	385	2,997	259
2. Urine Water Recovery			
Solid Waste Treatment	43	303	7
Waste Water Recovery	29	320	7
Food Management	35	442	7
Heat Leakage	19	69	
Cooling System	106		95
Misc. Hardware	5		60
	237	1,134	176

TOTAL NON-INTEGRATED SYSTEM WEIGHT = 385 + 237 = 622 LBS.

TOTAL NON-INTEGRATED SYSTEM POWER REQUIREMENT =

2,997 + 1,134 + 176 + 259 = 4,566 WATTS

4.6 INTEGRATED LIFE SUPPORT SYSTEM

4.6.1 GENERAL

In the integrated life support system the process energy is supplied wherever feasible by making use of the waste heat which normally would be rejected by the space power generators to space. The temperature level of the processes and of the available waste energy

is a most important factor. A quick review of Table 4-4 shows that most of the life support requirements can be grouped in two levels, the largest at 250-600°F, the second at 120°F. The overall quantities at 1800-2000°F will obviously have to be supplied by electrical heaters, the food preparation items at 170-180° can be preheated thermally to 120° with the additional heat supplied by electrical heaters. In this manner we have two basic heating circuits which are compatible with the temperature levels of the available waste energy. The two basic heating circuits are shown in the integrated system flow diagram, Figure 4-18.

A 600°F source forming the high temperature loop is used to heat the CO₂ desorber and the desiccant desorbing canisters.

The 155°F source (low temperature loop) is used to heat all of the remaining processes with the exception of sterilization and disinfection, which derive the small quantity of energy directly from the Sabatier exothermic reaction.

The equation location is in the center console as shown in the MORL cabin layout and artist concept sketches. This does not appear to be an optimum selection for an integrated power cycle-life support system, since the hot liquid piping would have to extend a considerable distance to the cabin walls. This distance becomes important in considering the heat leakage, and the weight of fluids in the tubing. In addition, it complicates the problem of initial system operation where, due to the great increase in viscosity of the heat transfer fluid from the 600° range to cabin temperature, other means such as electrical heating will have to be provided to supplement the temporarily inadequate pumping power.

Heat leakage for the high temperature loop has been estimated at 1200 BTU/HR. Approximately 142 BTU/HR leaks through the canisters (the 42 watts in Table 4-5, item 1) common to both integrated and non-integrated system, and 1060 BTU/HR. for a maximum length of 40 feet of tubing.

Relocation of the oxygen recovery system to an area as close as possible to the high temperature heat exchanger would minimize heat leakage, pumping power, weight and starting problem. However, since such relocation is more of a detail design problem, without significant effect on the scope of this study, no changes in the cabin layout have been made.

The heat transfer fluid considered for this operation is Therminol FR-1 (Monsanto Company, St. Louis, Missouri). Therminol is specially designed as a high temperature heat transfer fluid with low density and high specific heat in the 600°-400°F range. It is estimated that 1.0 GPM with a Δ T of 35°F is required to provide the $7,548 = (4168 + 2180 + 1200)$ BTU/HR. for the process. The 1.0 GPM provides the minimum recommended fluid velocity of 4 feet/second for good heat transfer performance as shown:

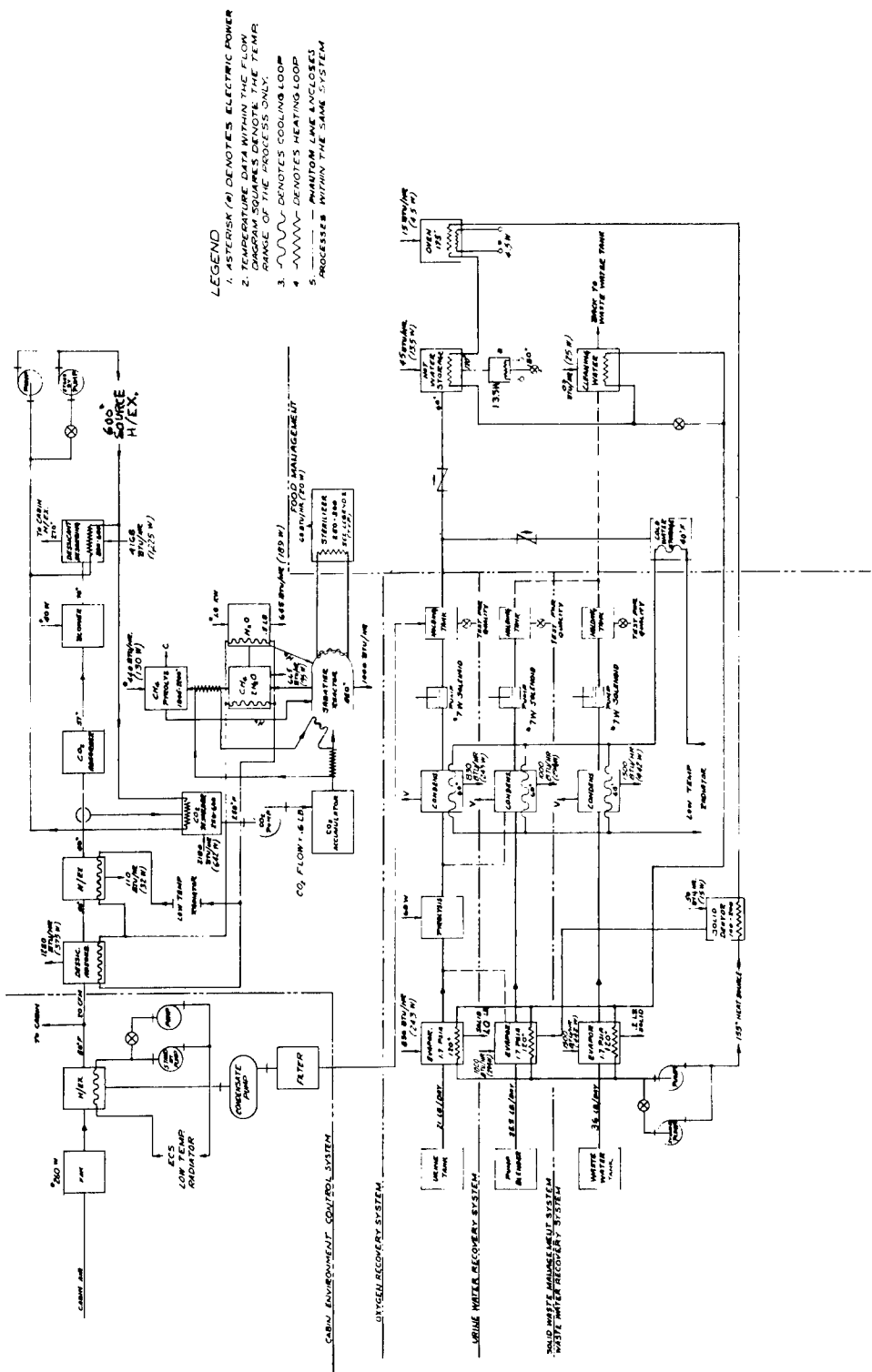


Figure 4-18. Flow Diagram - Life Supprt System - Integrated

GPM	$\Delta T ^\circ F$	U-FT/SEC	$\Delta P - \text{psi/FT}$	$\Delta P \text{ TOTAL}$	N_{RE}
0.7	50	3.15	.074	07.1	1.93×10^4
1.0	35	4.47	.137	13.2	2.7×10^4
1.35	26	6.0	.237	22.8	3.67×10^4

The total ΔP is based on an equivalent length of tubing (3/8 inch dia.) of 96 feet, calculated as follows:

Connecting tubing from equipment to wall 15 ft x 2 ft	30
From wall to heat exchanger 5 x 2	10
Equivalent tubing in heat exchanger	10
Equivalent tubing for fittings and controls	34
Equivalent tubing in canisters	12
TOTAL	= <u>96 ft.</u>

The pump power required to circulate the hot Terminol fluid is estimated at 1/8 HP (= 93 watts). This is based on off-the-shelf hardware: a high temperature pump with a long drive shaft to insulate the motor, as typical in sump pump design.

The low temperature loop supplies heat to a larger number of processes. However, due to the lower temperature differential between fluid temperature and ambient temperature it has a lower heat leakage of 550 BTU/HR. Approximately 325 BTU/HR. (95 watts) are due to heat leakage from within the system itself, i. e., the various containers and connecting tubing. This loss is common to both integrated and non-integrated systems, and is therefore tabulated in Table 4-5, item 2. The remaining 225 BTU/HR. is due to the interconnecting heating tubing where the total length has been estimated at 60 feet. The heat transfer fluid considered for the application is water-glycol (30% glycol mixture), flowing at the rate 1 GPM. The water glycol mixture appears to have the best heat transfer properties for this application. Other fluids such as Coolanol 34 and 35 or MIL-H-5606 could probably be used as well without significantly affecting either power or weight requirements.

The total pressure drop across the system is estimated at 20 psi. This quantity is based on an equivalent length of 150 feet of 3/8 inch diameter tubing at a calculated pressure drop of .129 psi/ft.

4.6.2 POWER REQUIREMENTS

The power requirements for the integrated life support system are listed in Table 4-6. This tabulation is restricted to electrical power only. A more complete tabulation of the entire life support system heat balance is shown in the heat load chart, Table 4-4.

The electrical requirements identified in Table 4-6 are basically those previously identified in Table 4-5 where waste heat could not be used either because of the temperature level such as for the pyrolysis unit, or because of the nature of the process such as for the electrolysis unit, which is strictly electrical. The only addition is that of the fluid pump power to circulate the heating fluid.

4.6.3 WEIGHT ESTIMATES

The weight of the integrated life support system is the same as that of the non-integrated system with the addition of the fluid heating circuits. Total weight estimates are shown in Table 4-7.

TABLE 4-6. INTEGRATED LIFE SUPPORT SYSTEM POWER REQUIREMENTS
ELECTRICAL ONLY

High Temperature Loop

Electrolysis Cells	1,000 Watts
Condenser Pump	7 Watts
Gas Pump	100 Watts
Pyrolyzation	130 Watts
Sabatier Cooling Pump	20 Watts
Blower	40 Watts
System Cooling Pump	50 Watts
Therminol Pump	93 Watts
	1,440 Watts

Low Temperature Loop

Pyrolysis	60 Watts
Condenser Pumps	21 Watts
Cooling Fluid Pumps	40 Watts
Heating Fluid Pumps	40 Watts
	161 Watts

TOTAL POWER = 1440 + 161 = 1601 WATTS

TABLE 4-7. INTEGRATED LIFE SUPPORT SYSTEM
WEIGHT REQUIREMENTS

High Temperature Loop

Weight of oxygen recovery system	=	385 Lb. (See Table 4.5)
Weight of fluid heating system	=	<u>40</u> 425 Lbs.

Low Temperature Loop

Weight of urine water recovery system	43
Waste Water Recovery System	35
Solid Waste Management	29
Food Management	19
Cooling and Miscellaneous	111
	= 237 (See Table 4-5)
Weight of fluid heating system	= 16
	253

TOTAL WEIGHT = 425 + 253 = 678 LBS.

4.6.4 INTEGRATION WITH BRAYTON CYCLE

The estimated weight and power requirements for the integrated life support system has been based on a 600°F and a 155°F heat sources. The Brayton Cycle cannot provide a 600°F waste heat energy as efficiently as it can provide 400° waste heat. This section evaluates the effect on system weight and power requirements due to the lowering of the heat source from the established 600° level. The affected components are the desiccant desorbing and CO₂ desorbing canisters of the CO₂ recovery unit in the oxygen recovery system.

It must be noted that due to various unknown factors in the heat transfer characteristics of the canisters, it is not possible to conduct a detailed analysis on the effect of the temperature variation. The approximate results plotted in Figure 4-19, are conservative and have been based on the following analysis.

4.6.4.1 Desiccant Desorbing Canister

Approximately 2888 BTU/HR of the total 4168 BTU/HR are required to heat the canister and incoming gas to 250°F. It is assumed that each phase of the same cycle is to be performed within the same time. A lower temperature heat exchanger would require an additional length of coil as the Δt between fluid and canister becomes smaller. However, the weight of the additional tubing is negligible as compared to the estimated effect on the actual desorption process.

The desorption process requires 1280 BTU/HR. This represents the amount of energy which must be absorbed by the molecular sieve to evaporate the entrapped water particles at 250°F. The amount of molecular sieve required in order to liberate .707 lbs. of water/hr. is calculated by referring to Table 4-4.

$$W = \frac{.707 \text{ lb./hr.} \times 1 \text{ cycle/hr.}}{(\text{percent H}_2\text{O adsorbed at } 250^\circ - \text{percent H}_2\text{O adsorbed at } 50^\circ) \times \text{adsorption efficiency}}$$
$$= \frac{.707}{(.29 - 0.8) \times 0.5} = 6.75 \text{ LB.}$$

The container weight was estimated at 6.0 lbs. Valves and other control equipment within or adjacent to the canister and, for thermal purposes, an integral part of the canister is then:

$$\text{Sieve} = 6.75 \text{ lbs.}$$

$$\text{Container} = 6.00 \text{ lbs.}$$

$$\begin{aligned} \text{Equipment} &= \underline{7.25 \text{ lbs.}} \\ &20.0 \text{ Lbs.} \end{aligned}$$

The heat transfer process within the sieve can be generally expressed as

$$Q = 1280 \text{ BTU/HR.} = U A \Delta t \text{ (overall)}$$

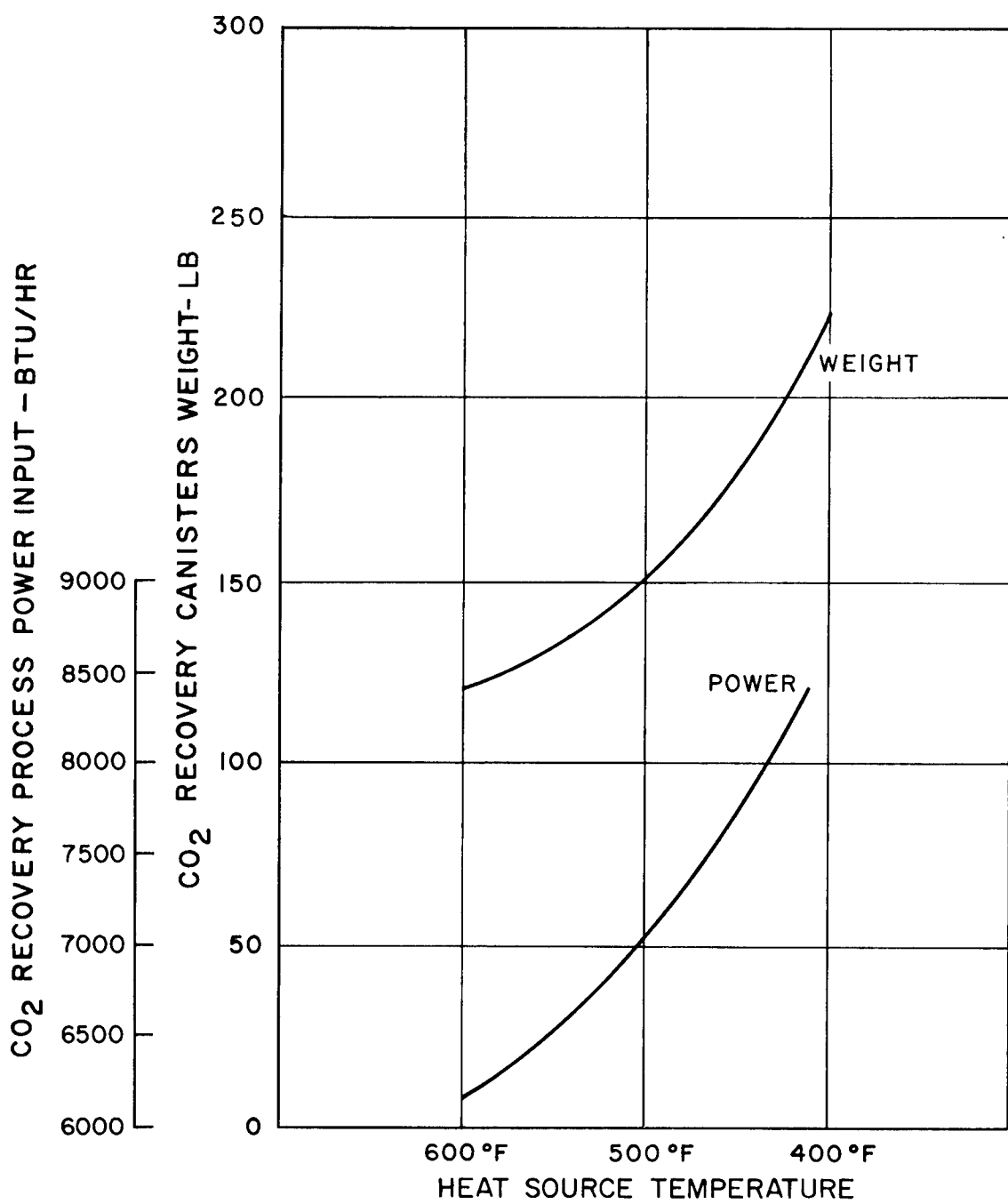


Figure 4-19. CO₂ Recovery Process Estimated Power and Weight Requirement Vs. Temperature of Heat Source

where Q is fixed and U is approximately constant. Then by changing the overall Δt from 350° ($= 600 - 250$) for a 600°F source to 150° ($= 400 - 250^{\circ}$) for a 400°F source, the sieve material must be increased so that the $A \times \Delta t$ value remains constant. Since the area of the sieve material is a function of the weight, the sieve weight for a 400° system is

$$6.75 \text{ Lb} \times \frac{350^{\circ}\text{F}}{150^{\circ}\text{F}} = 15.7 \text{ Lbs.}$$

The container size would accordingly increase to

$$6 \text{ Lb.} \times \frac{15.7}{6.75} = 14 \text{ Lbs.}$$

Assuming that the change in equipment weight is negligible the canister weight for a 400° system would then be

$$\text{Sieve} = 15.7 \text{ Lbs.}$$

$$\text{Canister} = 14.0 \text{ Lbs.}$$

$$\text{Equipment} = \underline{7.25 \text{ Lbs.}}$$

$$36.95 \text{ Lbs.}$$

The required heat input due to the additional canister weight, following the same calculations of Section 4.3.1.3 is

$$Q = 900 \text{ BTU/HR.} \times \frac{36.95}{20} = 1,660 \text{ BTU/HR.}$$

The desorption heat input for the 400° system is

$$\text{Canister Heating} = 1,660$$

$$\text{Sieve} = 1,280$$

$$\text{Atmosphere} = \underline{1,988}$$

$$4,828 \text{ BTU/HR.}$$

4.6.4.2 CO_2 Desorbing

The CO_2 desorbing process requires 180 BTU/HR. The remaining 2000 BTU/HR. is required to heat the entire canister to 250°F . Using the same approach as for the desiccant desorbing, the weight of the sieve can be calculated from Figure 4-4.

$$W = \frac{0.6 \text{ Lb.}}{(10.2 - 1.4) \times 0.5} = 13.6 \text{ Lbs.}$$

The weight of the container is estimated at 12 lbs. The remaining 14.4 lbs. are canister equipment. The estimated weight of the sieve material for a 400° system is

$$13.6 \times \frac{350}{150} = 31.8 \text{ Lbs.}$$

The container size increases to

$$12 \times \frac{31.8}{13.6} = 28 \text{ Lbs.}$$

The total canister weight is

Sieve	=	31.8
Canister	=	28.0
Equipment	=	14.4
		74.2 Lbs.

Heat input for canister is

$$2000 \text{ BTU/LB.} \times \frac{74.2}{40} = 3,700 \text{ BTU/HR.}$$

Total process heat input is then 3,880 BTU/HR. (=3700 + 180)

4.6.4.3 Total weight of canisters for a 400⁰ system is then

Desiccant Desorption	=	36.95 × 2 = 73.9
CO ₂ Desorption	=	74.2 × 2 = 148.4
		222.3 Lbs.

Total power requirement for a 400⁰ system is

Desiccant Desorption	=	4,828
CO ₂ Desorption	=	3,880
		8,708 BTU/HR.

Total weight increase = 222.3 - 120 = 102.3 Lbs.

Total power increase = 8,708 - 6,348 = 2,360 BTU/HR.

4.6.4.4 Similar calculations were made for a 500⁰ system. The results have been plotted in Figure 4-19.

4.6.5 LIFE SUPPORT SYSTEM RADIATORS

In evaluating the power and weights of the life support subsystems, estimates were made on the basis of two major cooling loops as shown in the flow diagram for both integrated and non-integrated systems. In actual design the two loops would go to a common radiator and the total heat load would be greater than the heat load shown on the flow diagram. The increase would be due to the additional cooling of electronic equipment, removal of heat leakage from the cabin air, metabolic heat, etc.

A complete heat balance for the Life Support system except for the Brayton cycle is shown in Table 4-8. The total heat rejected is 22,191 BTU/HR. This would be done by means of two radiators, one for the cabin environment control system (7,464 BTU/HR. load from the cabin air to ECS heat exchanger), the other (14,727 BTU/HR.) for all other direct glycol liquid cooling, such as condensers, CO₂ canisters, etc. Figure 4-20 and 4-21 give the size and weight for the two basic radiators as a function of heat load.

In the Brayton cycle an additional amount of 2,360 BTU/HR. is required due to the lower temperature fluid in the CO₂ recovery canisters, see Section 4.6.4. The liquid cooling load is increased from 14,727 to 17,087 BTU/HR. which corresponds to an increase of approximately 40 ft.² in radiator area and 5 lbs. in weight. These changes are negligible.

More important is the effect of the various cycles radiators on the environment control system. The 7,464 BTU/HR. load is based on the premise that there is no heat transfer from either side of the cabin walls. However, as the cabin is shrouded with the power system radiators, heat leakage into the cabin may become considerable since in addition to affecting the radiator, it will cause an increase in the ECS fan size. Figure 4-22 gives the ECS weight and power as a function of cabin heat load. A 2,360 BTU/HR. increase in this system will cause a weight increase of 45 Lbs. and an additional electrical power requirement of 150 watts. This is due to the fact that a larger size fan (and liquid pump) will be required to remove the heat from the air. In addition, the efficiency of the radiator for the ECS is not as good as the other life support system radiator, Figure 4-21, mainly due to the lower allowable ΔT in the ECS heat exchanger cooling fluid.

4.7 CONCLUSION

A comparison of the total power and weight requirements given in Tables 4-5, 4-6 and 4-7 shows that by integrating the Life Support System with the vehicle power source a total of 2,965 watts can be saved, at an estimated weight increase of 56 pounds of Life Support Equipment.

The total values of Tables 4-5, 4-6 and 4-7 are shown below for the convenience of the reader.

	WEIGHT	POWER
Non-integrated LSS	622 Lbs.	4,566 Watts
Integrated LSS	678 Lbs.*	1,601 Watts
WEIGHT INCREASE INTEGRATED LSS	56 Lbs.*	
ELECTRICAL POWER SAVING, INTEGRATED LSS		2,965 Watts

The thermally integrated life support sub-systems are not appreciably affected by the type of power cycle generating the spacecraft electrical energy, except in the case of the oxygen recovery system. This system is the most critical of all life support operations, on the basis of weight, power requirements, and additional development work required.

Another advantage of integration can be derived by the use of waste heat in conjunction with the Cabin Environmental Heat exchanger to minimize the repressurization load on the electrical power available.

*These values are 780 lbs and 68 lbs for Brayton powered systems.

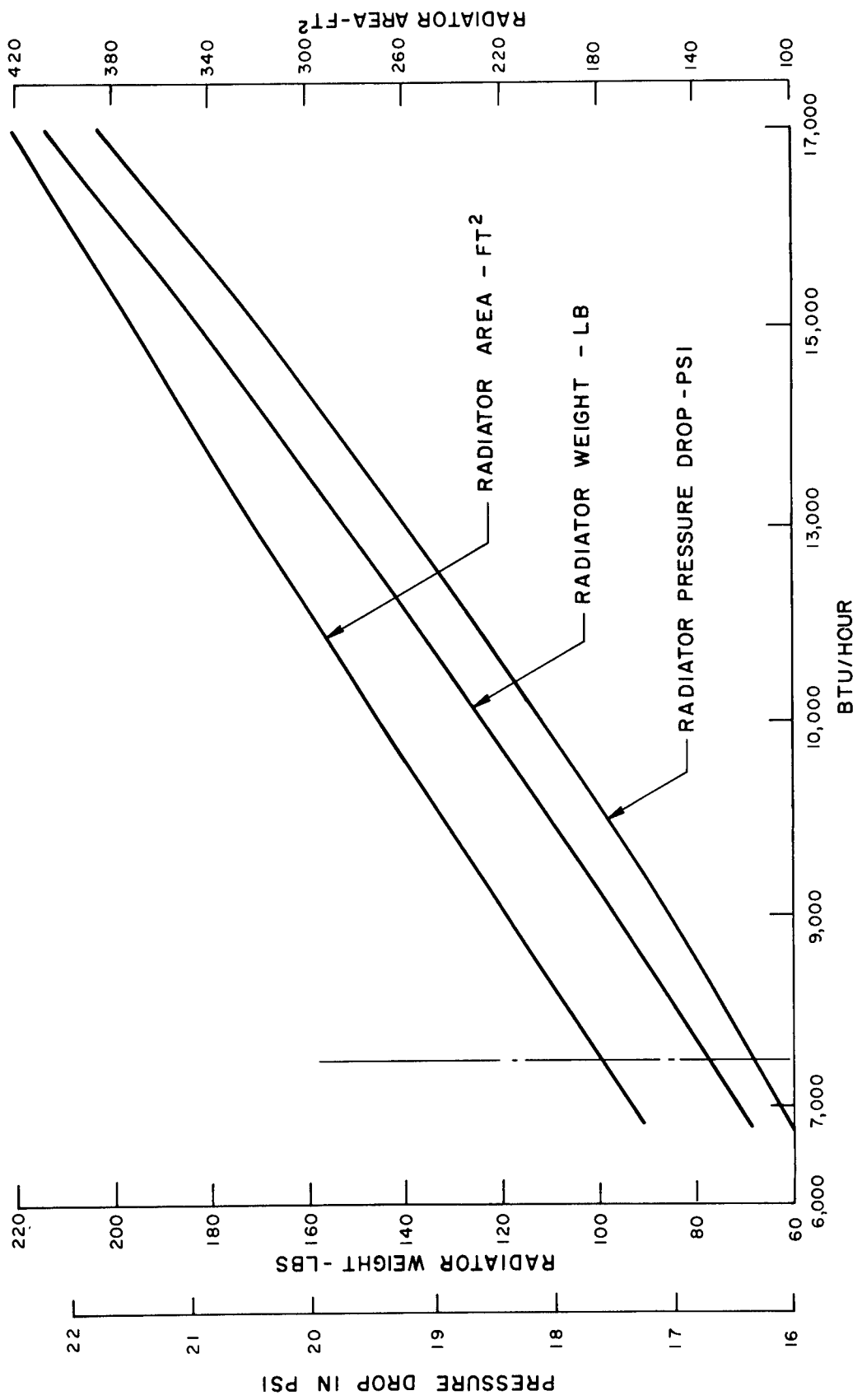


Figure 4-20. Environmental Control System Radiator Size

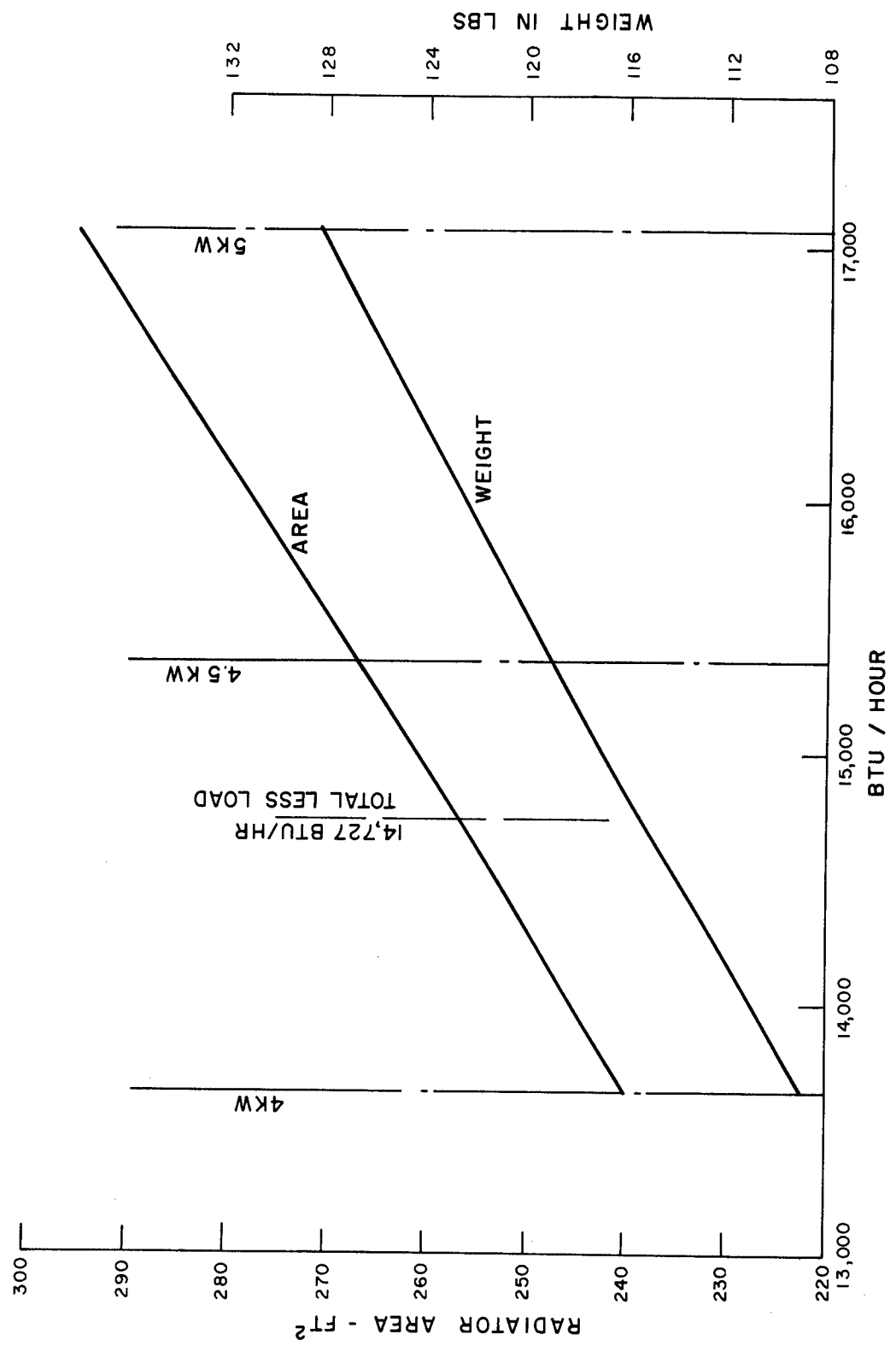


Figure 4-21. Life Support System (other than ECS) Radiator

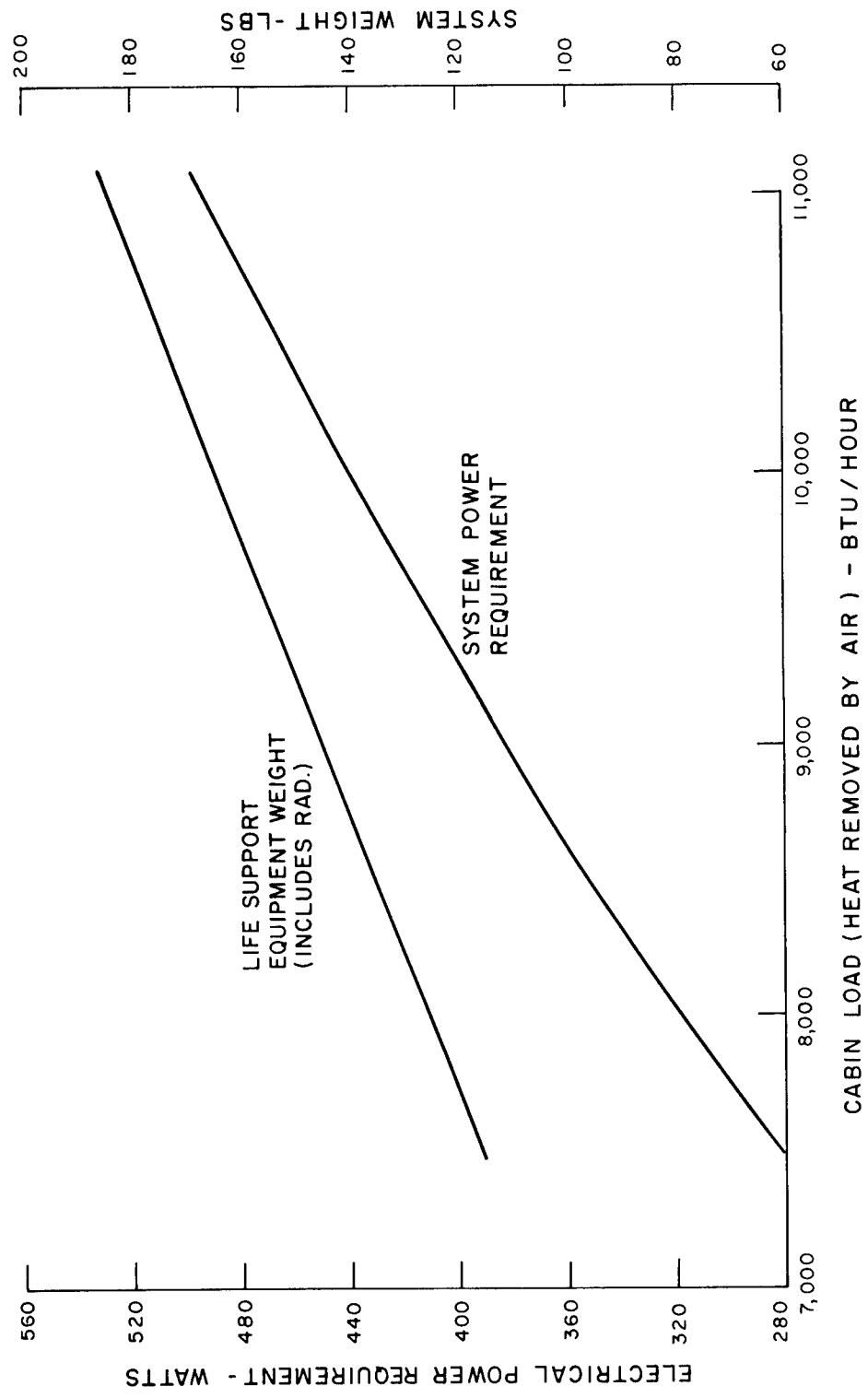


Figure 4-22. Environmental Control System Weight and Power Vs. Cabin Load Heat Requirements

TABLE 4-8. HEAT LOAD CHART INTEGRATED SYSTEM

* 4,900 Btu/hr. = 1.434 KW = 6.0 KW - 4.566 KW for non-integrated requirements.

4.8 REFERENCES

1. Perry, John H. (Editor), *Chemical Engineer's Handbook*, Third Edition, McGraw-Hill Book Company, New York, N. Y., 1950.
2. Ames, Robert K., "Present Status of the Sabatier Life Support System," *The American Society of Mechanical Engineers*, 63-AHGT-48, January 4, 1963.
3. Coe, C. S., Rousseau, J. and Shaffer, A., "Analytical Methods for Space Vehicle Atmospheric Control Processes," ASD-TR-61-162, Part II, AiResearch Manufacturing Co., prepared under contract AF33(616)-8323 for Wright-Patterson Air Force Base, Ohio, November, 1962.
4. "Molecular Sieve Air Purification System For a Space Vehicle," 87-CO₂-air, Linde Company, 1958.
5. "Air Conditioning-Refrigerating Data Book," *The American Society of Refrigerating Engineers*, 9th edition, 1955.
6. "Joy Fan Catalog," Joy Manufacturing Co., J-619, 1963.
7. "General Information on "Linde" Molecular Sieves Types 4A and 5A," Form 8605A, Linde Company, July, 1956.
8. Chandler, Horace W., and Pollara, Frank Z., "Carbon Dioxide Reduction Systems for National Aeronautics and Space Administration Report 5007-PR7-62, Isomet Corporation, 1962.
9. Rudek, Fred P., and Warner, Harold, "Research on Electric Arc Reduction of Carbon Dioxide," prepared by General Electric Company, under contract AF33(657)-11030 for Wright-Patterson Air Force Base, Ohio.
10. "Subsystem Design of Manned Orbital Research Laboratory (MORL) System," Prepared by the Boeing Company for NASA-Langley under contract number NAS1-2975, September 27, 1963.
11. Parker, F. A., Eckberg, D. R., Withey, D. J., "Atmospheric Selection and Environmental Control For Manned Space Stations," GE-MSD, July 23, 1964.

SECTION 5

STIRLING SYSTEM ANALYSIS

5.1 DESCRIPTION OF NON-INTEGRATED SYSTEM AND DESIGN

This section discusses the parameters associated with the Stirling power system as related to this study. The heat source is either a Solar-Collector-Absorber system or a Radio-Isotope package. The heat from either source is supplied to the engines by circulating NaK. Figure 5-1 is a schematic of the Stirling Non-Integrated System. The electrical power requirement for the non-integrated system is established as 6.24 KW_e to the station bus. This includes 4.57 KW_e required to supply the non-integrated life support systems. This demand will be satisfied by the parallel and independent operation of two advanced Stirling engines of the type discussed in Section 5.1.1. Each engine will drive one 12,000 rpm, 400 cps, 110/220 volt alternator. Each engine and corresponding alternator will be sized to supply one-half of the total electrical load. Each engine is heated by a Sodium Potassium (NaK) eutectic heat transfer loop.

There are two independent NaK loops linking the engines with the isotope heat source. The mass flow rates and temperatures, as listed on the schematic, are for normal orbital operation of the power system (i.e., all components operating at design point and supplying rated power to the station bus).

The power system energy balance for normal operation of the non-integrated system is tabulated in Table 5-1.

5.1.1 STIRLING ENGINE

The dynamic energy converted in the Isotope Stirling power system is the advanced Stirling cycle engine developed by the Allison Division, General Motors Corp. A

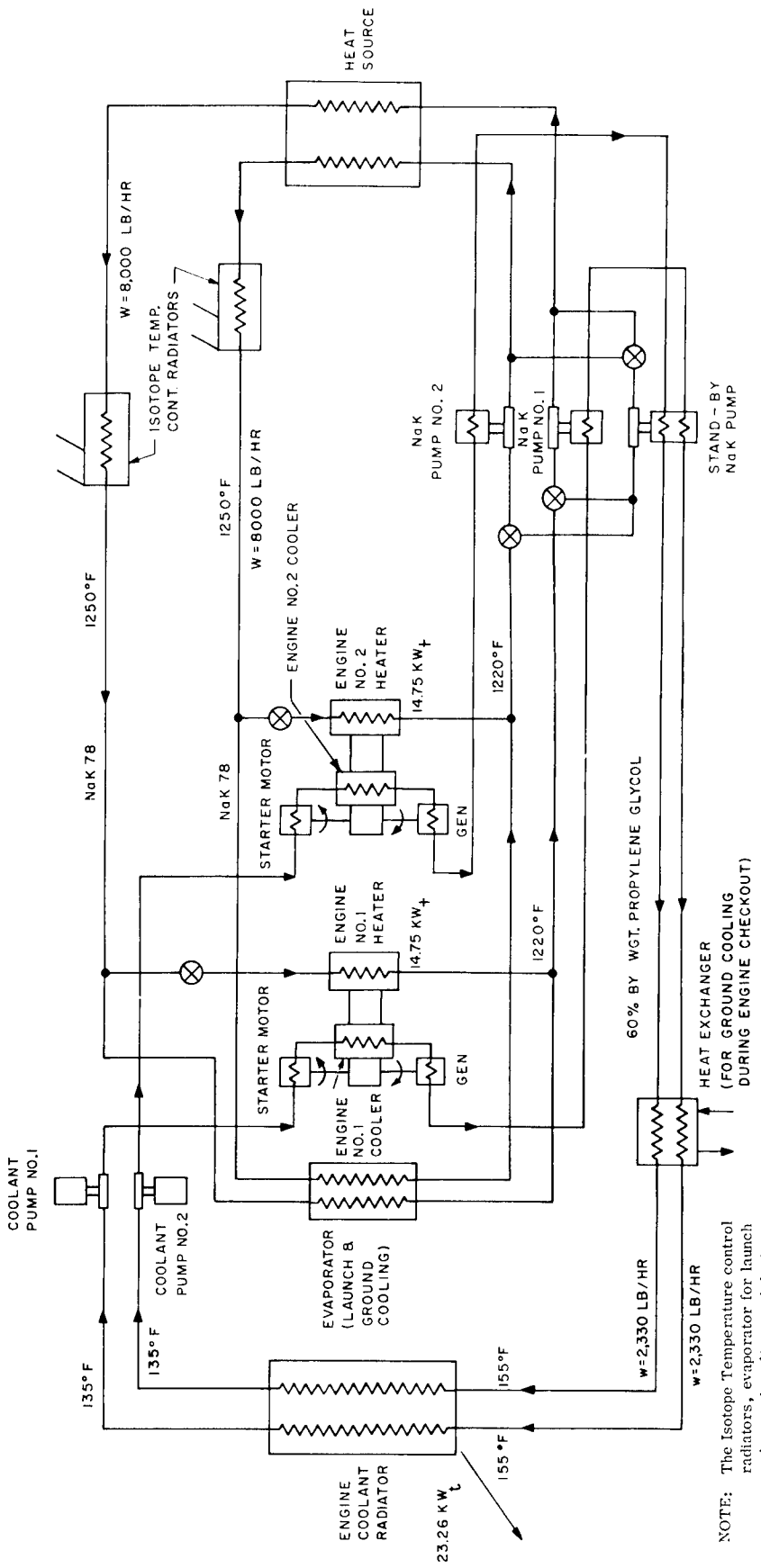


Figure 5-1. Stirling Cycle

TABLE 5-1. ENERGY BALANCE - NON-INTEGRATED SYSTEMS

a.	Electrical power to station bus	6.24 KW _e
b.	NaK pump-motor input	.44 KW _e
c.	Coolant pump-motor input	.36 KW _e
d.	Dissipative control (5% of load)	.31 KW _e
e.	Generator output	7.35 KW _e
f.	Generator efficiency	84.6%
g.	Gearing efficiency	98.0%
h.	Engine output	8.87 KW _e
i.	Brake thermal efficiency	30%
j.	Heat input to engines	29.50 KW _t
k.	Heat loss from NaK circuits and isotope heat source	2.50 KW _t
l.	Heat delivered by isotope heat source	32.00 KW _t
m.	Heat delivered by Solar Absorber	29.50 KW _t
n.	Heat rejected by engine coolant radiator	23.26 KW _t

brief description of the Stirling cycle is presented in this section. (Reference 1, 3 and 4)

The ideal Stirling cycle consists of two isothermal and two constant volume processes (see Figure 5-2). The process (A-B) is an isothermal compression during which heat is rejected by the system. The process (B-C) is a constant volume process during which heat is transferred from the regenerator to the working fluid. The process (C-D) is an isothermal expansion during which the work is performed and heat is added to the system in the engine heater. The process (D-A) completes the cycle and is a constant volume process during which heat is transferred from the working fluid to the regenerator.

The theoretical operation of the engine is governed by the motion of the two pistons as shown in Figure 5-3. The lower (or power) piston does the compression and expansion work. The upper (or displacer) piston is used to transfer the working fluid from the lower to the upper spaces through the heat exchangers. In the process from A to B, the power piston is moved from bottom dead center (BDC) to top dead center (TDC). This compresses the working fluid in the cold space since the displacer piston is in the uppermost position. To maintain the temperature constant it is necessary to remove the heat of compression in the cooler. In the second process (B to C), the displacer piston is moved down to force the working fluid through the cooler, regenerator, and heater into the hot space. During this process, stored heat in the regenerator is transferred to the working fluid. In the third process (C to D), both the power piston and the displacer piston move down together and heat is added to the working fluid from the heater. This is the power stroke of the cycle. The cycle is completed (D to A) by the movement of the displacer piston from BDC to TDC. This forces the working fluid through the heater, regenerator and cooler into the cold space. During this process, heat is rejected from the working fluid and stored in the regenerator. The actual cycle differs from the ideal cycle, which has been discussed above, because of the difficulty in maintaining constant temperature during the isothermal compression and expansion processes. Also, the ideal cycle necessitates that the working fluid be either in the hot space or in the cold space. In the actual engine, there is always a small amount of fluid in the heater, regenerator, and cooler.

Figure 5-4 is a schematic of the mechanical arrangement for the engine. It shows the power piston, the displacer piston, the heater-regenerator-cooler side circuit, and the rhombic drive crank mechanism which provides the required phasing between the two pistons. For this application, it will be assumed that one crank shaft is geared to an alternator and the other crank shaft is geared to a starter motor. With proper counterweight on the gears, the inertia forces due to the reciprocating pistons can be cancelled to obtain very low vibration levels. All torsional moments

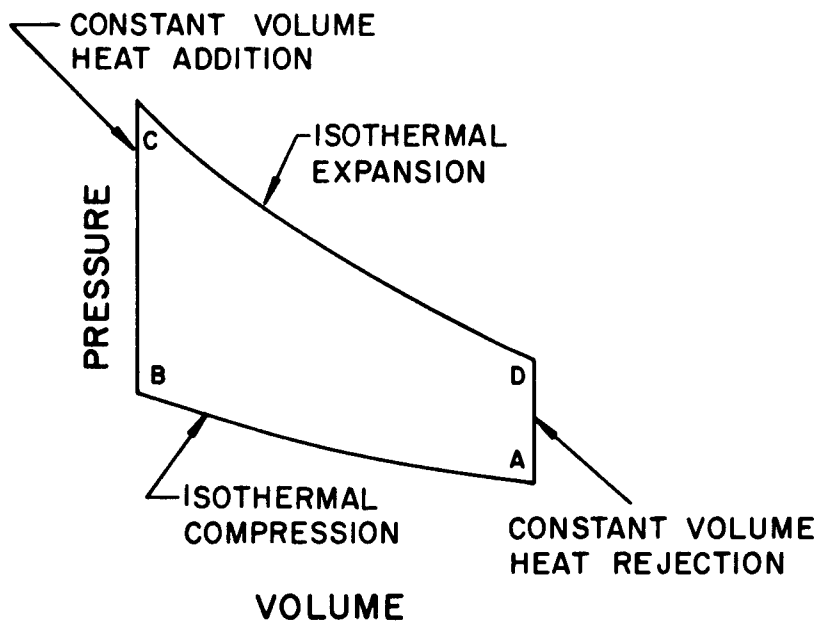


Figure 5-2. Pressure Volume Diagram for Ideal Stirling Cycle

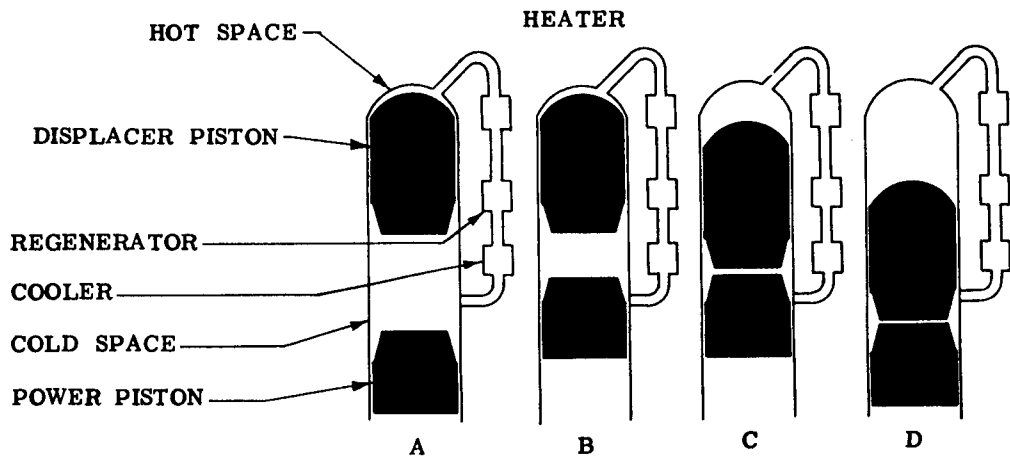


Figure 5-3. Stirling Engine Cycle Phases

can be cancelled by proper selection of the alternator and starter motor rotors.

The operating conditions for the Stirling Engines in the non-integrated power system are given in Table 5-2.

TABLE 5-2. STIRLING ENGINE OPERATING CONDITIONS

Brake output (per engine)	4.43 KW
Crankshaft speed	2400 rpm
NaK inlet temperature	1250° F
NaK Δ T	30° F
Mean cycle pressure	1500 psi
Working fluid	Dry Helium
Brake thermal efficiency	30%
Coolant inlet temperature	135° F
Coolant type	Propylene Glycol (60% by weight)

5.1.2 ALTERNATOR

The alternator selected for this application is a permanent magnet generator (PMG) with the following specifications:

1. Speed : 12,000 rpm
2. Rated Output : 3.68 KVA, 110/220 volt
3 φ , 400 cps
3. Efficiency at Rated Output : 84.6%

The two generators (one per Stirling engine) will be paralleled to supply the rated power to the station bus of 6.24 KW_e . The generator speed selected will result

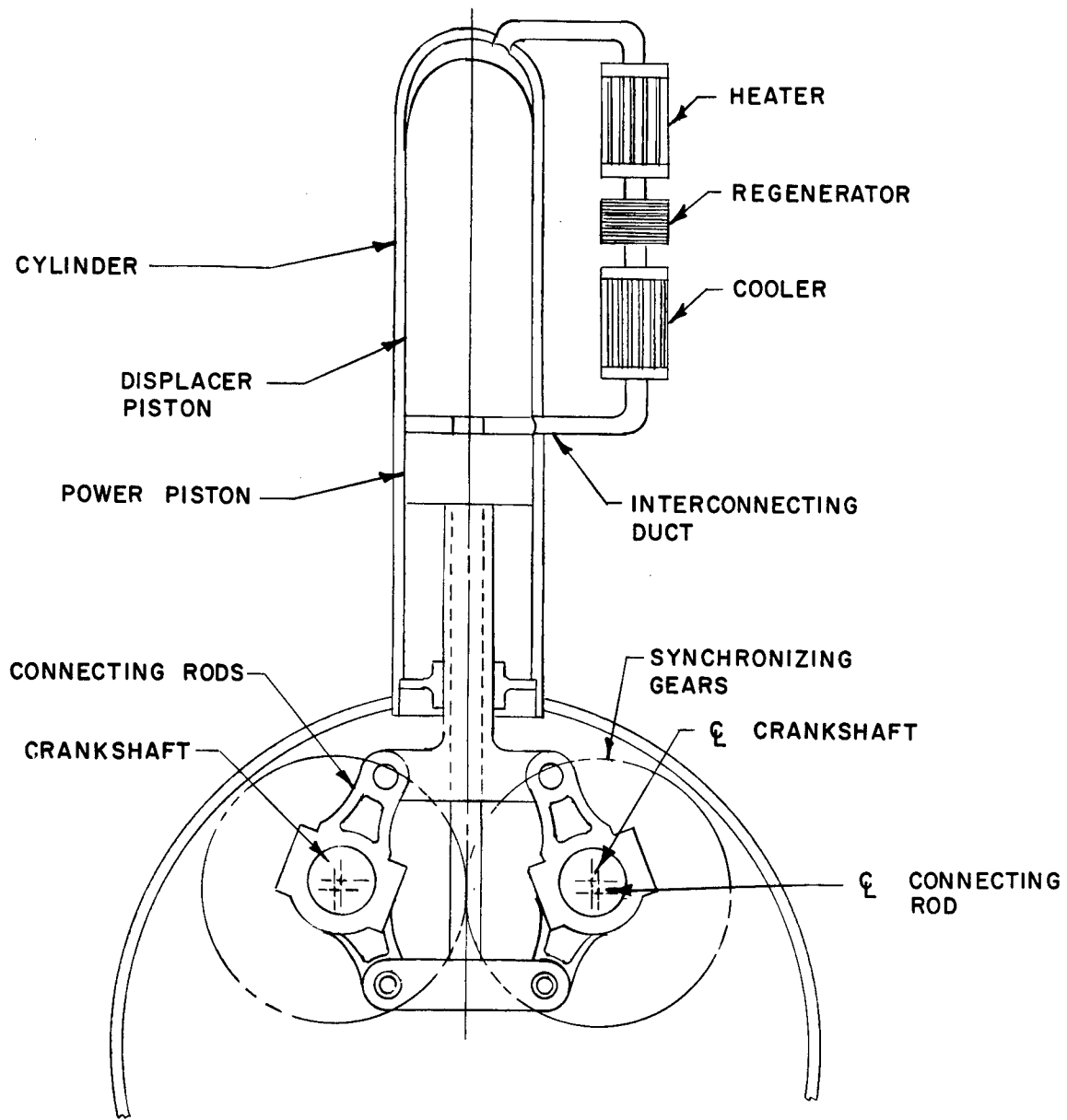


Figure 5-4. Schematic of Basic Stirling Cycle Engine

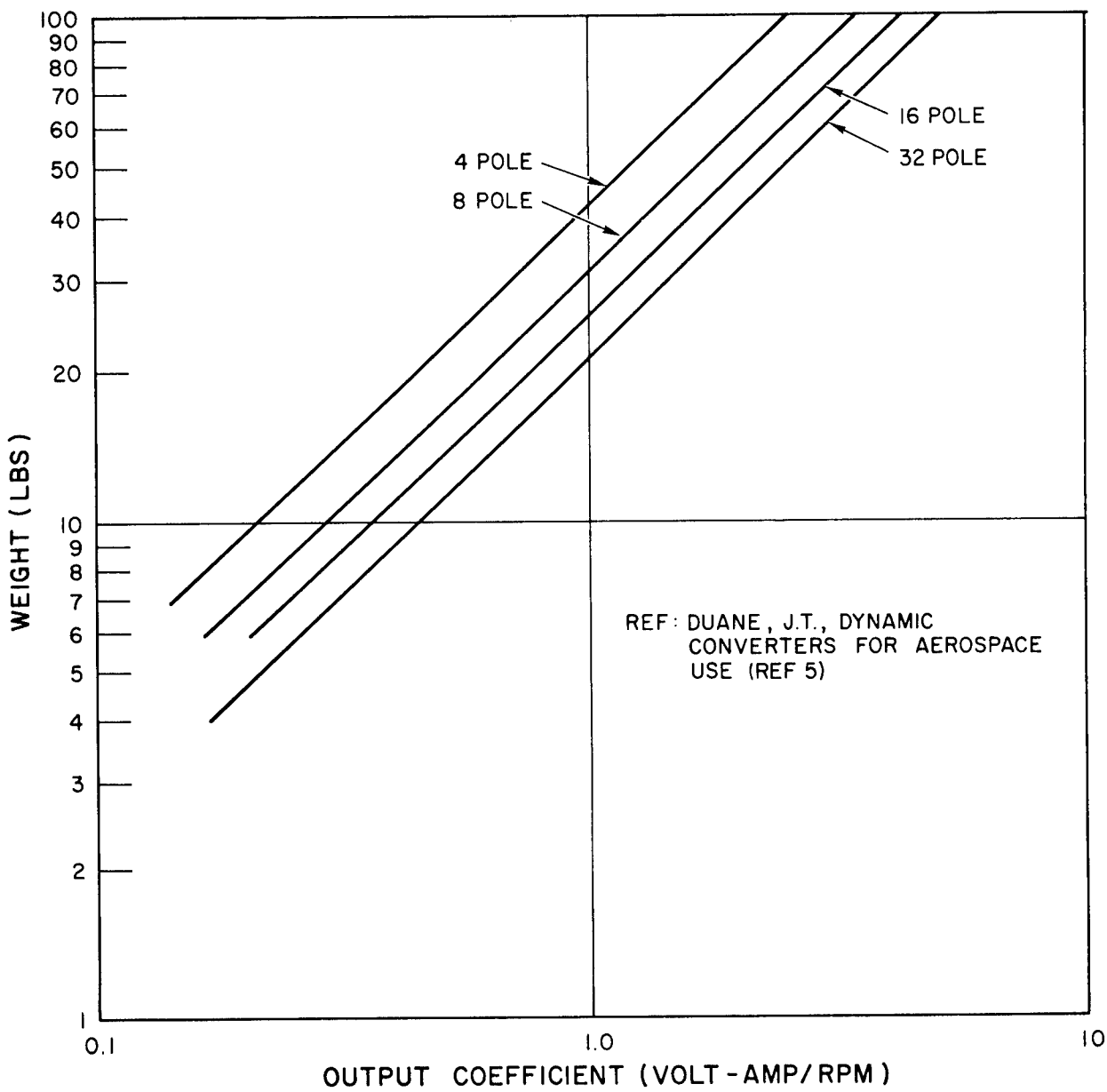


Figure 5-5. Weight Variation with Output for Space Application
Type Solid Rotor AC Generator

in a smaller generator size and weight if compared to a generator which is run at the crankshaft speed of 2,400 rpm. For example, two cases are considered to illustrate the generator weight saving by using a higher speed machine.

Case I: (generator speed = 12,000 rpm)

$$p = \frac{120f}{N}$$

where p = number of poles

f = frequency in cps

N = speed in rpm

$$p = \frac{120 (400)}{(12,000)} = 4 \text{ poles}$$

$$\text{Output coefficient} = \frac{\text{volt-ampere}}{\text{rpm}}$$

$$= \frac{3,680}{12,000} = .306 \frac{\text{V-A}}{\text{rpm}}$$

Referring to Figure 5-5 the generator weight for this output coefficient and number of poles is 14 pounds.

Case II: (generator speed = 3,000 rpm)

$$p = \frac{120f}{N} = \frac{120 (400)}{3,000} = 16 \text{ poles}$$

$$\text{Output coefficient} = \frac{3,680}{3,000} = 1.23 \frac{\text{V-A}}{\text{rpm}}$$

Referring to Figure 5-5, the generator weight for the output coefficient and number of poles is 31 pounds.

Alternator efficiency varies with power output as shown in Figure 5-6. This curve was obtained by utilizing the general shape of a similar curve obtained from Reference 6, and adjusting this "normalized shape" to agree with performance data on two General Electric brushless alternators.

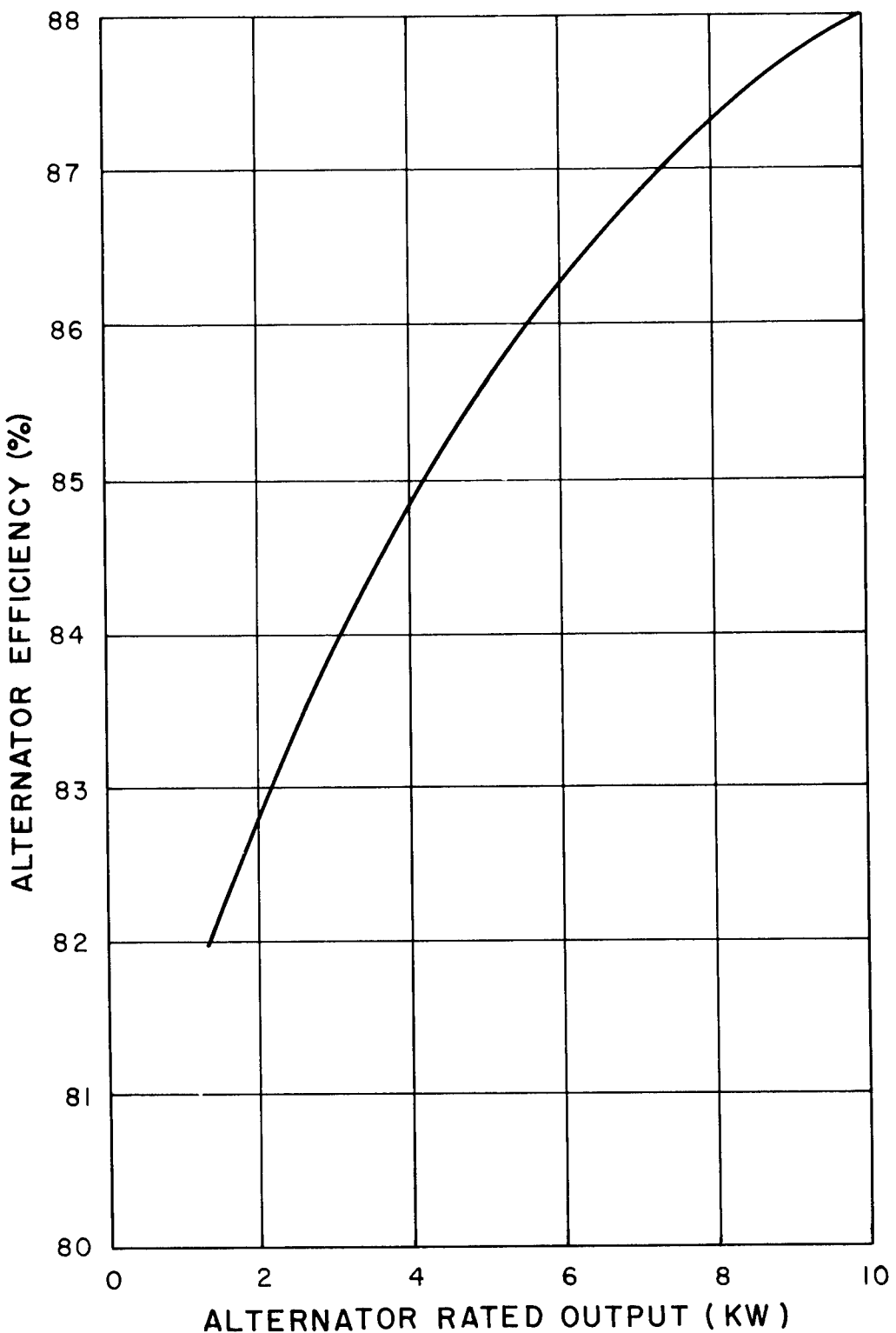


Figure 5-6. Estimated Alternator Performance

For this application, a 12,000 rpm, 4 pole, 400 cps Permanent Magnet unit was selected. Overall efficiency and starting considerations indicated the advisability of a single alternator per engine rather than two. This leaves the displacer crank available for a starter motor.

5.1.3 STARTER MOTOR

Starting of the engine is accomplished with an auxiliary starter motor. For this, a 400 cps induction motor is considered, geared to the displacer crank. Accordingly, rotation of the motor is opposite to the alternator direction of rotation. Assuming the motor weight and moment of inertia are made equal to that of the alternator, dynamic balance exists at all times.

5.1.4 ALTERNATOR AND STARTER MOTOR GEARING

With the synchronous speed of the alternator 12,000 rpm and the engine speed 2,400 rpm, a 5:1 speed increase is necessary between the engine cranks and the alternator and starter motor. For 6.24 kw net output, the weight associated with the gearing is estimated to be 6 lbs. With 3.12 kw net output, the weight is reduced to about 4 lbs.

5.1.5 SPEED CONTROL

Speed control is provided for by a dissipative load. At the design operating condition, it is estimated that 5% of the alternator net capacity will be dissipated as heat across a resistor. Considering that synchronous speed must be maintained for any fractional load, the estimated weight for the speed control is 140 lbs.

5.1.6 NaK AND COOLANT PUMPS

Pumping requirements are believed best met with a "canned" rotor pump configuration. This provides reliable operation without excessive losses (as, for example, might occur with a static, electro-magnetic pump for the NaK). Overall efficiencies (Hydraulic power output ÷ electrical power input) for the NaK and water pumps are assumed to be 20 percent and 30 percent respectively.

5.1.7 COOLANT RADIATOR

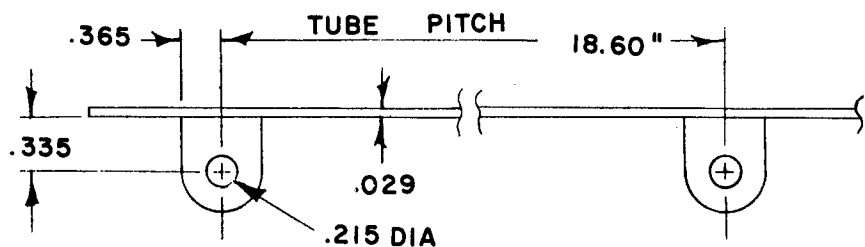
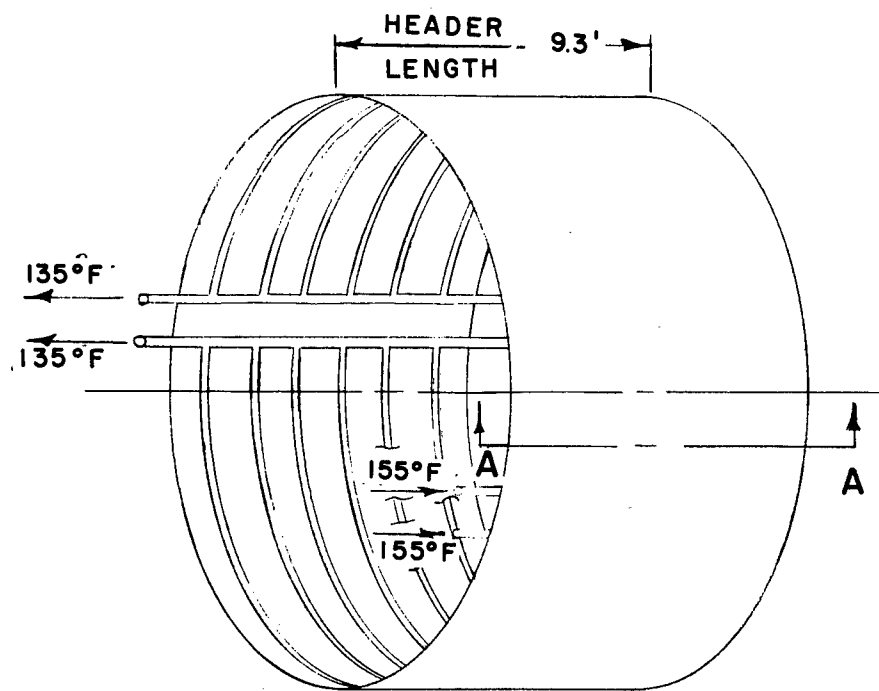
5.1.7.1 Isotope Stirling

The radiator selected for use with the Isotope Stirling power system is a cylindrical structure which is integral with the skin of the vehicle, as shown in Figure 5-7. Two independent circuits have been selected to be consistent with the redundant cooling of the isotope heat source. An aqueous solution of propylene glycol (60 percent by weight) has been selected for use as a coolant because the freezing point of -74° is well below the radiator effective sink temperature of -60°F . Consequently, if the circulation is stopped in one circuit, the coolant will not freeze in the radiator. The radiator was designed for a 1 percent probability of failure due to micrometeroid penetration in the course of a year's life. Table 5-3 gives the pertinent design parameters for the engine coolant space radiator for the non-integrated power systems. Figures 5-8 and 5-9 show the total weight, total area, pressure drop and header length of the radiator as a function of the total radiated power.

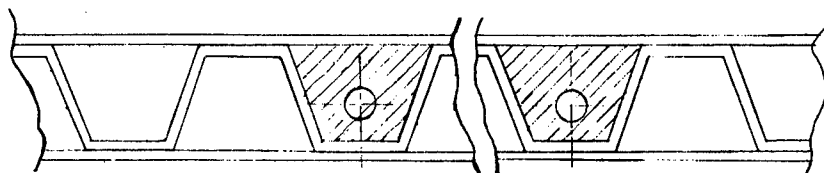
5.1.7.2 Solar Stirling Non-Integral Radiator

The radiator considered for this application is a 250-inch cylinder, separated from the vehicle to allow both cylindrical surfaces to radiate. Inlet and outlet coolant

**NON - INTEGRATED SYSTEM RADIATOR
INTEGRAL WITH SKIN**



**SECTION A-A
IDEALIZED INTEGRAL RADIATOR**



**SECTION A-A
PRACTICAL INTEGRAL RADIATOR**

Figure 5-7. Isotope Stirling System Radiator Integral with Skin

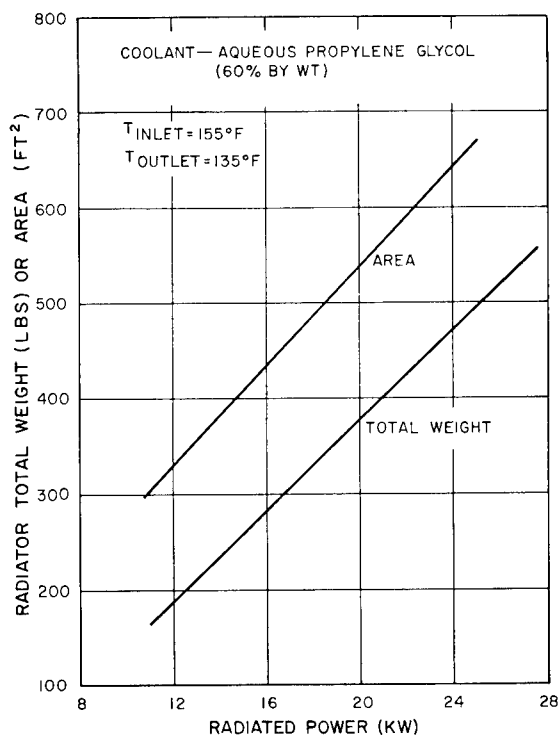


Figure 5-8. Characteristics of Engine Coolant Radiator
(Integral with MORL Vehicle)

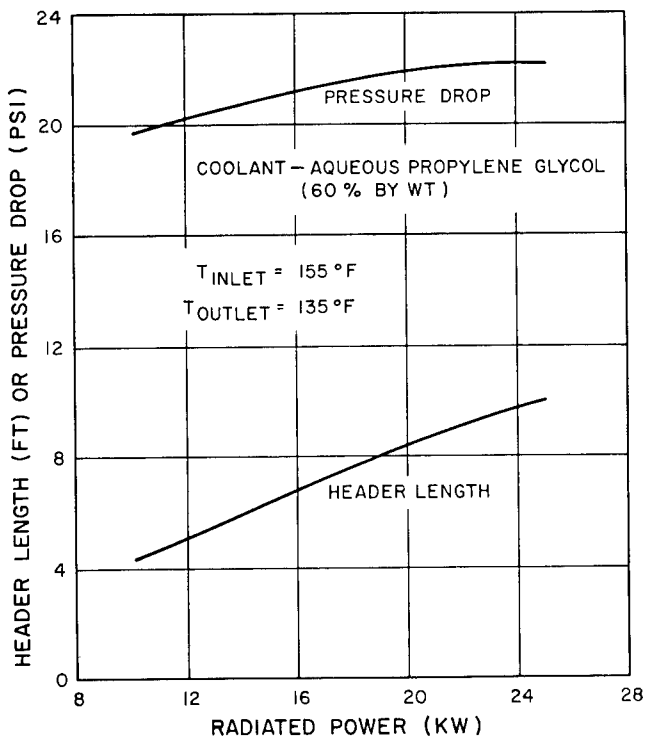


Figure 5-9. Characteristics of Engine Coolant Radiator
(Integral with MORL Vehicle)

TABLE 5-3. COOLANT RADIATOR DESIGN PARAMETERS

Radiated Power	23.26 KW
Header Length	9.3 ft
Tube Length	34 ft
Total Radiator Area	625 ft ²
Inlet Temperature	155° F
Outlet Temperature	135° F
Number of Tubes/Circuit	6
Tube ID	.215 in
*Total Radiator Weight	455 lbs
Coolant Type	60% by Wt Propylene Glycol
Total Flow Rate	4,670 lbs/hr
Pressure Drop/Circuit	22 psi
Ideal Pump Power	.088 KW
Fin Thickness	.029 in
Header ID	.385 in
Header OD	.900 in

temperature are, respectively 155° F and 135° F. Line sizes are established based upon minimum system weight, using .30 as the combined coolant pump-motor efficiency , and 125 lbs/kw system weight. Accordingly, the pumping penalty is 417 lbs/kw of hydraulic power output. Combining this pumping penalty with an effective sink temperature of 400° R results in the radiator characteristics shown in Figures 5-10 and 5-11.

*The radiator weight includes the weight of the fins, tubes, headers, and fluid inventory , but does not include the weight of the associated structure required to make the radiator integral with the vehicle skin.

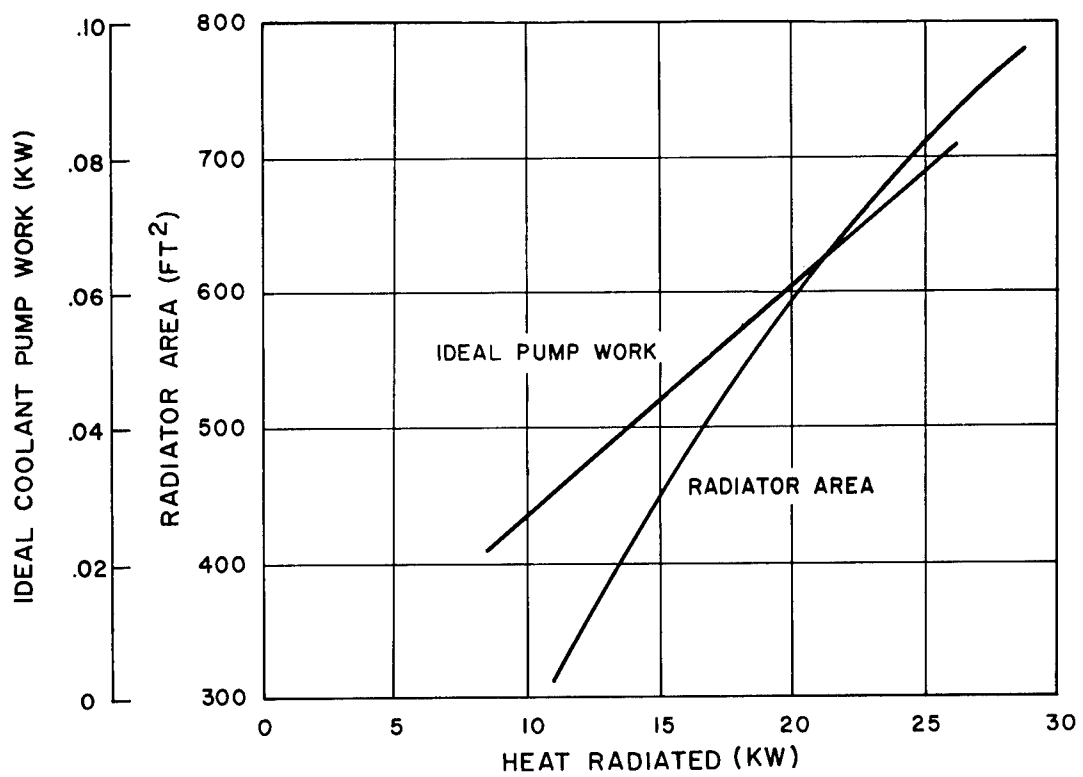


Figure 5-10. Solar Stirling Cycle Radiator Characteristics

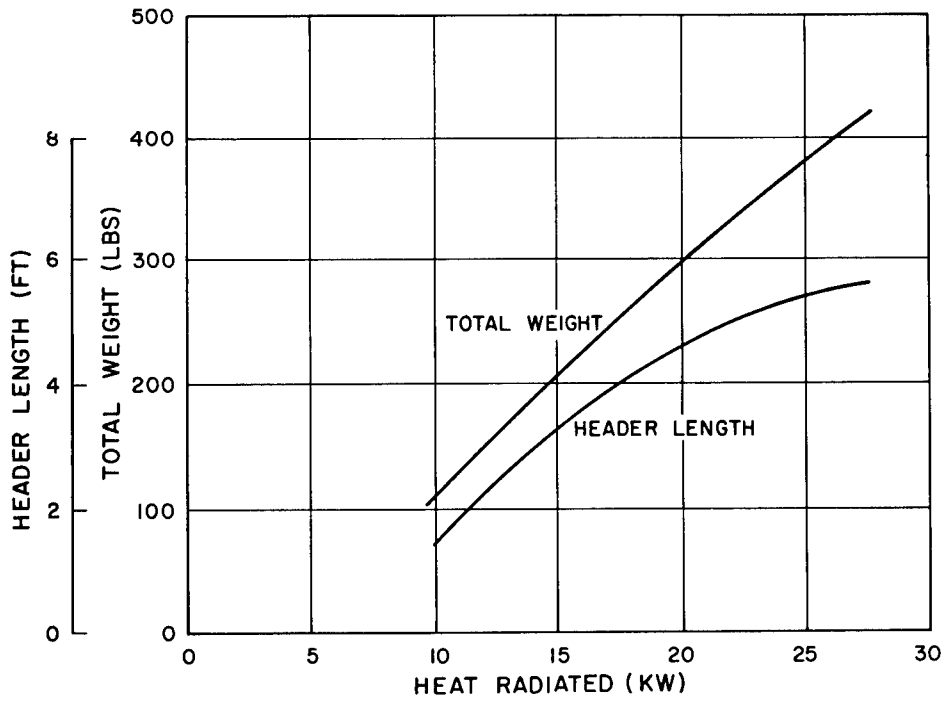


Figure 5-11. Solar Stirling Cycle Radiator Characteristics

5.2 NON-INTEGRATED SOLAR STIRLING SYSTEM

In this system radiation impinging upon the collector surface is reflected into the absorber cavity where it heats circulating NaK. An excess of heat flux into the absorber during operation in sun light effects a phase change in the Lithium Hydride, storing thermal energy to enable engine operation in darkness.

5.2.1 SOLAR COLLECTOR AND ABSORBER

Size and weight estimates for the solar collector and absorber are based on an overall collection efficiency incorporating .90 reflectivity, 0.1° misorientation error and 6 percent shadow. Accordingly, for an absorber whose temperature is 1710°R , optimum performance occurs with an aperture to collector diameter ratio

$$D_a/D_c = .0208,$$

which yields an overall collection efficiency

$$\text{OCE} = .817$$

With an absorber sized for sufficient heat storage to afford operation in darkness, and with an optimum amount of insulation thickness (based upon minimum system weight), the absorber heat losses

$$Q_{A_{\text{ABS}}} = 0.04 \text{ kw}$$

Accordingly, for a given heat input to the engine, $Q_{A_{\text{ENG}}}$, and a 94 minute period of which 58 minutes (minimum) are in light, the heat required by the absorber

$$Q_{A_{\text{ABS}}} = \frac{94}{58} (Q_{A_{\text{ENG}}} + 0.04 \text{ kw})$$

The absorber consists of two parallel tubes through which the NaK flows. The LiH is located in the shaded space shown in Figure 5-12. The weights quoted do not include the conical shell located in front of the absorber surface itself. The pumping power reported is the actual pumping power, using an overall pump efficiency of 20 percent. The LiH weight estimate includes 10 percent contingency.

The sizing of the absorber elements is based upon two primary requirements:

(a) enough Lithium Hydride (with a 10 percent contingency) must be contained to provide energy for operation during periods of darkness, and (b) the system must be designed for minimum weight. A pump with an over-all motor-pump efficiency of 20 percent was selected. The pump weight is 125 lbs/KW of net power output (or 625 lbs/KW of hydraulic output power). Accordingly with 1220°F NaK inlet temperature, the absorber characteristics as a function of its steady state power capability is shown by Figures 5-13, 5-14 and 5-16.

In accordance with guide-lines established for the collector, it is assumed to be of rigid construction, and to weigh $1.0 \text{ lb}/\text{ft}^2$ of projected area.

5.2.2 TEMPERATURE CONTROL

Temperature control is effected by means of a disk which covers the aperture of the absorber. The disk is solid, covering the absorber during periods of darkness to keep the re-radiation losses of the absorber to a minimum. During light operation, the aperture is uncovered until the NaK temperature becomes greater than 1255°F. When this occurs, the disk is actuated to re-cover the aperture thus maintaining the NaK temperature at its nominal value of 1255°F. An estimated weight for the temperature control disk and associated sensing and actuation is six pounds. Average power requirements for this can be made very low and are assumed negligible.

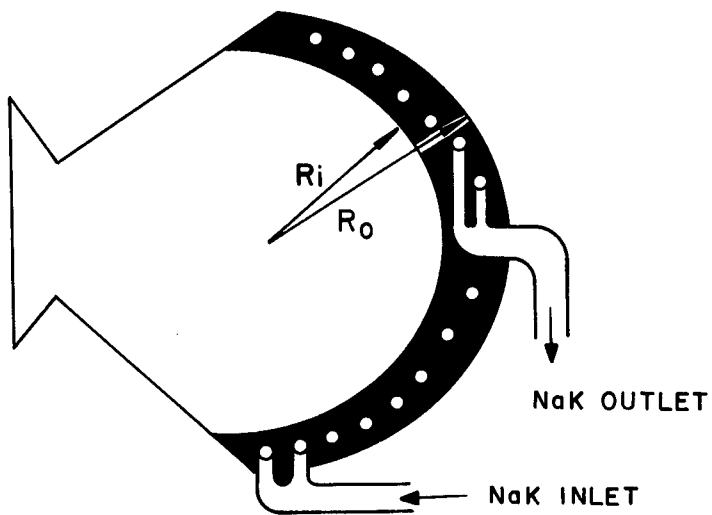


Figure 5-12. Converging-Diverging Conical Shell Aperture

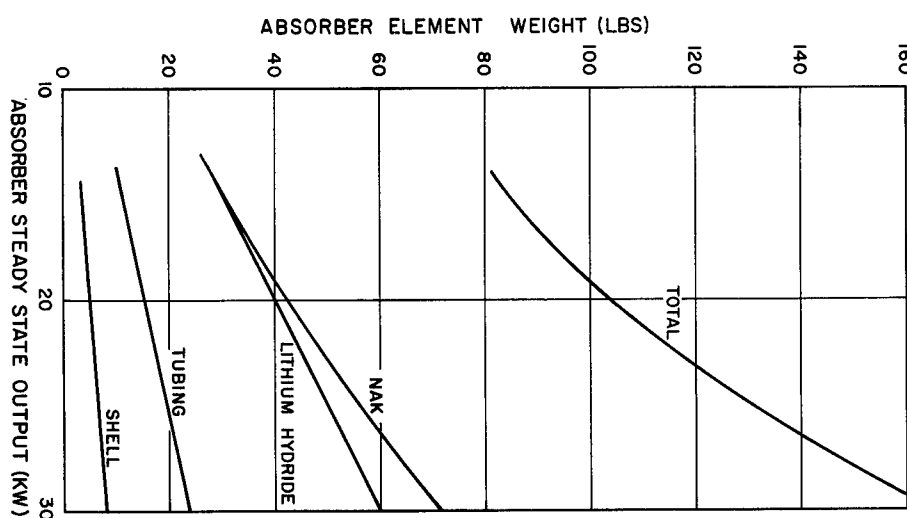


Figure 5-13. Stirling Cycle Absorber Characteristics:
Element Weight Vs. Output Power

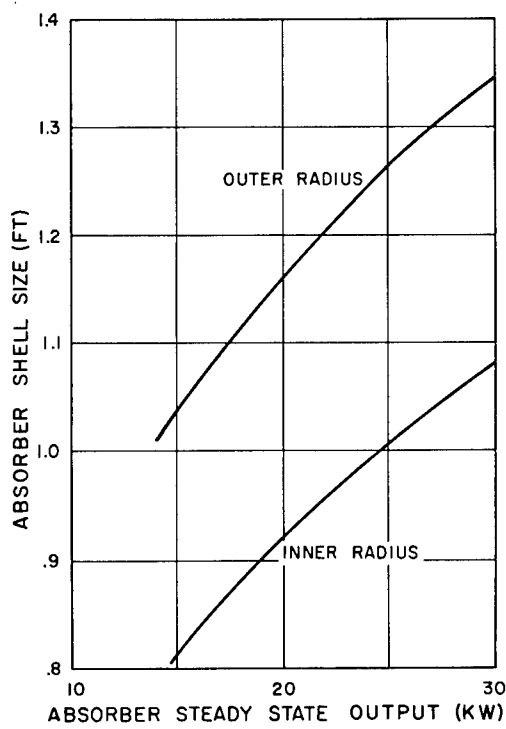


Figure 5-14. Stirling Cycle Absorber Characteristics:
Shell Size Vs. Output Power

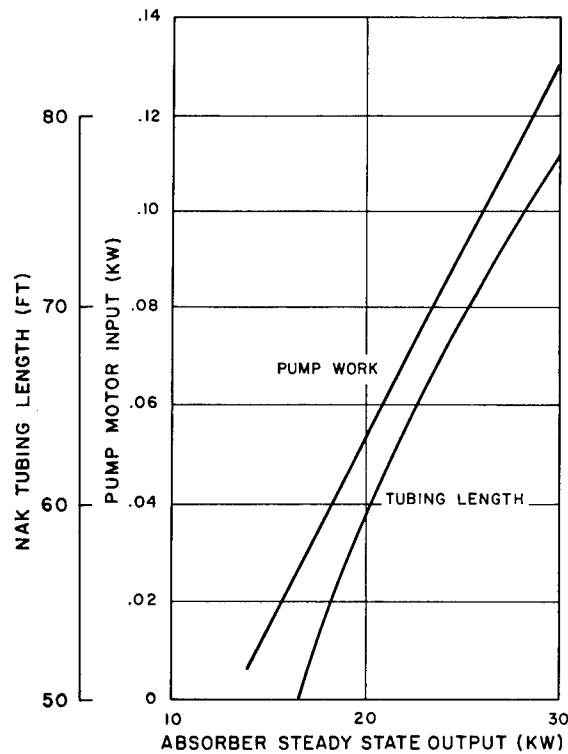


Figure 5-15. Stirling Cycle Absorber Characteristics:
NaK Tubing Length Vs. Output Power

TABLE 5-4. WEIGHT ESTIMATE FOR NON-INTEGRATED SOLAR STIRLING CYCLE

The estimated weight for the non-integrated Solar Stirling Power Cycle producing 6.24 net kw, with two parallel systems sharing the load is:

Batteries	600 lbs
Collector	449
Absorber	162
Stirling Engines (2 @ 80 lbs)	160
Radiator (including coolant)	365
Alternator Gearing (2 @ 6 lbs)	12
Alternators (2 @ 14 lbs)	28
Starter Motors (2 @ 14 lbs)	28
Speed Control	140
Coolant Pump (2 @ 9 lbs)	18
NaK Pumps (3 @ 23 lbs)	69
NaK Inventory	3
Piping	54
Structure	<u>229</u>
Total Non-Integrated System Wt	2,317
Life Support System	<u>622</u>
Total Non-Integrated System Wt	2,939

5.3 DESCRIPTION OF INTEGRATED SOLAR STIRLING SYSTEM AND DESIGN

The integrated, solar energy powered Stirling cycle interface with the Life Support equipment is shown by the system flow schematic Figure 5-16. Heat is provided to the Life Support equipment from two sources, the 155° F coolant and the 1250° F NaK.

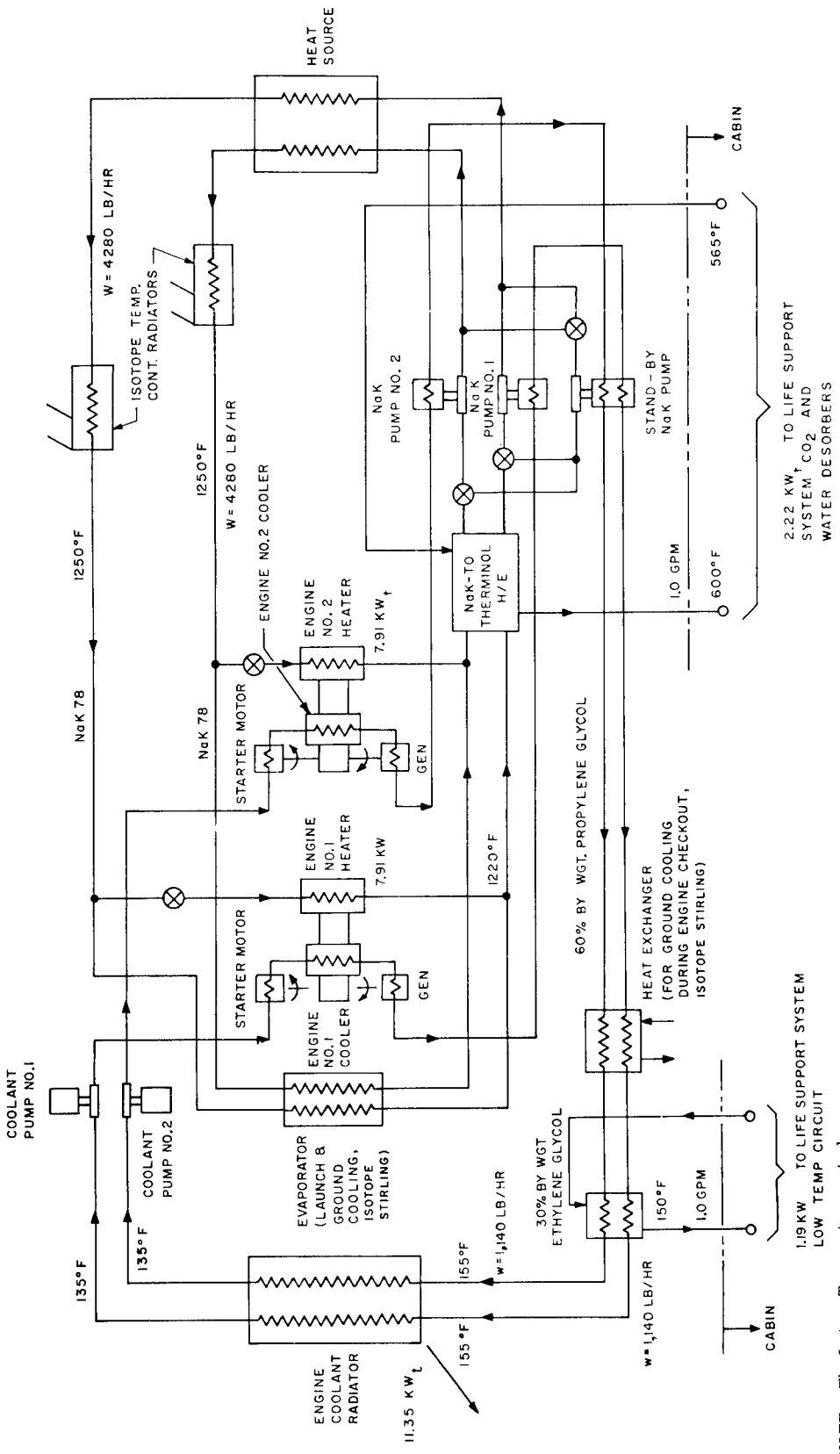


Figure 5-16. Stirling Cycle

Figure 5-17 shows the layout of the integrated power system components.

With thermal integration, the electrical load is modified by two factors:

1. It is reduced by the equivalent amount of heat transferred to the life support equipment.
2. It is increased by the pumping requirements necessary to the circulation of the heat transfer fluids.

The energy balance for the integrated power system is as follows:

TABLE 5-5. ENERGY BALANCE FOR INTEGRATED SOLAR STIRLING CYCLE

Electrical load to station bus (non-integrated system)	6.24 kw _e
Net electrical power saving as the result of thermal integration	2.96 kw _e
Electrical load to station bus (integrated)	3.28 kw
NaK pumping power	0.23 kw _e
Coolant pumping power	0.18 kw _e
Dissipative control (5% of load)	0.16 kw _e
Generator output	3.85 kw _e
Engine output ($\eta_{gear} = .98$ $\eta_{alt} = .827$)	4.75 kw _e
Heat input to engine ($\eta_{eng} = .30$)	15.82 kw
Total life support heat loss from high temperature loop	0.35 kw _t
Usable heat transferred from NaK circuits to life support system	1.87 kw _t

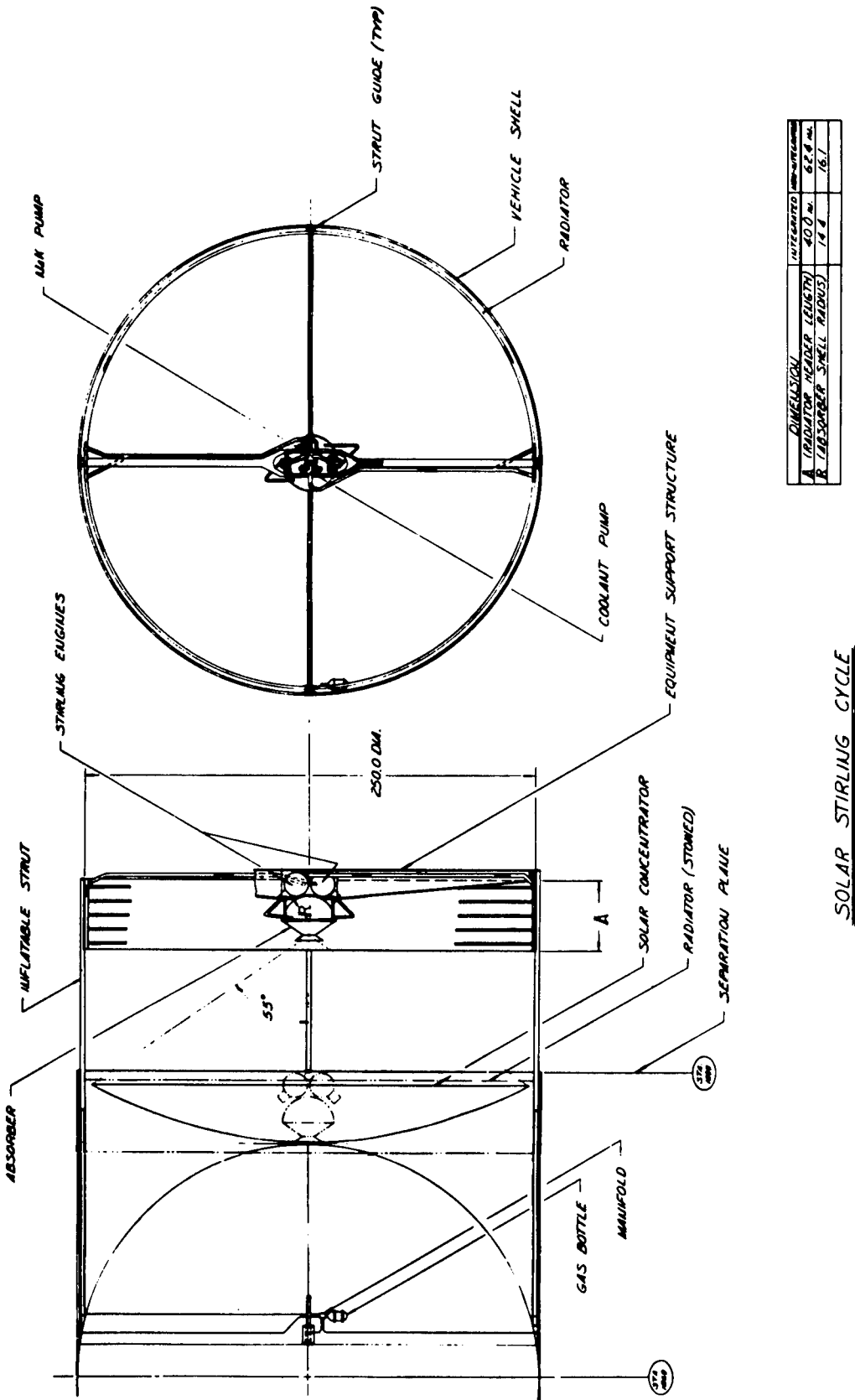


Figure 5-17. Power System Component Layout - Solar Stirling

Heat delivered by absorber	18.04 kw _t
Total life support from low temperature circuit	0.16 kw _t
Usable heat transferred from engine coolant circuits to life support system	1.03 kw _t
Net heat rejected by engine coolant radiation	11.35 kw _t

TABLE 5-6. WEIGHT ESTIMATES FOR INTEGRATED SOLAR STIRLING CYCLE

The estimated weight for the integrated Solar Stirling Cycle is as follows:

Batteries	600 lbs
Collector	300 lbs
Absorber	105 lbs
Stirling Engines (2 @ 60 lbs)	120 lbs
Radiator (includes Fluid inventory)	180 lbs
Alternator Gearing (2 @ 5 lbs)	10 lbs
Alternators (2 @ 8 lbs)	16 lbs
Start Motors (2 @ 8 lbs)	16 lbs
Speed Control	80 lbs
Coolant Pumps (2 @ 7 lbs)	14 lbs
NaK Pumps (3 @ 17 lbs)	51 lbs
NaK Thermal Heat Exchanger	2 lbs
NaK Inventory	2 lbs
Thermal Pump	10 lbs
Piping	38 lbs
Structure	<u>151</u> lbs
Total Integrated Power System Wt	1695 lbs
Life Support System	<u>678</u> lbs
Total Integrated System Wt	2373 lbs

5.4 NON-INTEGRATED ISOTOPE STIRLING CYCLE POWER SYSTEM ANALYSIS

5.4.1 INTRODUCTION

This section discusses the system parameters and components associated with the thermal integration of an Isotope Stirling power system with the life support systems. It has been assumed for this comparative study that the system constraints be consistent with the Manned Orbital Research Laboratory (MORL) being sponsored by NASA. A weight breakdown of the non-integrated Stirling power system is given in Table 5-7.

TABLE 5-7. POWER SYSTEM WEIGHT BREAKDOWN, NON-INTEGRATED SYSTEM

1. Isotope heat source	
a. Fuel and heat exchanger	= 237 lbs
b. Shielding	= 530
	767 lbs
2. Heat source temperature control radiators (2)	35 lbs
3. Engines (2 @ 80 lbs)	160 lbs
4. Engine speed and power controls	140 lbs
5. Alternators (2 @ 14 lbs)	28 lbs
6. Alternator gearing (2 @ 6 lbs)	12 lbs
7. Starter motors (2 @ 14 lbs)	28 lbs
8. Coolant pumps (2 @ 9 lbs)	18 lbs
9. NaK pumps (3 @ 23 lbs) (includes one stand-by)	69 lbs
10. Engine coolant radiator (integral with MORL structure and includes fluid inventory inside radiator)	455 lbs
11. Ground cooling heat exchanger	4 lbs

12.	Piping	69 lbs
13.	NaK inventory (includes 10% contingency)	3 lbs
14.	Structure	
	Additional structure to mount engines and to support isotope heat source	117 lbs
	Savings in structural weight as the result of using an integral engine coolant radiator	-180 lbs
15.	Batteries	<u>600</u> lbs
	Power System Total Weight	2,286 lbs

5.4.2 ISOTOPE HEAT SOURCE

The heat for the Isotope Stirling power system is supplied by the radioisotope Plutonium 238. The following design guidelines apply to the isotope heat source and associated heat exchanger:

- a. The fuel package shall be designed to survive and maintain containment of the fuel for any conceivable accident; either on the pad, during launch, or in orbit.
- b. The fuel package shall be designed to contain fuel for the length of time required for nuclear safety considerations in case it is jettisoned at sea and sinks and cannot be recovered.
- c. The fuel package shall be designed for separation, atmospheric re-entry, and recovery for re-processing.
- d. The isotope heat exchanger shall be designed with two independent isotope coolant circuits, one for each of the Stirling engines, to maximize reliability.

- e. The fuel shall be loaded aboard the spacecraft prior to launch. No refueling is planned for the duration of the mission (one year).
- f. Consideration of safety requirements in depth is beyond the scope of the study.

5.4.2.1 Shielding

Shielding is provided based on allowing a maximum dose of 30 rem per year. The heat exchanger is located comparatively close to the crew quarters and, consequently, the fraction of time spent by the crew at various stations within the pressure vessel can have a significant effect on the shielding required. To account for this factor, the time estimates for the various duty stations were made for this study. These estimates are given in Table 5-8. Based on a one year duty cycle, the times listed are those expected to be spent in the various occupations. The corresponding distances considered average for each of these occupations are also listed in Table 5-8 and shown in Figure 5-18.

The dose due to gamma will be 9.6 rem, or 32% of the total dose. This is based on the assumption that no gamma shielding is provided except that of the heat exchanger and vehicle structure and that these structures are equivalent to 1 cm of steel. The thickness of lithium hydride required to limit the neutron dose to 20.4 rem is shown as a function of power level in Figure 5-19.

TABLE 5-8. AVERAGE CREW DUTY STATIONS

<u>Location No.</u>	<u>Purpose</u>	<u>Time (Hours)</u>	<u>Distance (Inches)</u>
1	Sleep	2900	210
2	Recreation	1600	120
3	Duty	4100	255
4	Inside Maintenance	120	45
5	Outside Maintenance	15	125

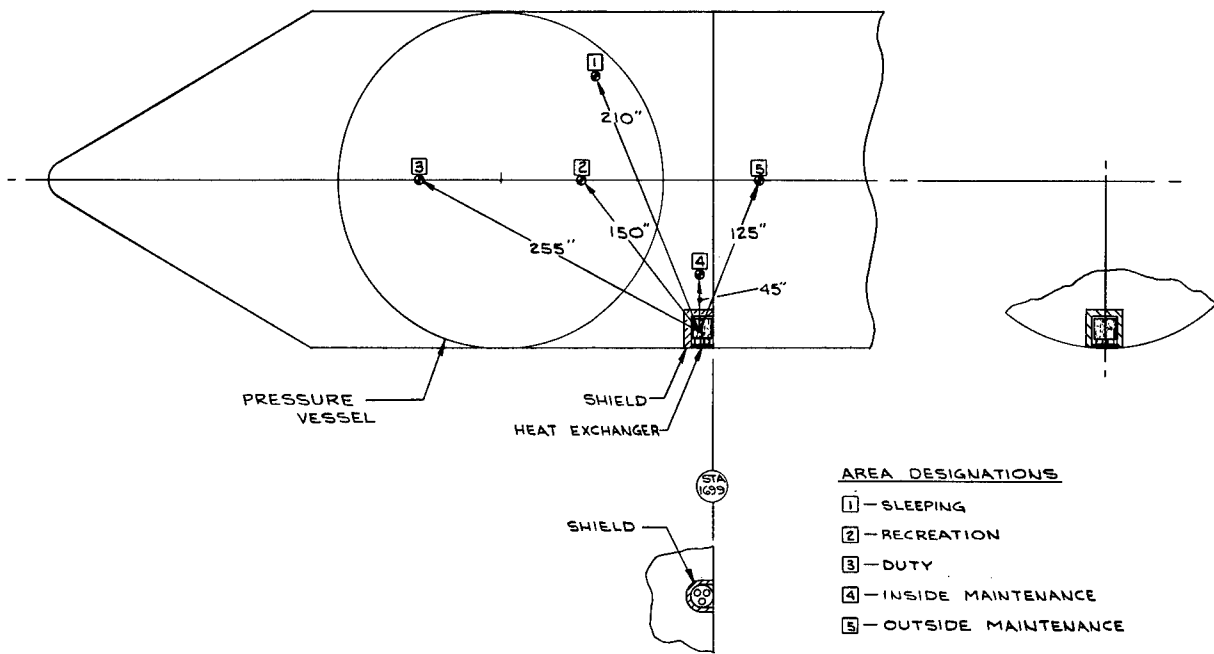


Figure 5-18. Heat Exchanger Location on Vehicle

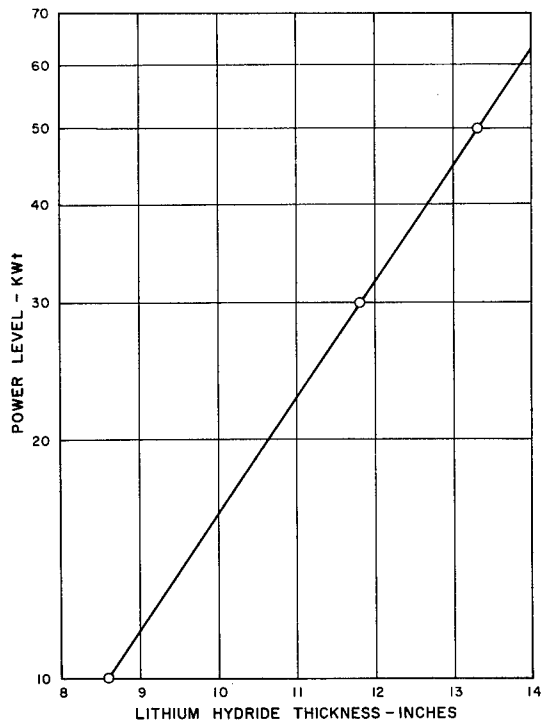


Figure 5-19. Lithium Hydride Shield Thickness

5.4.2.2 Isotope Cooling

The isotope must be cooled, essentially, continuously. During the loading period, during the waiting period on the launch pad, and during launch, this can be accomplished by the operation of one or more of the coolant loops with heat rejection via the space radiator or by suitably designing the heat exchanger so as to allow direct evaporative cooling.

If significant thickness of shielding is required, it is not practical to disperse the individual fuel capsules to allow direct radiation heat rejection because of the significant weight penalty incurred in the shielding of individual capsules rather than clusters of fuel capsules.

Upon completion of the mission, cooling must also be provided during the return of the fuel capsules to earth. The combined factors of the high cost of Pu-238 (about \$63,000,000 for 30 KW) and the significant radiological hazards resulting from the dispersal of the isotope in the atmosphere in the event of capsule burnup will likely require that provision be made for the intact return of the capsules at mission conclusion. The design criteria will also likely require that the capsules survive all forms of vehicle abort, partial orbit injection, etc.

5.4.2.3 Fuel Capsule

The fuel capsule design is shown in Figure 5-20. The fuel material is PuO_2 and the clad may be Haynes -25 or Hastelloy C. Both of these materials are adequate to 1650°F . The capsule includes a void volume to allow for the pressure buildup due to the helium produced in the decay of Pu-238. The void may be included as shown in Figure 5-20 by separating the fuel with a perforated plate or by reducing fuel density to provide interstitial voids.

The clad thickness must be sufficient to contain the PuO_2 during accidents and for about 10 half lives (~890 years). The thickness required for intact accident survival will depend upon the safety criteria, the mission and launch vehicle and the particulars of the heat exchanger design. The heat exchanger structure, in particular, can provide significant protection in the survival of high velocity impact.

The maximum helium pressure will occur many decades after encapsulation, depending upon the details of the capsule design. For constant temperature environment with convective cooling the pressure is approximately given by:

$$P(t) = \frac{W_{238} R}{V} \left[1 - e^{-t\lambda} \right] \left[(\bar{T} - T_0) e^{-t\lambda} + T_0 \right]$$

where:

$P(t)$ = pressure

t = time

W_{238} = moles of Pu-238

R = gas constant

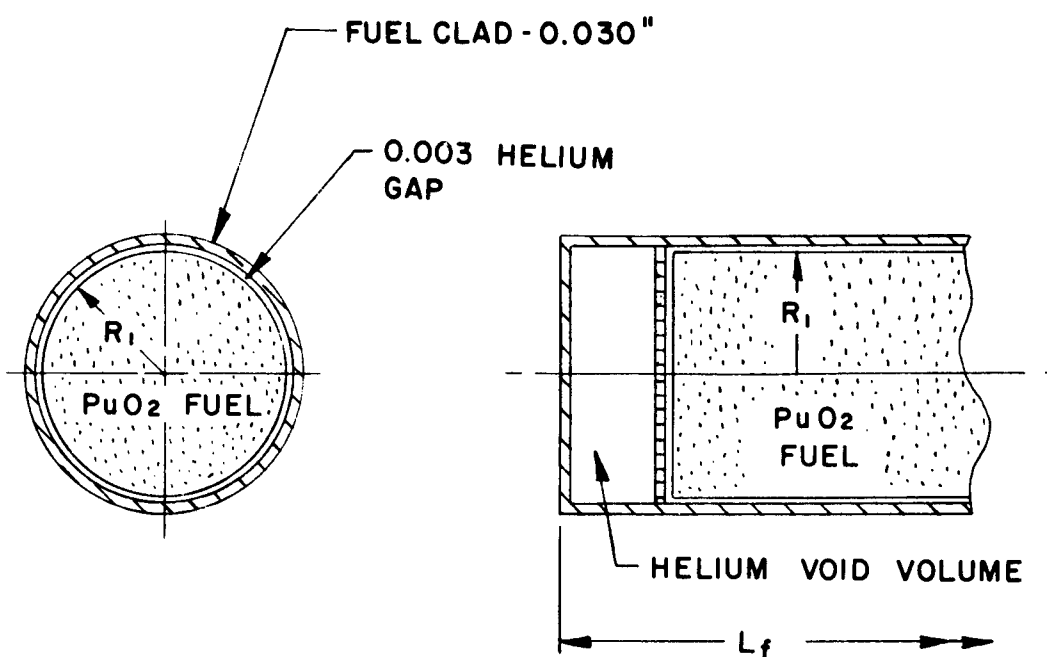


Figure 5-20. Fuel Capsule

λ	= decay constant of Pu-238
\bar{T}	= average fuel temperature at beginning of life
T_o	= ambient temperature
V	= void volume

5.4.2.4 Heat Exchanger - General

The heat exchanger design must be such as to allow the capsules to be loaded only a short time prior to launch and the loading operation must be simple to minimize the time and, therefore, the dose received during the loading operation. In addition, to assure continued cooling of the isotope in the event of failure of a loop, two complete cooling loops must be provided.

To meet these requirements, a "pressure-tube" type of heat exchanger is used. The basic pressure tube is shown in Figure 5-21. It consists of two concentric tubes which form an annular flow passage. Dividers are used between the tubes to provide separate flow passages. In Figure 5-21 flow channels "A" are fed from a common header and channels "B" are fed from a common but independent header. The design must meet maximum fuel and clad temperature limitations when only one loop is operable. The individual tubes are positioned horizontally on the vehicle and the fuel capsules slide into the fuel cavity. The heat from the capsule may be conducted or radiated to the inner wall of the heat exchanger tube. The temperature differential across the gap is substantial in radiation, and therefore a conduction medium is desirable. Conduction can be provided by wrapping the fuel capsule with indium or lead foil which will fuse to both walls to provide the necessary heat transfer path, or the gap may be flooded with a liquid metal such as NaK. A cross-section of an assembled tube using a NaK heat transfer medium is shown in Figure 5-22.

The individual tubes may be assembled on a triangular pitch, as shown in Figure 5-23 to form a heat exchanger. A compact array, with a length to diameter ratio

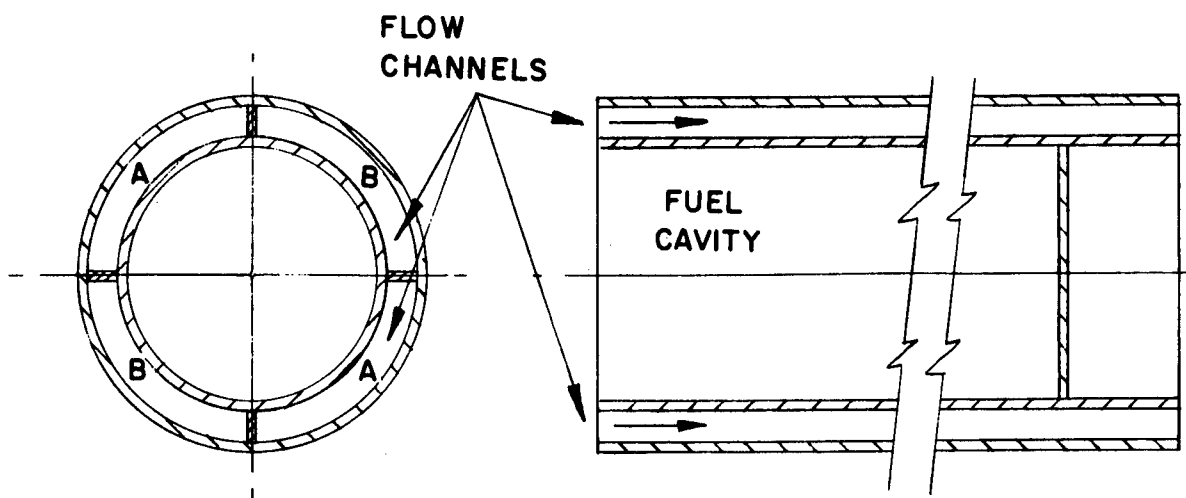


Figure 5-21. Individual Heat Exchanger Tube

of about 1.0, will result in minimum shield weight. Consideration of the criticality problem with a close-packed array of Pu-238 was excluded from the study scope.

The flow channels are provided with suitable inlet and outlet connections, as shown in Figure 5-24. The inner tubes of each heat exchanger tube are extended to the side of the vehicle and welded into a common tube sheet. After the fuel capsules are inserted, a blind cover plate is fitted over the tube sheet and bolted tight. It may also be seal welded. The fuel cavity is flooded with NaK to provide a heat transfer medium between capsule and heat exchanger tube.

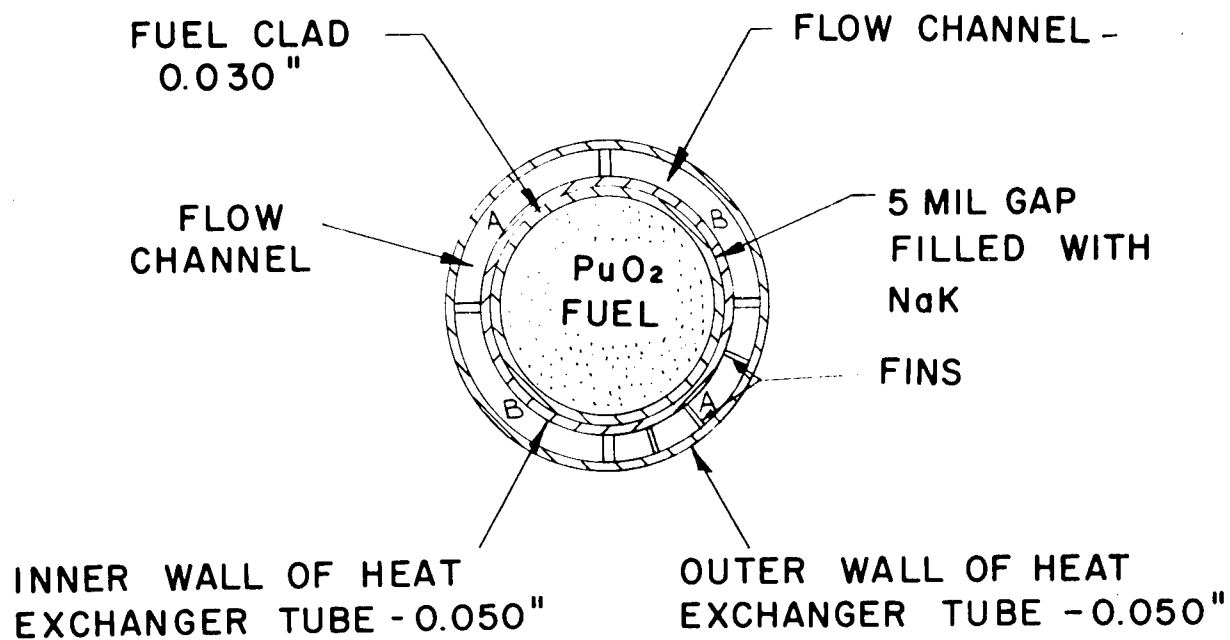


Figure 5-22. Fuel Capsule and Heat Exchanger Tube

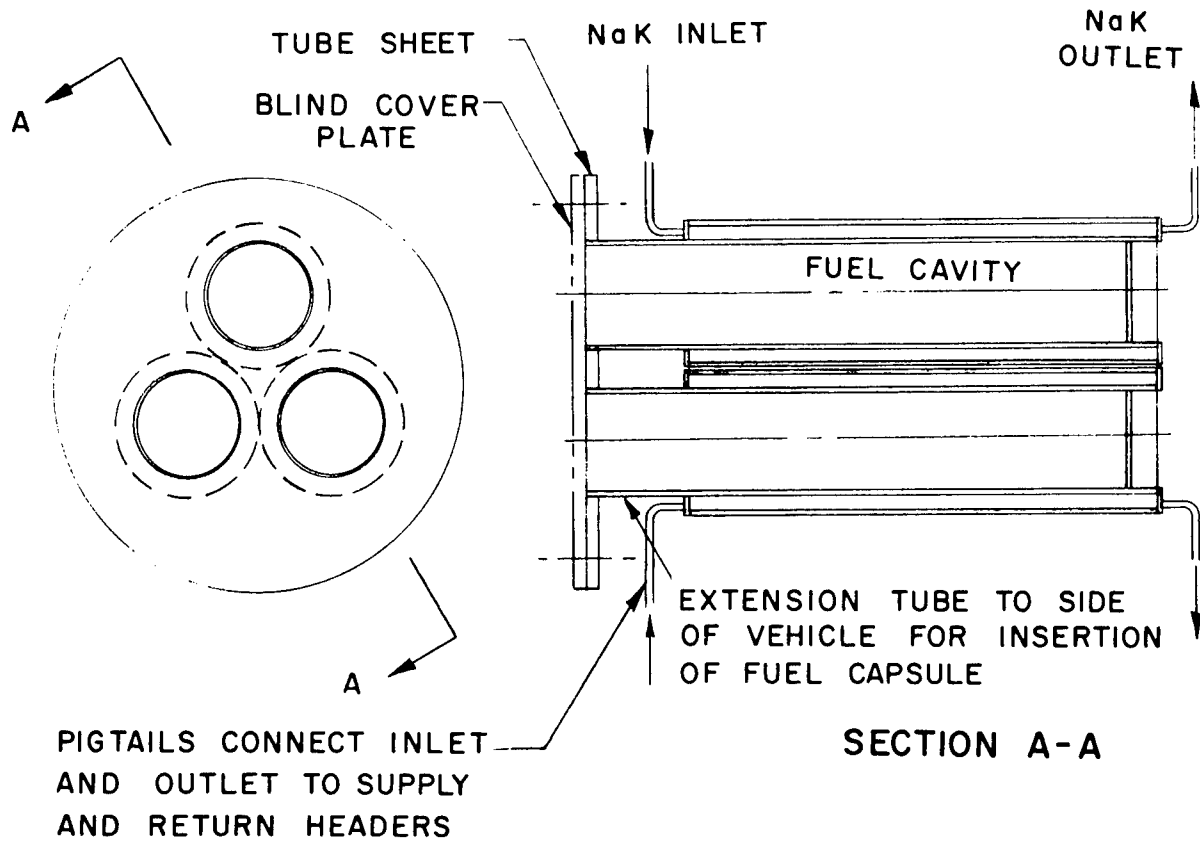


Figure 5-23. Heat Exchanger Assembly

If the flow loops are inoperative during the loading operation, the capsule heat may be removed by passing air over the exterior of the heat exchanger tubes or by enclosing the tubes in a shell and providing evaporative cooling.

The heat exchanger fits within the shield, as shown in Figure 5-25, and the exchanger and shield are mounted in the vehicle as shown in Figure 5-18. The shield is open on the two sides that face away from the crew compartments because there is no structure in these directions that can cause neutron scattering.

5.4.2.5 Heat Exchanger Design

The heat exchanger is provided with two independent NaK cooling loops, as shown in Figure 5-22. Either loop can remove design power of 32 KW with a maximum NaK temperature of 1250° F.

Minimum generator weight is obtained with large diameter fuel elements, as shown in Figure 5-16. This relationship is a result of the lower fraction of weight that must be used to contain the PuO₂ fuel in larger capsules. Though weight decreases with capsule radius, temperature increases as shown in Figure 5-27. The maximum design clad temperature of 1650° F is not limiting. The melting point of PuO₂ is about 4100° F and a margin of 500° F was provided for hot spots and emergency cooling. This limited capsule radius to 1.5 inches.

At a fuel radius of 1.5 inches, a total capsule length of 67.7 inches is required for 32 KW, as shown in Figure 5-28. This is based on PuO₂ that is compacted to 90 percent theoretical density (10.3 gr/cc) and a power density of 4.06 watts/cc.

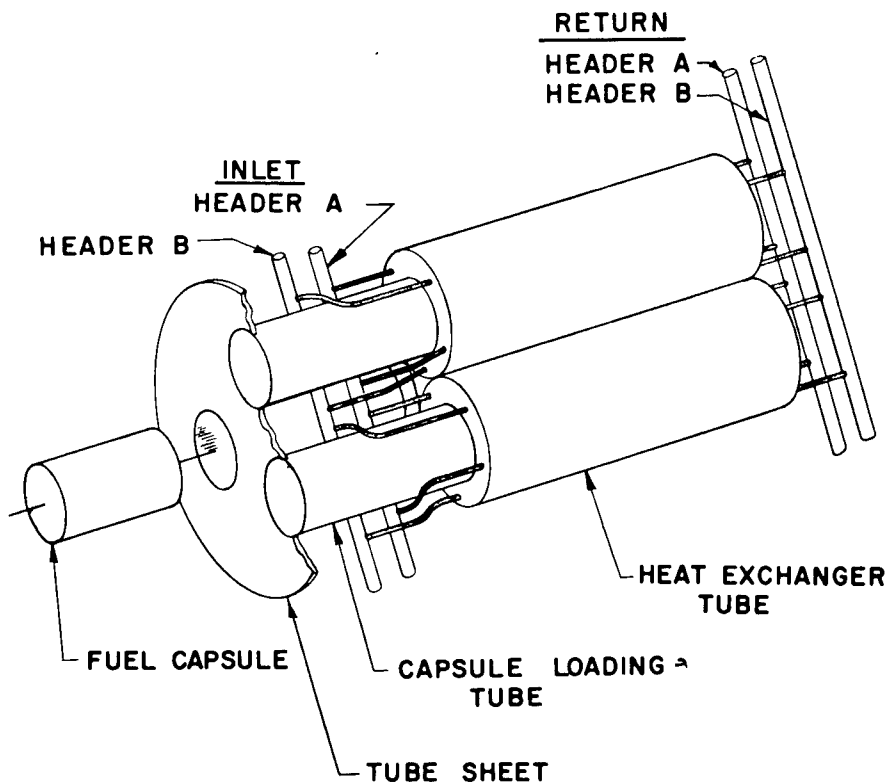


Figure 5-24. Heat Exchanger Header Arrangement

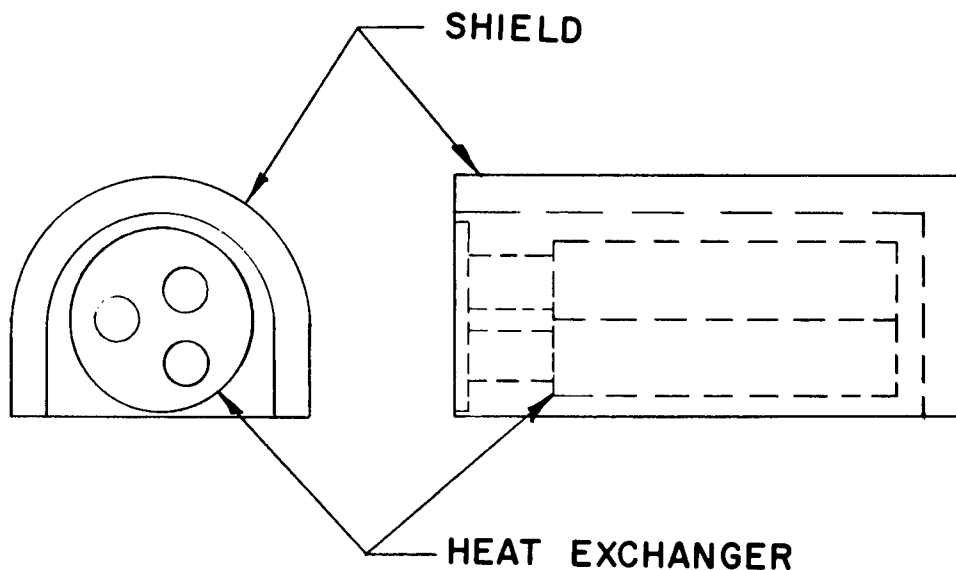


Figure 5-25. Heat Exchanger and Shield

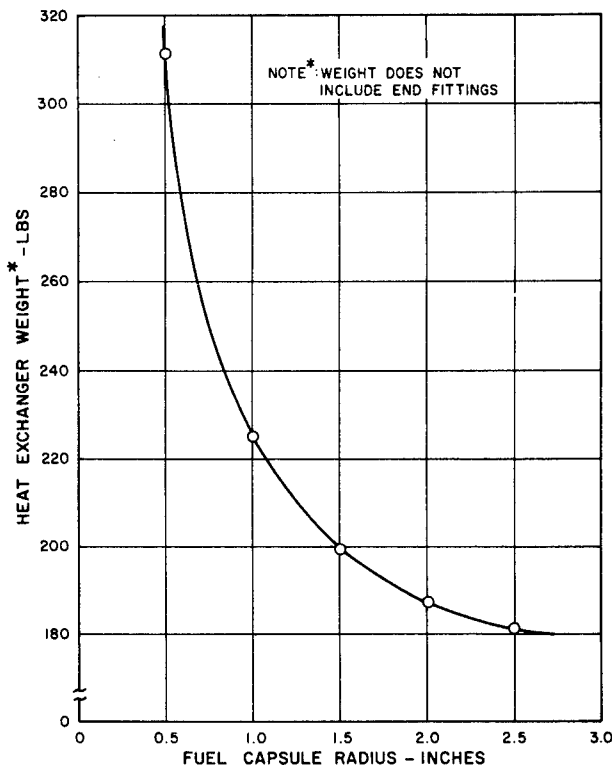


Figure 5-26. Heat Exchanger Weight - Isotope Stirling Cycle

Heat exchanger weight is minimized by using the minimum number of tubes because of the decreased weight required in capsule and fittings and in piping connections. However, heat exchangers that have high length-to-diameter ratios make inefficient use of shielding materials. This effect is shown in Figure 5-29. The heat exchanger weight increases slowly with number of tubes as shown; however, there is a significant reduction in shield weight in going from one to three fuel capsules.

The combined weight of heat exchanger and shield is almost invariant over the range from 3 to 12 capsules and since it is desirable for ground handling considerations to handle the minimum number of capsules, the three tube heat exchanger is used.

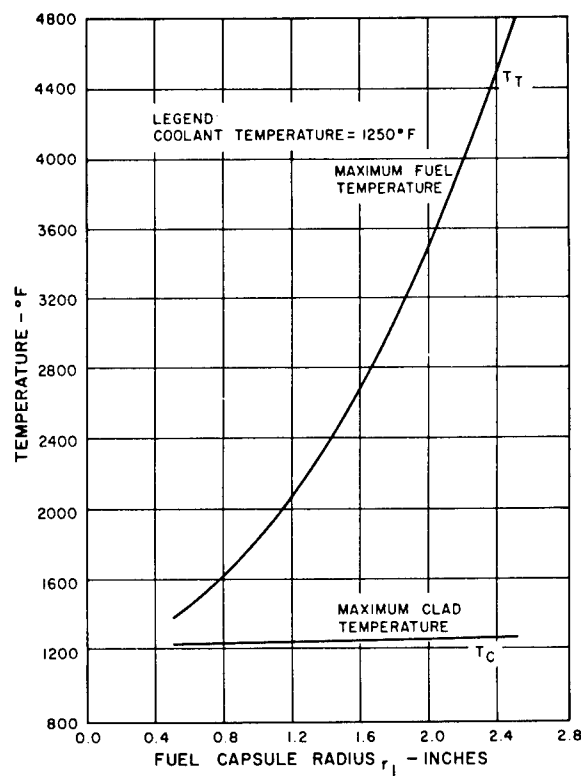


Figure 5-27. Fuel Capsule Temperatures

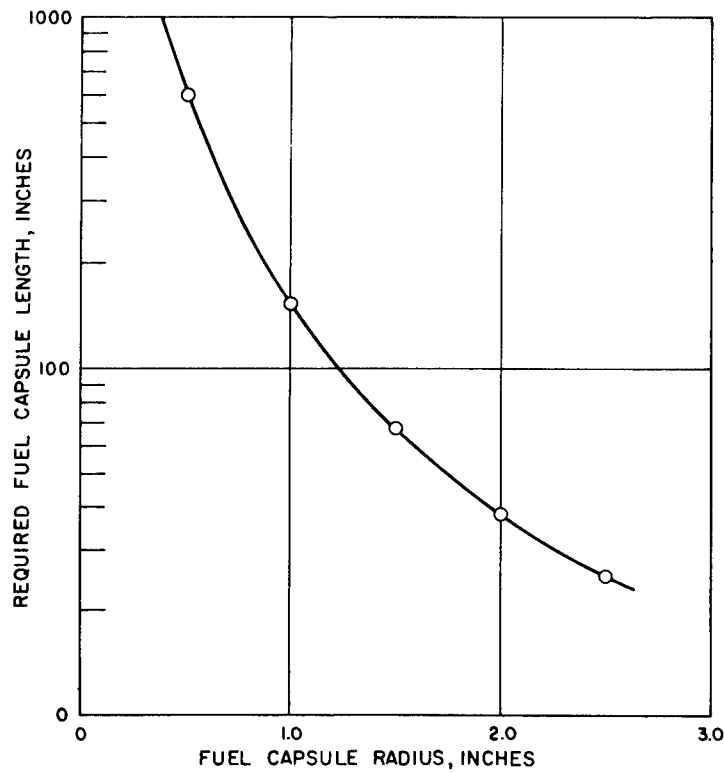


Figure 5-28. Total Fuel Capsule Length Versus Capsule Radius

The dimensions and weights of the exchanger and shield are given in Table 5-9.

TABLE 5-9. ISOTOPE HEAT EXCHANGER CHARACTERISTICS

Thermal Power	32 KW
Coolant	Eutectic NaK
Flow Rate (per loop)	8000 lbs/hr
NaK outlet Temperature	1250° F
Maximum Fuel Temperature	2540° F
Maximum Clad Temperature	1270° F
Fuel Capsule Radius	1.5 inches
Fuel Clad Inside Radius	1.503 inches
Fuel Clad Thickness	0.030 inches
Heat Exchanger Tube Inside Radius	1.538 inches
Inner Tube Thickness	0.050 inch
Outer Tube Thickness	0.050 inch
Annular Flow Channel Width	0.100 inch
Heat Exchanger Tube Outside Radius	1.738 inches
No. of Tubes	3
No. of Fins	None
Active Fuel Length per Tube	23.6 inches
Circumscribed Diameter of Heat Exchanger	7.4 inches
Overall Length of Heat Exchanger (including extension tubes and inlet/outlet headers)	29.6 inches
Shield Thickness (Lithium Hydride)	11.8 inches
Shield Length	41.4 inches
Shield Width	31.0 inches
Shield Height	18.2 inches
Shield Weight	530 pounds
Heat Exchanger Weight	235 pounds
Total Weight	765 pounds

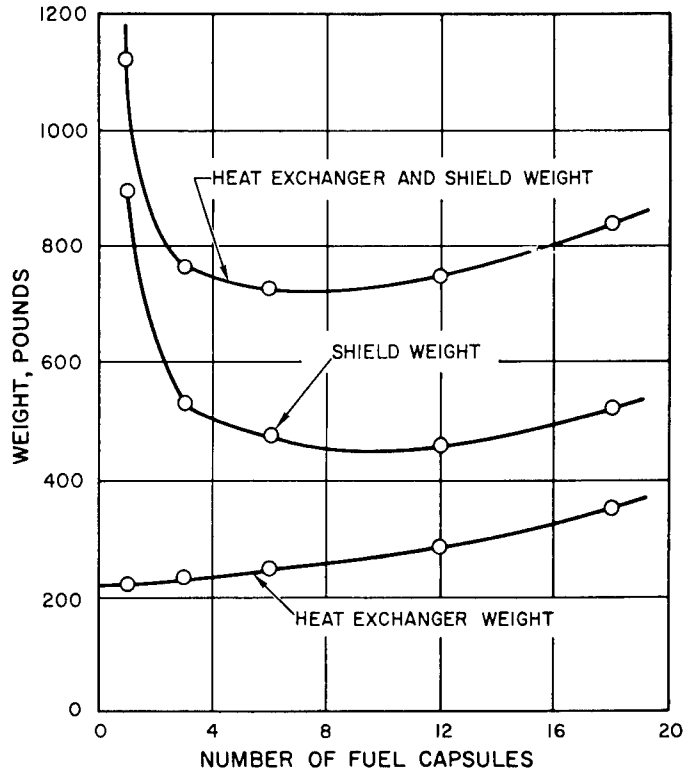


Figure 5-29. Heat Exchanger and Shield Weight

5.4.2.6 Isotope Source Temperature Control

Temperature control for the isotope heat source is provided by the use of high temperature NaK radiators which are in series with the flow through the isotope heat exchanger. One such radiator has been provided for each isotope coolant loop to provide independent control of NaK temperature. The temperature control is effected with a number of insulated doors which will rotate open or closed to control the radiator outlet temperature.

With the doors fully open, each radiator will be sized to dissipate one-half the heat generated by the isotope package. The heat loss from the NaK circuits has been

estimated at 2.5 KW_t, with the major part of this being contributed by the losses from the temperature control radiators with the shutters fully closed.

Figure 5-30 shows the weight and area of the isotope temperature control radiators as a function of power dissipation. The weight of the shutters and associated linkages has been estimated at 0.4 lbs/ft².

5.4.3 NaK PUMPS

The NaK pumps selected for use in this study are the canned-rotor type. The canned-rotor pumps have a high efficiency and are light weight when compared to equivalent electromagnetic liquid metal pumps. Three NaK pumps have been included in the isotope cooling loops, one pump for each independent coolant circuit and one standby pump with necessary valving to allow for switching into either NaK circuit. Note that the primary NaK pumps are each cooled by the corresponding

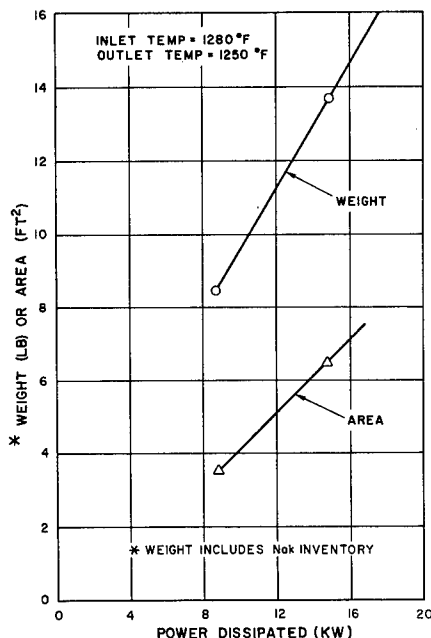


Figure 5-30. Isotope Temperature Control Radiator

engine coolant circuits (see Figure 5-1). Consequently, the loss of circulation in one engine coolant circuit will result in the overheating of the corresponding NaK pump. Since the standby pump is cooled by both engine coolant circuits, it may be used to replace the pump which has lost its coolant flow. The overall efficiency $\left(\frac{\text{ideal pump power}}{\text{electrical power input}} \right)$ of each NaK pump-motor combination will be assumed to be 20 percent.

The ideal pump power is given by

$$P_{\text{Ideal}} = (5.42 \times 10^{-5}) \frac{w \Delta p}{\rho}$$

where

P_{Ideal}	= Ideal pump power (KW)
w	= Mass flow rate $\frac{\text{lb}}{\text{hr}}$
Δp	= Static pressure drop $\frac{\text{lb}}{\text{in}^2}$
ρ	= Density $\frac{\text{lb}}{\text{ft}^3}$

For the non-integrated power system

w	= 16,000 lbs/hr (total for both circuits)
Δp	= 4.5 psi
ρ	= $44.7 \frac{\text{lb}}{\text{ft}^3}$ @ 1235°F (Ref 2)

$$P_{\text{Ideal}} = \frac{(5.42 \times 10^{-5})(16,000)(4.5)}{44.7}$$

$$P_{\text{Ideal}} = 0.0872 \text{ KW}$$

$$\text{Power Input} = \frac{0.0872}{.20} = .44 \text{ KW}$$

5.4.4 COOLANT PUMPS

The engine coolant pumps will circulate an aqueous solution of propylene glycol (60 percent by weight) through the engine coolers, oil coolers, alternators, NaK pumps, and radiator to dissipate the waste heat from the power system. One coolant pump will be used in each of the two independent coolant circuits. The pump-motor combination will be hermetically sealed to ensure leakproof operation. The overall efficiency $\frac{\text{ideal pump power}}{\text{electrical power input}}$ of each pump will be assumed to be 30 percent.

The ideal pump power is given by

$$P_{\text{Ideal}} = (5.42 \times 10^{-5}) \frac{w \Delta p}{\rho}$$

where P_{Ideal} = Ideal pump power (KW)

w = Mass Flow Rate $\frac{\text{lb}}{\text{hr}}$

Δp = Static pressure drop $\frac{\text{lbs.}}{\text{in}^2}$

ρ = Density $\frac{\text{lb}}{\text{ft}^3}$

For the non-integrated power system

w = 4,670 lbs/hr (total for both circuits)

Δp = 27 psi

ρ = 63.1 lb/ft³ @145°F (Ref 2)

$$P_{\text{Ideal}} = \frac{(5.42 \times 10^{-5}) (4,670) (27)}{63.1}$$

$$P_{\text{Ideal}} = .108 \text{ KW}$$

$$\text{Power Input} = \frac{.108}{.30} = .36 \text{ KW}$$

5.4.4.1 Evaporator

An evaporator has been proposed as a necessary component in the Isotope Stirling power system for the following reasons:

1. Cooling of the isotope package prior to launch when the engines are not operating. In this case, the evaporative fluid (water) will be supplied by the ground support equipment (G.S.E.).
2. Cooling of the isotope package during launch. In this case, the water will be supplied for storage on-board the vehicle.
3. Cooling of the isotope package in an emergency situation when the cooling cannot be accomplished by the engines, engine coolant radiators, or isotope temperature control radiators. In this case, the necessary water will be directed from the supply in the life support system.

The size of this evaporator cannot be determined until specific information is available on the time between disconnect of the umbilical and insertion into orbit.

5.4.4.2 Ground Cooling Heat Exchanger

Ground cooling during engine checkout prior to launch can be accomplished by incorporating a compact heat exchanger in series with the flow through the engine coolers. The G.S.E. will connect to this heat exchanger and pump water through the secondary circuit of the heat exchanger to provide the necessary cooling of the propylene glycol. The weight of a heat exchanger which is capable of transferring 23.26 KW_t to the water has been calculated as 4 pounds. This weight is based on a counterflow, double-concentric, pipe type heat exchanger.

5.4.5 DISCUSSION OF POWER SYSTEM

5.4.5.1 Effects of Component Failure on System Operation

Table 5-10 has been prepared to show the effects of various combinations of component failures on the system operation. It has been assumed in this tabulation that, at most, only two major components will experience a failure at the same time. The evaporator will be employed for emergency isotope cooling during certain combinations of component failures. When the evaporator is required, its operation is necessarily on a short time basis because of the limited supply of stored water onboard the vehicle. Consequently, if it is not possible to correct the malfunction within a short time period, it will be necessary to abort the mission. A standby NaK pump-motor has been incorporated into the system so that it may be valved into either NaK loop to replace an inoperable primary pump. As can be seen from Table 5-10, there is only one condition which results in an inability to cool the isotope package with the present design.

5.4.5.2 Packaging of System Components Within MORL Vehicle

Figure 5-31 shows the relative position of the power system components with respect to the MORL vehicle. All components have been clustered around the isotope heat source to minimize the power system volume and to minimize the pressure drop in the NaK circuits and the engine coolant loops. The inlet to the engine coolant radiator is as near as possible to the engines. The entire power system package will be enclosed with high temperature insulation to minimize the heat loss from hot parts. The isotope heat exchanger has been situated so as to allow ready access for loading of the fuel. Maintenance of power system components will require entrance into the insulated compartment through the micrometeoroid shield at the end of the vehicle (STA 1699). The packaged volume is estimated as 75 cubic feet and the overall dimensions are shown in Figure 5-31.

TABLE 5-10. EFFECT OF COMPONENT FAILURES ON SYSTEM OPERATION

	Engine #1	Engine #2	NaK Pump #1	NaK Pump #2	Standby NaK Pump	Rupture NaK Line #1	Rupture NaK Line #2	Engine Coolant Rad. #1	Engine Coolant Rad. #2	*Temp. Control Rad. #1	*Temp. Control Rad. #2
Engine #1	E ₂	E ₄	E ₂	E ₂	E ₂	E ₂	E ₅	E ₂	E ₄	E ₂	E ₂
Engine #2	E ₄	E ₂	E ₂	E ₂	E ₂	E ₅	E ₂	E ₄	E ₂	E ₂	E ₂
NaK Pump #1	E ₂	E ₂	E ₁	E ₂	E ₂	E ₂	E ₂	E ₂	E ₂	E ₁	E ₁
NaK Pump #2	E ₂	E ₂	E ₂	E ₁	E ₂	E ₂	E ₂	E ₂	E ₂	E ₁	E ₁
Standby NaK Pump	E ₂	E ₂	E ₂	E ₂	E ₁	E ₂	E ₂	E ₂	E ₂	E ₁	E ₁
Rupture NaK Line #1	E ₂	E ₅	E ₂	E ₂	E ₂	E ₂	A	E ₂	E ₅	E ₂	E ₃
Rupture NaK Line #2	E ₅	E ₂	E ₂	E ₂	E ₂	A	E ₂	E ₅	E ₂	E ₃	E ₂
Engine Coolant Rad. #1	E ₂	E ₄	E ₂	E ₂	E ₂	E ₂	E ₅	E ₂	E ₄	E ₂	E ₂
Engine Coolant Rad. #2	E ₄	E ₂	E ₂	E ₂	E ₂	E ₅	E ₂	E ₄	E ₂	E ₂	E ₂
*Temp. Control Rad. #1	E ₂	E ₂	E ₁	E ₁	E ₁	E ₂	E ₃	E ₂	E ₂	E ₁	E ₁
*Temp. Control Rad. #2	E ₂	E ₂	E ₁	E ₁	E ₁	E ₃	E ₂	E ₂	E ₂	E ₁	E ₁

where E₁ emergency operation - full electrical power

E₂ emergency operation - reduced electrical power (one engine)

E₃ emergency operation - reduced electrical power (one engine) - must use evaporator

E₄ emergency operation - battery power

E₅ emergency operation - battery power - must use evaporator

A abort - system cannot remove heat from isotope package

*In this tabulation, the temperature control radiator failure mode considered was the doors jammed in the fully closed condition (i.e., minimum heat radiation capability).

5.4.5.3 System Start-Up Procedure

It has been assumed that the MORL vehicle will be launched with the engines non-operating, but it will be necessary to run the NaK pump-motors to dissipate the isotope heat in the evaporator. Consequently, it will be necessary to start the power system engines as soon as possible after orbit has been achieved in order to minimize the time that the NaK pump-motors are operated from battery power. This consideration will probably dictate the use of a programmed start-up which is initiated by telemetry. Start-up is relatively simple with the isotope heat source since heat is always available at the engines. Each engine is started by applying power to the starter motor which is geared to the rhombic drive mechanism. The engine coolant pump-motors must be designed to enable start-up with the increased viscosity which will result from the low radiator temperature.

5.5 INTEGRATED POWER AND LIFE SUPPORT SYSTEMS

5.5.1 DESCRIPTION OF SYSTEM AND DESIGN

The electrical power requirement for the integrated power and life support system will be 6.24 KW_e , less the net electrical power savings as the result of thermal integration of the power system with the life support systems. This net electrical power savings has been established at 2.96 KW_e , so that the resultant electrical power to the station bus is 3.28 KW_e as compared to the 6.24 KW_e for the non-integrated system. This 3.28 KW_e demand will be satisfied by the parallel and independent operation of two advanced Stirling engines of the type discussed in Section 5.1. Each engine will drive one 12,000 rpm, 400 cps, 110/220 volt alternator. Each engine and corresponding alternator will be sized to supply one-half of the total electrical load. As in the non-integrated system, each engine is heated by a Sodium Potassium (NaK) eutectic heat transfer loop. There are two independent NaK loops linking the engines with the isotope heat source. Figure 5-16 shows the flow diagram for the integrated systems. This diagram is similar to the corresponding diagram for the non-integrated system (Figure 5-1), with the exception of

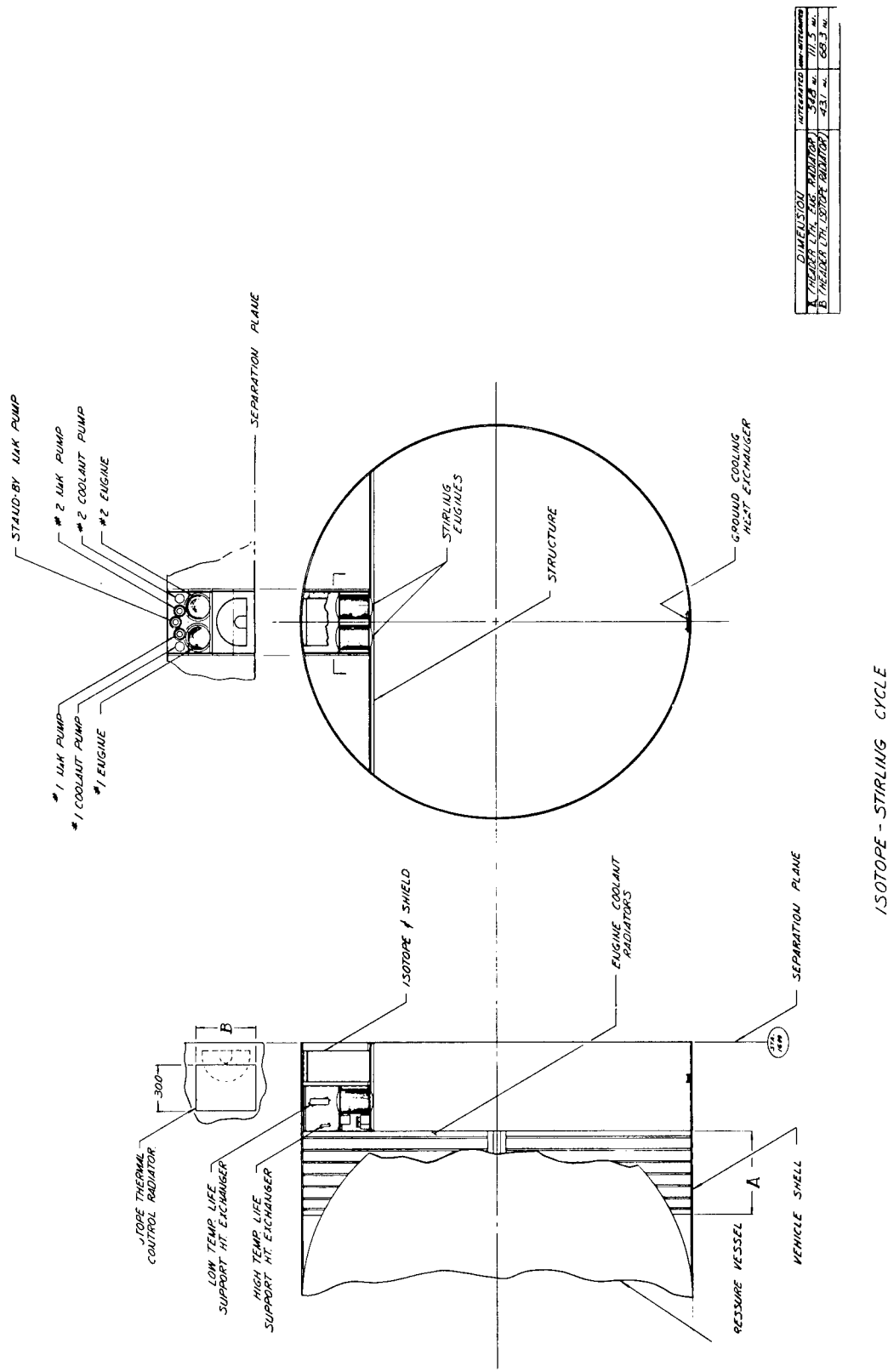


Figure 5-31. Power System Component Layout - Isotope Stirling

the two heat exchangers necessary to transfer heat from the power system to the life support system. One heat exchanger supplies the high temperature (600°F) requirements of the life support CO_2 and water desorbers by transferring 2.22 KW_t from the NaK loops. The other heat exchanger supplies the low temperature (150°F) requirements of the life support evaporators, etc., by transferring 1.19 KW_t from the waste heat in the engine coolant circuits.

The power system energy balance for normal operation of the integrated system is tabulated in Table 5-11 and the corresponding weight breakdown is shown in Table 5-12.

TABLE 5-11. ENERGY BALANCE, INTEGRATED ISOTOPE STIRLING SYSTEM

a. Electrical load to station bus (non-integrated system)	6.24 KW_e
b. Net electrical power saving as the result of thermal integration	2.96 KW_e
c. Electrical load to station bus (integrated)	3.28 KW_e
d. NaK pumping power	0.23 KW_e
e. Engine coolant pumping power	0.18 KW_e
f. Dissipative control (5% of load)	0.16 KW_e
g. Generator output	3.85 KW_e
h. Generator efficiency	82.7%
i. Gearing efficiency	98%
j. Engine Output	4.75 KW_e
k. Brake thermal efficiency	30%
l. Heat input to engine	15.82 KW_t
m. Heat loss from isotope temperature control radiators	2.00 KW_t
n. Total life support heat loss from high temperature loop	0.35 KW_t
o. Usable heat transferred from NaK circuits to life support system.	1.87 KW_t
p. Heat delivered by isotope heat source	20.04 KW_t
q. Total life support heat loss from low temperature circuit	0.16 KW_t
r. Usable heat transferred from engine coolant circuits to life support system	1.03 KW_t
s. Net heat rejected by engine coolant radiator	11.35 KW_t

TABLE 5-12. SYSTEM WEIGHT BREAKDOWN, INTEGRATED SYSTEMS

A. Power system

1.	Isotope heat source	
a.	Fuel and heat exchanger = 157	
b.	Shielding = 500	657 lbs.
2.	Heat source temperature control	24
3.	Engines (2 @ 60 lbs.)	120
4.	Engines speed and power controls	80
5.	Alternators (2 @ 8 lbs.)	16
6.	Alternator gearing (2 @ 5 lbs.)	10
7.	Starter motors (2 @ 8 lbs.)	16
8.	Coolant pumps (2 @ 7 lbs.)	14
9.	NaK pumps (3 @ 17 lbs. (includes one standby)	51
10.	Engine coolant radiator (integral with vehicle structure and includes fluid inventory inside radiator)	170
11.	Ground cooling heat exchanger	3
12.	NaK-to-therminol heat exchanger	2
13.	Engine coolant-to-L.S. low temperature heat exchanger	4
14.	Piping	49
15.	NaK inventory (includes 10% contingency)	2
16.	Structure	
a.	Additional structure to mount engines and to support isotope heat source	117
b.	Savings in structural weight as the result of using an integral engine coolant radiator	(-86)
17.	Batteries	600
	Power System Total Weight	1849 lbs.

B. Life Support System

1.	CO ₂ recovery canisters	120 lbs.
2.	Electrolysis cells	100
3.	Pyrolyzation	20
4.	CO ₂ Accumulator Pump	7

TABLE 5-12. SYSTEM WEIGHT BREAKDOWN, INTEGRATED SYSTEMS (Cont)

5. Accumulator, reactor, condenser	26
6. Cooling system	206
7. High temperature fluid heating system	40
8. Urine water recovery	43
9. Solid waste treatment	29
10. Waste water recovery	35
11. Food management	19
12. Low temperature fluid heating system	16
13. Miscellaneous hardware	17
Life support system total weight	678 lbs.
Integrated System Total Weight	2,527 lbs.

5.5.2 ALTERNATORS, STARTER MOTORS, AND ELECTRICAL CONTROLS

As a result of the thermal integration, the electrical output from each alternator has been reduced to 1.93 KW_e . With this rated output, Figure 5-5 indicates an alternator weight of eight pounds. From Figure 5-6 the lower rated generator output will result in a reduction in generator efficiency to 82.7 percent.

5.5.3 ISOTOPE HEAT SOURCE

Since the thermal output from the isotope heat exchanger for the integrated system is approximately $2/3$ of the output for the non-integrated system, an approximation for the design in the integrated power system can be obtained by removing one of the three heat exchanger tubes. This will result in a reduction of approximately $1/3$ in the weight of the isotope heat exchanger. The shield weight associated with the integrated isotope heat exchanger will not be reduced by as significant a factor. Figure 5-32 shows the shield configuration for the integrated isotope heat source. The required shield thickness has been obtained from Figure 5-19 for a thermal power output of 21.3 KW_t . This configuration results in a shield weight of 500 pounds. It

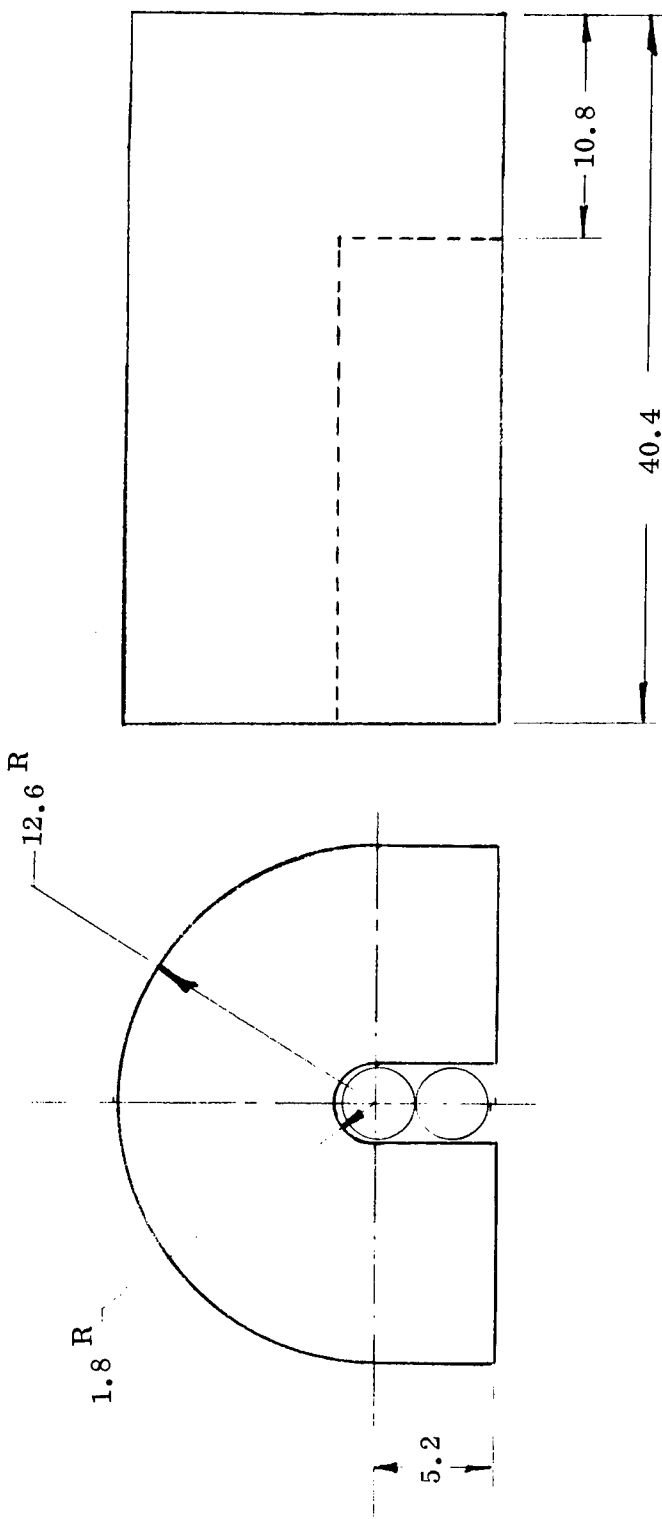


Figure 5-32. Shield Configuration - Integrated System

is not expected that this isotope heat exchanger and shield arrangement will result in the minimum weight. For minimum weight, it will probably be necessary to shorten the tube length and increase the number of tubes to at least three.

5.5.4 NaK PUMPS

For the purposes of this study, it has been assumed that the efficiency of the NaK pump motors does not change as the capacity is decreased from that required for the non-integrated system to that required for the integrated system. It has also been assumed that a canned rotor pump will be used in the integrated system.

Based on these assumptions, the NaK pump-motor power required for the integrated system will be given by:

$$\begin{aligned} P_{\text{actual}} &= \frac{(5.42 \times 10^{-5}) w \Delta p}{\eta \rho} \\ &= \frac{(5.42 \times 10^{-5}) (8560) (4.5)}{(.20) (44.7)} \\ &= .23 \text{ KW(e)} \end{aligned}$$

5.5.5 COOLANT PUMPS

The assumption has been made that the coolant pump-motors for the integrated system are just as efficient as the larger pumps used in the non-integrated system.

Therefore, the coolant pump-motor power requirement will be given by:

$$\begin{aligned} P_{\text{actual}} &= \frac{(5.42 \times 10^{-5}) w \Delta p}{\eta \rho} \\ &= \frac{(5.42 \times 10^{-5}) (2280) (27)}{(.30) (63.1)} \\ &= .18 \text{ KW (e)} \end{aligned}$$

5.5.6 ENGINE COOLANT RADIATOR

As the result of thermal integration, the power dissipated by the engine coolant will be reduced to 11.35 KW_t . Figure 5-8 indicates that the weight and area corresponding to this rate of heat rejection are 170 pounds and 310 ft^2 , respectively.

5.5.7 ISOTOPE TEMPERATURE CONTROL RADIATOR

The size and weight of the isotope temperature control radiators will be reduced due to the decrease in heat source thermal output. Figure 5-30 shows that the weight per radiator for the integrated power system will be 10.2 pounds, and the corresponding area of 4.5 ft^2 will require approximately 1.8 pounds of thermal shutters.

5.5.8 EVAPORATOR

The decrease in thermal output from the isotope heat source will cause a corresponding decrease in size and weight of the evaporator. The magnitude of this reduction can not be assessed without complete mission definition.

5.6 DISCUSSION OF INTEGRATED POWER AND LIFE SUPPORT SYSTEMS

5.6.1 POWER SYSTEM-TO-LIFE SUPPORT SYSTEM HEAT EXCHANGERS

The thermal integration of the power system with the life support system will require the addition of two heat exchangers, as shown in Figure 5-16. The NaK-to-therminol heat exchanger supplies the high temperature (600°F) requirements to the life support equipment. This heat exchanger is a counterflow tube-and-shell type which is shown schematically in Figure 5-23. The weight of this component has been calculated as two pounds.

The lower temperature (150°F) requirements of the life support systems are satisfied by transferring waste heat from the engine coolant circuits to the 30 percent ethylene glycol life support heat transfer loop in another counter-flow tube-and-shell type exchanger.

5.6.2 PACKAGING OF POWER SYSTEM IN RELATION TO LIFE SUPPORT SYSTEM

The integrated power system is packaged in the same way as the non-integrated power system (see Figure 5-31). There is very little change in the packaged volume between the integrated and non-integrated power system because of the relatively small change in isotope shield volume which is the major part of the system volume. The angular relationship between the cabin and the power system is such that the solid waste management and urine treatment subsystems in the cabin are as close as possible to the power systems. The therminol and glycol heat transfer loops will enter and leave the cabin near the toilet compartment.

5.6.3 EFFECTS OF HEAT LOSSES

Thermal integration causes an additional load on the cabin environmental control system due to the heat losses from the hot fluid lines which transport the heat from the power system to the life support systems inside the cabin. This will be reflected by increased weight for the environmental control system heat exchanger and radiator.

5.7 REFERENCES

1. "Potential Capabilities of the Stirling Engine for Space Power," Technical Documentary Report, No. ASD-TDR-62-1099, March 1963.
2. Geiringer, Paul L., "Handbook of Heat Transfer Media," Reinhold Corp., New York, 1962.

3. Welsh, H.W.; Poste, E.A.; and Wright, R.B., "The Advanced Stirling Engine for Space Power," ARS-1033-59 (November 1959).
4. Stephens, C.W.; Spies, R.; and Menetrey, W.R.; "Energy Conversion Systems Reference Handbook, Volume III, Dynamic Thermal Converters," WADD Technical Report 60-699.
5. Duane, J.T., "Dynamic Converters for Aerospace Use" Electrical Engineering, October, 1962, p 776.
6. "The Size and Performance of Dynamic Electric Generators for Space Power," ASTRA, Inc., Raleigh, North Carolina.

SECTION 6.

BRAYTON SYSTEM ANALYSIS

6.1 NON-INTEGRATED SYSTEM

6.1.1 INTRODUCTION

This study is concerned with the advantages of thermally integrating the Life Support System (LSS) with the Spacecraft power system. In order to establish a reference point, it was necessary to design a non-integrated power system and LSS for comparison to the integrated system.

By definition, one of the cycles studied was an Argon gas Brayton cycle employing a two spool turbine. The energy source was to be gas cooled, and the cycle was to employ a gas filled radiator. One heat source was to be Plutonium 238, and the other heat source a solar collector/absorber. The Isotope fuel capsule clad temperature was limited to 1650°F and the temperature of the turbine inlet gas was not to exceed 1500°F . This was done so that a conservative, state of the art design could be derived.

6.1.2 CYCLE DESCRIPTION

The cycle is conventionally depicted on a temperature - entropy diagram in Figure 6-1.

Referring to Figure 6-1 process 1 - 2 is the compression of the working fluid. This process is not isentropic due to the inefficiencies in the compressor, and as a result the temperature rise exceeds that of an ideal compressor. Process 2 -2.5 represents nearly constant pressure heating of the compressor discharge gas in the recuperator, and Process 2.5 - 3.0 nearly constant pressure heating of the working fluid in the energy source heat exchanger. Process 3 - 4 is the nearly isentropic expansion of the gas through the compressor turbine and Process 4 - 5 expansion of the gas through the generator turbine. Temperature drop of the gases during the expansion processes is less than that for an ideal cycle due to the losses in the expansion process. Process 5 - 6 represents heat transferred from the exhaust gas to the compressor discharge gas through the recuperator, and finally Process 6 - 1 represents heat rejected before the gas is returned to the compressor unit.

6.1.3 DESCRIPTION OF SYSTEM AND DESIGN

The power plant system is shown schematically in Figure 6-2 as a single loop system where the Argon gas flows through all components in the power system. Two separate parallel systems are used for reliability. In operation, the working fluid leaves the engine coolant radiator where it enters the compressor section of the turbo-compressor, and is compressed to a selected pressure. It then flows through the cold side of the recuperator where it picks up heat from the turbo-alternator discharge before being ducted

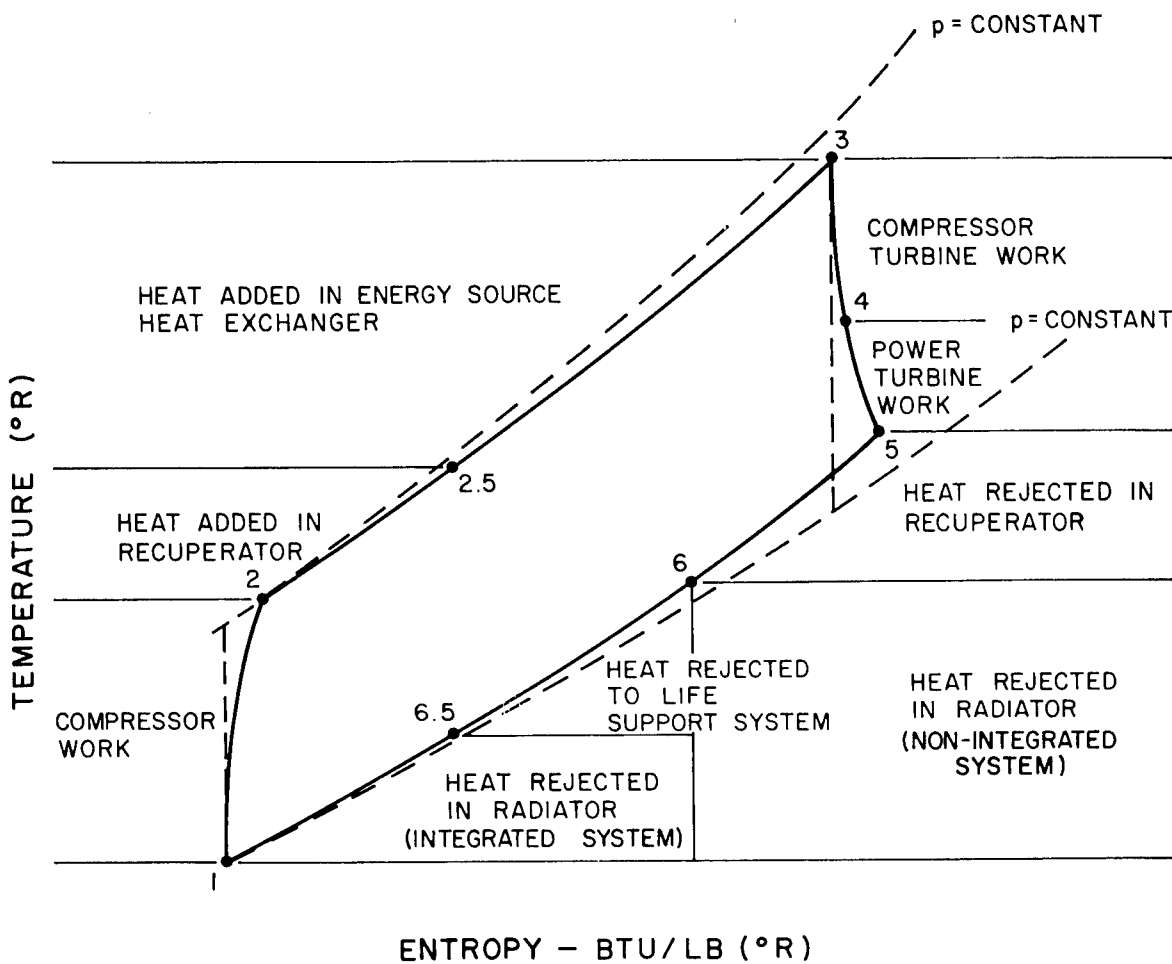


Figure 6-1. Recuperated Brayton Cycle

through the isotope heat source, where it is heated to design temperature. After passing through the turbo-compressor turbine, the gas is ducted to the power turbine where energy is removed to drive the generator. Some of the waste heat is then removed by passing the Argon stream through the hot side of the recuperator where energy is given up to the compressor discharge flow. After leaving the recuperator, the Argon is passed through the radiator where it is cooled to the design compressor inlet temperature by radiation of energy to space. Speed control of the gas generator unit is accomplished by by-passing a small percentage of the total flow around the gas generator turbine to control the amount of turbine work available. Turbo generator speed is controlled by varying the load on the generator by loading parasitic load resistors.

The generator, turbo compressor, and turbo generator bearings are cooled by auxiliary liquid cooling loops employing electrically driven pumps and small space radiators.

High pressure Argon storage bottles serve both as a gas source for startup and for make-up in the event of small amounts of leakage from the system.

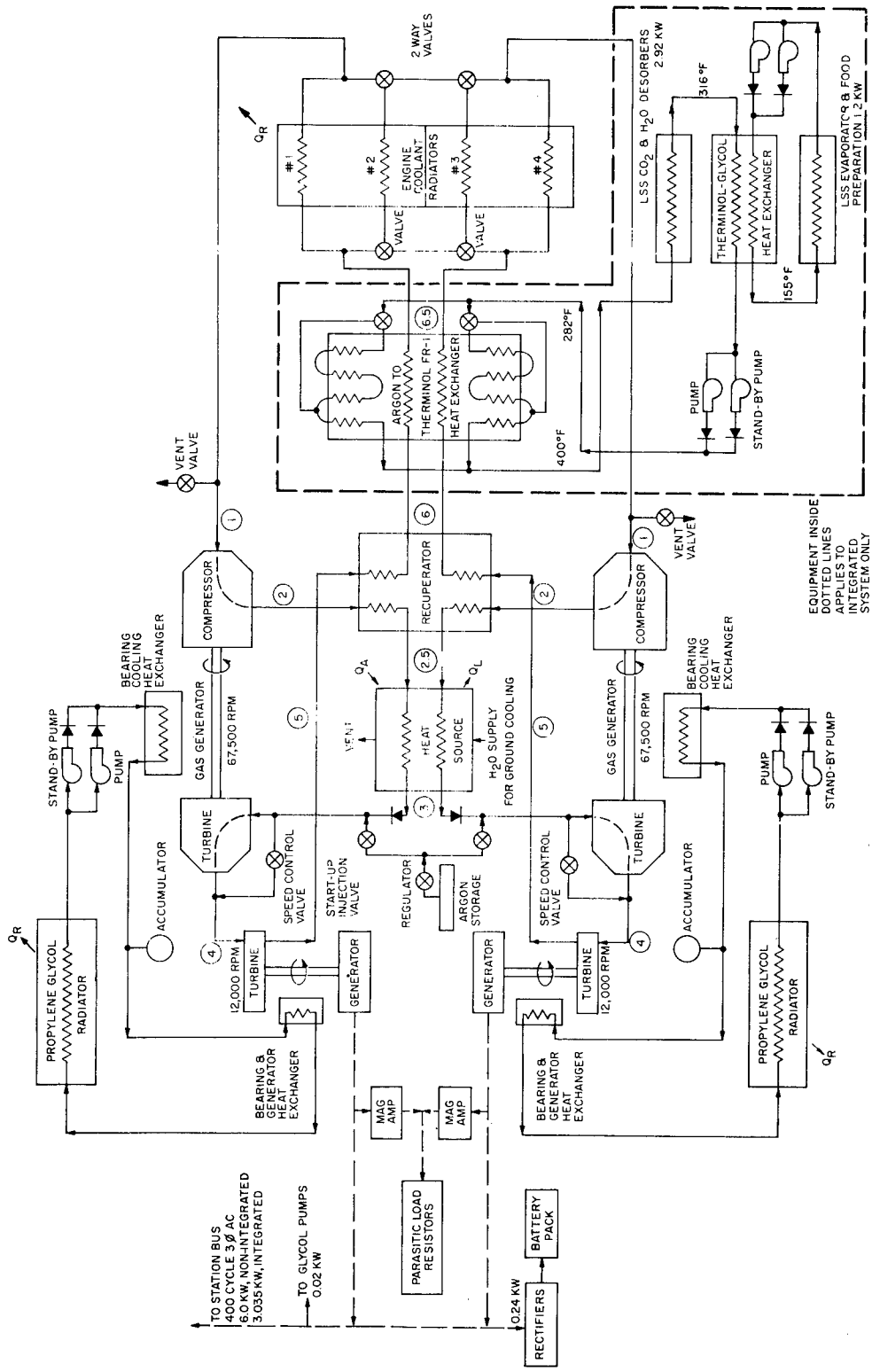


Figure 6-2. Brayton Cycle Functional Diagram

HEAT SOURCE IS ISOTOPE FOR THE ISOTOPIC BRAYTON CYCLE
HEAT SINK IS ABSORBER FOR THE SOLAR BRAYTON CYCLE

6.1.4 SYSTEM CONFIGURATION

6.1.4.1 Solar Brayton

A general configuration is shown on Figure 6-3 which depicts a possible equipment arrangement plan. This layout actually shows the "Integrated System"; however, the differences between the Non-Integrated and Integrated systems are primarily in the categories: (a) weights and sizes, (b) additional heat exchangers for the integrated and (c) mirror tip folding requirement for the non-integrated system.

The general equipment location and structural support means will be identical for the two systems. The solar collector will be rigidly attached to the vehicle skin at eight circumferential points (or along four sectors, each sector several feet long). The absorber, turbo-machinery and recuperator "package" will be supported from four telescoping tubes which are structurally attached to the vehicle skin at points coincident with the mirror support sectors. The other ends of these tubes will be attached to the Absorber structure. The turbo-machinery and recuperator will be attached to the absorber by means of the interconnecting argon ducts. The four gas radiator panels will be spaced along the circumference of a 250 in. diameter circle, thus presenting a minimum shadow to the solar collector. The panels will be physically attached and the entire ring type unit will be tied to the "absorber-turbo-machinery-recuperator package" by means of four tubular supports which also serve as argon carrying ducts to and from the radiator.

Figure 6-3 depicts the system in the fully deployed configuration. However the stowed or launch configuration is also shown in phantom. The deployment sequence is described in Section 6.1.12.3.

6.1.4.2 Isotope Brayton

Figure 6-4 shows the layout of the major equipment items in the spacecraft. The heat source, recuperator, and turbo machinery are close coupled to minimize occupied volume and to minimize the ducting length to reduce friction pressure drop and thermal losses from the hot portion of the system. Thermal losses from the ducting to and from the radiator will have no adverse effect on system performance since this is the low temperature portion of the system where waste heat is being rejected anyway.

The Isotope Package in its shield is located as far as possible from the cabin area to reduce the radiation shielding requirements. One end of the Isotope Source Heat Exchanger is located behind a hatch and immediately adjacent to the outer wall of the spacecraft to facilitate loading of fuel slugs just prior to launch. Waste heat radiators are integral with the vehicle skin on the cylindrical skirt section surrounding the power plant system.

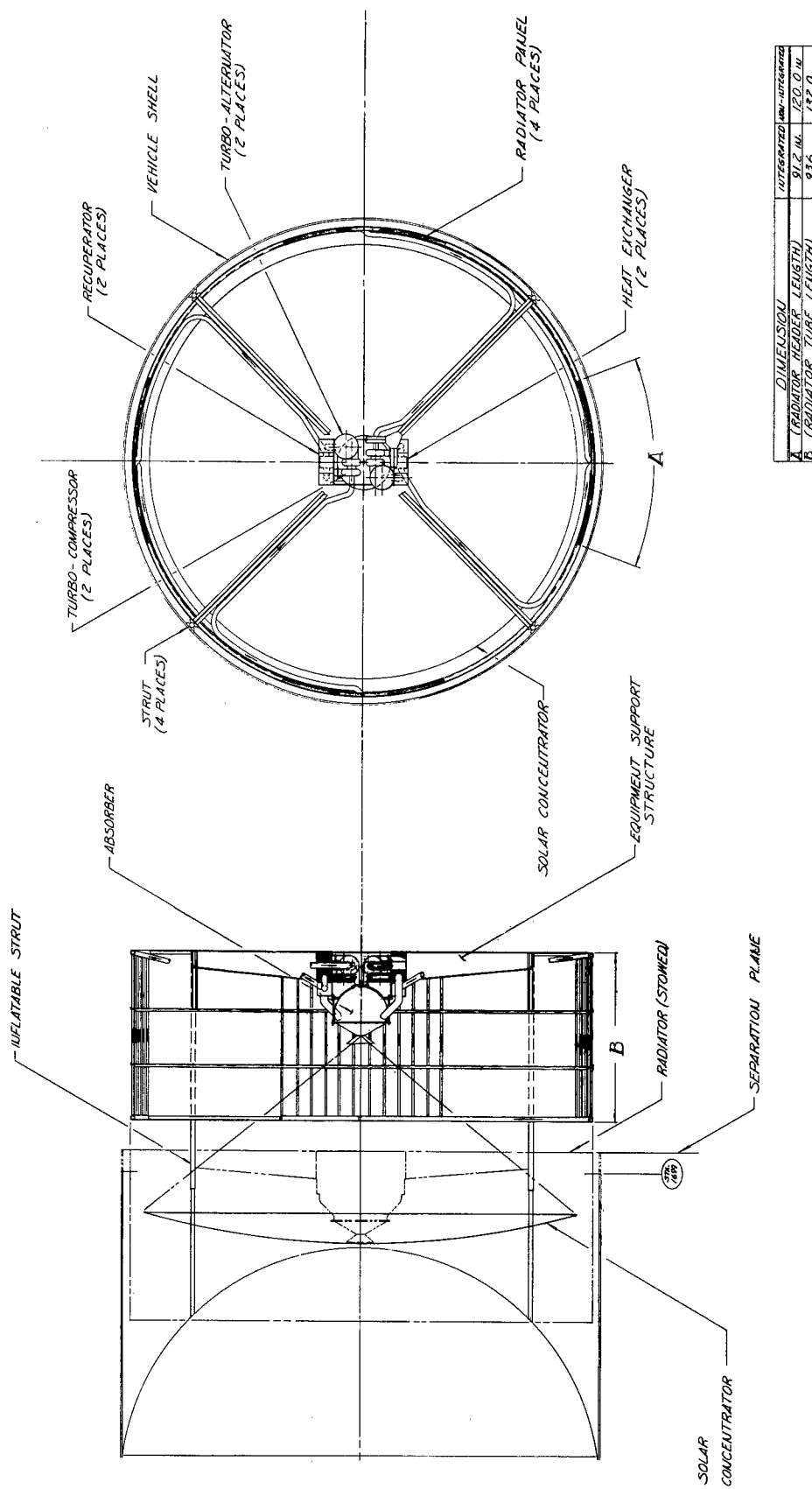


Figure 6-3. Solar Brayton Power System Layout

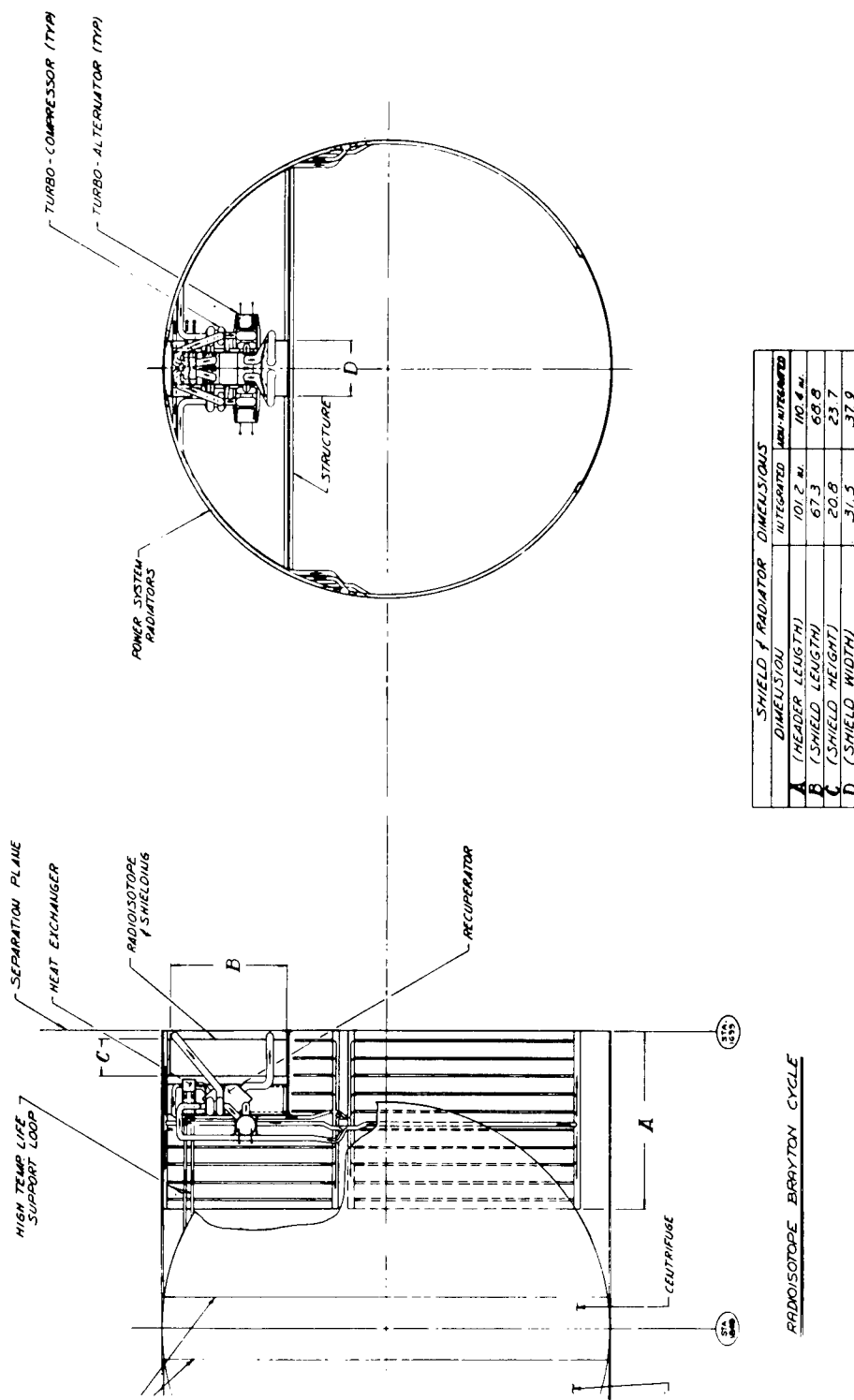


Figure 6-4. Power System Component Layout - Isotope Brayton

One of the distinct advantages of this package arrangement is that all power plant components are stowed within the confines of the spacecraft during both launch and operation and no deployment is required. Tables 6-6 and 6-14 list design parameters and component weights, respectively.

6.1.5 HEAT SOURCE DESIGN

6.1.5.1 Solar Collector

The solar collector chosen for this study is a rigid parabolic reflector of honeycomb aluminum structure, weighing approximately one pound per square foot of projected area.

The size of the mirror was determined by the amount of heat required for steady daylight operation plus the amount of heat necessary to be stored in the absorber for operation during the night portion of the orbit. An overall collection efficiency of 79 percent was used in the sizing calculation. This number was determined by making use of the information contained in Appendix B. For a cavity temperature of 2010°R , the efficiencies were plotted to determine the locus of peak efficiencies and cross-plotted to determine the overall collection efficiency at a D_a/D_c of 0.0192 and a misorientation of 6 minutes. (See Figure 6-5.) The result is an overall collection efficiency of 80.5 percent.

This efficiency assumes a mirror reflectivity of 0.90 and is applicable to a 55° included rim angle. It also assumed a vehicle misorientation of six minutes of arc to account for average vehicle-sun misalignment. Surface slope errors were assumed to have a Gaussian distribution with a standard deviation of 6 minutes. A 6 percent shadow area is also assumed.

The 80.5% efficiency was decreased an additional 0.5 percent to account for thermal losses through the absorber structure and insulation. (Re-radiation from the Aperture was already included.) An additional 1 percent was allowed for the effects of surface degradation. The overall collector-absorber efficiency was thus set at 79 percent.

The daylight heat requirement is 37.93 KW. This is increased by the ratio of the orbital period to the daylight time (1.62) to 61.50 KW. Using a solar flux density of 130 watts/ ft^2 , results in the required mirror area of 473 ft^2 or a diameter of 24.58 feet. For a $D_a/D_c = 0.0192$ the aperture diameter is 5.66 inches. Using a mirror specific weight of 1 lb/ ft^2 , the mirror weight is 473 pounds.

It was not the purpose of the study to optimize the mirror design. Mirror performance was based on a rigid parabolic reflector, for both the non-integrated and integrated systems. Detailed hardware design would require consideration of the decreased efficiency caused by folding the mirror, with a resulting increase in mirror size.

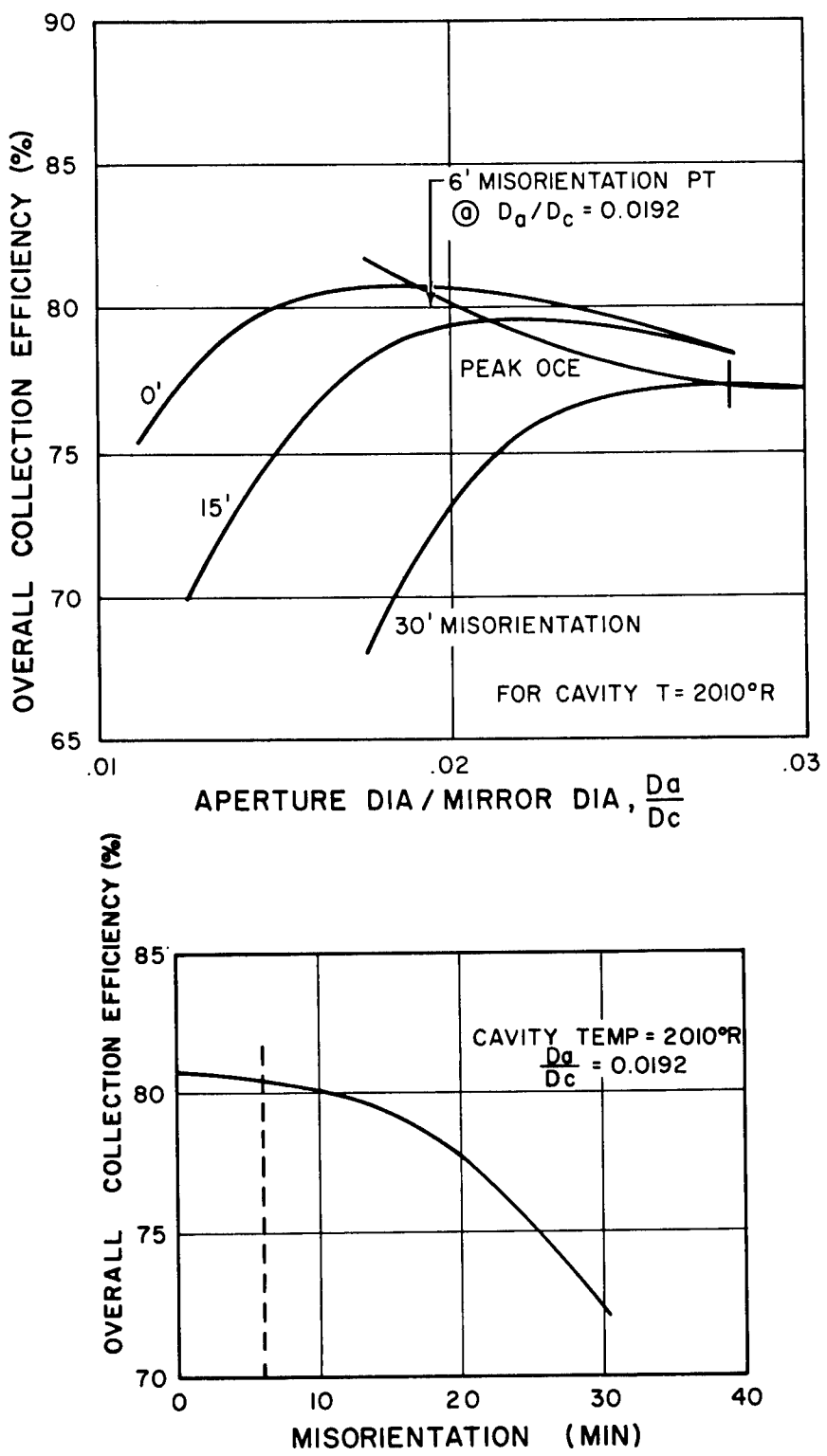


Figure 6-5. Overall Collector Efficiency Vs. Misorientation

Since the diameter of the Saturn IV vehicle is 21.6 feet, the mirror for this non-integrated design would require a tip folding capability similar to the one proposed for the Solar Mercury Rankine cycle. This mirror diameter exceeds the vehicle by approximately 3.9 feet, therefore a two foot rim (four - 90° sectors) requires folding. The unfolding procedure would be part of the deployment sequence.

Since the power plant package shadows approximately a five-foot diameter area at the center of the mirror, this area can be used as an additional structural support point, if it is required for launch considerations.

The actual calculations for the required collector area are shown in Table 6-1. For convenience, the numbers for the Integrated design are also shown on this table and will be referenced in subsequent paragraphs.

TABLE 6-1. SOLAR BRAYTON -- COLLECTOR REQUIREMENTS

	Non-Integrated System	Integrated System
1. Absorber Heat Requirements (KW) (BTU/Hr.)	29.98 (102, 400)	18.00 (61, 400)
2. Overall Collector Efficiency (%)	79	79
3. Collector Input Requirements (KW)	37.93	22.80
4. Total Requirements (Incl. Night) = ($\frac{94}{56}$) x Item 3 (KW)	61.50	37.95
5. Solar Constant (KW/ft ²)	0.130	0.130
6. Projected Mirror Area Required (ft ²)	473	284
7. Mirror Diameter (ft)	24.58	19.06
8. Mirror Weight @ 1.0 lb/ft ² (lbs)	473	284
9. Optimum Aperture Dia./Mirror Dia.	0.0192	0.0192
10. Aperture Diameter (for Absorber Design) (Inches)	5.66	4.39
Mirror Weight Elec. Output (Lbs.) $\frac{\text{Lbs.}}{\text{KW}_e}$	75.8	45.5*

*Mirror Weight/KW_e - Equivalent System

6.1.5.2 Solar Heat Absorber

The Solar Absorber used in this study is essentially a scaled version of the Thompson Ramo Wooldridge Semi-spherical cavity design.

The heat storage medium is Lithium Fluoride with a melting temperature of 1560°F. The amount of LiF required is based on the night-time heat requirement plus a 10 percent

margin to insure that some portion of the total inventory remains in the liquid state at all times. With a heat requirement of 30KW (102,000 BTU/hr.), 61,440 BTU are required during the dark period of the orbit. Allowing a 10 percent margin, the actual heat to be stored is 67,584 BTU/orbit. Since the latent heat of vaporization for LiF is 450 BTU/lb., the total inventory required is 150 pounds.

An optimum weight tube in shell type absorber was investigated by means of a computer program; however, in the final analysis, a compromise was necessary between weight and a practical number of gas carrying tubes. The design selected is one with 36 tubes (18 each loop); with individual tube lengths of 6.98 feet, tube thickness is 10 mils and shell thickness is 30 mils. The tube inside diameter for the design pressure drop of 5 percent (0.68 psi) is 0.67 inch.

The aperture diameter for the 24.6 foot mirror and the optimum $D_a/D_c = 0.0192$ is 5.66 inches.

Figure 6-6 plots absorber pressure drop versus inside tube diameter for various numbers of tubes. Figure 6-7 is a plot of absorber component weight (not including headers, insulation, or conical front section) also as a function of tube inside diameter. The information from Figure 6-6 defines lines of constant pressure drop on Figure 6-7.

Figure 6-8 is then a plot of tube inside diameter versus heat added for the case of 36 tubes. From this plot, the tube I.D. was determined to be 0.67 inch.

Figure 6-9 is a plot of the tube length versus tube I.D. for lines of constant heat added (Q_a). Using the tube I.D. as found from Figure 6-8, Figure 6-9 allows the determination of tube length as a function of Q_a which appears as Figure 6-10. For this non-integrated design, the tube lengths should be 6.98 feet. Figure 6-11 is an overall plot of total absorber weight as a function of heat transferred. The total weight includes inlet and outlet headers, front conical section, insulation and an allowance for a temperature control.

As a means of cavity temperature control, the method suggested in the TRW Quarterly Report, ER-5905 (January-March 1964) on Brayton Cycle Cavity Receiver Development is used. It consists of a front conical section which is split into four quadrants each actuated by a temperature controlled bellows, so that if the cavity temperature exceeds a pre-selected limit, these quadrants open. This allows cavity heat to be radiated to space. An alternate approach would be the use of several shutter sections equally spaced on the conical section. This would require the use of only one bellows and actuating linkage (two, if redundancy is desirable).

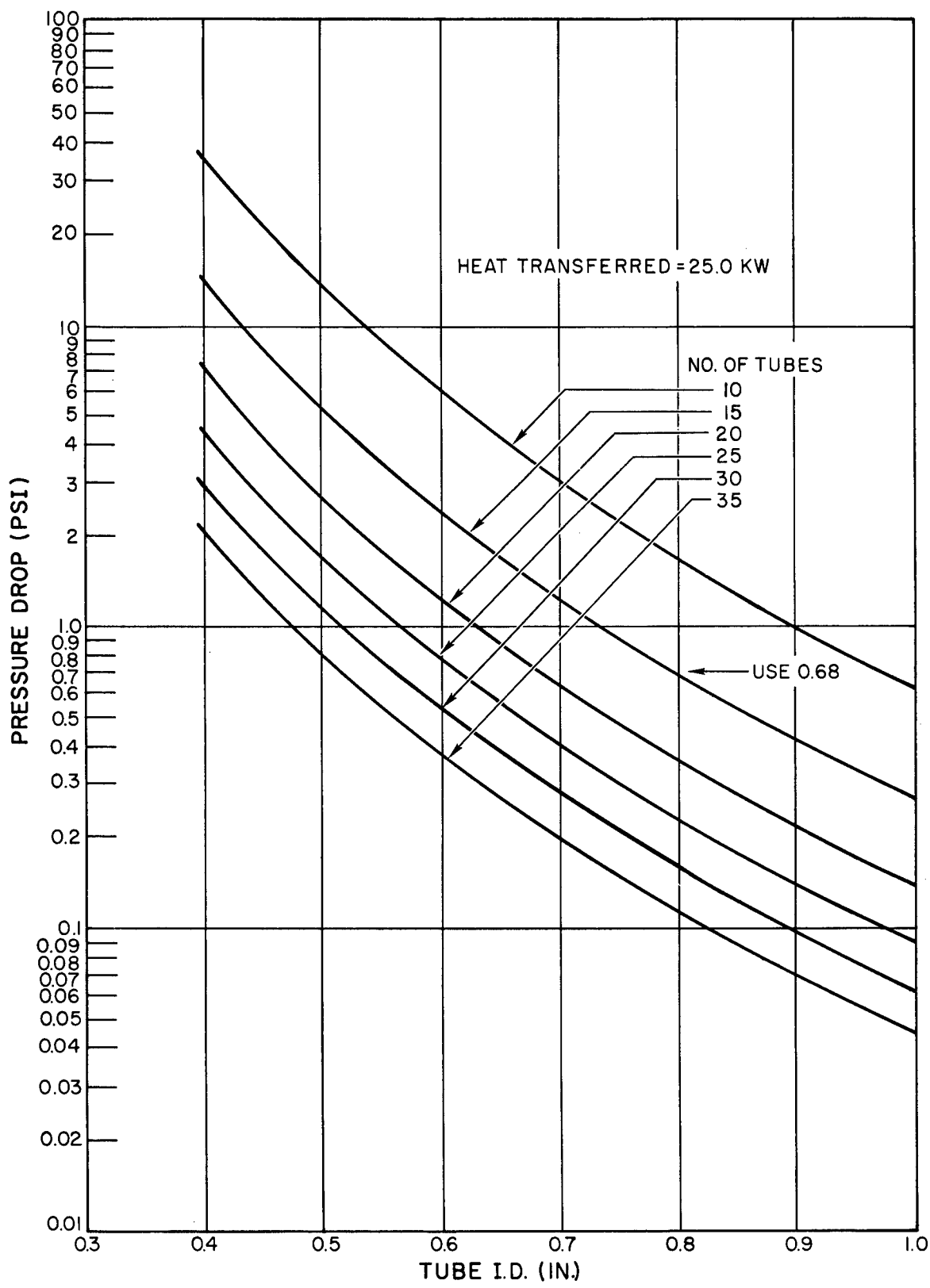


Figure 6-6. Absorber ΔP Vs. Tube I.D.

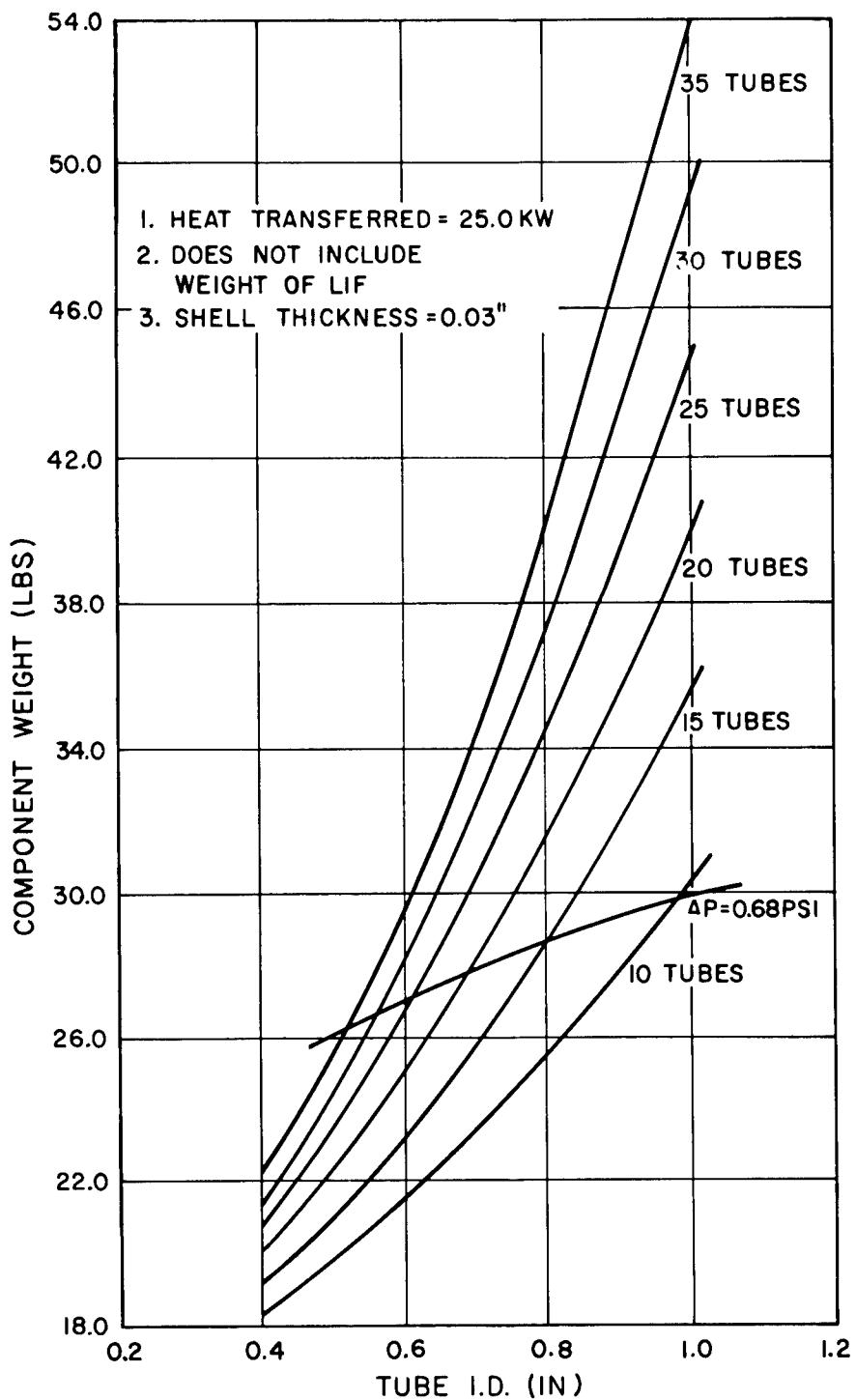


Figure 6-7. Absorber Component Weight Vs. Tube I.D.

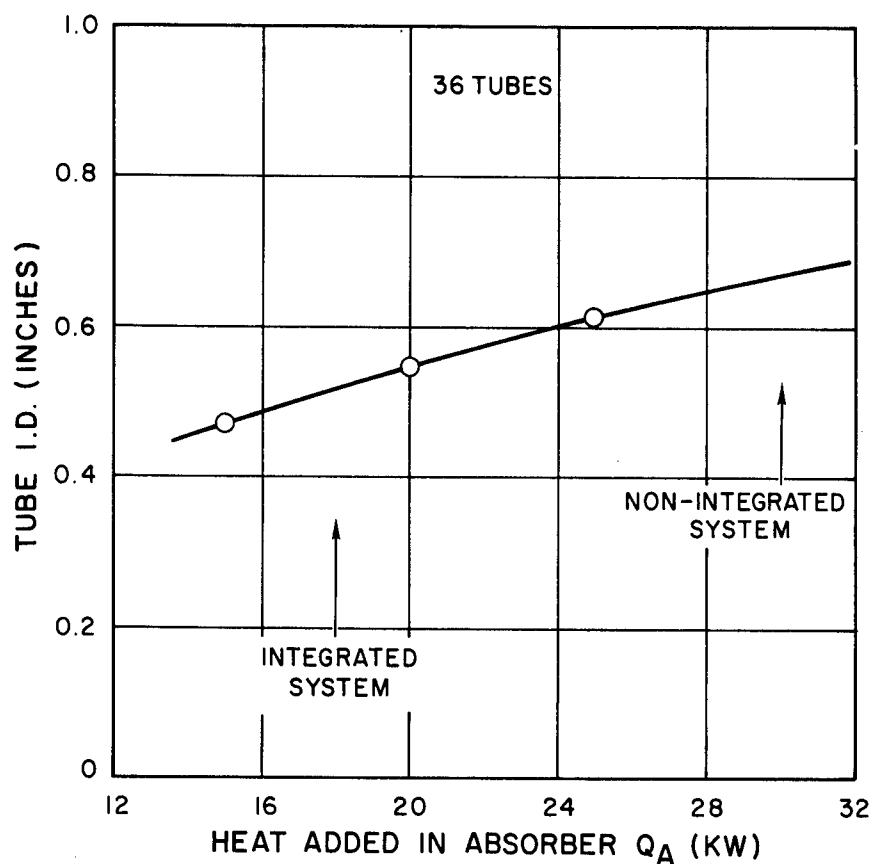


Figure 6-8. Absorber Heat Vs. Tube I.D.

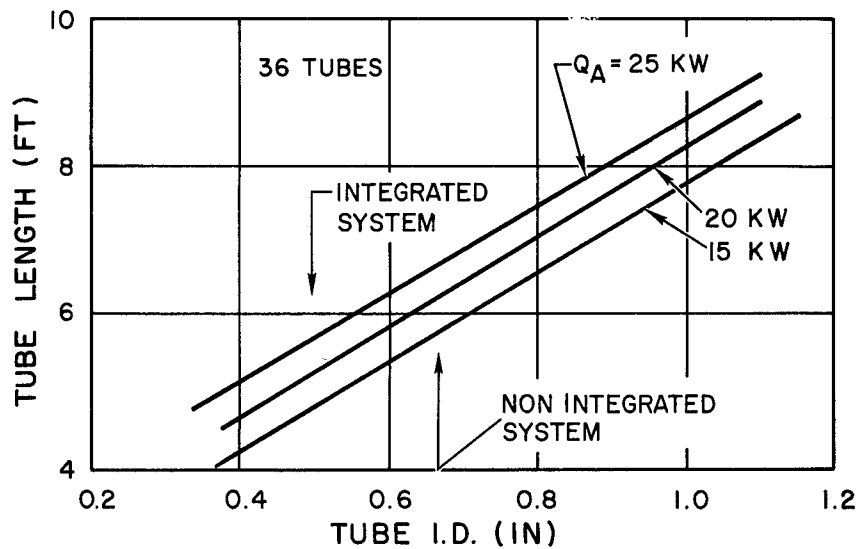


Figure 6-9. Absorber Tube Length Vs. Tube I.D.

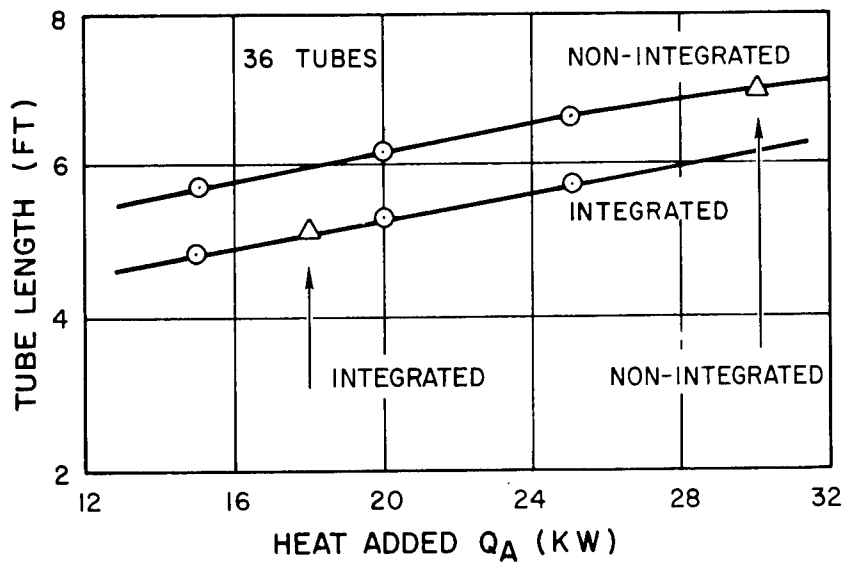


Figure 6-10. Absorber Heat Vs. Tube Length

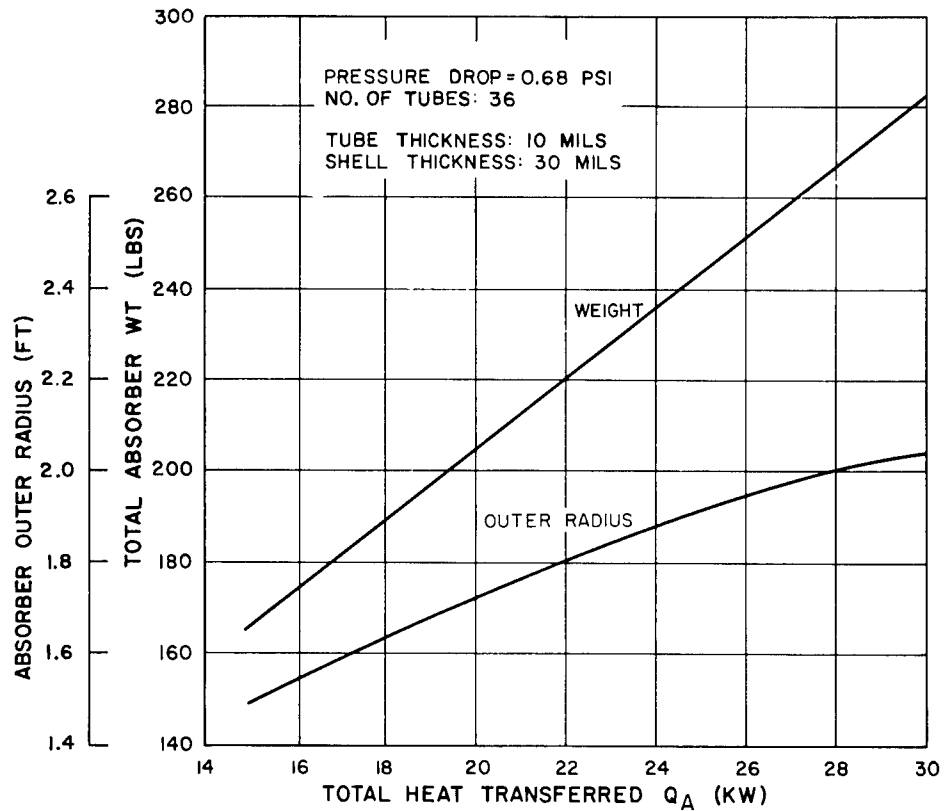


Figure 6-11. Absorber Weight Vs. Heat Transferred (Q_A)

To close the aperture during darkness to prevent large radiation loss, the TRW design again suggests the use of four quadrant sections each operated by a temperature sensor and bellows. This control could be simplified by the use of a conical shade door and a single temperature sensitive actuation device which would cause the door travel to be parallel to the absorber focal plane and would assume either an open or closed position.

6.1.5.3 Isotope Heat Source

6.1.5.3.1 Introduction

This section presents the conceptual designs for isotope heat exchangers for use in Brayton Cycle power conversion systems. The heat exchangers and cycles are not optimized, rather the heat exchangers are optimized to meet given cycle conditions of temperature, flow rate, and pressure. Stated operating conditions for the exchangers are given in Table 6-2.

Cooling the isotope package during the re-entry phase and detailed safety considerations were beyond the scope of this study.

Cooling the isotope package during launch preparations, the launch phase and prior to start up of the system was considered, but not to a significant technical depth.

Cooling problems associated with single engine operation and emergency conditions significantly affect the system design and are considered in depth.

TABLE 6-2. ISOTOPE HEAT EXCHANGER REQUIREMENTS

	<u>Non-Integrated</u>	<u>Integrated</u>
Heat Source	Pu-238	Pu-238
Coolant	Argon	Argon
Flow Rate (per loop)	0.235 lb/sec.	0.140 lb/sec.
Inlet Pressure	13.66 psia	13.66 psia
Pressure Drop (desired)	5%	5%
Argon Outlet Temperature T_3	1490°F	1490°F
Maximum Clad Temperature	1650°F	1650°F
Thermal Power Required	29.65 KW	17.65 KW
Thermal Power Provided (1% Margin) Non-Integrated (2% Margin) Integrated	30 KW	18.0 KW

The radio-isotope, Pu-238, can be produced by the irradiation of Neptunium-237 (Np-237). The Np-237 is a waste by-product that must be separated from the radioactive wastes of reactors, either U. S. Government reactors or commercial power reactors.

The supply of Pu-238 is thus linked to:

1. The amount of Np-237 available in reactor waste products
2. The capacity of separation facilities
3. The availability of reactors to convert the Np-237 to Pu-238.

The US Atomic Energy Commission presently estimates, (Ref. 1), that within these limitations, the amounts of Pu-238 shown in Table 6-3 will be available for isotopic power applications at the dates shown.

The values shown assume that Pu-238 is produced as a by-product of other irradiations. It is also possible to operate a reactor so as to produce Pu-238 as the prime objective. In such a case, amounts of Pu-238 significantly greater than those given below can be provided. However, the lead time necessary to obtain funds, modify and/or construct new processing facilities, and make necessary change-overs would be 6 to 8 years. Therefore, the values given above are maximum until the 1970's.

The present cost of Pu-238 is 1000 \$/gram (2,100,000 \$/Kwt). The increased capacity of the late 1960's is expected to reduce this price to about 500 \$/gram (1,050,000 \$/Kw_t).

TABLE 6-3. ESTIMATED PU-238 AVAILABILITY

Year	Production Rate, Kg/year		Total	Total Production Kw _t /year
	Commercial Power Reactors	US Government Reactors		
1965	3.0	13.0	16.0	7.7
1966	3.3	18.0	21.3	10.2
1967	4.6	24.0	28.6	13.7
1968	6.3	32.0	38.3	18.4
1969	8.6	36.0	44.6	21.5
1970	12.4	42.0	54.4	26.1
1971	16.7	47.0	63.7	30.6
1972	23.0	51.0	74.0	35.5

6.1.5.3.2 Integration Factors

6.1.5.3.2.1 Heat Exchanger Location

To obtain maximum benefit of distance for shielding, the isotope is located at the extreme corner of the vehicle as shown in Figure 6-12. This location has other benefits in that:

- (a) The heat exchanger is accessible for the loading of the isotope when the vehicle is on the launch pad and
- (b) Two surfaces of the exchanger face away from the crew compartments and therefore require no shielding or only partial shielding.

6.1.5.3.2.2 Shielding

Shielding is provided based on allowing a maximum dose of 30 rem per year. The heat exchanger is located comparatively close to the crew quarters and, consequently, the fraction of time spent by the crew at various stations within the pressure vessel can have significant effect on the shielding required. To account for this factor, the time estimates for duty stations given in Table 6-4 were made. Based on a one year duty cycle, the times listed are those expected to be spent in the various occupations. The corresponding distances considered average for each of these occupations are also listed in Table 6-4 and shown in Figure 6-12.

TABLE 6-4. AVERAGE CREW DUTY STATIONS

<u>Location No.</u>	<u>Purpose</u>	<u>Hours</u>	<u>Distance Inches</u>
1	Sleep	2900	210
2	Recreation	1600	150
3	Duty	4100	255
4	Inside Maintenance	120	45
5	Outside Maintenance	15	125

The dose due to gamma will be 9.6 rem or 32% of the total dose. This is based on the assumption that no gamma shielding is provided except that of the heat exchanger and vehicle structure and that these structures are equivalent to 1 cm of steel. The thickness of lithium hydride required to limit the neutron dose to 20.4 rem is shown as a function of power level in Figure 6-13.

Presently, there is not a uniform set of criteria that defines the allowable radiation dose to be received by an astronaut on a single mission or a series of missions. Consequently, it is necessary to develop a rationale for criteria that can be supported by logic.

In the commercial handling of radioactive materials, all licenses are required by the U. S. Atomic Energy Commission to adhere to the radiation protection standards set forth in the Federal Register, 10 CFR Part 20. These standards relate to allowable dose rate, permissible air concentrations, waste disposal, etc., and, of interest here, define the maximum whole body dose* for industrial workers to be 1.25 rem per calendar quarter. In commercial practice, this is applied as 5 rem per calendar year and all continuous occupancy areas are provided with sufficient shielding to assure that the 5 rem per year whole body dose will not be exceeded.

*The whole body dose affecting the blood forming organs will determine the allowable dose when the eyes are shielded from radiation.

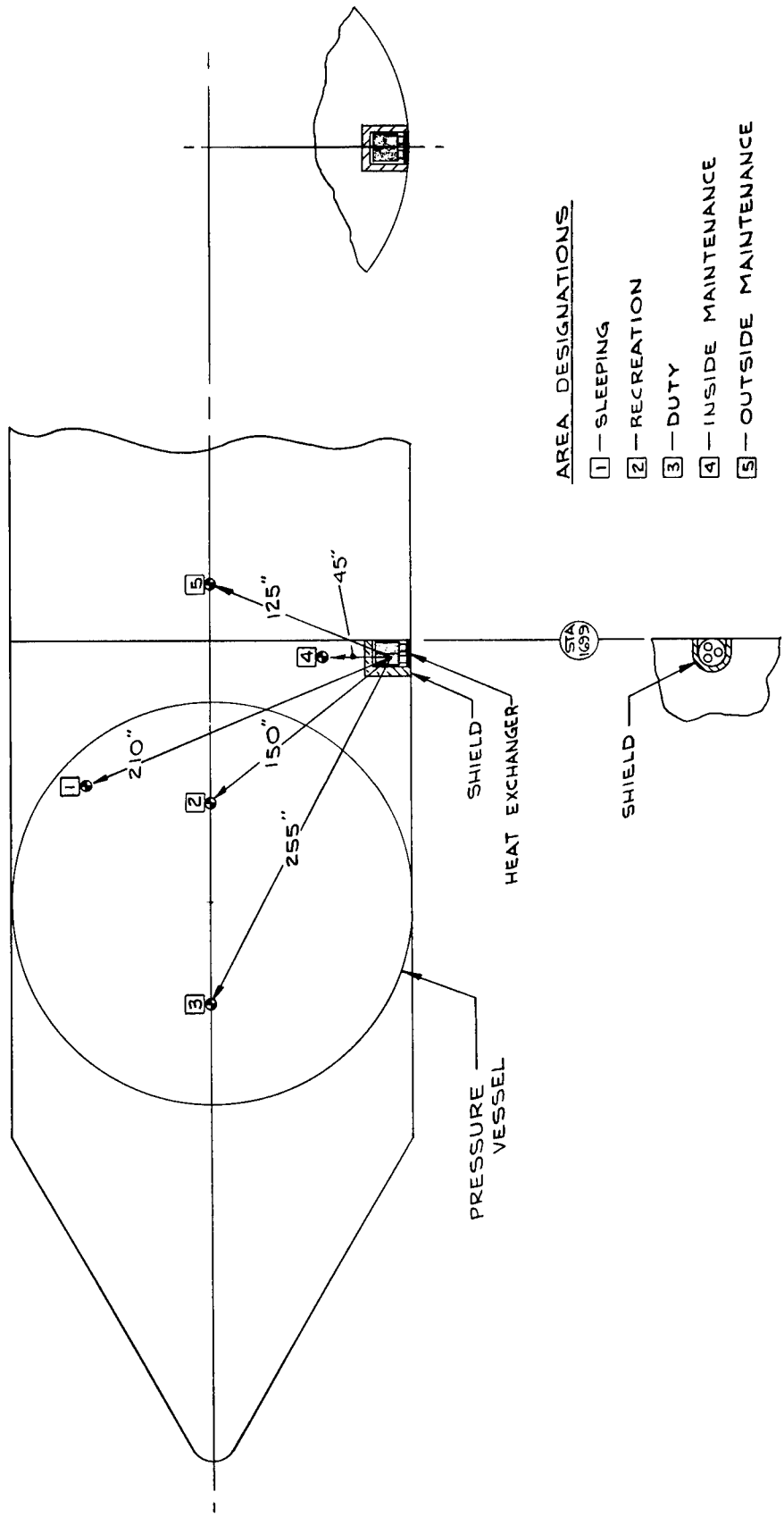


Figure 6-12. Heat Exchanger Location on Vehicle

It is generally concluded that an astronaut will be expected to endure a risk that is one order of magnitude higher than that of an industrial worker. If this guideline is applied, the design dose rate for astronauts aboard the station is 50 rem per year.

The astronaut will be subject to space radiation in addition to the radiation from the radio-isotope and both sources will require shielding to meet the 50 rem per year limit. The optimum division between dose contributions from the space and radio-isotope sources is that which will result in minimum total shield weight; however, it is not possible to parametrically consider the effect of various divisions between the two dose contributors in this study. Consequently, it is assumed that a yearly dose of 30 rem will result from radio-isotope radiation and 20 rem will result from space radiation. The value of 30 rem per year generally agrees with that used in other space station studies. (See reference 2.)

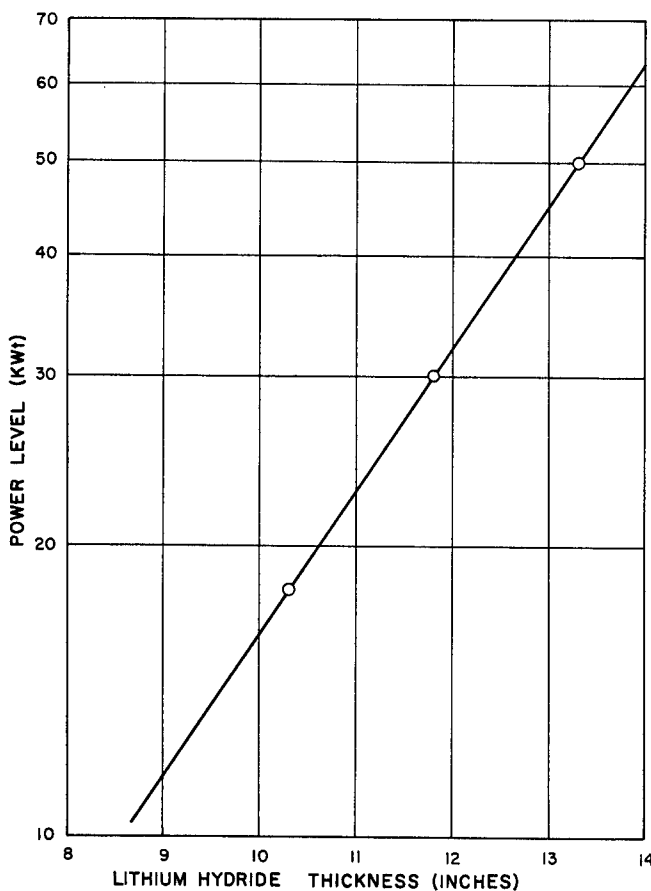


Figure 6-13. Isotope Brayton Lithium Hydride Shield Thickness

The radio-isotope will be provided with sufficient shielding to assure that a 30 rem per year whole body dose will not be exceeded considering that the astronaut will move relative to the isotope for sleeping (33 percent), recreation (18 percent), duty (47 percent), inside and outside maintenance (1.4 and 0.2 percent), and rendezvous operations. The astronaut is assumed to spend the percentages of time noted in parenthesis in the various occupations.

6.1.5.3.2.3 Isotope Cooling

The isotope must be cooled essentially continuously. During the loading period, during the waiting period on the launch pad, and during launch this can be accomplished by the operation of one or more of the coolant loops with heat rejection via the space radiator, an evaporator, or by suitably designing the heat exchanger so as to allow direct evaporative cooling.

If significant thicknesses of shielding are required, it is not practical to disperse the individual fuel capsules to allow direct radiation heat rejection because of the significant weight penalty incurred in the shielding of individual capsules rather than clusters of fuel capsules.

Upon completion of the mission, cooling must also be provided during the return of the fuel capsules to earth. The combined factors of the high cost of Pu-238 (about \$63,000,000 for 30 kW_t) and the significant radiological hazard resulting from the dispersal of the isotope in the atmosphere in the event of capsule burnup will likely require that provision be made for the intact return of the capsules at mission conclusion. The design criteria will also likely require that the capsules survive all forms of vehicle abort, partial orbit injection, etc.

6.1.5.3.3 Fuel Capsule

The fuel capsule design is shown in Figure 6-14. The fuel material is PuO₂ and the clad may be Haynes -25 or Hastelloy C. Both of these materials are adequate to 1650°F. The capsule includes a void volume to allow for the pressure buildup due to the helium produced in the decay of Pu-238. The void may be included as shown in Figure 6-14 by separating the fuel with a perforated plate, or by providing a void along the fuel centerline or by reducing fuel density to provide interstitial voids.

The clad thickness must be sufficient to contain the PuO₂ during accidents and for about 10 half lives (~890 years). The thickness required for intact accident survival will depend upon the safety criteria, the mission and launch vehicle and the particulars of the heat exchanger design. The heat exchanger structure, in particular, can provide significant protection in the survival of high velocity impact. The maximum helium pressure may occur many decades after encapsulation, depending upon the details of the capsule design. For a constant temperature environment with convective cooling the capsule pressure varies as:

$$P(t) = \frac{W_{238} R}{V} \left[1 - e^{-t\lambda} \right] \left[(\bar{T} - T_0) e^{-t\lambda} + T_0 \right]$$

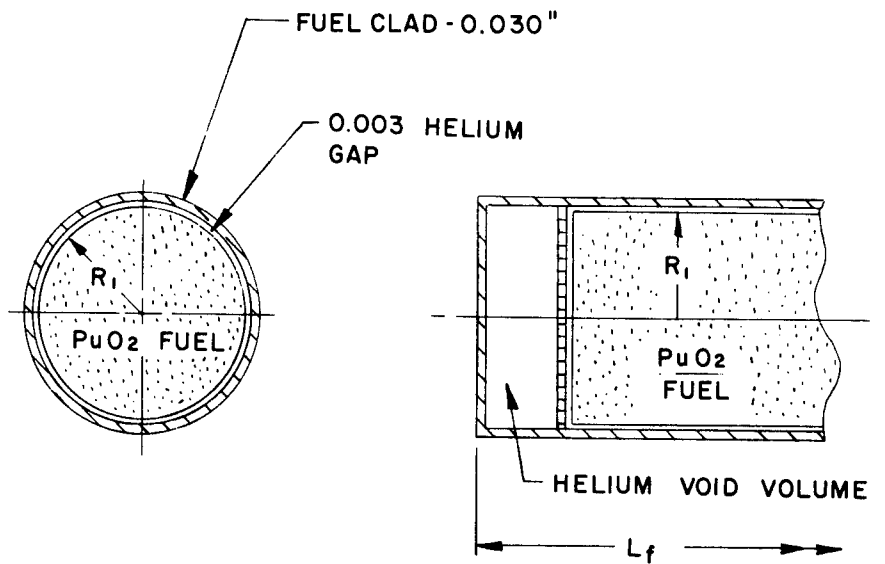


Figure 6-14. Fuel Capsule

Where:

$P(t)$	=	Pressure
t	=	Time
W_{238}	=	Moles of Pu-238
R	=	Gas Constant
λ	=	Decay constant of Pu-238
\bar{T}	=	Average fuel temperature at beginning of life
T_o	=	Ambient temperature
V	=	Void volume

6.1.5.3.4 Heat Exchanger Description

The heat exchanger design must be such as to allow the capsules to be loaded only a few minutes prior to launch and the loading operation must be simple to minimize the time and therefore dose received during the loadings operation. In addition, to assure continued cooling of the isotope in the event of failure of a loop, two complete cooling loops must be provided.

To meet these requirements, a "pressure-tube" type of heat exchanger is used. The basic pressure tube is shown in Figure 6-15. It consists of two concentric tubes which form an annular flow passage. Dividers are used between the tubes to provide

separate flow passages. In Figure 6-15 flow channels "A" are fed from a common header and channels "B" are feed from a common but independent header. The design must meet maximum fuel and clad temperature limitations when only one loop is operable. The individual tubes are positioned horizontally on the vehicle and the fuel capsules slide into the fuel cavity. The heat from the capsule may be conducted or radiated to the inner wall of the heat exchanger tube. The temperature differential across the gap is large enough that a conduction medium is desirable. Conduction can be provided by wrapping the fuel capsule with indium or lead foil which will fuse to both walls to provide the necessary heat transfer path, or the gap may be flooded with a liquid metal such as NaK. A cross section of an assembled tube using a NaK heat transfer medium is shown in Figure 6-16.

The individual tubes may be assembled on a triangular pitch as shown in Figures 6-17 and 6-18 to form the heat exchanger. A compact array with a length to diameter ratio of about 1.0 will result in minimum shield weight. Consideration of the criticality problem with a close-packed array of Pu-238 was outside the scope of the study.

For an argon cooled exchanger, the inlet and outlet headers and connectors would be contoured to minimize pressure drop. The inner tubes of each heat exchanger tube are extended to the side of the vehicle and welded into a common tube sheet. After the fuel capsules are inserted, a blind cover plate is fitted over the tube sheet and bolted tight. It may also be seal welded. The fuel cavity is flooded with NaK to provide a heat transfer medium between capsule and heat exchanger tube.

If the flow loops are inoperative during the loading operation, the capsule heat may be removed by passing air over the exterior of the heat exchanger tubes or by enclosing the tubes in a shell and providing evaporative cooling.

The heat exchanger fits within the shield as shown in Figure 6-17 and the exchanger and shield are mounted in the vehicle as shown in Figure 6-12. The shield is open on the two sides that face away from the crew compartments because there is no structure in these directions that can cause neutron scattering.

6.1.5.3.5 Heat Exchanger Analysis

The low system pressure (13 psia) that allows the attainment of reasonable efficiencies in small size Brayton cycle components makes it extremely difficult to remove the heat from the radioisotope heat source without exceeding limiting conditions of pressure drop, maximum clad temperature, or Reynolds number. Limits were established as a pressure drop ($\Delta P/P$) less than 5 percent, a maximum clad temperature of 1650°F , and a minimum Reynolds number of 3000. The heat removal problem is

further aggravated by the requirement that a single loop be capable of maintaining maximum clad temperature.

There are many heat exchanger parameters that may be varied to meet the specified cycle operating conditions. Some of these are:

- . Number of Heat Exchanger Tubes in Parallel
- . Length of Tubes
- . Number and Thickness of Fins
- . Width of Annular Flow Passage
- . Fuel Effective Density

The effects of these parameters were investigated and are discussed in the following paragraphs. It was found necessary to use a low effective fuel density to satisfy the requirements.

6.1.5.3.5.1 Number of Parallel Tubes

Figures 6-19a through 6-19j show the effect of the number of parallel heat exchanger tubes as a function of fuel capsule length and annular flow passage width. The heat exchanger parameters that are of primary interest (Maximum Clad Temperature, Reynolds Number, Heat Exchanger Total Weight, and Pressure Drop) are plotted.

In Figure 6-19a, a clad temperature of 1650°F can be obtained with a flow passage width of 0.1 inch and a fuel capsule length of 23 inches; however, these conditions result in a pressure drop ($\frac{\Delta P}{P}$) of 16%. The Reynolds number at 3500 is marginally acceptable as it is greater than the minimum acceptable of 3000. Weight is 370 pounds. (Weights do not include end fittings and flow connections which are estimated at 5 pounds per tube.) Figure 6-19b shows that a decrease in the number of tubes from 60 to 40 will result in a clad temperature of 1650°F at a length of 23 inches, a Reynolds number of 4700, and a weight of 320 pounds. The higher Reynolds number and lower weight are both desirable; however, the pressure drop exceeds 30.4% and is, therefore, unacceptable.

Figures 6-19c and 6-19d show that with continued reduction of the number of tubes to 30 and 20, respectively, a clad temperature of 1650°F cannot be obtained irrespective of the allowable pressure drop. The results of Figures 6-19a through 6-19d indicate that a pressure drop of 5 percent may be obtainable with a number of tubes greater than 60; however, a greater number of tubes will reduce the Reynolds number below 3000.

6.1.5.3.5.2 Finned Flow Channels

Fins may be included in the flow channels as shown in Figure 6-16 to reduce the maximum clad temperature. The fins have a significant effect and as shown in Figure 6-19c. Twenty parallel tubes with ten 20 mil thick fins per flow channel can provide 1650°F clad temperatures with coolant channel widths of 0.2 or 0.3 inches. Weight is 300 to 330 pounds; however, the Reynolds number is below 3000 and the pressure drop is excessive.

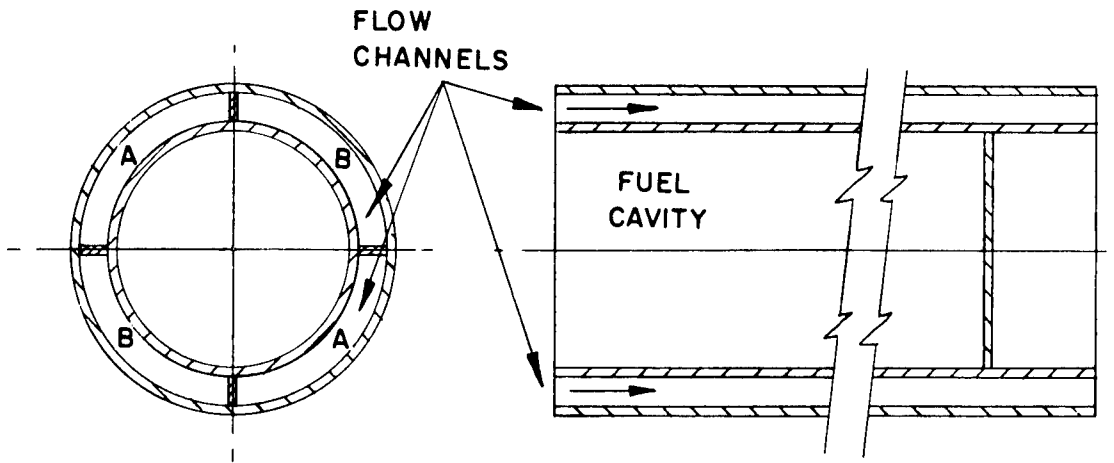


Figure 6-15. Individual Heat Exchanger Tube

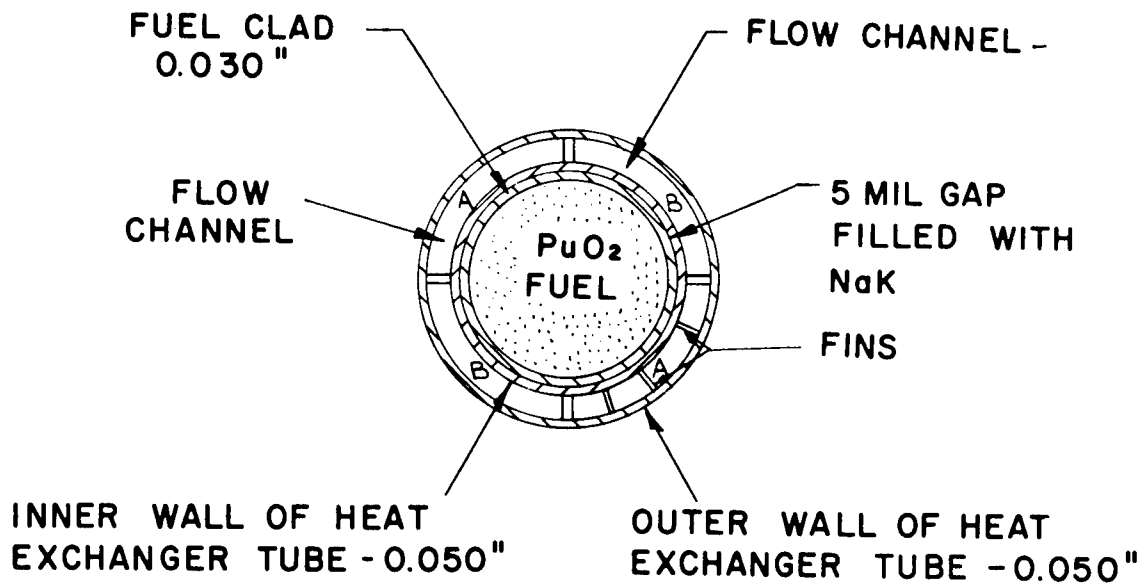


Figure 6-16. Fuel Capsule and Heat Exchanger Tube

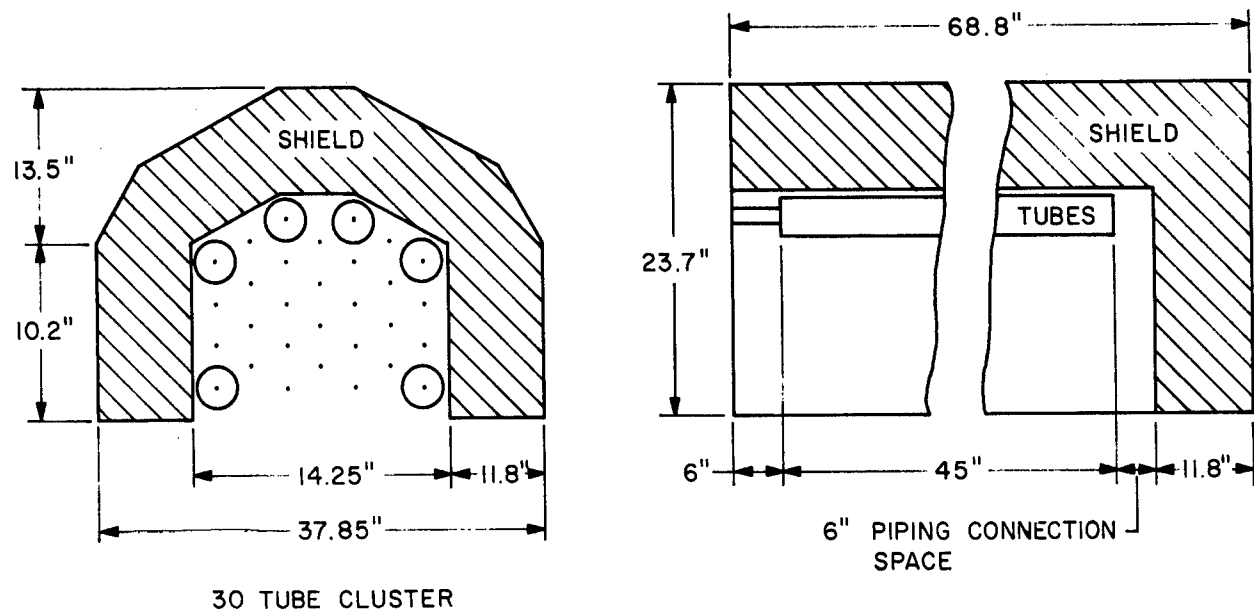


Figure 6-17. Isotope Heat Exchanger and Shield, Non-Integrated System

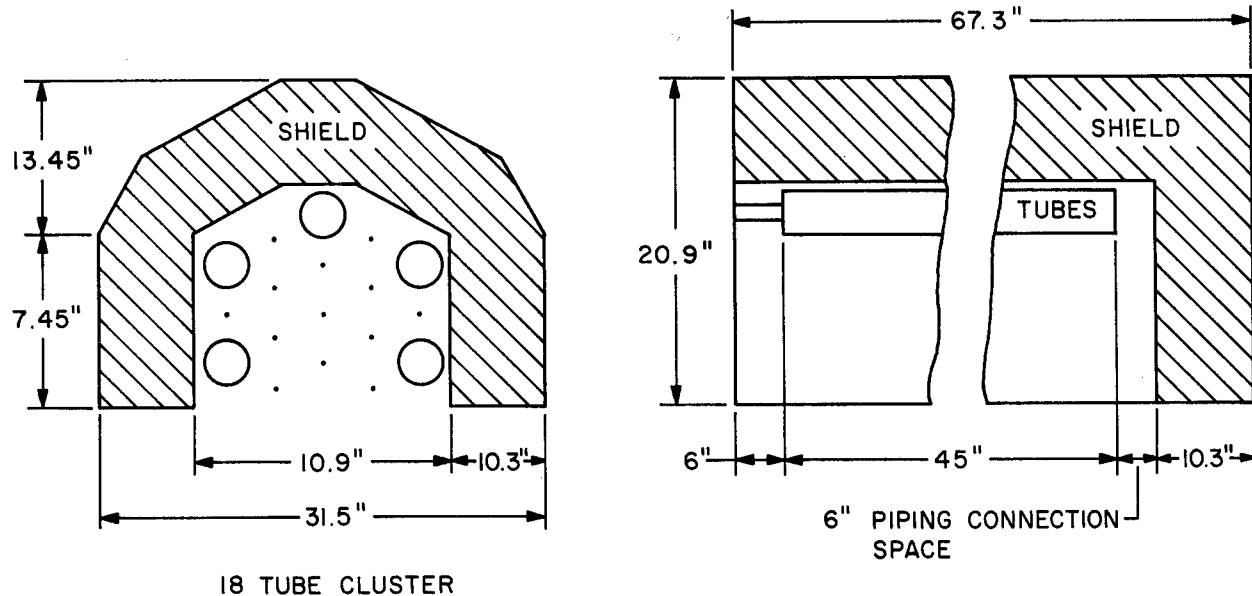


Figure 6-18. Isotope Heat Exchanger and Shield, Integrated System

ISOTOPIC HEAT EXCHANGERS

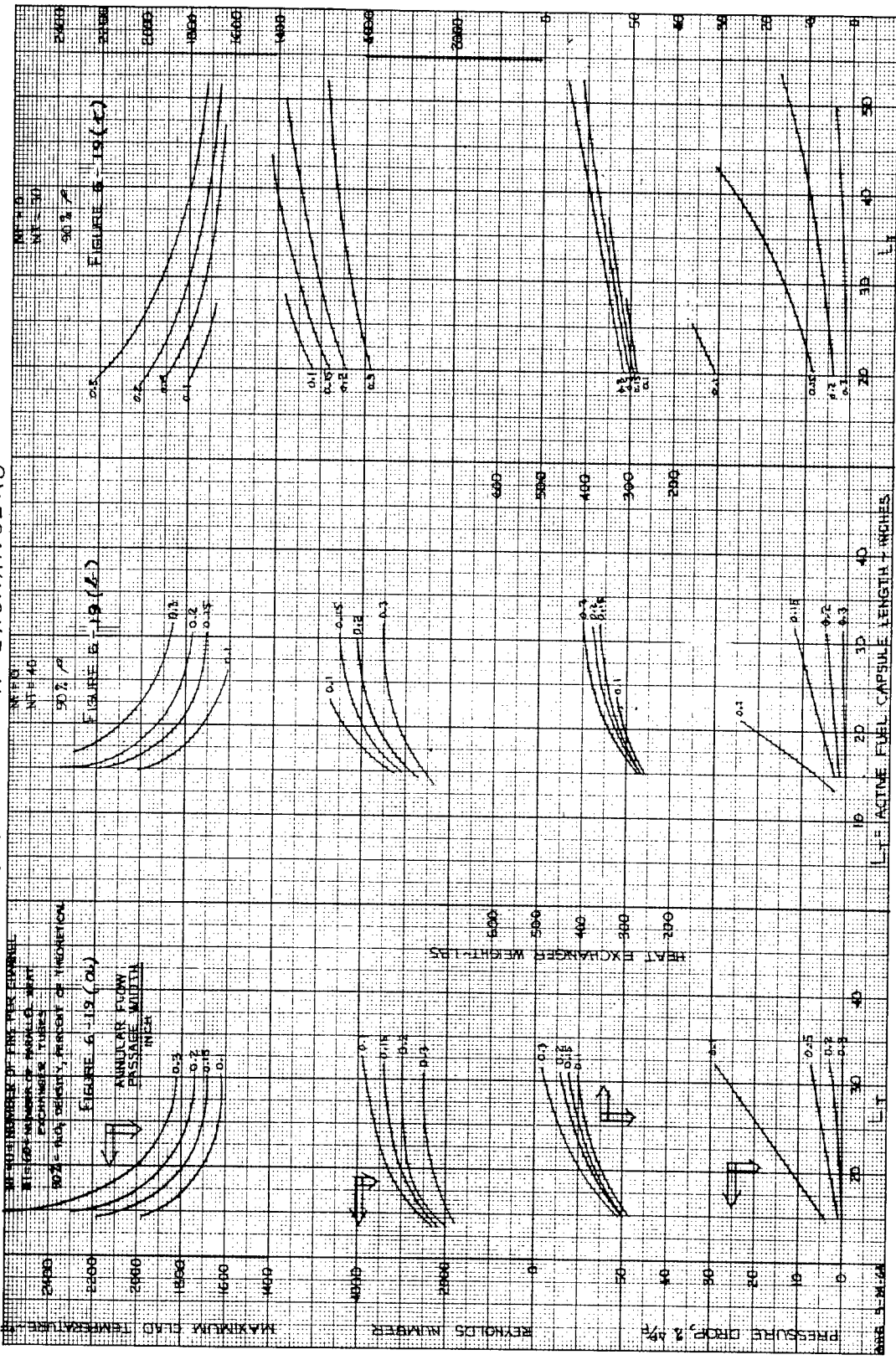


Figure 6-19a, b, c

ISOTOPIC HEAT EXCHANGERS

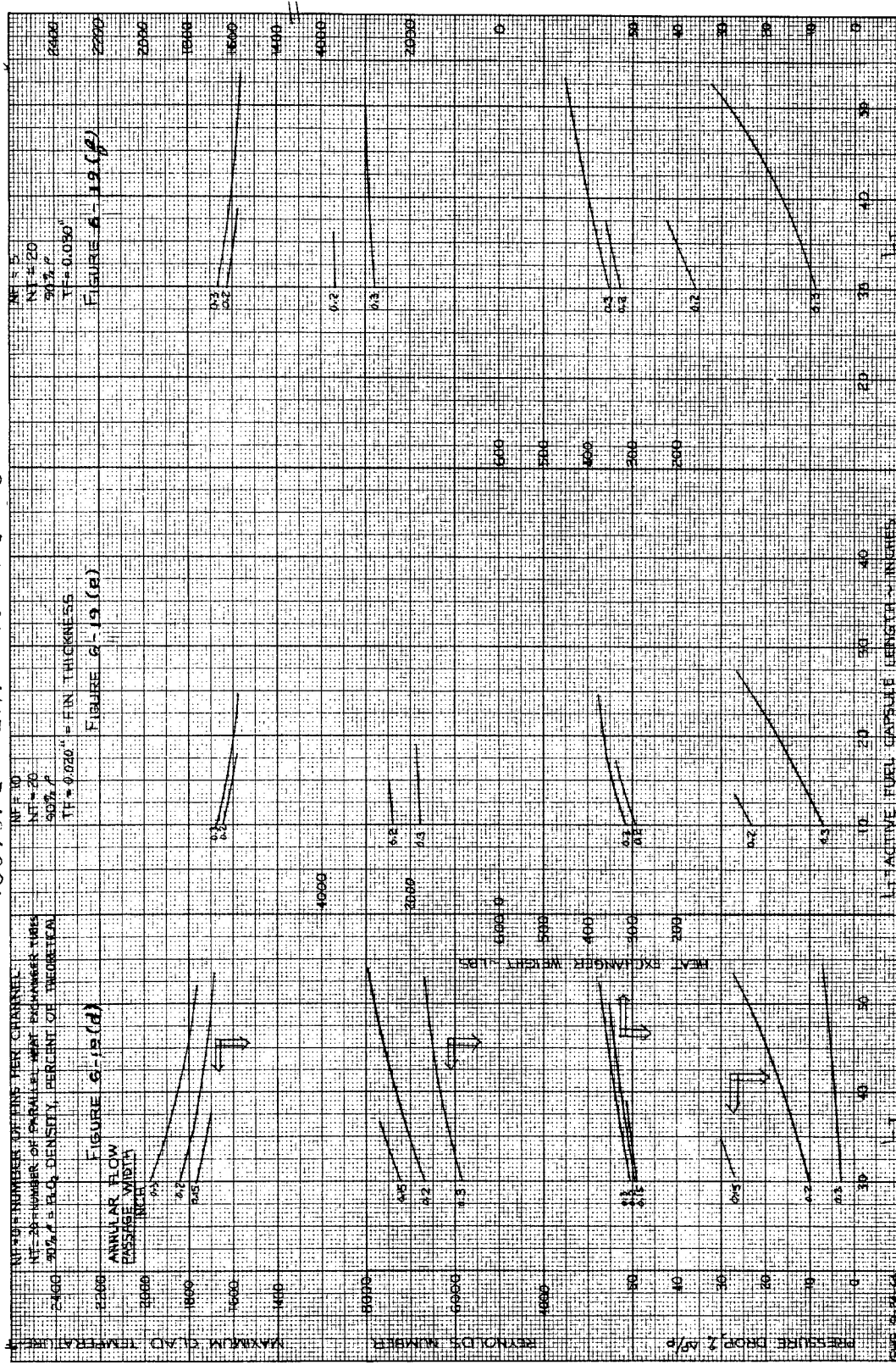


Figure 6-19d, e, f

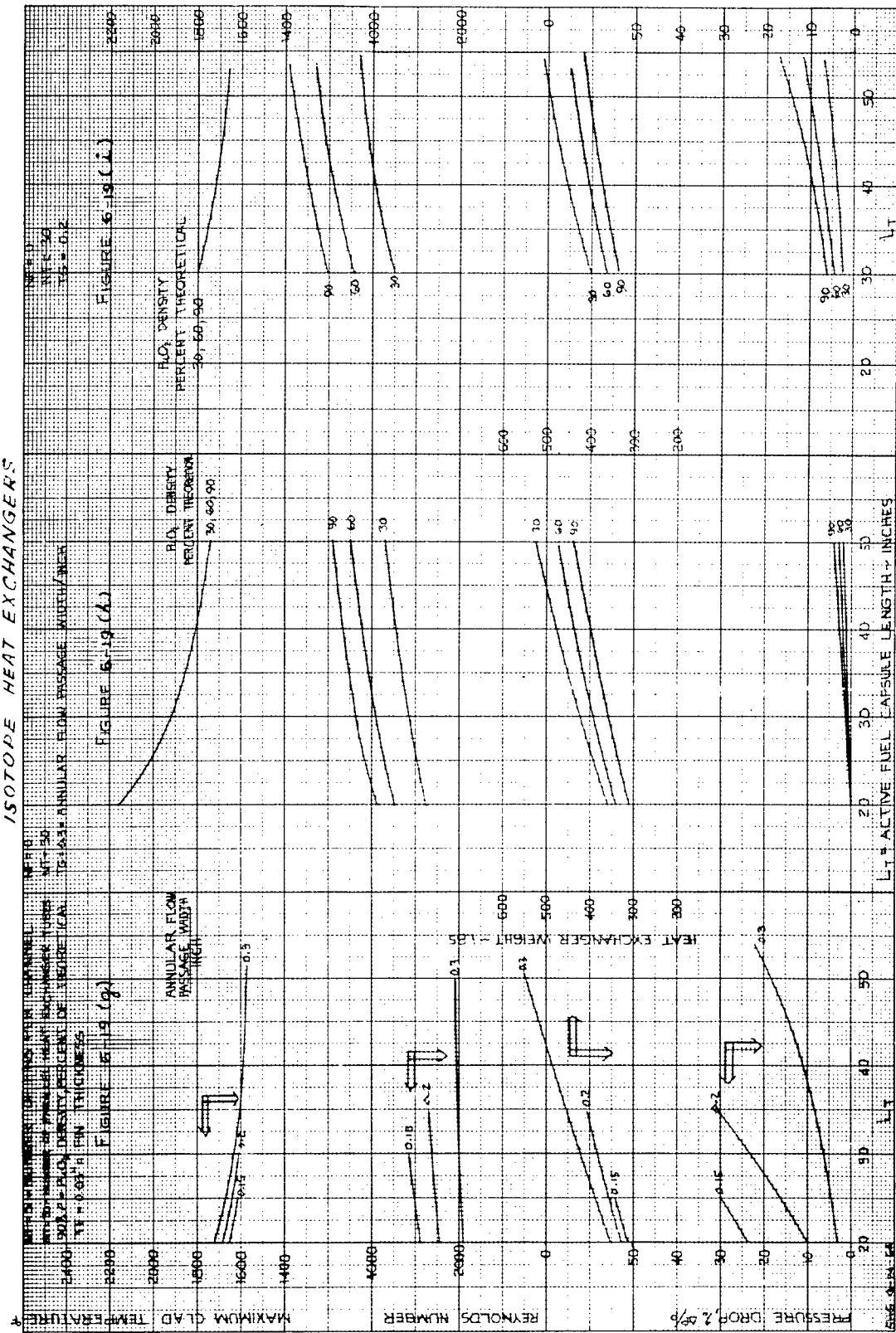


Figure 6-19g, h, i

ISOTOPE HEAT EXCHANGERS

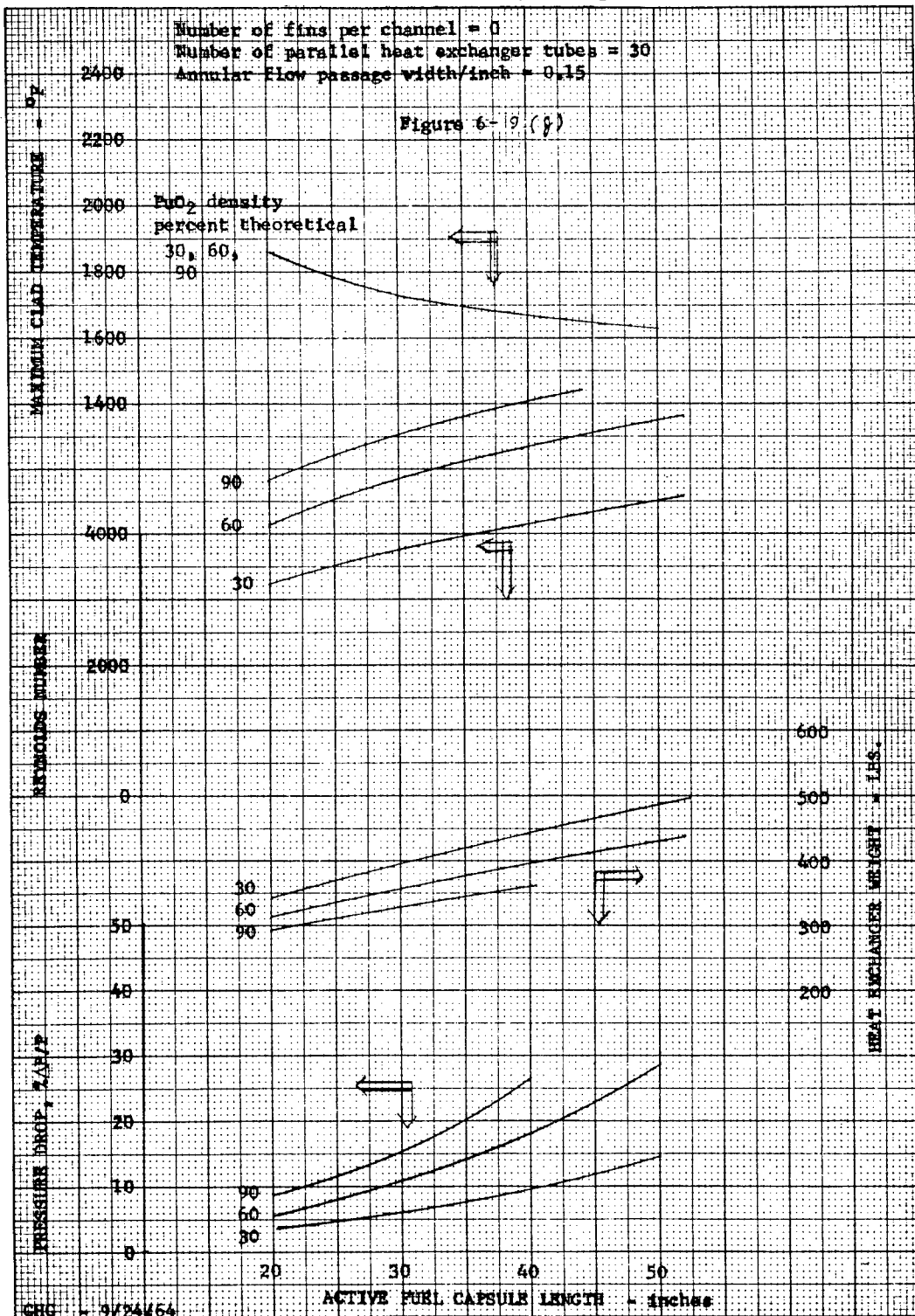


Figure 6-19j

A decrease in the number of fins to five that are 30 mils thick has the effect shown in Figure 6-19f. A 0.3-inch flow channel provides a 1650°F clad temperature but is unacceptable due to low Reynolds number and high pressure drop. A 0.2-inch channel provides a higher Reynolds number, but results in excessive pressure drop.

The number of tubes may be increased to 30 with the same five fins that are 30 mils thick and as shown in Figure 6-19g, clad temperature of 1650°F may be obtained with channel widths of 0.15, 0.2 and 0.3 inches. The two smaller widths result in pressure drops greater than 5 percent. The pressure drop in the 0.3-inch channel is 5 percent at a 1650°F clad temperature; however, the Reynolds number is below 2000.

Figures 6-19a to 6-19g show the effect of number of tubes, length of tube, and number of fins and the results indicate that a design cannot be obtained that will simultaneously satisfy the requirements on clad temperature, Reynolds number, and pressure drop. These results are for the PuO_2 fuel with a density that is 90% of theoretical. It is also possible to reduce the fuel density in order to obtain increased heat transfer area. Fuel density can be reduced by compacting and sintering to a lower density or by using an annular fuel pellet with a central void.

6.1.5.3.5.3 Fuel Density Effects

The effect of fuel density is shown in Figures 6-19h through 6-19j. In Figure 6-19h, a 0.3-inch flow channel will not provide a 1650°F clad temperature up to lengths of 50 inches. In Figure 6-19i, a 0.2-inch flow channel will provide the necessary temperature at a length of 55 inches and a pressure drop of 5 percent with a density slightly lower than 30 percent. Generator weight exceeds 500 pounds. In Figure 6-19j, clad temperature is attained with a length of 45 inches. A pressure drop of 5 percent is attainable at a density below 30 percent of theoretical.

Figures 6-19i and 6-19j indicate that acceptable designs can be attained with fuel lengths of 55 and 45 inches, respectively. The lower length will result in lower shield weights and is, therefore, more desirable. The data from Figure 6-19j is cross-plotted as a function of fuel density at a fuel length of 45 inches with the results shown in Figure 6-20. A pressure drop of 5 percent is obtained at a fuel density of 14 percent and with a Reynolds number of 3300 and a weight of 510 pounds.

A heat exchanger design that meets all of the cycle requirements is obtained by reducing fuel density to provide increased heat transfer area. The decreased fuel density results in a higher heat exchanger weight because more material is used in fuel cladding and tubing.

The dimensions and weights of the heat exchanger are given in Table 6-5.

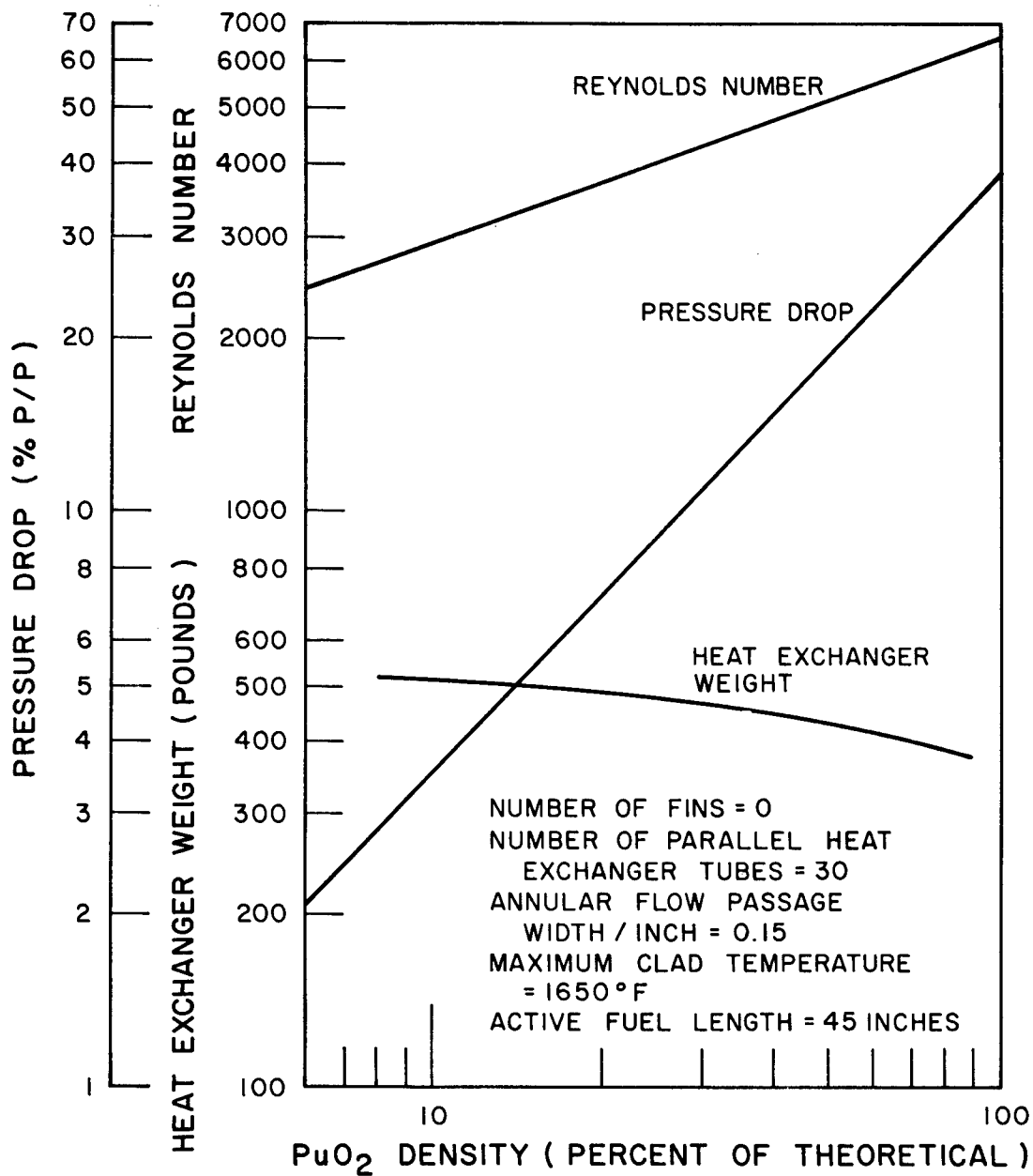


Figure 6-20. Characteristics of Isotope Brayton Cycle Heat Exchanger

TABLE 6-5. ISOTOPE HEAT EXCHANGER

	<u>Non-Integrated</u>	<u>Integrated</u>
Thermal Power	30 KW	18 KW
Coolant	Argon	Argon
Flow Rate (per loop)	0.235 lb/sec.	0.14 lb/sec
Argon Outlet Temperature T_4	1490°F	1490°F
Maximum Clad Temperature (one Loop Operation)	1650°F	1650°F
Fuel Capsule Radius	0.827 inch	0.827 inch
Fuel Clad Inside Radius	0.830 inch	0.830 inch
Fuel Clad Thickness	0.030 inch	0.030 inch
Heat Exchanger Tube Inside Radius	0.865 inch	0.865 inch
Inner Tube Thickness	0.050 inch	0.050 inch
Outer Tube Thickness	0.050 inch	0.050 inch
Annular Flow Channel Width	0.150 inch	0.150 inch
Heat Exchanger Tube Outside Radius	1.115 inches	1.115 inches
Number of Tubes	30	18
Number of Fins	None	None
Active Fuel Length per tube	45 inches	45 inches
Circumscribed Diameter of Heat Exchanger	See Figure 6-17	See Figure 6-18
Overall Length of Heat Exchanger	See Figure 6-17	See Figure 6-18
Shield Thickness (Lithium Hydride)	11.8 inches	10.3 inches
Shield Length	68.8 inches	67.3 inches
Shield Width	37.85 inches	31.5 inches
Shield Height	23.70 inches	20.8 inches
Shield Weight	1520 pounds	967 pounds
Heat Exchanger Weight (Included End Connections and Fittings)	730 pounds	438 pounds
Total Weight	2250 pounds	1405 pounds

6.1.6 TURBOMACHINERY

6.1.6.1 Selection of Design Point

Cycle thermodynamic efficiency is a function of compressor inlet temperature, recuperator effectiveness, compressor and turbine efficiencies, compressor pressure ratio and the system loss pressure ratio $\Delta P_t/\Delta P_c$, where ΔP_t is the pressure drop across the turbines, and ΔP_c is the pressure rise of the compressor. Figure 6-21 is a plot of cycle thermodynamic efficiency versus compressor ratio with turbine inlet temperature a parameter. Other component performance parameters are listed in Table 6-6. The effects of gas bearing losses are not included in these efficiency numbers. As can be seen from Figure 6-21 the efficiency curves peak from P_2/P_1 of 2.3 to 2.4 depending on compressor inlet temperature T_1 .

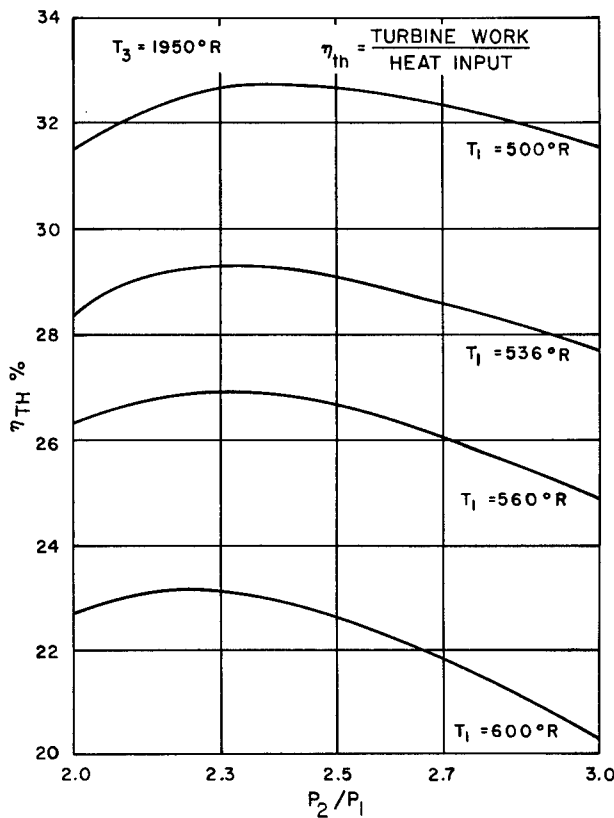


Figure 6-21. Brayton Cycle Thermodynamic Efficiency

TABLE 6-6. SUMMARY OF DESIGN PARAMETERS
BRAYTON CYCLE POWER SYSTEM

		<u>Non-Integrated</u>	<u>Integrated</u>
Net Electrical Power Output	KW	6.57	3.46
Working Fluid		Argon	Argon
Turbine - Inlet Temperature	T_3	1950°R	1950°R
Compressor Inlet Temperature	T_1	536°R	536°R
Compressor Efficiency	η_c	0.80	0.79
Compressor Turbine Efficiency	η_{T1}	0.83	0.82
Power Turbine Efficiency	η_{T2}	0.84	0.83
Loss Pressure Ratio		0.846	0.846
Type of Alternator		4 Pole Homopolar Generator -	
Alternator Efficiency	$\eta_a \%$	86.2	84.5
Recuperator Effectiveness	ϵ	0.90	0.90
Gas Bearing Losses	KW	1.10	1.10
Parasitic Load	KW	0.31	0.165
Gas Cycle Efficiency	η	0.267	0.248
Overall Cycle Efficiency	$n \%$	20.8	18.2
Radiator Area (Isotope Brayton)	Ft. ²	615	310
Radiator Area (Solar Brayton)	Ft. ²	944	500
Average Orbital Sink Temperature	°R	400°R	400°R

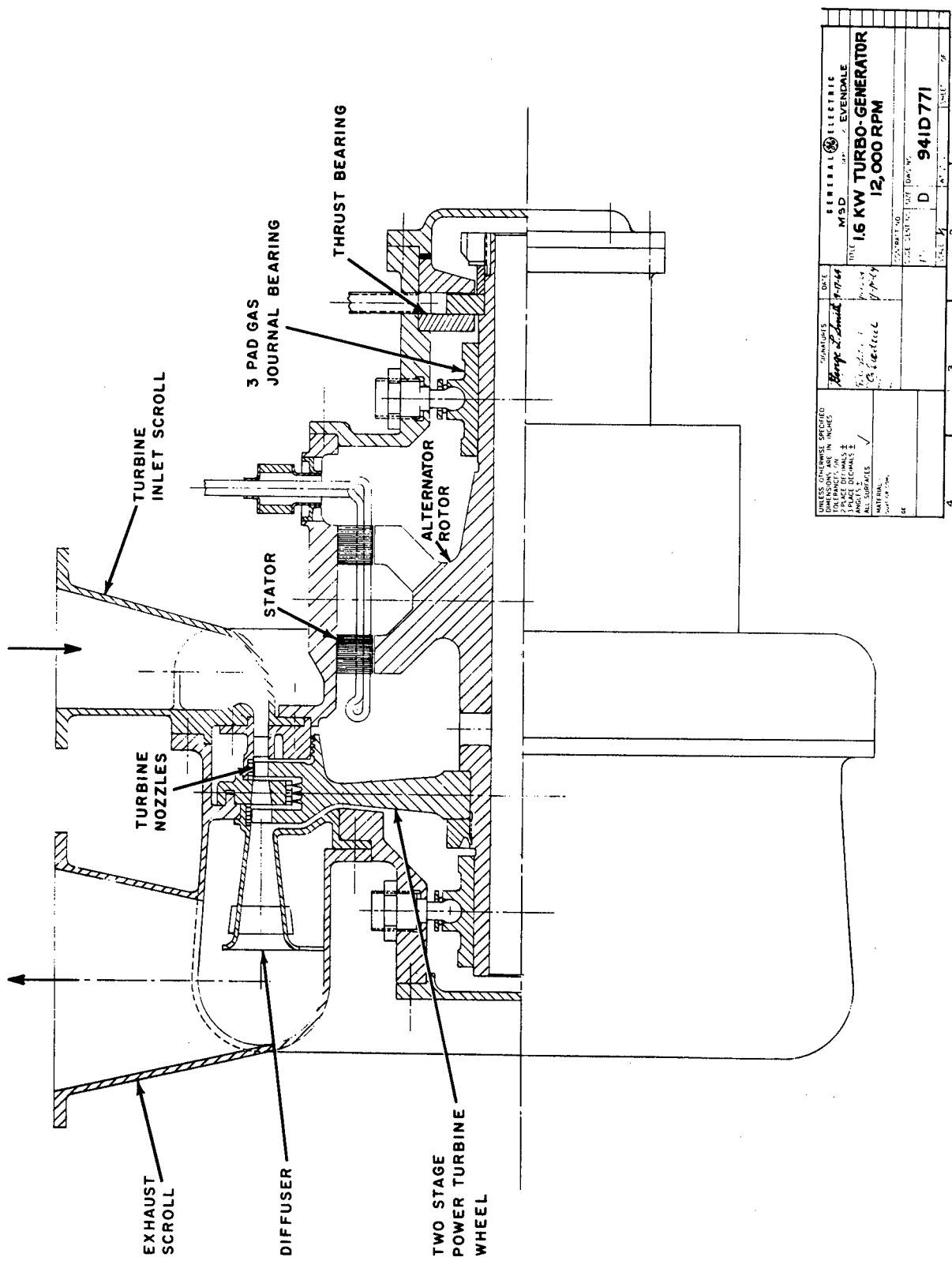
6.1.6.2 Power Turbine Performance

An initial power turbine design was made for a 2-stage unit running at 36,000 RPM with an estimated efficiency of over 0.86. Since it would produce electrical power at 12,000 cps which would have to be converted to 400 cps at a 0.91 efficiency its overall efficiency was about 0.78. A single stage turbine operating at 12,000 RPM was estimated to have an efficiency of slightly over 0.80 with the reduced efficiency due to tip clearance and Reynolds number losses due to the small blade heights. A radial flow turbine was not considered because the specific speed is around 35.

6.1.6.3 Turboalternator

The general arrangement of the turboalternator package is illustrated in Figure 6-22 which is a cross-section of the study design. The overall dimensions without the ducts are approximately:

Diameter	12.0 inches
Length	14.0 inches



UNLESS OTHERWISE SPECIFIED DIMENSIONS ARE IN INCHES PRINTED DETAILS PLATE DETAILS ALL SURFACES MATERIAL COAT & CO.	GENERAL ELECTRIC M&D INC. GENERAL ELECTRIC M&D INC. GENERAL ELECTRIC M&D INC.
	GENERAL ELECTRIC M&D INC. GENERAL ELECTRIC M&D INC.
	GENERAL ELECTRIC M&D INC.
	GENERAL ELECTRIC M&D INC.
	GENERAL ELECTRIC M&D INC.

16 KW TURBO-GENERATOR
12,000 RPM

941D771

Figure 6-22. Turbo-alternator - Reference Design

On the left is the hot turbine portion. On the right side is the turboalternator portion. Turbine and alternator stator parts are integrally mounted. This facilitates the alternator stator cooling and the turbine insulation. The hot gas to drive the turbine enters between the turbine and the alternator and leaves on the side away from the alternator to achieve the most favorable passage from the diffuser outlet and to minimize interference with generator cooling.

The ducting is arranged so that the argon gas enters the inlet scroll flowing in a radial direction. From the inlet scroll it flows axially through the turbine nozzles, turbine blades and diffuser into the exhaust scroll. All of the flow energy is converted to rotative speed of the turbine. Recovery of the velocity energy (dynamic pressure) of the high velocity gas occurs in the cylindrical exhaust scroll where most of the losses occur. This must be designed for optimum aerodynamic performance and very smooth surface finishes to minimize the flow losses.

The outlet and inlet housings are structural members. For this reason, they consist of symmetrical round and conical shells and flanges in order to accommodate thermal expansion without distortions which would destroy the centering ability required for the gas bearings. The inlet and outlet housings and connecting pipe will be insulated to prevent excessive heat loss.

The bearing housings, at least on the turbine end of the unit, will be insulated from the hot gas path to keep the bearing parts cool. This is necessary to control the very critical radial clearances in the gas bearings.

The turbine bearing housing and the alternator bearing housing are centered and supported by the outlet duct structure and alternator stator housing. Both are sub-assemblies and carry the adjustable, pivoted, three-pad bearings. The axial thrust bearing, which has to be able to take axial thrust in both directions, is located at the extreme right on the drawing. Normally, the axial thrust of the system is primarily that of the turbine wheel, which will be small because the design is principally an impulse turbine. A small additional amount of thrust load will come from the alternator when the centerline of the poles does not match the centerline of the stator core stacks.

The design approach, as shown in Figure 6-22, provides for the journal bearing housings as separate parts. These have their own precision machining tolerances, their own pivoted three-pad bearing, and locating and gas feeding devices. By this design, the rotor can be balanced and run-in on its own gas bearings.

The front portion of the bearing housing has stationary removable inserts for the thrust bearings. The thrust bearing disk can be adjusted by shims relative to the turbine wheel and the magnetic center of the alternator. Both bearing housings are hermetically sealed.

The alternator speed is established by the frequency and power requirements, in combination with the desire to avoid wound-rotor construction. A homopolar alternator has been selected in order to achieve maximum reliability and longer life through simplicity.

This type of alternator with its no-winding type rotor is limited to a minimum of two pole pairs, and must be operated at 12,000 rpm to achieve 400 cps. The power output fixes the size of the pole faces required, the magnetic path, and size and weight of the alternator rotor. Alternator efficiency as a function of size is shown in Figure 6-23.

The gas turbine wheel must be designed to satisfy the requirements of the alternator in both speed and power. The turboalternator rotor must, in turn, be designed to satisfy the limitations imposed by the self-acting gas bearings.

Careful consideration of many arrangements resulted in the selected two-bearing, straddle-mounted, rotor design shown. With this design, the bearing diameters for both bearings can be made equal.

The most severe mechanical limitations affecting the rotor design are the restrictions imposed by the gas bearing characteristics. The very low spring rate assignable to these bearings, combined with the close running clearances require a high degree of accuracy of alignment, balance, roundness, surface finish and freedom from distortions while running. The dynamic characteristics of the rotor are also limited by the gas bearing capabilities. The systems natural frequency must be designed such that no critical vibration occurs at operating speed. It is possible to operate such a rotor on gas bearings by passing quickly through critical speeds in the conical and transverse modes, but it is not possible to have a critical speed in the bending mode in the design speed range. The only reason for wanting to design for more than two bearings would be if the rotor's first bending mode critical speed could not be satisfactorily controlled with a two bearing design. Extra bearings, beyond two, introduce many mechanical problems, both in construction and operation. Accessibility, adjustment, and alignment of the bearings between the turbine wheel and alternator all become difficult and should be avoided.

The rotor and bearing combination will pass through a system critical in a conical whirl mode at about two thirds its operating speed and will probably operate below its first systems critical in the transverse mode. Careful attention to detail in the final design will allow these system criticals to be adjusted over a small range without reducing the shaft stiffness or adversely affecting the bending critical speeds.

The rotor illustrated in Figure 6-22 shows the turbine wheel supported by a shrink fit on the main alternator shaft. It is necessary to make these pieces separate due to the difference in properties of the materials. The alternator rotor material, with

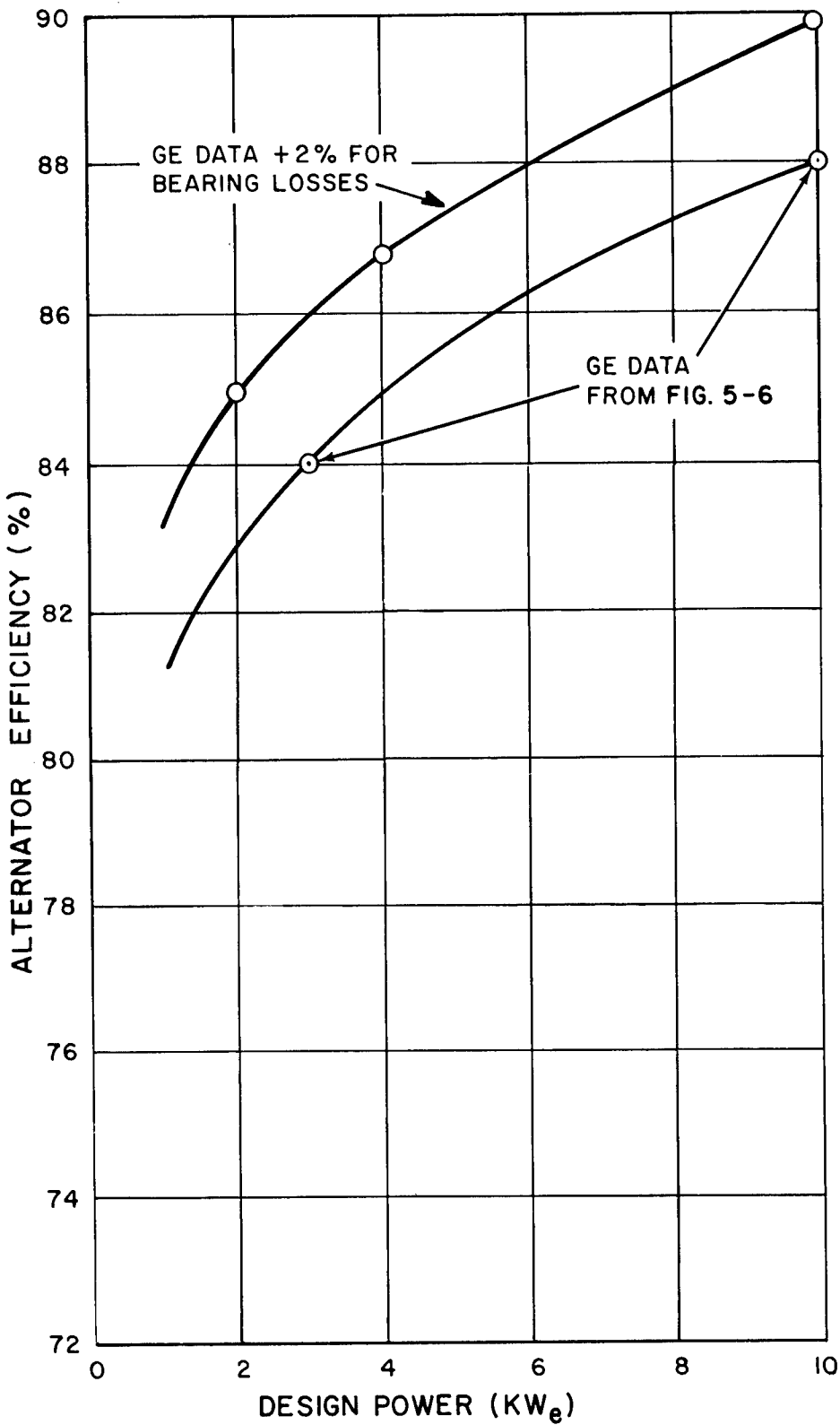


Figure 6-23. Brayton Cycle Alternator Performance

its high magnetic permeability, and its relatively low temperature capability, is not suitable for the stress and temperature conditions in the turbine and conversely the turbine wheel material does not have suitable magnetic properties. It is, therefore, planned to use A286 for the turbine and 4130 for the rotor and shaft to accomplish both magnetic and mechanical design requirements. If final detail analysis shows that a shrink fit is unsuitable, the wheel will be joined to the rotor by electron beam welding techniques.

The turbine wheel will be made with integral blades which will be fitted with separate segmented shroud bands. The use of integral blades eliminates the complications of dovetail attachments and makes a narrower, lighter wheel possible. The lack of a dovetail also assures that the balance will not shift, once obtained, because of the rigid assembly. The shrouds will incorporate sealing bands to control by-pass leakage. In addition, the shrouds will contribute to the mechanical design by providing vibration damping for the buckets. Vibration damping is normally missing in integral wheel designs.

The rotor and gas bearings will be assembled to each other and adjusted for proper clearance and concentricity prior to final balance. The rotor will be given a preliminary balance in a conventional manner before assembling the gas bearings. With the gas bearings assembled and with external gas provided to operate the bearings as externally pressurized units to prevent rubs and give increased stiffness at the low balance-machine speeds, the unit will be balanced in a conventional sensitive balance machine. Without further adjustment, the rotor unit and its bearings will be assembled into its stator members and operated to speed. This system is feasible due to the relatively low operating speed of 12,000 rpm.

Heat generated in the gas bearings and in the generator parts will be removed by a Propylene Glycol coolant circulated through cooling coils appropriately located on the turbo alternator assembly.

Weight of the turbine and generator system as a function of generator capacity is shown in Figure 6-24.

6.1.6.4 Turbo-Compressor

Preliminary analysis indicates that a single stage centrifugal compressor rotating at 67,500 rpm will satisfy the compressor requirements. For a compressor inlet pressure of 6 psia, the specific speed is 88, which is in the peak efficiency range. Centrifugal compressors are less sensitive to blade imperfections and for small sizes it is easier to obtain high efficiency in a centrifugal compressor than in an axial

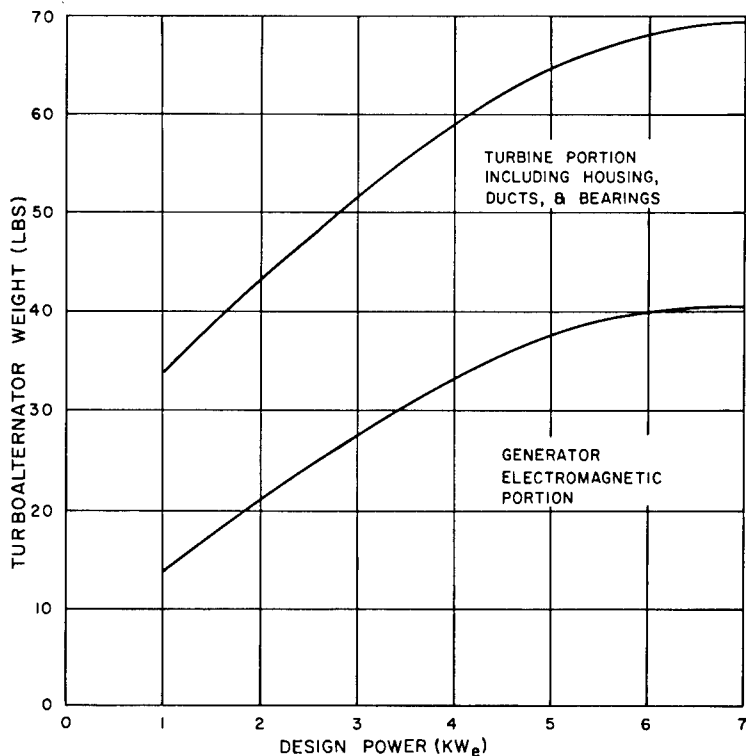


Figure 6-24. Brayton Turboalternator Weight

compressor. Tip clearance becomes very critical for an axial compressor and for blade heights less than 0.5 inch centrifugal compressors are usually indicated. An axial flow compressor would require at least four stages, with blades less than 0.25 inch high, and would have a low efficiency due to tip clearance and Reynolds Number effects. The multi-stage axial compressor would also cause critical speed problems due to the longer bearing span. Gas bearings have low stiffness and small radial clearances; therefore it is essential to have high critical speeds above the operating range of the machine.

Using a slip factor of 0.85 and the temperature rise from the cycle calculations, the required tip speed is 990 ft/sec. For 67,500 rpm, the tip diameter is 3.36 inches. The inlet velocity/tip speed ratio was chosen as 0.3 for maximum efficiency. The flow Mach number at the rotor exit is 0.76.

A radial design was chosen for the compressor turbine because the specific speed of 95 is in the peak efficiency region, and the radial inflow design permits a compact arrangement of the gas generator. An axial flow turbine design is possible, but was not considered to be superior. The turbine was designed for a tip speed/jet velocity ratio of 0.7 resulting in a tip speed of 990 ft/sec at 67,500 rpm for a tip diameter of 3.36 inches. The exit velocity/tip speed ratio was chosen as 0.4.

Figure 6-25 shows the gas generator unit. It consists of a cylindrical midframe with a compressor housing attached to one side and a turbine housing attached to the other side. The midframe is designed as a bearing housing for the two self-acting pivoted-pad journal gas bearings.

The radial inflow turbine is integral with the shaft and the compressor is attached. Two torque pins and a central nut in front of the compressor and axial shim stock locate the rotor with minimum axial movement and the desired clearance in the compressor housing. The axial thrust of the compressor and turbine wheels will be balanced by holes located in the back plates of the compressor and turbine housings. The axial thrust bearings are located behind the compressor-rotor. In this way, the rotor will be precisely located axially.

The rotor shaft is designed to be very stiff and the bearings are located near the "Bessel Points" resulting in minimum shaft deflection under load. The manufacturing tolerances must be controlled very tightly so that the eccentricity between the rotor and stator will be less than 0.002-inch. Tilting pad self-acting hydrodynamic gas bearings have been successfully tested with 1.5 inch shaft diameter. The diameter for this design is 1.6 inches. The bearings have three segments, each including an angle of 105 degrees, and are pressurized by compressor discharge gas at a temperature of 340°F. The angle between the pivot and leading edge is 70 degrees. The preferred way to introduce the lifting gas is directly through the pivots. If the machinery must be rotating during launching operations, the gas bearings may have to be pressurized during this period by an external high pressure gas supply to withstand the high G loadings.

The compressor casing is attached to the midframe in such a way that the diffuser and impeller shroud is sandwiched between the compressor scroll and the front disk of the midframe. The bullet nose is attached by three struts to a cylindrical piece joining the compressor scroll structure with the impeller shroud. The outlet of the compressor scroll is in the tangential direction.

The hot argon gas will enter the turbine scroll tangentially. The nozzle diaphragm is a separate piece of sheet metal design located in the part which forms the turbine shroud and the outlet duct. The outlet bullet nose is held concentrically by three struts. The entire gas generator rotor can be removed by disconnecting the compressor scroll and pulling off the impeller.

The rotor will be made of Rene 41 or Udimet 700 and will weigh about three pounds. The static bearing load is 0.7 lb/in^2 . This conservative loading gives some margin to withstand high G loadings during launch operations and increases the reliability

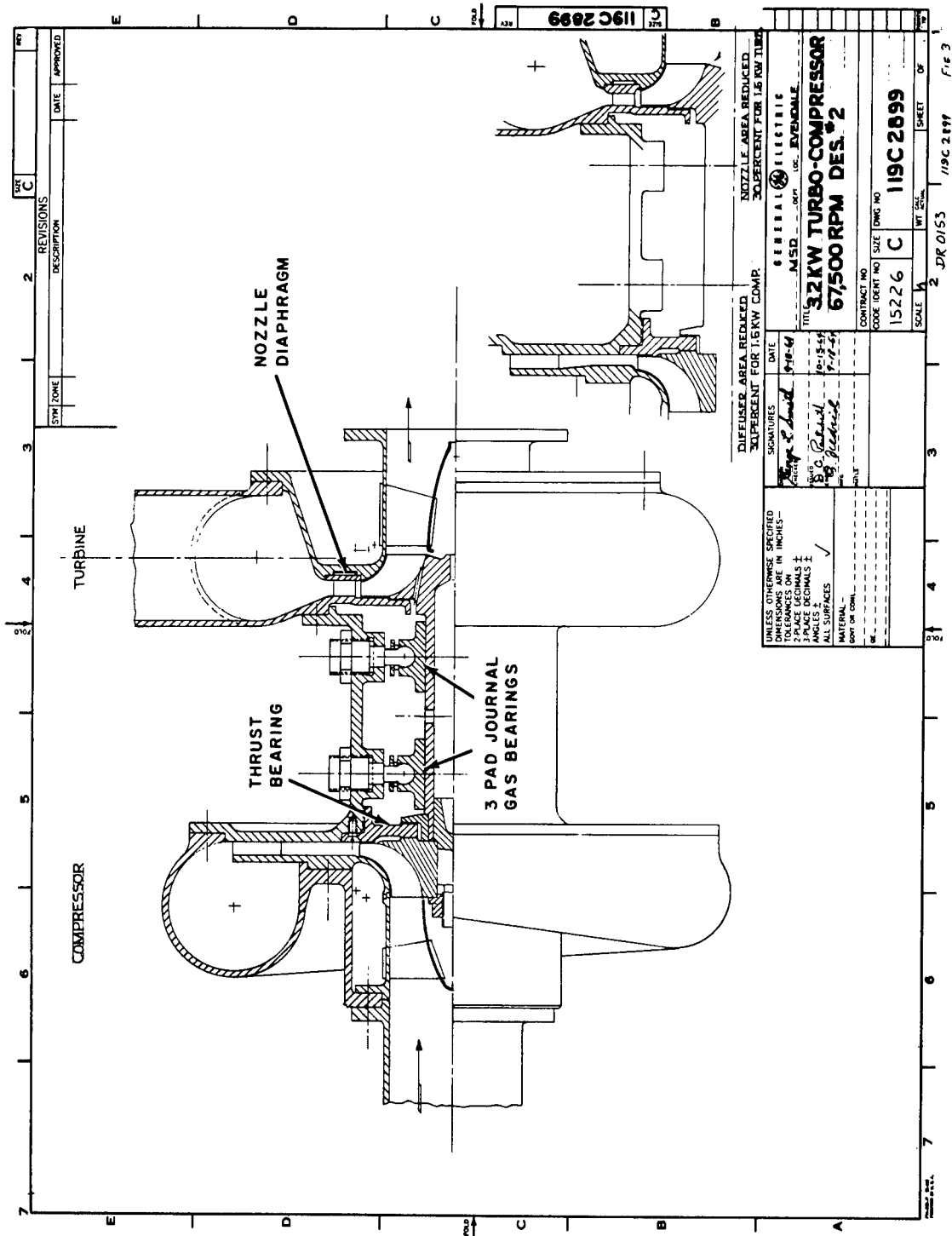


Figure 6-25. Turbo-compressor Reference Design

of normal operation. The stationary parts will weight about 31 pounds. This yields a total weight of 34 pounds. Diameter without ducts is approximately 10.2 inches and length approximately 10.2 inches.

6.1.7 RADIATORS

6.1.7.1 Isotope Powered System

The argon filled radiators to reject engine waste heat to space are shown in Figure 6-26a.

Figure 6-26b depicts the idealized radiator design used in a computer program to calculate a minimum radiator weight system. Figure 6-26c indicates how this radiator design is incorporated in the corrugated skin of the vehicle. The fin forms the outer skin of the vehicle while the tubes replace a section of corrugations. A significant saving in power system weight results from making the radiator fin do double duty by also acting as the outer vehicle skin. Table 6-7 lists the pertinent performance parameters for the radiator design selected.

Each engine has its own radiator circuit consisting of two panels connected in parallel. The coolant circuits for the two engines are kept separate to maximize reliability. Exhaust gas from the recuperator enters the headers to the two radiator panels through a Y connection where it is distributed to the individual tubes. The argon then flows circum-

TABLE 6-7. SUMMARY OF DESIGN PARAMETERS
ISOTOPE BRAYTON CYCLE
POWER PLANT WASTE HEAT RADIATORS

<u>Parameter</u>	<u>Non-Integrated</u>	<u>Integrated</u>
Heat Rejected KW	20.98	8.40
Area Ft. ²	615	310
Weight lbs	1000	410
Number Panels	4	4
Argon Temp. In, T ₆ °R	875	763
Argon Temp. Out, T ₁ °R	536	536
Argon Weight Flow lb/sec.	0.470	0.280
Radiator Pressure Drop psi	0.32	0.25
Vehicle Outer Skin Weight Replaced by Radiator — Lbs.	-177	-89
Net Increase in Vehicle Weight — lbs	823	321
Orbital Sink Temperature °R	400	400

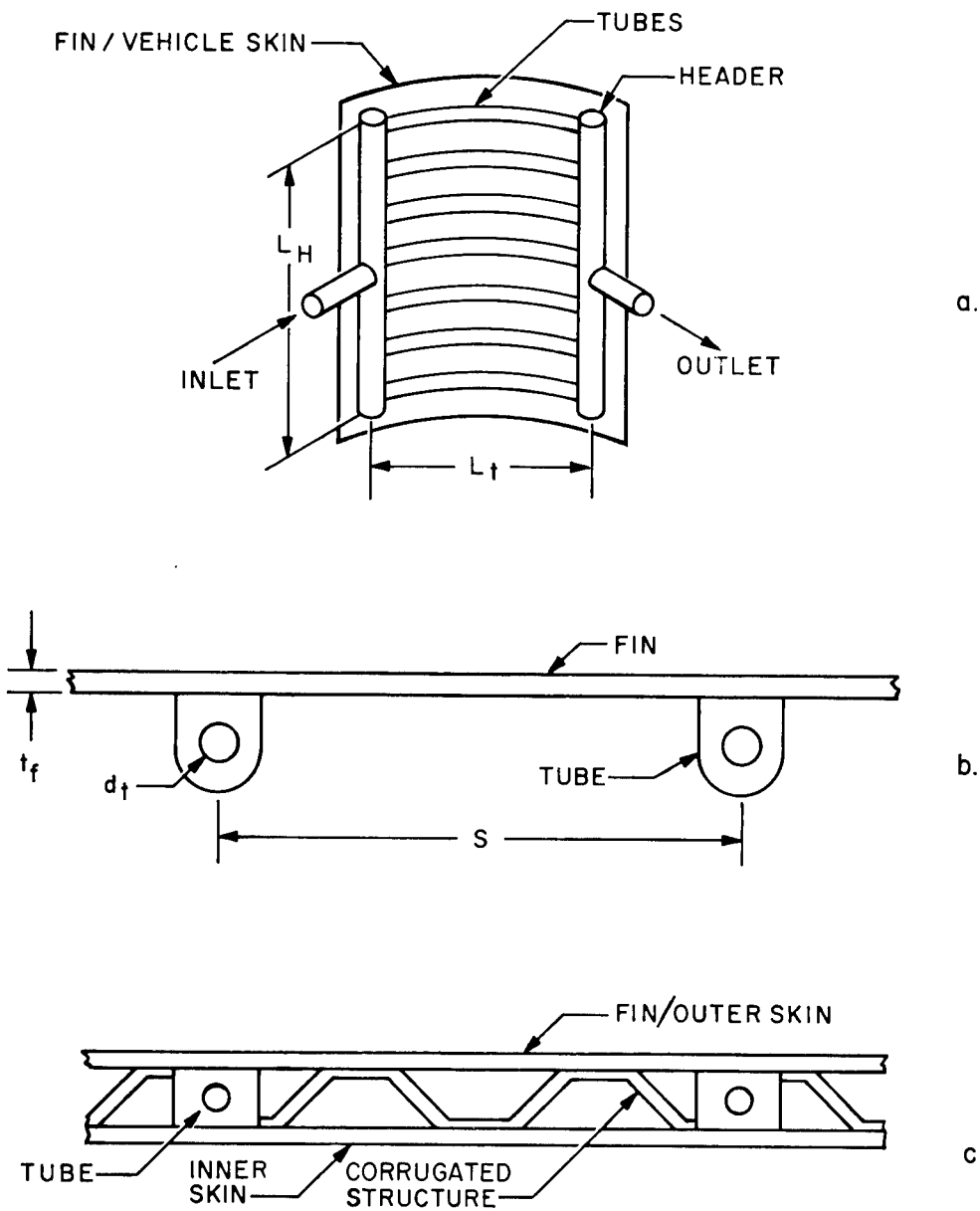


Figure 6-26. Waste Heat Radiator

ferentially through the tubes giving up energy by forced convection to the tube walls, which are brazed to a fin as shown in Figure 6-26b. The waste heat is transferred to the fin by conduction where it is radiated to space.

6.1.7.2 Solar Powered System

The radiator selected for this study is not an integral part of the vehicle skin. It was considered undesirable to extend long and relatively large gas ducts from the power plant package forward beyond the solar collector and to the vehicle proper because of the requirement of joint sealing after deployment.

A minimum weight aluminum radiator was determined by a Computer Program using a 0.99 Meteoroid Protection Probability and the 1963 NASA Whipple Flux model. The radiator is designed for a 5% pressure drop (0.32 psi). For the non-integrated version, the heat required to be radiated is 21.0 KW; inlet temperature being 875°R and outlet temperature is 536°R. A 400°R sink temperature was assumed and a radiator effectiveness of 0.7, along with an outside heat transfer coefficient of 5 BTU/hr°ft² and a surface emissivity of 0.86. (See Appendix C.)

The resulting weight and area requirements are 1215 lbs. and 944 square feet. Figure 6-27 is an approximate sketch of the radiation configuration and a table which lists additional information.

This radiator is approximately 20 percent heavier than one designed as an integral part of the vehicle skin. The reasons for this are the following:

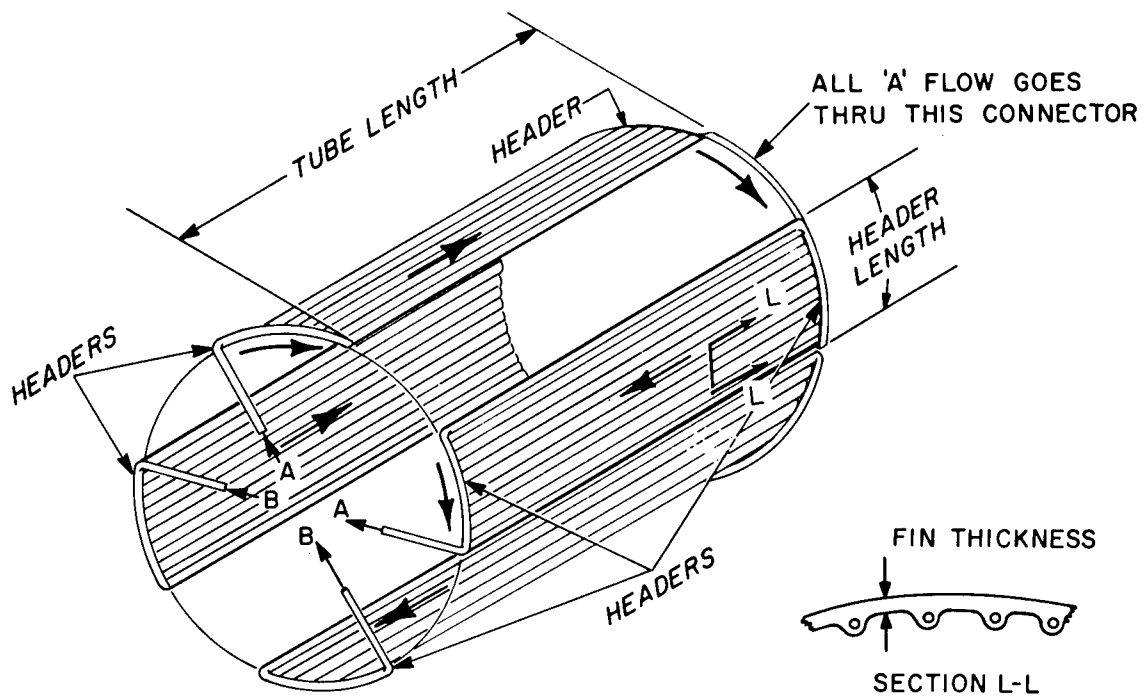
1. It is necessary to "armor plate" both outside and inside surfaces for meteoroid protection.
2. The divorced radiator does not possess twice the available area for radiation that an integral design would since the associated view factor improves by only 30% (approximately).
3. There is no vehicle skin present to reduce the amount of armor required (specifically the skin internal corrugated sheets).

6.1.8 RECUPERATOR

Size and weight of the recuperator used in this system is scaled from data supplied by NASA-Lewis Laboratories for a recuperator for a 10 KW_e system.

Recuperator inlet temperature and pressure for the 6.24 KW_e system under study in this contract are approximately the same as for the 10 KW_e reference system which had the characteristics listed in Table 6-8. If the recuperator effectiveness remains constant, the ΔT of the working fluid remains the same in all cases. The core length for the recuperators designed for both the integrated and non-integrated system were held constant and flow area through the core scaled down to hold gas flow per unit area constant. A dual recuperator design was employed for compactness and is shown in Figure 6-28. Table 6-8 lists the pertinent characteristics.

The recuperator design for the Solar Brayton Cycle is identical to that of the Isotope Brayton cycle except that it is packaged in two single loop packages to minimize mirror shadow area, and to keep the axial length of the "absorber-turbo-machinery-recuperator" package as short as possible, and to keep the plumbing to a minimum practical length.



FOUR PANELS: Two for Loop A and two for Loop B

	NON-INTEGRATED	INTEGRATED
Number of Tubes per Panel	48	36
Header Length (Each)	11 Ft	7.8 Ft
Tube Length	10 Ft	7.6 Ft
Fin Thickness	.031 In	.028 In
Total Radiation Area (Inside & Outside)	944 Ft^2	500 Ft^2
Total Weight	1215 Lbs	520 Lbs
Total Heat Radiated	21 KW	8.4 KW
Radiator ΔT	339°	227°

Figure 6-27. Solar Brayton Radiator

TABLE 6-8. RECUPERATOR CHARACTERISTICS
BRA YTON CYCLE POWER SYSTEM

<u>Parameter</u>	<u>Reference Design</u>	<u>Non-Integrated</u>	<u>Integrated</u>
Electrical Power KW _e	10.0	6.57	3.46
Thermal Power KW _t	-	30.0	18.0
Wt. Flow Lb/Sec.	0.612	0.470	0.280
T ₂ °R	801	801	801
T ₅ °R	1560	1544	1544
P ₂ psia	13.8	13.80	13.80
P ₅ psia	6.73	6.38	6.37
Δ P/P Hot Side %	1%	1%	1%
Δ P/P Cold Side %	1%	1%	1%
Effectivity ϵ	0.9	0.9	0.9
Flow Area in. ²	625	485	287
Weight Lbs.	300	236	135

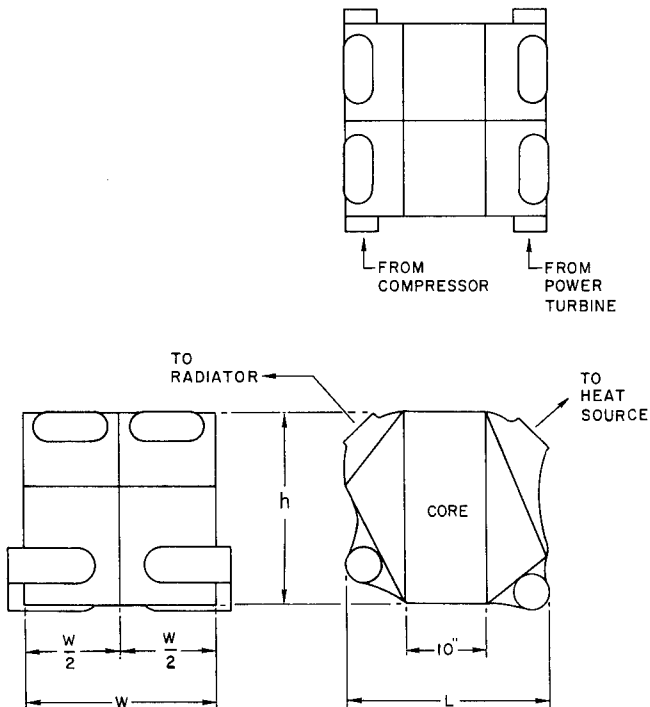


Figure 6-28. Recuperator

6.1.9 CYCLE ANALYSIS

Calculation of solar collector and radiator weights performed early in the study indicated that a pressure ratio of 2.5 and a compressor inlet temperature of 536°R would be near optimum. A pressure ratio of 2.3 would increase compressor efficiency and reduce stresses in rotating parts with little loss in cycle performance. For this reason, 2.3 was chosen for the cycle pressure ratio, with 1950°F as turbine inlet temperature.

Advantages of a minimum weight system and the high cost coupled with the limited availability of Pu-238 indicated the desirability to operate at the same design point for the Isotope Brayton Cycle.

Detailed design of the Isotope Heat Source and shield yields a specific weight of approximately 75 lbs/KW_t for the non-integrated system.

The minimum weight radiator for the non-integrated system indicates a specific weight of about 1.6 lbs/ft^2 and an area of 620 ft^2 for a radiator with a 536°R outlet temperature. This yields a specific weight of 47.5 lbs/KW_t .

Estimates were made for the combined heat source and radiator weight for the Isotope Brayton System as follows:

$$\frac{Q_{\text{shaft}}}{\eta_T \text{ (from Figure 6-21)}} = Q_A$$

but $Q_{\text{shaft}} = 7.62 \text{ KW}$ (from Table 6-9).

$$Q_R = Q_A - Q_{\text{shaft}}$$

$$W_I \text{ (weight of isotope source)} = Q_A \times 75 \frac{\text{lb}}{\text{KW}}$$

$$\Delta T \text{ (thru radiator)} = 875 - 536 = 339^{\circ}\text{R}$$

$$T_{\text{avg}} \text{ (Argon in radiator)} = \frac{339}{2} + T_{\text{out}}$$

but T_{AVG} (Argon in radiator) $\approx T_*$ (effective radiator surface temperature)

since ΔT through gas film is small.

$$\frac{Q_R}{A} \propto \left(T_*^4 - T_S^4 \right)$$

$$\text{where } T_* \approx \frac{339}{2} + T_{\text{out}}$$

$$T_S = 400^{\circ}\text{R}$$

This ratio R is defined as follows:

$$R = \frac{\left(\frac{Q_R}{A}\right)_{T_{out}}}{\left(\frac{Q_R}{A}\right)_{536^0R}}$$

R is then calculated for $T_{out} = 500,560^0R$. The area required for a new T_{out} is given by: RA_{536^0R}

where $A_{536^0R} = 615 \text{ ft}^2$ from Table 6-7. The radiator weight (W_R) is given by:

$$W_R = R(615) \left(1.6 \frac{\text{lb}}{\text{ft}^2}\right)$$

The total weight of isotope source and radiator (W_T) is given by:

$$W_T = W_I + W_R$$

This data is plotted in Figure 6-29. Even though the split between heat source and radiator weight is different from the solar powered system, the pressure ratio of 2.3 and T_1 of 536^0R selected for the solar powered system yields a near optimum weight system. A pressure ratio of 2.5 and a T_1 of 500^0R appears to be a slightly better choice for the isotope powered system.

6.1.9.1 Cycle Operating Points

When the compressor inlet temperature, turbine inlet temperature and pressure ratio have been selected, the component efficiencies can be used to calculate the state of the working fluid at each point in the cycle. A digital computer program developed by the General Electric Company, Jet Engine Department, was used for this calculation. The absolute pressure level in the loop was chosen to yield reasonable specific speed in the compressors and turbines in combination with the reasonable fluid velocity and component diameters. The cycle performance is calculated on the basis of "per unit weight flow" of working fluid with the turbine flow work and heat input on a per unit weight flow basis being tabulated in Table 6-10.

6.1.9.2 Power Plant Energy Balance

The requirements for this power system are to supply a 6.0 KW_e steady state load plus $.24 \text{ KW}_e$ for charging a battery pack to supply a peak load of 9 KW_e for one hour out of each 24 hours. The power plant must also supply power to operate its own coolant pumps and to dissipate 5 percent of the load for speed control. Required generator output is 6.57 KW_e . When generator efficiency and turbo alternator gas bearing losses are taken into account, the required turbine power is 7.92 KW .

Using the values for heat added, heat rejected and turbine work per unit flow listed in Table 6-10, the required power plant gas flow and heat source and radiator size can be calculated.

The overall power plant energy balance is listed in Table 6-9.

TABLE 6-9. BRAYTON CYCLE ENERGY BALANCE
NON-INTEGRATED SYSTEM

Electrical Power to Station Bus	6.24 KW _e
5% of Load for Speed Control	0.31
Coolant Pump Power	<u>0.02</u>
Generator Output	6.57 KW _e
Generator Efficiency (neglecting bearing losses)	86.2%
Net Shaft Power to Generator	7.62 KW
Gas Bearing Losses to Turbo-Alternator	<u>0.30</u>
Required Turbine Power	7.92 KW
Required Turbo-Power = 7.50 BTU/sec.	
Turbine Flow Work = 15.97 BTU/Lb (per cycle analysis)	
Argon Flow Required $\frac{7.5}{15.97} = 0.470$ Lb/sec.	
Heat Added = 59.76 BTU/lb (per cycle analysis)	
Heat Rejected = 42.2 BTU/lb. (per cycle analysis)	
Heat Added by Heat Source (59.76) (0.470) = 28.1 BTU/sec.	
Heat Rejected by Radiator (42.2) (0.470) = 19.83BTU/sec.	
Heat Source Input to Gas Stream	29.65 KW
Assumed Thermal Losses	<u>0.35</u>
<u>For the Isotope Brayton Cycle</u>	
Heat to be Supplied by Isotope Source	30.00 KW _t
Generator	6.57 KW
Generator Coolant	1.05
Bearing Coolant	1.10
Thermal Losses	<u>0.35</u>
	<u>9.07</u>
Heat Rejected by Radiators	20.93 KW _t
<u>For the Solar Brayton Cycle</u>	
Heat to be Supplied by Absorber	30.00 KW _t
Generator Output and Losses	7.92 KW
Gas Gen. Bearing Losses	0.80 KW
Ducting Thermal Losses	<u>0.30</u> KW
	<u>9.02</u>
Total Heat to be Rejected by Radiator	<u>9.02</u> KW _t
	20.98 KW _t

TABLE 6-10. THERMODYNAMIC CYCLE OPERATING POINTS
BRAYTON CYCLE
NON-INTEGRATED SYSTEM

Station	Location	T_1 °R	P psia
1	Compressor Inlet	536	6.0
2	Compressor Outlet	801	13.80
2.5	Heat Source Inlet	1470	13.66
3	Compressor Turbine Inlet	1950	12.97
4	Power Turbine Inlet	1672	8.10
5	Power Turbine Outlet	1544	6.37
6	Radiator Inlet	875	6.32

Turbine Work
Pounds of Argon = 15.97 BTU/lb

Heat Added
Pounds of Argon = 59.76 BTU/lb

Heat Rejected
Pounds of Argon = 42.2 BTU/lb

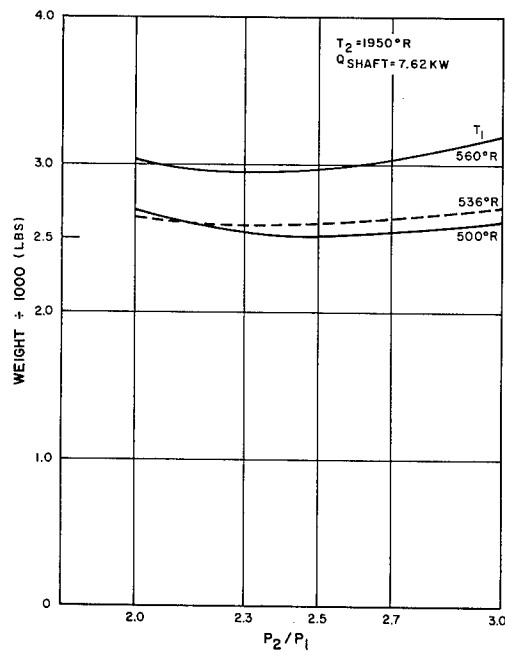


Figure 6-29. Isotope Brayton Cycle Isotope Source/Shield and Radiator Weight

6.1.10 AUXILIARY COOLANT SYSTEM

The frictional heat generated in both the turbo generator gas bearings, as well as the heat generated in the alternator due to windage, magnetic, and electrical losses, must be rejected from these components to control temperature. Computer studies indicate that a severe penalty is incurred in cycle efficiency if compressor bleed gas is used as the coolant fluid (Table 6-11). To avoid a large weight penalty as a result of reduced cycle efficiency, an auxiliary liquid coolant system is employed as shown in Figure 6-2.

A 60 percent by weight solution of Propylene Glycol in water was selected as the heat transfer media for this system because its freezing temperature of 386°R is below the sink temperature of 400°R so freeze-up of an inoperable system should be no problem. The boiling point of 685°R is sufficiently high so that local boiling in the gas generator bearing heat exchanger and the turbo generator heat exchanger should not be a problem.

Assuming a 20°R rise through the turbo machine heat exchangers and an equal drop through the radiator, the flow rate for the non-integrated system can be calculated as below:

$$Q_r = W C_p \Delta T \quad \Delta T = 20^{\circ}\text{R} \text{ assumed at } 605^{\circ}\text{R}$$

$$W = \frac{Q}{C_p \Delta T} \quad C_p = 0.85 \text{ BTU/lb.} - ^{\circ}\text{F}$$

$$W = \frac{2.15 \times .948}{0.85 \times 20} = .12 \text{ lb/sec.} \quad Q = 2.15 \text{ KW}$$

$$\rho = 63.1 \text{ lbs./ft}^3$$

Volumetric flow is .856 gallons per minute (GPM).

A similar calculation for the integrated system indicates a flow rate of .685 GPM is required to remove the 1.73 KW of waste heat.

Detailed analysis for the propylene glycol radiators for the engine coolant loop for the Isotope Stirling system yields a specific weight of 14.05 lbs./KW_t and a specific area of $13.95 \text{ ft}^3/\text{KW}_t$ for a 20 KW_t radiator operating at 605°R mean temperature with a 20°R rise. Specific pumping power was calculated to be $.0105 \text{ KW}_e/\text{KW}_t$. Applying those values to the systems for the Brayton cycle auxiliary coolant loop yields the values listed in Table 6-12.

Separate coolant circuits are maintained for each set of turbo machinery to increase reliability. Two pumps are provided for each circuit for redundancy since the penalty is very small. An accumulator will be required to handle changes in fluid volume with varying temperature.

6.1.11 GROUND COOLING AND CHECKOUT

The assumption has been made for this study that the isotope fuel capsules will be installed on the pad prior to launch. The cooling water requirements for the isotope package heat exchanger during ground hold are as follows. The cells of the isotope source will be surrounded by a can around which will be wrapped the insulation to control thermal energy leakage from the isotope source. This can will serve to contain water which will be sprayed on the heat exchanger from an external source. Both sensible heat in raising the water from an assumed temperature of 70°F to 212°F and the latent heat of evaporation will be utilized. The weight penalty for such a ground cooling system will be very small since the only extra equipment needed is a line to supply less than .2 GPM of water and a vent line to carry off the saturated steam since all control valves pumps, etc. can be a part of the Ground Support Equipment and need not be carried aboard the space vehicle.

It must be pointed out that if the space station is to be launched with the power plant not operating, a similar cooling problem exists between launch and activation of the turbo machinery, at which time the isotope will be cooled by the Argon stream. If the cooling water is stored aboard the spacecraft at 70°F, the same mass flow of cooling water will be required as for ground cooling. In addition, pumps and a power source (batteries) for the pumps will be required. Since the time period between launch and equipment start-up is undefined at this time, no analysis will be made of the weight penalty for post-launch cooling.

Water requirements for evaporative cooling are:

(Assumed water temperature is 70°F)

$$\text{at } 212^{\circ}\text{F } h_g = 1150.4 \text{ BTU/lb}$$

From "Thermodynamic Properties of Steam" by Keenan and Keyes

$$\text{at } 70^{\circ}\text{F } h_f = 38.04 \text{ BTU/lb}$$

$$\text{therefore, } h_g - h_f = 112.36 \text{ BTU/lb}$$

$$\text{Water Requirements} = \frac{56.8 \text{ BTU/min - KW}_t}{112.36 \text{ BTU/lb}} = .0512 \text{ lb/KW}_t\text{-minute}$$

In order to operate the power system/life support system on the launch pad for the purposes of pre-launch checkout, special provisions will have to be made to remove waste heat from the system. The waste heat radiators are designed to reject energy to a 400R sink temperature while in space. The effective sink temperature while the spacecraft is on the launching pad will be much too high for the radiators to perform at their design point and deliver 76°F gas to the compressor inlets.

To control compressor inlet temperatures, the radiator area will be covered with a shroud and series of spray nozzles. Chilled water sprayed on the radiator will be regulated to provide the proper heat rejection rate.

TABLE 6-11. COMPRESSOR GAS BLEED PENALTIES
BEARING AND GENERATOR COOLING
BRAYTON SYSTEM

<u>Performance Index</u>	<u>Non-Integrated</u>	<u>Integrated</u>
$\frac{Q_a}{Q_a}$ Gas Loaded Bearing only		
$\frac{Q_a}{Q_a}$ Liquid Cooled Bearing and Generator	1.105	1.190
$\frac{Q_a}{Q_a}$ Gas Cooled Bearing and Generator		
$\frac{Q_a}{Q_a}$ Liquid Cooled Bearing and Generator	1.200	1.280
$\frac{Q_r}{Q_r}$ Gas Cooled Bearing only		
$\frac{Q_r}{Q_r}$ Liquid Cooled Bearing and Generator	1.195	1.360
$\frac{Q_r}{Q_r}$ Gas Cooled Bearing and Generator		
$\frac{Q_r}{Q_r}$ Liquid Cooled Bearings and Generator	1.375	1.600
<u>W compressor</u> <u>Gas Cooled Bearing only</u>		
<u>W compressor</u> <u>Liquid Cooled Bearing and Generator</u>	1.115	1.21
<u>W comp.</u> Gas Cooled Bearing and Generator		
<u>W comp.</u> Liquid Cooled Bearing and Generator	1.23	1.32

Q_a = Heat added

Q_r = Heat rejected from radiator and to the Life Support System

W = Compressor work

TABLE 6-12. AUXILIARY COOLING SYSTEM PARAMETERS
BRAYTON SYSTEM

<u>Parameter</u>	<u>Non-Integrated</u>	<u>Integrated</u>
Q_r KW	2.15	1.73
Radiator Area Ft. ²	30	24.1
Radiator Weight Lbs.	30.2	24.3
Pump Power KW	0.0218	0.0176

This system will result in no weight penalty to the spacecraft since the shroud, nozzles, pumps, chiller and control valves are all Ground Support Equipment and need not be carried aboard the space vehicle, and any sealants required to waterproof the vehicle in this area should have a negligible weight.

6.1.12 START-UP AND CONTROL

6.1.12.1 Start-Up Subsystem

The start-up subsystem consists of the High Pressure Argon Storage Bottle, a pressure regulator, and the solenoid operated start-up ejection valves connected into the ducting

between the heat source and the gas generator turbine. Enough bottled gas will be stored to complete a total of five system starts. Evacuation of the system before a re-start in orbit would be accomplished by dumping the charge to space through the vent valves located near the compressor inlet and then re-starting in the same manner as the original start-up.

The system would be launched, evacuated, and start-up accomplished by injecting argon gas directly into the gas turbine inlet nozzles. Results from analog computer studies performed at NASA-Lewis Laboratories indicated that a burst of gas of approximately 10 seconds duration is required to spin the turbine up to speed so that the system becomes self-sustaining.*

6.1.12.2 Speed Control Subsystem

Speed control for the gas generator turbo-compressor rotor will be achieved by by-passing a small percentage of the total flow around the turbine wheel. A proximity pick-up, mounted on the compressor section where it will not be exposed to high temperature gases, will count the rate at which the compressor vanes pass the pick-up head. This frequency will be compared to a fixed frequency oscillator, oscillating at a rate equivalent to 67,500 RPM and the differential signal as a result of the two frequencies used to control the speed control/by-pass valve.

The speed of the turbo generator unit will be controlled by varying the load. A frequency sensing device in the generator output will control magnetic amplifiers to shunt a portion of the generator output to a set of parasitic load resistors mounted on the skin of the spacecraft where they can radiate the dissipated energy to space. Weight estimates for the load resistors, magnetic amplifiers, cabling and harnesses, etc., were scaled from data furnished by NASA-Lewis Laboratories for the 30 KW_e Snap 8 System.

The magnetic amplifiers and load resistors are sized to handle the entire output of the generators so that the power system may be started without activating any other spacecraft electrical equipment to act as a load.

6.1.12.3 Solar Brayton Initial Deployment and Startup

The initial activation of the deployment sequence may be accomplished either by RF command link from earth or initiated manually by the crew at the time of their arrival.

*These studies were part of another program and are not reported in detail here.

In either case, the physical extension of the power plant aft of the solar collector may be accomplished mechanically by means of pneumatically actuated telescoping tubes and appropriately placed dampers (dashpots) near the end of travel. This is one method which readily suggests itself. The optimum manner of deployment would require design outside the scope of this study.

The configuration and the method of deployment involve no requirement for the sealing of joints in outer space, thus avoiding a major problem area.

Once the deployment has been completed and the station oriented to the sun, the absorber cavity will begin to heat. As soon as the cavity design temperature is obtained, the power plant is ready for immediate start up.

Initial start-up of the solar powered system must occur during the day portion of an orbit. To collect sufficient heat for operation during the next night portion it is probably necessary to admit heat to the absorber soon after "sunrise." This is not considered a serious restraint as the initial choice of start-up time is arbitrary. There may be an increase in the size of the auxiliary power source used to provide power during launch, orbit inject on, and power system start-up if start-up does not occur early in the station activation sequence. Heat is available at all times from the isotope heat source.

6.1.13 EMERGENCY OPERATION

6.1.13.1 Isotope Brayton Cycle

One of the inherent characteristics of an isotope heat source is that it cannot be turned off or its power reduced. Once the fuel capsules are installed in the heat exchanger, the generated energy must be removed to control the temperature.

This consideration has led to the concept of the dual loop isotope heat exchanger where each element of isotope is equally cooled by each of the two power plant gas streams. If one of the turbo-compressor units fail, half of the cooling mass flow is lost. Since the heat exchange process is essentially a constant pressure process, $Q = WC_P \Delta T$, and the heat generation rate Q cannot be reduced. Either W or ΔT must be doubled in the remaining circuit to cool the isotope package.

The simplest way to increase W is to increase the absolute pressure in the system. This allows the ΔT through the isotope package to remain near the design temperature levels and maintains constant turbine inlet temperature to the turbo compressor. The gas generator turbine will now deliver higher shaft horsepower which is absorbed by the compressor demanding increased power to compress the higher mass flow.

If the increased mass flow is all ducted through the one radiator loop consisting of only two panels, the radiator temperature must increase (by the fourth power law) to reject the increased load. This causes the compressor inlet temperature to rise from 76°F to 301°F , which reduces the available energy to the turbo-alternator to 34.6 percent of the original design value. As a result the generator output will be reduced to approximately 1.2 KW_e , which does not meet the study requirement of a minimum power availability of 1.4 KW_e .

A second consideration was the installation of a pair of valves to connect all four radiator panels in parallel to dump the waste heat. This results in a decrease in compressor inlet temperature from 76°F to 57°F with a 114 percent increase in generator output. In addition to adding approximately 28 lbs. of extra generator weight to be able to produce the larger electricity load generated, the redundancy of two separate radiators is lost in that if any one of the four radiator panels is punctured, the entire system is out of operation.

An alternate method of dissipating the heat from the isotope package when one loop is inoperative is to hold W constant and increase the ΔT of the working fluid as it passes through the isotope heat exchanger. If the turbine inlet temperature is to be held constant at 1490°F and the maximum clad temperature is not to exceed the 1650°F limit, the inlet temperature must be reduced. This can be accomplished by by-passing some of the flow around the hot side of the recuperator to reduce the effectiveness. This will result in an increase in radiator inlet temperature from 415°F to 1012°F . This results in radiator metal temperatures higher than acceptable for aluminum radiators.

The assumption is made that if both sets of turbo machinery fail, the mission will be terminated and the isotope package separated from the spacecraft for return to earth and reprocessing. Cooling of the isotope package during the re-entry phase is beyond the scope of this study.

The design solution chosen for this study consists of doubling the pressure in the one system remaining in operation to double mass flow through the heat source. The valving in the radiator inlet and outlet ducting is now positioned so that three of the four radiator panels are dumping waste heat. The radiator temperature rises, and compressor inlet temperature rises to approximately 140°F , reducing the power-turbine shaft work per unit flow rate to about 77 percent of design; but since the mass flow has doubled, the shaft work increases to 154 percent of the 3.54 KW design output.

As a result, the remaining generator will now deliver approximately 4.5 KW_e which is well above the 1.4 KW_e required for emergency operation. One disadvantage of this system is that the generator must be capable of operating at 150 percent of design load during emergency conditions. A second disadvantage is that if a puncture of either of the

two radiator panels that are common to both loops for emergency operation occurs, the capability of cooling the isotope source is lost. Addition of more valving to isolate any one of the four radiator panels eliminates this problem.

6.1.13.2 Solar Brayton Cycle

In the event of a failure of any of the components in one of the two argon loops, the turbo-machinery may be shut down by venting the affected loop. This will cause the cavity temperature in the solar absorber to begin to rise, since one half of the absorbed heat is no longer being utilized (carried away from the absorber). However, the cavity temperature control on the Absorber will immediately begin to open the front segments (or shutters) thus allowing heat to be radiated back into space. The temperature control will limit the temperature to 1950°R in the cavity. The overall effect is that only one-half of the power will now be available in the station, or 3.24 KW, however, this is still more than twice the minimum requirement of 1.4 KW for emergency operation. This would allow extended operation while the failure is being remedied.

6.1.14 SYSTEMS SUMMARY

Tables 6-13 and 6-14 list the component volumes and sizes for the two systems. Tables 6-15 and 6-16 are compilations of component weights for the Isotope and Solar Brayton systems.

6.2 INTEGRATED BRAYTON POWER PLANT AND LIFE SUPPORT SYSTEM

6.2.1 INTRODUCTION

This section discusses the changes in and effects on the power plant described in Section 6.1 of this report when it is thermally integrated with the Life Support System.

In the Brayton power cycle, the most logical source of heat is just before the heat rejection phase of the cycle. This is just before the hot gas enters the radiator and is the point in the cycle where an abundance of waste heat is available at a specific temperature, in this instance 875°R (415°F). In order to obtain thermal energy at a higher temperature it would be necessary to extract heat immediately after the power turbine (turbo-alternator) and before entering the recuperator. If this were done it would be necessary to add an equal amount of heat in the source in order to maintain the cycle design points. This in turn requires the radiator to reject additional heat. The end result would be an increase in power system weight, size and complexity. A systems weight analysis indicates that it is more desirable to supply only waste heat to the Life Support System.

TABLE 6-13. COMPONENT VOLUMES
ISOTOPE BRAYTON CYCLE POWER SYSTEM

<u>Component</u>	<u>Non-Integrated</u>	<u>Integrated</u>
Isotope Package and Shield	35.6 ft. ³	29.3 ft. ³
Turbo-Compressor (2 each)	1.4 ft. ³	1.4 ft. ³
Turbo-Alternator (2 each)	1.8 ft. ³	1.6 ft. ³
Recuperator	7.5 ft. ³	3.9 ft. ³
Batteries	4.0 ft. ³	4.0 ft. ³
Argon Filled Radiators	Integral	Integral
Glycol Filled Radiators	Integral	Integral
Argon to Therminol Heat Exchanger	-	0.3
Therminol to Glycol Heat Exchanger	-	Negligible
Start-up Controls	<u>4.0 est.</u>	<u>4.0 est.</u>
Sum of Component Volumes	54.3 ft. ³	42.5 ft. ³
Package Volume (Approx.)	95 ft. ³	89 ft. ³

TABLE 6-14. COMPONENT SIZES
SOLAR BRAYTON CYCLE POWER SYSTEM

<u>Component</u>	Approximate Size (inches except as noted)	
	<u>Non-Integrated</u>	<u>Integrated</u>
Turbo-Compressor	12 Dia., 10 Long	12 Dia., 10 Long
Turbo-Alternator	12 Dia., 14 Long	12 Dia., 12 Long
Recuperator (each of two)	24 x 24 x 12	17 x 9 x 10
Absorber	*56 Dia. x 42 Long	39 Dia. x 33 Long
Radiator (each of four panels)	10 ft. x 11 ft. x 1.5	7.6 ft. x 7.8 ft. x 1.5
Solar Collector	24.6 ft. Diameter	19.0 ft. Diameter
Battery Package	(4 cu. ft.)	(4 cu. ft.)
Additional Heat Exchanger	-	7 x 7 x 12
Total Radiator Area	944 ft. ²	500 ft. ²
Total Collector Projected Area	473 ft. ³	279 ft. ²
Approx. Total "Stowed" Volume	1400 ft. ³	1150

*1/2 sphere plus frustum of a cone

TABLE 6-15. SUMMARY OF COMPONENT WEIGHTS
ISOTOPE BRAYTON CYCLE POWER SYSTEM

<u>Component</u>	<u>Non-Integrated</u>	<u>Integrated</u>
Shielded Heat Source		
Shielding Weight	1520 lbs.	967 lbs.
Fuel Inventory	190 lbs.	114 lbs.
Heat Exchanger and Headers	540 lbs.	324 lbs.
Energy Conversion System		
Turbo-Compressors (2 each)	68 lbs.	68 lbs.
Turbo-Generator (2 each)	110 lbs.	82 lbs.
Recuperator (Dual Passage)	236 lbs.	135 lbs.
Batteries	600 lbs.	600 lbs.
Support Structure and Plumbing	404 lbs.	291 lbs.
Heat Rejection Subsystem		
Argon Filled Radiators (2)	1000 lbs.	410 lbs.
60% P.G. Filled Radiators (2)	24 lbs.	19 lbs.
60% P.G. Pumps (4) (included in Plumbing, above)		
Argon to Therminol FR1 Heat Exchanger	-	14.5 lbs.
Therminol to 30% Ethylene Glycol Heat Exchanger	-	Negligible
Skin Structure Saved by Integral Radiator	-117 lbs.	-89 lbs.
Controls Subsystem	<u>114 lbs.</u>	<u>73 lbs.</u>
	4684 lbs.	3008 lbs.
Life Support System	<u>622 lbs.</u>	<u>780 lbs.</u>
TOTALS	5306 lbs.	3788 lbs.

TABLE 6-16. SUMMARY OF COMPONENT WEIGHTS,
SOLAR BRAYTON CYCLE POWER SYSTEM

<u>Component</u>	Weight (Lbs.)	
	<u>Non-Integrated</u>	<u>Integrated</u>
Turbo-Compressor (2)	68	68
Turbo-Alternator (2)	110	82
Absorber	281	189
Collector	473	279
Recuperator	236	135
Radiator	1215	520
Speed Control	114	73
Piping	81	78
Structure	286	191
Other		
Additional Heat Exchanger	-	14
Sub-Total	2864	1629
Life Support Equipment	622	780
Battery Package	600	600
TOTAL	4086	3009

6.2.1.1 Cycle Description

This cycle, like the one described in Section 6.1.2 is a recuperated, closed Brayton Cycle with one minor change. A heat exchanger has now been installed between the recuperator and radiator to extract waste heat for use in the endothermic process in the Life Support System, (LSS).

Referring to Figure 6-1, all processes are the same as described in Section 6.1.2 until the argon leaves the recuperator at station 6. Some of the waste heat is now rejected to the LSS heat exchanger represented by process 6 - 6.5. Process 6.5 - 1 represents the heat rejected in the radiator before the process fluid is returned to the compressor.

6.2.1.2 Description of System and Design

The power plant system is shown schematically in Figure 6-2. It is the same as the system described in Section 6.1.3 of this report with the following changes and additions.

- a. Almost all major components are both smaller and lighter than for the non-integrated system because the total electrical power requirements have been reduced.
- b. A large percentage of the waste heat is rejected to the Life Support System instead of to the space radiator. This not only reduces radiator size, but also reduced the isotope source and turbo machinery size by reducing the electrical requirements for the power generating system.

6.2.1.2.1 Life Support System Heat Supply

Referring to Figure 6-2, an Argon to Therminol FR-1 Heat Exchanger has been installed between the recuperator outlet and radiator inlet. The Therminol circulating through this heat exchanger by an electrically driven pump is heated to 400°F by the hot argon and passes through the LSS to provide the energy for desorption of CO₂ and H₂O from the Silica Gel and molecular sieve beds. It then passes through a Therminol to Ethylene Glycol heat exchanger where it gives up energy to the Glycol.

Valves are provided to isolate one side of the Argon to Therminol heat exchanger when one loop is inoperative.

The Ethylene Glycol leaves the Therminol to Glycol heat exchanger at 155°F and is circulated through the evaporators and food preparation areas of the LSS system by a pump. Here it provides endothermic heat to evaporate the waste wash water and urine in the reclamation cycle and to heat water for food preparation.

All of the LSS energy supply equipment will be located inside the cabin where it is accessible for maintenance and repair except the Argon to Therminol heat exchanger and the isolating valves, which will be located in the power supply package.

6.2.2 TURBOMACHINERY

6.2.2.1 Discussion

There are at least two ways to design for the lower mass flow rate for the integrated system. One is to maintain the pressure level and design smaller machinery. The other is to keep the larger machinery and reduce the pressure level.

Available data indicate that, in the small sizes, Brayton cycle turbomachinery efficiency decreases with size, partly due to Reynolds number effects and partly due to manufacturing accuracy. For Reynolds numbers greater than about 50,000, turbomachinery losses change approximately in proportion to the -0.2 power of Reynolds number. Applying this relationship to the case where the dimensions are unchanged and pressure level is reduced, component efficiencies would decrease about 1.7 points for the compressor and 1.4 points for the turbines. The shaft power cycle efficiency would decrease from 0.294 to 0.272 exclusive of generator and bearing losses. Heat transfer components would also be adversely affected by the lower pressure level.

Considering the case where pressure level is maintained and the dimensions are reduced, the Reynolds number effect would be only about half as great, but there would be additional losses due to the smaller size. Clearance, blade edge thickness, and surface roughness cannot continuously decrease to remain in constant proportion to the wheel diameter. Since the turbomachinery losses are about the same for either case, the effect of pressure level on the heat transfer components is the significant factor because the heat exchangers and radiator are the largest and heaviest components of the system.

The first approach to scaling down the components was to maintain the specific speed, resulting in higher rotative speed and smaller tip diameters. This approach did not look attractive from mechanical design considerations. The second approach was to maintain rotative speed and diameter and reduce the flow passages 30 percent. This results in a 16 percent decrease in specific speed, but Reference 3 indicates no penalty in turbine efficiency and only one point decrease in compressor efficiency for the components. The power turbine will have the same pitch diameter with 30 percent smaller flow passages.

Since the pressure level and required temperature rise remains the same for the integrated system as for the non-integrated system, the flow passage length was kept the same and the number of tubes reduced to keep the mass flow per tube constant in the isotope package. The reduced power level decreases the required shielding thickness as shown in Figure 6-13.

The smaller number of tubes reduces the volume that the shield must enclose and further reduces shield volume.

Figure 6-18 shows the isotope heat exchanger and shield including pertinent dimensions. Other pertinent parameters are listed in Table 6-5.

6.2.2.2 Turbo Alternator

The turbo alternator package for this power plant system is the same as described in Section 6.1.6.3 with the following exceptions:

- a. Both the diameter and width of the pole pieces in the rotating portion of the alternator, as well as the stator windings, are reduced in size and weight to reflect the reduced electrical output of 1.73 KW_e .
- b. The turbine wheel diameter is kept constant but the flow passages and inlet and outlet scrolls are reduced in cross-sectional area approximately 30 percent to keep velocities and turbine RPM constant at the reduced flow rate.

Gas bearing losses were assumed to be the same as for the 3.28 KW_e generator since the speed remains the same and the turbine/rotor weight does not decrease in proportion to the electrical output. This probably is a conservative approach.

Component weights and efficiency can be found from Figures 6-24 and 6-23, respectively.

6.2.2.3 Turbo Compressor

The gas generator is identical to the one described in Section 6.1.6.4 except both nozzle area and diffusor area are reduced 30 percent to keep RPM and gas velocities constant at the reduced mass flow.

Gas bearings are assumed to be the same as for the gas generator described in Section 6.1.6.4 since rotative speed and compressor and turbine weights are constant.

6.2.3 RECUPERATOR

The recuperator is a slightly smaller version of the one described in Section 6.1.8 and pictured in Figure 6-28. Pertinent dimensions are listed in Table 6-8.

6.2.4 RADIATORS

The argon filled radiators to reject the waste heat to space are shown in Figures 6-26 and 6-27. They are the same as described in Section 6.1.7 with the following exceptions.

- a. Weight is considerably less due to the smaller mass flow and heat rejection rate. This reduces both the header and tube diameter and fin thickness.
- b. Area is reduced due to the lower heat rejection rate, but not in the same proportion as weight due to the lower radiator temperature.

Table 6-7 and Figure 6-27 list the pertinent performance parameters and dimensions.

6.2.5 AUXILIARY COOLANT SYSTEM

The auxiliary coolant system to cool generator and turbo machinery gas bearings is identical to that shown in Figure 6-2 and described in Section 6.1.10 except the size is smaller to reflect the reduced generator losses. Pertinent performance parameters are listed in Table 6-12.

6.2.6 ISOTOPE HEAT SOURCE

The Isotope Heat Exchanger and Shield is as described in Section 6.1.5.3 with the following exceptions:

- a. Energy input has been reduced from 30 KW_t to 18 KW_t due to the smaller electrical requirements. This only requires 18 of the individual heat exchanger tubes and fuel capsules to supply the required 18 KW_t .

6.2.7 SOLAR BRAYTON SYSTEM CONFIGURATION

The system configuration will be as shown on Figure 6-3 which is identical to the Non-Integrated System except for the following differences:

1. Because of the smaller solar collector diameter, the integrated system has no requirement for a "tip folding mechanism."
2. The integrated design involves an argon gas to therminol liquid heat exchanger in the gas loop just prior to the space radiator. This is a comparatively small heat exchanger and fits neatly in the power package within the projected area of the absorber and occupies otherwise unused space.

The Therminol lines to and from this heat exchanger which carry heat to the life support equipment will be ducted from the power plant package to the vehicle by way of the telescoping tubes which support the power package.

6.2.8 SOLAR COLLECTOR

The integrated system solar collector does not require the tip-folding capability because of its reduced diameter which is made possible because of the significantly lower cycle heat requirement. Referring to Table 6-1, it is seen that the total heat input requirement for the collector is decreased from 37.9 KW to 22.8 KW for a 40 per cent reduction in collector area and weight. The overall collector efficiency is the same for both systems since by definition it is not a function of the required input power.

6.2.8.1 Solar Absorber

The solar absorber for the Integrated System was chosen using the same criteria as for the non-integrated design. With the required amount of heat to be transferred to the gas cycle set at 18 KW, the overall weight and size requirements were established as shown in Tables 6-14 and 6-16 and Figure 6-11.

Again making use of the computer generated data and Figures 6-8, 6-9 and 6-10 for the 36 tube in shell configuration, tube dimensions were determined: inside diameter 0.52 inch, length 5.1 feet. Tube thickness and shell thickness remain the same as for the Non-Integrated systems, 10 and 30 mils, respectively.

The aperture diameter for the 19 ft. mirror is 4.39 inches. Except for weights and dimensions, all other design features are the same as the non-integrated design.

The following percentages represent the improvement in ratio of integrated to non-integrated parameters due to thermal integration.

Heat Absorbed	60%
Weight Ratio	67%
Size Ratio	80%

6.2.9 LIFE SUPPORT SYSTEM INTERFACE

The life support system and its weight and power requirements are described in Section 4 of this report.

The equipment to supply the endothermic power requirements to the LSS is described in the following two paragraphs.

6.2.9.1 Argon to Therminol Heat Exchanger

This heat exchanger is located in the power plant process gas piping between the discharge of the recuperator and the inlet to the waste heat radiator. It transfers the thermal energy required for the endothermic processes in the LSS from the argon process gas to a heat transport medium (Therminol FR-1) which is then pumped into the LSS equipment in the cabin area.

The heat exchanger is a cross counter-flow plate-fin type with the geometry shown in Figure 6-30, having a single pass on the argon side and four passes on the Therminol side.

In order to supply the low temperature heat requirements to the life support process, the high temperature Therminol loop is passed through a pure counterflow heat exchanger, counter to the ethylene-glycol solution (30 percent glycol by weight). The design conditions are given below:

<u>Ethylene Glycol</u>	<u>Therminol</u>
W = 222 lbs/hr	W = 368 lbs/hr
T _{in} = 135°F	T _{in} = 312°F
T _{out} = 155°F	T _{out} = 278°F
Q = 4080 BTU/hr	

The final design characteristics arrived at, which minimize both the component weight and the pumping power, are given below:

Ethylene Glycol Tube i.d. = .3 inch
Heat Exchanger o.d. = .52 inch
Length = 23 inch
Ethylene Glycol Weight = .0602 lb
Structural Weight (aluminum .03 inch wall) = .172 lb
Therminol Weight = .064 lb
Total Weight = .3 lb
Ethylene Glycol Pressure Drop = Negligible
Therminol Pressure Drop = Negligible

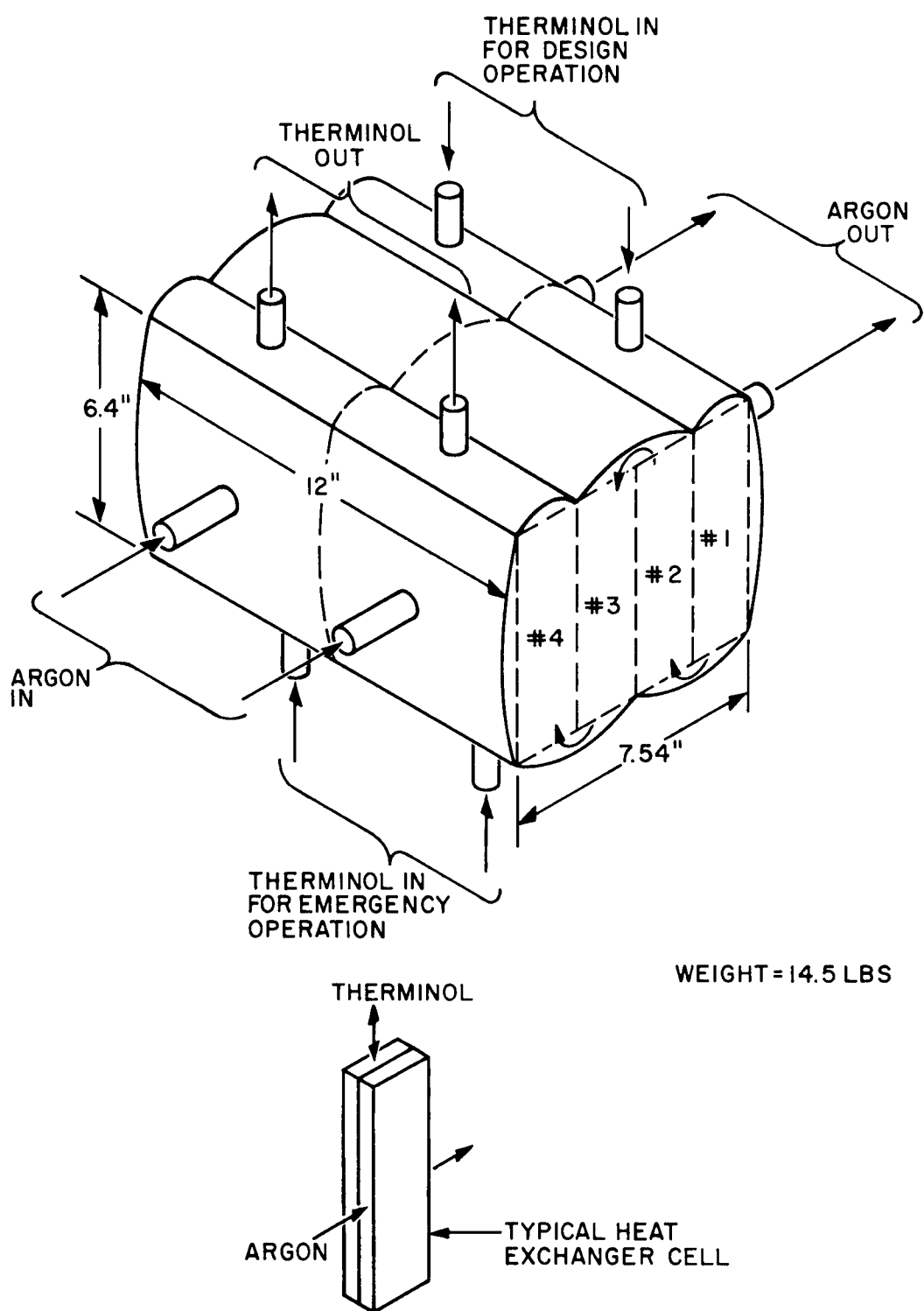


Figure 6-30. Dual Argon to Therminol FR-1 Heat Exchanger

The configuration for this heat exchanger is shown in Figure 6-31.

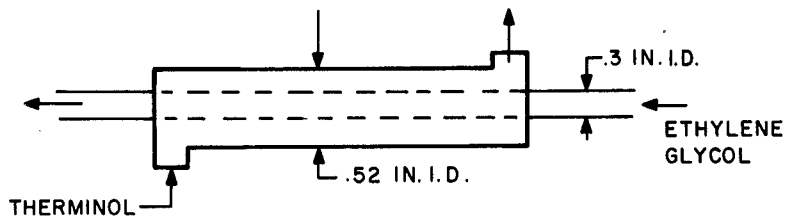


Figure 6-31. Therminol FR-1 to Ethylene Glycol Heat Exchanger

This heat exchanger will be located in the LSS racks inside the cabin to minimize piping length and to eliminate penetrating the cabin pressure wall with an extra set of lines.

6.2.10 DISCUSSION OF THE SYSTEM

6.2.10.1 Selection of the Design Points

The same factors affecting the selection of the design point as described in Section 6.1.6.1 apply to the integrated power system as well as to the non-integrated system. Since all component efficiencies are constant as discussed in Section 6.2.2, the same design point of $P_2/P_1 = 2.3$ and $T_1 = 536^{\circ}\text{R}$ was chosen for the integrated system. Compressor inlet pressure was held constant at 6 psia for the reasons discussed in Section 6.2.2.

6.2.10.2 Isotope Brayton Heat Source and Radiator

Detailed design of the isotope heat source and shield yields a specific weight of approximately $78\text{lb}/\text{KW}_t$ and radiator weight of $1.4 \text{ lb}/\text{KW}_t^2$ with an area of 310 ft^2 for a 536°R outlet temperature. This yields a specific radiator weight of $51.2 \text{ lbs}/\text{KW}_t$. Since these values are not greatly different from those shown in Figure 6-29, it was assumed that the pressure ratio of 2.3 and T_1 of 536°R will still yield a near optimum system.

Figure 6-32 shows a plot of radiator weight as a function of Argon ΔP . It can be seen that weight is quite strongly influenced by pressure drop. A pressure drop of .25 psi was chosen for the radiator, leaving an allowable pressure drop of 0.12 psi through the Argon to Therminol heat exchanger to make up the allowable .32 psi drop through the heat rejection system. This results in a heat exchanger weight of 14.5 lbs. and radiator weight of 410 lbs for a total heat rejection system weight of 424.5 lbs.

6.2.10.3 Solar Brayton Radiator

The design criteria were the same as used for the non-integrated system with regard to meteoroid protection, heat transfer coefficients, surface emissivity, radiator effectiveness, etc. However, one parameter was changed, i.e., the allowable pressure drop through the radiator. It is desirable to maintain the same over-all system pressure loss ratio for the integrated as the non-integrated system. Since the integrated system requires the use of an additional heat exchanger in argon loop, it was decided to keep the

total loss from the recuperator discharge to the compressor inlet set at 5 percent as in the non-integrated design. This 5 percent (0.32 psi) was therefore split by approximately 2 to 1 between the radiator and heat exchanger respectively. The actual losses were set at 0.20 psi for the radiator and 0.12 psi for the heat exchanger.

The heat to be rejected to space for this system is 8.4 KW compared to the 21 KW of the non-integrated design. This 60 percent reduction is due to: (a) the addition of 40 percent less heat to the integrated cycle and (b) supplying about 30 percent of the waste heat to the life support system.

The total weight of this radiator (i.e., four parallel panels - each with 36 tubes) is estimated at 520 pounds and a total area of 500 ft^2 . Other characteristics are shown on Figure 6-33. Weight and Area for this design is shown as a function of heat radiated on Figure 6-34.

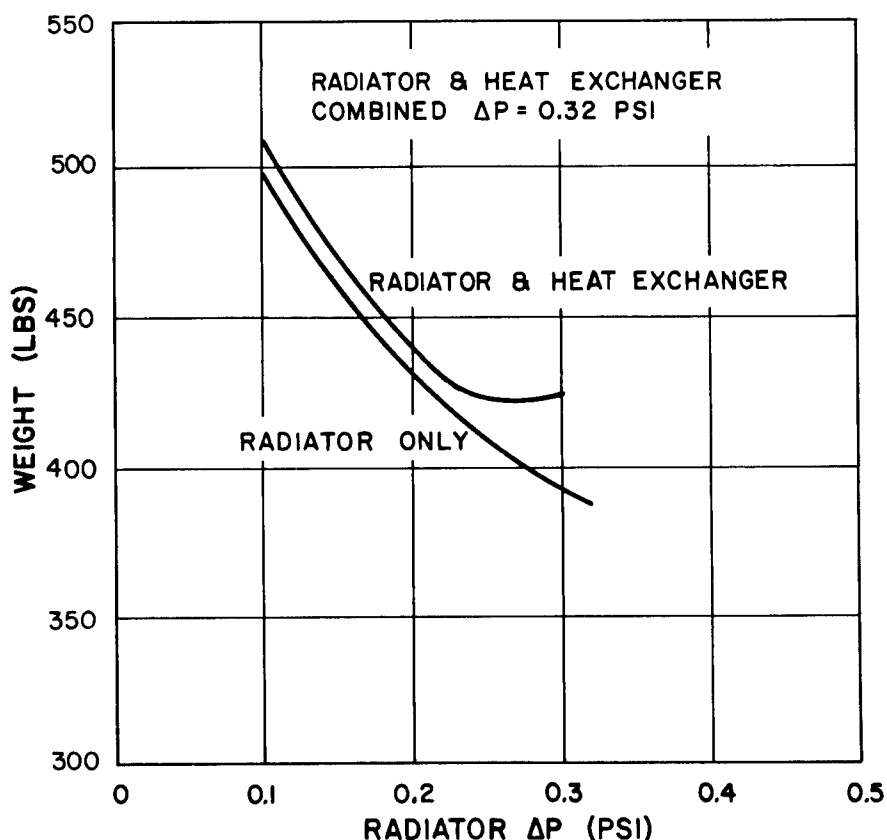


Figure 6-32. Radiator and LSS Heat Exchanger Weight

6.2.10.4 Cycle Operating Points

The same procedure was used to calculate the cycle operating points as is described in Section 6.1.9.1 and the results are tabulated in Table 6-17.

TABLE 6-17. BRAYTON CYCLE THERMODYNAMIC CYCLE OPERATING POINTS INTEGRATED SYSTEM

Station	Location	T °R	P psia
1	Compressor Inlet	536	6.0
2	Compressor Outlet	801	13.8
2.5	Heat Source Inlet	1470	13.66
3	Compressor Turbine Inlet	1950	12.97
4	Power Turbine Inlet	1663	7.97
5	Power Turbine Outlet	1544	6.37
6	LSS Heat Exc. Inlet	875	6.32
6.5	Radiator Inlet	763	6.12

Turbine Work
Pounds of Argon = 14.83 BTU/lb

Heat Added
Pounds of Argon = 59.73 BTU/lb

Heat Rejected
Pounds of Argon = 42.20 BTU/lb

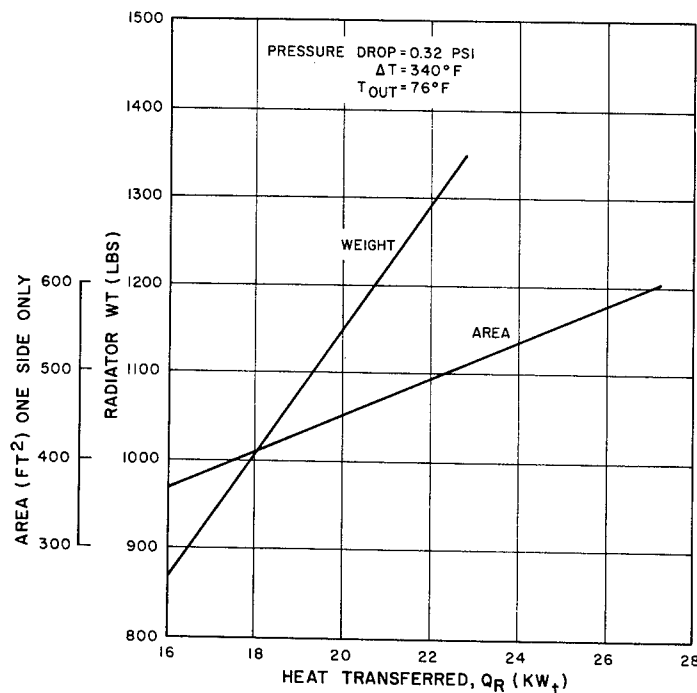


Figure 6-33. Solar Brayton Cycle Radiator Characteristics

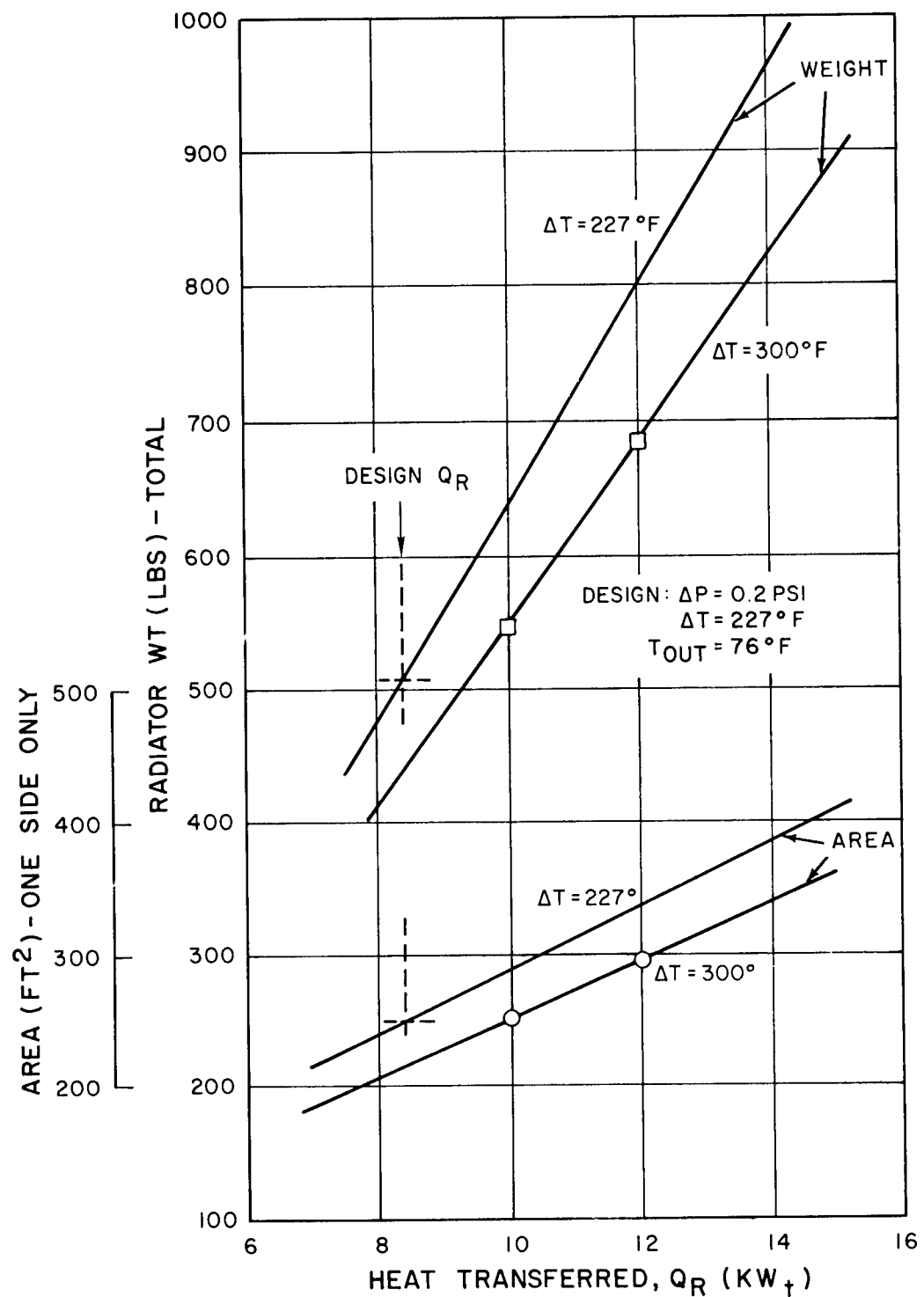


Figure 6-34. Solar Brayton Cycle Integrated Radiator Characteristics

6.2.10.5 Power Plant

The assumption was made that the electrical load, excluding requirements of the power plant and life support system, would remain constant. The generators were then sized to produce this power plus that required for the integrated life support system and the power plant auxiliaries. This results in a required generator output of 3.46 KW_e . When generator efficiency and gas bearing losses are taken into account the required turbine power is 4.39 KW .

Using the values for heat added, heat rejected, and turbine work per unit flow listed in Table 6-17, the required power plant gas flow rate and heat source and heat rejection weight can be calculated.

The over-all power plant energy balance is listed in Table 6-18. Component volumes were listed in Tables 6-13 and 6-14.

6.2.11 START AND RE-START CAPABILITY

The initial start-up of this system is discussed in Section 6.1.12 this report with the exceptions listed below:

1. It may be necessary to electrically heat the Therminol loop as discussed in Section 6.2.13 to establish flow of the therminol before start-up of the LSS system.
2. The life support system absorbs approximately $1/3$ of the waste heat during normal operation. If the LSS is not to operate to remove heat from the process stream, the radiator temperature must increase according to the fourth power law to radiate the excess heat. If all four radiator panels are used to radiate energy, the compressor inlet temperature will increase from 536°R to approximately 576°R , resulting in a 14 percent decrease in turbine power to the generator. The net result is a maximum of 2.96 KW_e generated with an inlet temperature to the radiator of approximately 920°R .

6.2.12 EMERGENCY OPERATION

The first four paragraphs of Section 6.1.1.3 apply to the integrated system as well as the non-integrated system. However, effects of the energy removed by the LSS heat exchanger on single engine performance must be considered.

When the assumption is made that the 4.11 KW to the LSS is still removed in the argon to Therminol heat exchanger, the turbine inlet temperature rises from 536 to 597°R , reducing the power turbine shaft work per unit flow rate to about 77.7 percent of the design. But since the argon mass flow rate is doubled, the turbine work increases to 155 percent

TABLE 6-18. ISOTOPE BRAYTON CYCLE ENERGY BALANCE
INTEGRATED SYSTEM

Non-Integrated Electric Power to Station Bus	6.24 KW _e
Non-Integrated Electrical Power to LSS	<u>4.566</u>
Non-Integrated Electrical Power to Other Loads	1.674 KW _e
Integrated Electrical Power to LSS	1.601
Coolant Pump Power	0.02
5% of Load for Speed Control	<u>0.165</u>
Generator Output	3.460 KW _e
Generator Efficiency (neglecting bearing losses) 84.5 %	
Net Shaft Power to Generator	4.09 KW
Gas Bearing Losses in Turbo-Alternator	<u>0.30</u>
Required Turbine Power	4.39 KW
Required Turbine Power = 4.16 BTU/sec.	
Turbo Flow Work = 14.83 BTU/lb.	
Argon Flow Required $\frac{4.16}{14.83} = 0.280 \text{ Lb/sec.}$	
Heat Added by Source (59.73) (0.280) = 16.74 BTU/sec.	
Heat Rejected to LSS and Radiator (42.2) (0.280) = 11.8 BTU/sec.	
Heat Source Input to Gas Stream	17.65 KW _t
Assumed Thermal Losses	<u>0.35</u>
Heat to be Supplied by Isotope Source	18.0 KW _t
Generator Output	3.46 KW
Generator Coolant	0.63
Bearing Coolant	1.10
Thermal Losses	0.35
LSS System	<u>4.11</u>
	9.65
Heat Rejected by Radiator	8.35 KW
<u>Solar Brayton Cycle</u>	
Total Heat to be supplied by Absorber	18.00 KW _t
Total Heat required by cycle:	
Generator output and losses:	4.4 KW
Gas Generator bearing losses:	0.8 KW
Total Heat to Life Support:	<u>4.4 KW</u>
	9.6 KW
Total Heat to be rejected by Radiator	<u>9.6 KW</u>
	8.4 KW _t

of design. As a result, the remaining generator will now deliver approximately 1.82 KW_e which is above the 1.4 KW specified for emergency operation and is slightly more than the 1.6 KW_e required for the LSS system. This means that the LSS system could operate at 100 percent capacity for an indefinite time on one set of turbo-machinery if necessary.

To hold the heat removed rates and Therminol temperatures in the LSS constant, the flow of Therminol through the heat exchanger will have to be diverted so that only 8 percent, of three heat exchangers in operation. This reduces the effective heat transfer area to 12.5 percent of the design value resulting in an increase in therminol temperature delivered to the LSS of 69°F, to 468°F. The LSS should have no difficulty in handling this moderate increase in temperature.

To hold the heat removal rate and Therminol temperatures in the Life Support System constant, the flow of Therminol through the heat exchanger would have to be diverted so that ideally only 8 percent of the total heat transfer area is used. Since this is not practical, a more realistic approach would be to bypass the first three of the four heat exchanger sections comprising the total radiator area. This reduces the effective heat transfer area to 25 percent of design value, resulting in a 69 degree F increase in Therminol temperature delivered to the Life Support System. The Life Support system should have little difficulty in handling this moderate increase in temperature.

The disadvantages of this system are the same as discussed in Section 6.1.13.

The assumption is made that if both sets of turbo-machinery fail, the mission will be terminated, and the isotope package separated from the spacecraft for return to earth. Cooling of the isotope package during the re-entry phase is beyond the scope of this study.

6.2.13 START-UP AND CONTROL

6.2.13.1 Start-up Sub-system

The start-up sub- system is the same as the system described in Section 6.1.12.1 with the following exceptions:

1. The high pressure argon storage bottles will be slightly smaller and lighter due to the reduced volume in the integrated power plant.
2. The Therminol heat exchanger and lines may need electrical heaters to pre-heat the liquid prior to the start up so that viscosity may be reduced to an acceptable level to allow pumping. The power for energizing the heaters will come from the batteries.

6.2.13.2 Speed Control Subsystem

The speed control system will be identical to that described in Section 6.1.12.2 with the following exceptions:

1. The magnetic amplifiers and parasitic load resistors will be smaller and lighter due to the reduced electrical capacity of the system. Weights were shown in Table 6-15.

6.2.14 GROUND COOLING AND CHECKOUT

The ground cooling and checkout pressures for the integrated system are the same as those described for the non-integrated system in Section 6.1.11.

6.3 REFERENCES

1. "Present and Potential Annual Availability, of Isotope Power Fuels," Division of Isotopes Development, United States Atomic Energy Commission, April 1963, Revised February 1964.
2. "Study on Application of Nuclear Electric Power to Manned Orbiting Space Stations: Phase I" General Electric Company Document Number 68SD865, December 20, 1963.
3. "Gas Medium Selection and Turbo-Machinery Matching for Closed Brayton Cycle Space Power Systems" by Yabutoshi Senoo, ASME 63-WA-86, November 17, 1963.

Other references pertinent to this section are:

- a. "Feasibility of Radioisotope Power for Manned Orbiting Space Stations," Martin Company Document Number MND-3085, Report Classified Confidential, September 20, 1963.
- b. "Conceptual Design of a Radioisotope Power System for a Manned Orbiting Research Laboratory," Martin Company Document Number MND-3125, Report Classified Confidential, February 1964.

SECTION 7.

SOLAR MERCURY RANKINE SYSTEM ANALYSIS

7.1 INTRODUCTION

The Mercury Rankine auxiliary power system is a solar energy power conversion system using a mercury vapor turbine to drive a permanent magnet alternator, producing A. C. power at 2000 cps.

The major components of the system are:

1. A solar collector in the form of a parabolic reflector.
2. A boiler absorber containing lithium hydride between concentric hemispherical shells, utilizing a single spiral boiler tube to carry the working fluid.
3. A single shaft, sealed turbine-alternator-pump unit of the TRW Sunflower type.
4. A tube and header condenser-radiator made integral with the vehicle skin.

Auxiliary components, such as starter and speed controls, are assumed similar to the corresponding components of the Sunflower system described in References 1 and 2.

Structure, plumbing and heat exchangers were designed specifically for this study.

The following paragraphs describe the assumptions made and the logic followed in the selection of major system parameters for both integrated and non-integrated Mercury Rankine power systems. Unless otherwise indicated, assumed values are taken from Section 3.2 Design Guidelines.

Table 7-1 summarizes the system output characteristics, heat balance and components weights.

7.2 NON-INTEGRATED SYSTEM

7.2.1 OUTPUT - 6.24 KW

This system is sized to provide a continuous useable output of 6.24 KW with complete redundancy of rotating machinery necessary to accomplish emergency power requirements.

6.0 KW is delivered to provide continuous load requirements, while .24 KW is required to charge batteries for use in meeting peak load conditions.

The alternators are designed to deliver an additional 340 watts (5% of output) to operate the turbine speed control and 270 watts to make up frequency conversion losses.

7.2.2 HEAT BALANCE

See Table 7-1.

7.2.2.1 Alternator Output

$$6.24 + .34 + .27 = 6.85 \text{ KW or } 3.43 \text{ KW per parallel unit.}$$

7.2.2.2 Pumping Power .18 KW

Based on References 1 and 2 pump power was assumed independent of system size. This is reasonable for the range of flow rates considered since pumping efficiency tends to increase with pump size and flow rate and the pressure differential is the same for all cases.

TABLE 7-1. CYCLE COMPARISONS MERCURY RANKINE

PARAMETER	VALUE Integrated	VALUE Non-Integrated
Total Electrical Output, KW	3.60	6.85
Load	3.28	6.24
Speed Control	.18	.34
Converter Loss	.14	.27
Heat Balance		
Heat Added to Boiler, KW	39.7	60.0
Heat Rejected to Radiator	35.0	51.7
Load	3.28	6.24
Speed Control	.18	.34
Converter	.14	.27
Pumps	.36	.36
Alternator Losses	.78	1.12

Weight Summary

ITEM	WEIGHT
Battery	600
Solar Collector	606
Boiler - Absorber	227
Turbo-Alternator (2)	48
Condenser - Radiator	79
Saving in Vehicle Structure Wt (Integral Radiator Design)	-(28)
Mercury Inventory	18
Speed Control	50
Auxiliaries (2)	114
Structure and Piping	146
Heat Exchangers	80
Total Power Systems	1940
Life Support System Wt (lbs)	678
Total System Weight (lbs)	2618
	2379
	622
	3001

NOTE: The turbo alternator output is delivered at a frequency of 2000 cps. In order to compare on an equal basis with the other systems in the study, a conversion penalty was assessed. It is assumed that the frequency converter can be incorporated into the power conditioning unit and that no additional component weight penalty need be assessed.

7.2.2.3 Alternator Losses: 1.12 KW

Efficiency is assumed to be 86% (See Figure 7-1). The curve is extrapolated from Advanced Sunflower Comparison data.

7.2.2.4 Heat Added to Boiler: 60.0 KW

Assuming a turbine efficiency of 49% (See Figure 7-2), a mercury flow rate of 1434 lb. per hour was calculated.

Values for enthalpy of the mercury at the boiler outlet (161.8 BTU/lb) and inlet (18.7 BTU/lb) were obtained from thermodynamic data provided by the General Electric Company and plotted in Reference 3.

Pump work was derived from inlet and discharge pressures of 7 psia and 240 psia, respectively. These values were typical of the Sunflower 3 KW system.

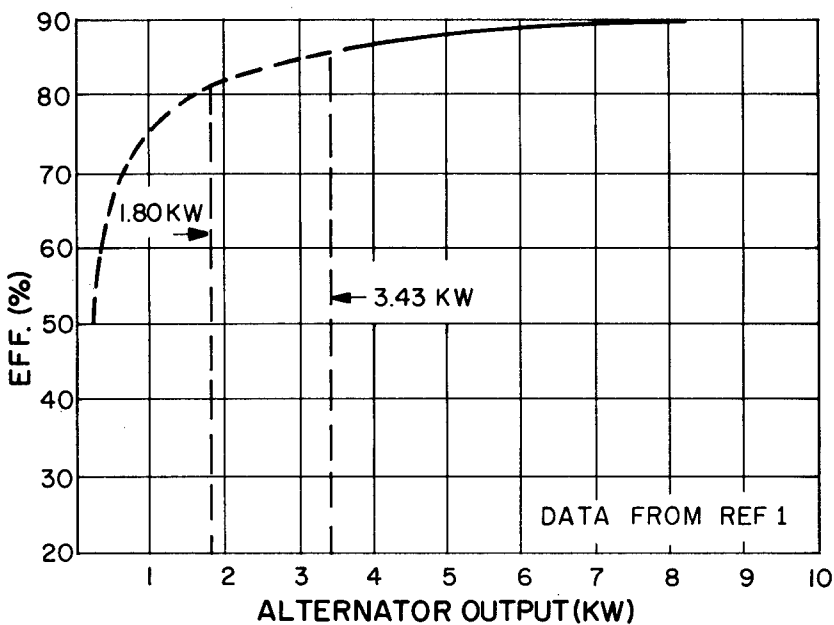


Figure 7-1. Mercury Rankine System PM Alternator Efficiency Vs. Alternator Output

Using the data shown above, the heat added was calculated from the relationship

$$Q_A = W_f (h_1 - h_{f2} - PW)$$

7.2.2.5 Heat Rejected at Condenser. 51.7 KW

Turbine exhaust conditions, h_2 , were established from the relationship $W = h_1 - h_2$.

Then the heat rejected (Q_R) is given by $Q_R = W_f (h_2 - h_{f2})$.

7.2.3 POWER SYSTEM COMPONENTS

7.2.3.1 Turboalternator (Figures 7-3 and 7-4)

The unit weight was determined by interpolating the curve of Figure 7-3 which shows Sunflower turboalternator weight plotted against net system output. The dimensions shown in Figure 7-4 are scaled from Sunflower drawings and photos, then adjusted to match selected component weight.

7.2.3.2 Condenser - Radiator (Figure 7-5)

It is assumed that the radiator will be integral with the station structure, occupying 164 square feet of skin area aft of the cabin. The size and weight are based upon heat rejection of 51.7 KW at 605°F. The design curves for this radiator are shown in Figure 7-5.

The heat losses from the piping, structure, and turbine housing were considered to be approximately 1 percent of the heat delivered from the boiler and were neglected in sizing the components.

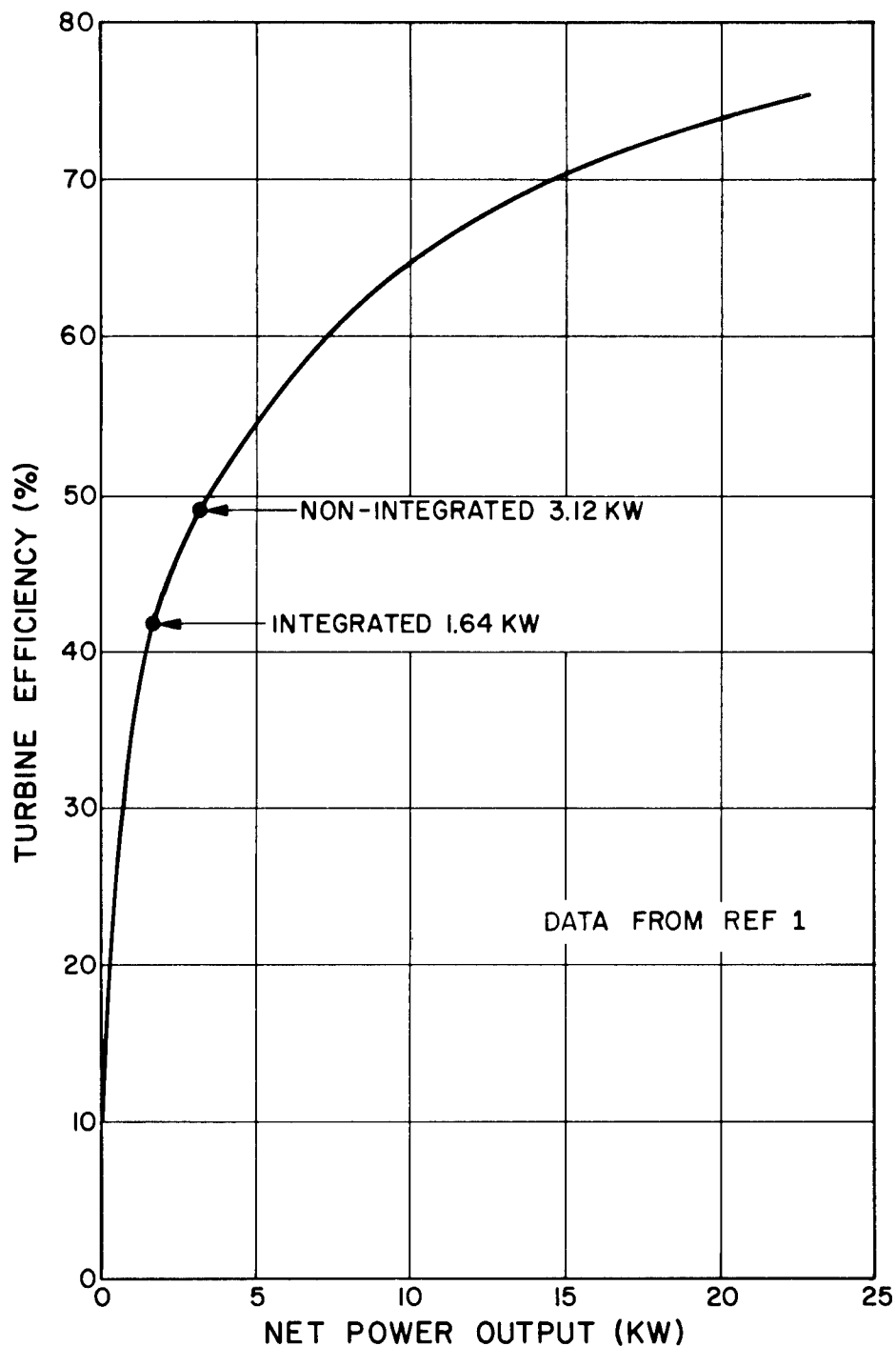


Figure 7-2. Sunflower Turbine Efficiency Data

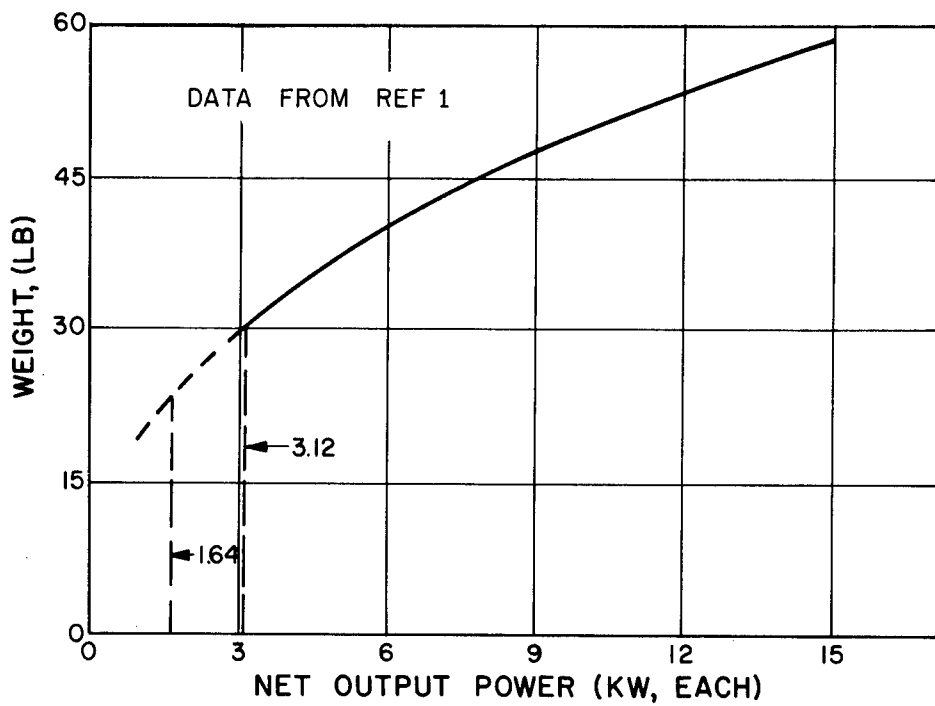


Figure 7-3. Mercury Rankine System Turbo-alternator Weight Vs. Net Output Power (PIC-SOL 209/4, SEC B-1, Fig. 39)

SPECIFICATIONS

LENGTH, 13.0 IN
 DIAMETER, D 4.5 IN
 WEIGHT 30 LB
 OUTPUT 3.43 KW AT
 2000 CPS
 MERCURY FLOW RATE
 717 LB/HR
 INLET CONDITIONS
 PRESSURE 240 PSIA
 TEMP. 1250°F
 EXHAUST CONDITIONS
 PRESSURE 7.0 PSIA
 TEMP. 605°F

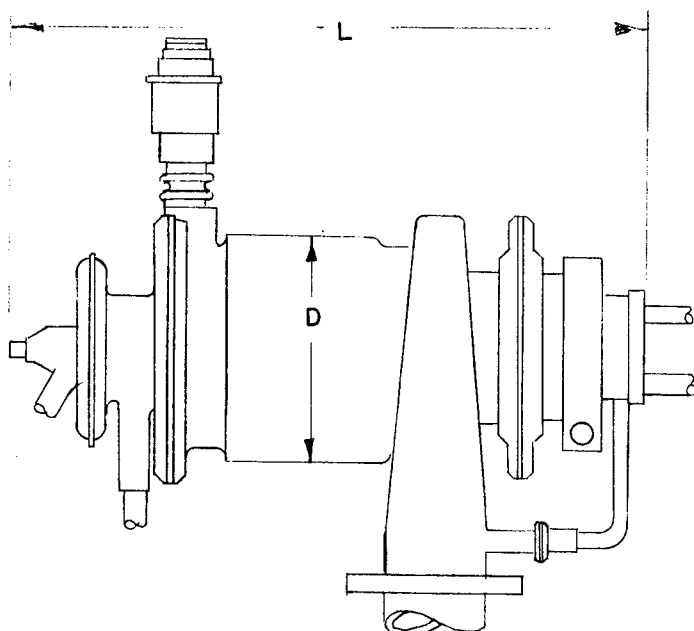


Figure 7-4. Turbo-alternator and Pump

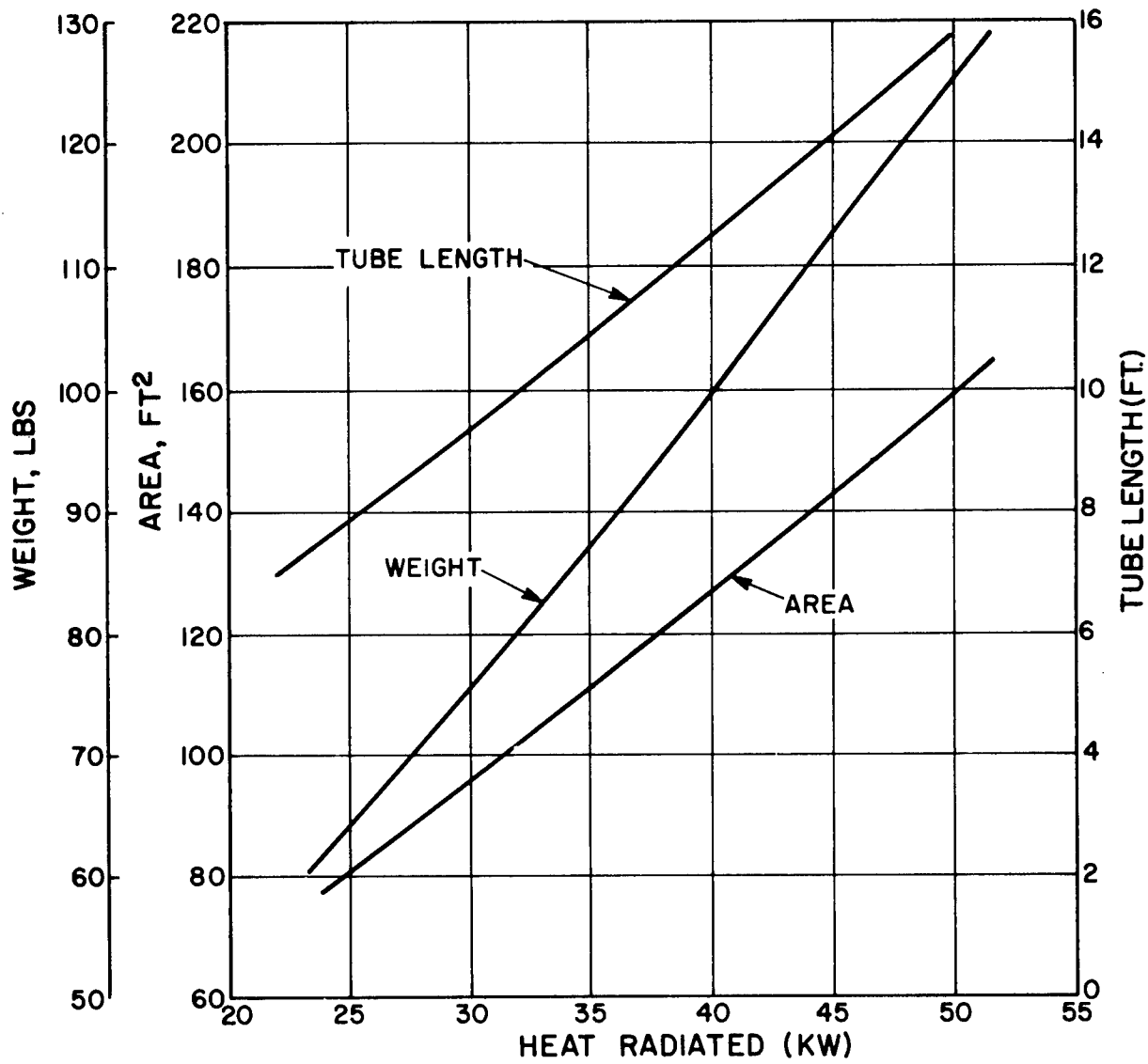


Figure 7-5. Design Characteristics of Rankine Cycle Radiator Integral with MORL Structure

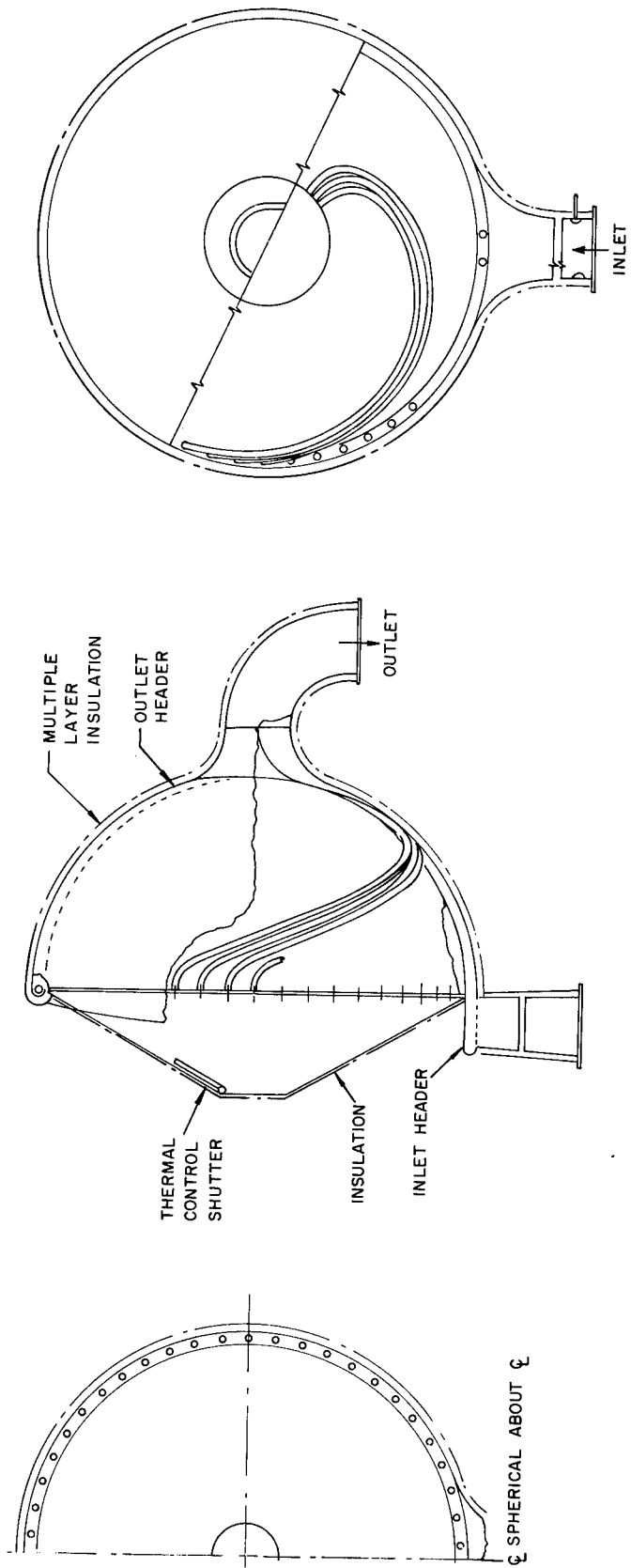


Figure 7-6. Solar Absorber Configuration

7.2.3.3 Boiler Absorber (Figure 7-6 and 7-7)

The design of this unit is based upon the double -shell concept described in the Sunflower reports. The weight of lithium hydride used is selected for 36 minutes shadow time, plus a 10 percent contingency factor for delivery of 60.0 KW average heat input.

The weight of the boiler absorber unit has been determined by extrapolation of a curve based upon Sunflower absorber weight vs. net heat to boiler. The heat lost by radiation from the absorber surface was assumed negligible because the use of super insulation provides a low conductivity from the interior to the surface.

7.2.3.4 Solar Collector

An overall collection efficiency of .816 was assumed from the data provided in Appendix B. The collector was sized to provide power at the rate of 97.2 KW for the period of sun-light, or an average of 60.0 KW. A time average mis-orientation of $0^{\circ}6'$ and a 6 percent shadow factor were assumed. Using a solar constant of 130 watts per square foot, the reflector for the non-integrated system requires 916 square feet of projected area and weighs 916 pounds.

7.2.3.5 Speed Control and Auxiliary Equipment

The design effort for these units was minimal since all auxiliary equipment was assumed to be similar to corresponding Sunflower units. The weight estimates for the turbine speed control, starting auxiliaries and mercury inventory were obtained by extrapolation of curves of component weight vs. system power output, based on Sunflower data. The curves are shown in Figures 7-8, 7-9, 7-10 and 7-11.

Speed controls actually built for Sunflower were twice as heavy as originally estimated. To derive the weight vs. output curve, Figure 7-8, the speed control weights reported in Reference 1 were doubled.

7.3 INTEGRATED SYSTEMS

7.3.1 OUTPUT - 3.28 KW

Integrating the thermal requirements of the life support and power systems resulted in a 47 percent reduction in electrical power output and a 13 percent reduction in overall system weight. The final output figure was based on a total system output (thermal plus electrical) equivalent to that postulated for the non-integrated system. (See Table 7-2.) Complete redundancy of the rotating equipment necessary to supply emergency power was a requirement.

7.3.2 HEAT BALANCE (See Table 7-1)

Figure 7-12 shows the schematic flow diagram for the integrated system. The power system component layout is shown in Figure 7-13. The cycle calculations for the integrated system, were made in the same manner as the non-integrated system

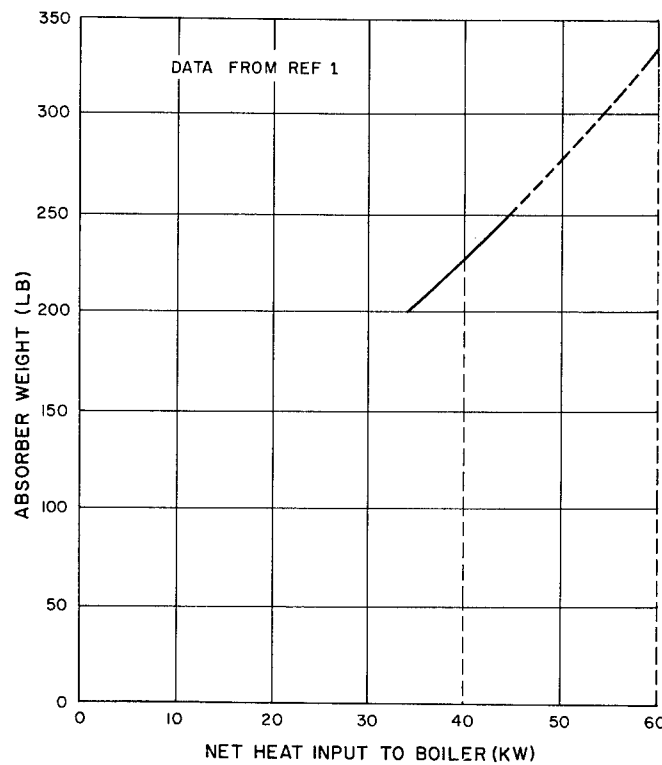


Figure 7-7. Mercury - Rankine System Absorber Weight Vs. Net Heat Input to Boiler (PIC-SOL 209/4, SEC B-1, Fig. 51, 53)

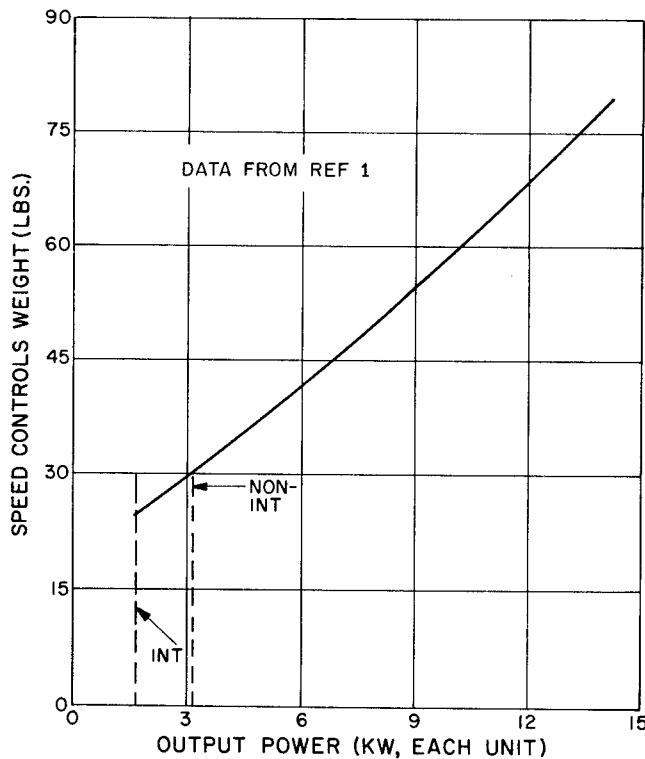


Figure 7-8. Mercury-Rankine System Speed Control Weight Vs. Power (PIC-SOL 209/4, SEC B-1, Fig. 39)

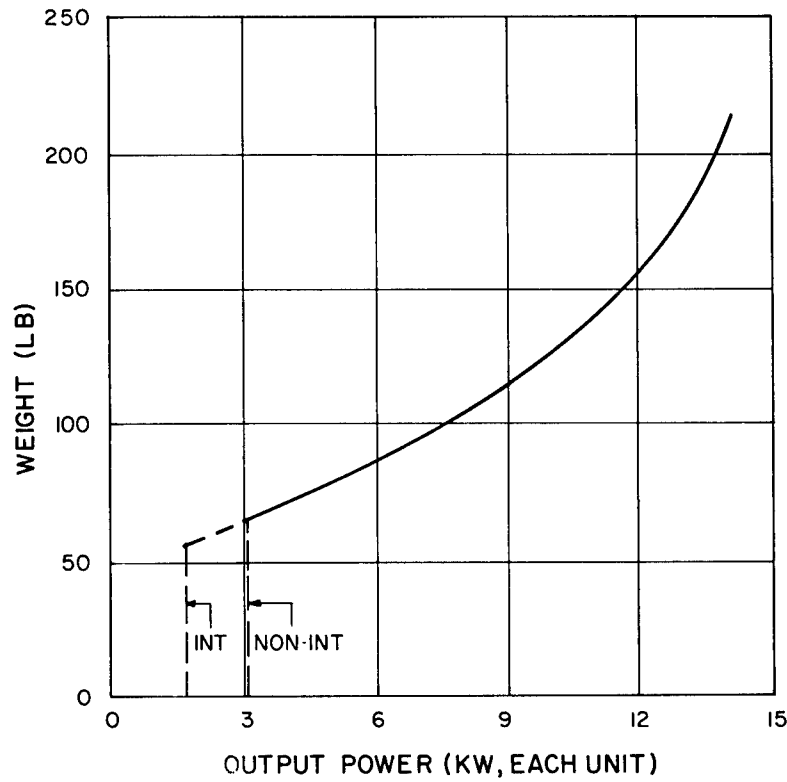


Figure 7-9. Mercury-Rankine System Start Auxiliaries Weight Vs. Output Power (PIC-SOL 209/4, SEC B-1, Fig. 39)

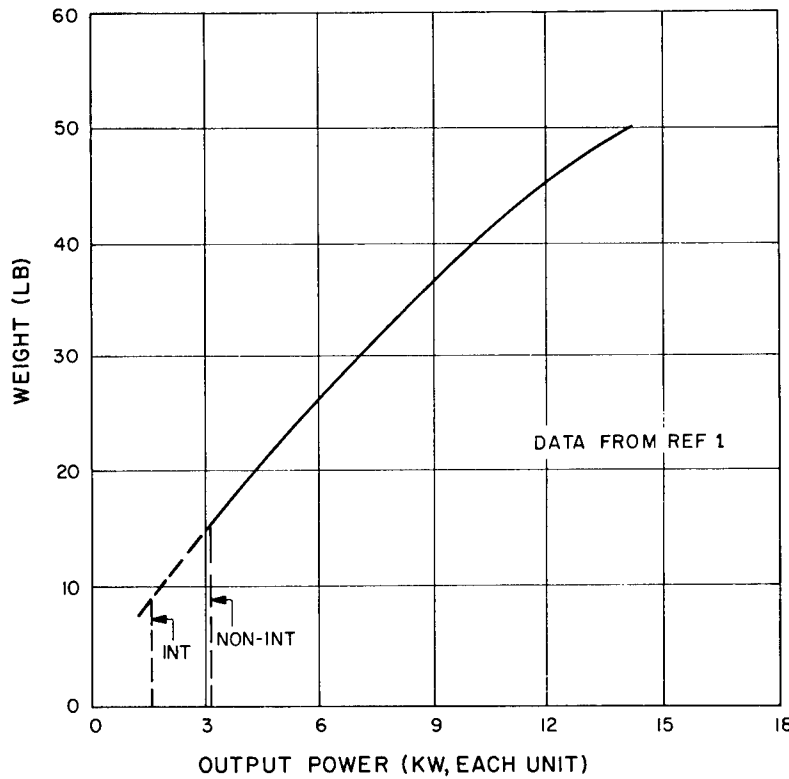


Figure 7-10. Mercury-Rankine System Mercury Inventory Weight Vs. Output Power (PIC-SOL 209/4, SEC B-1, Fig. 39)

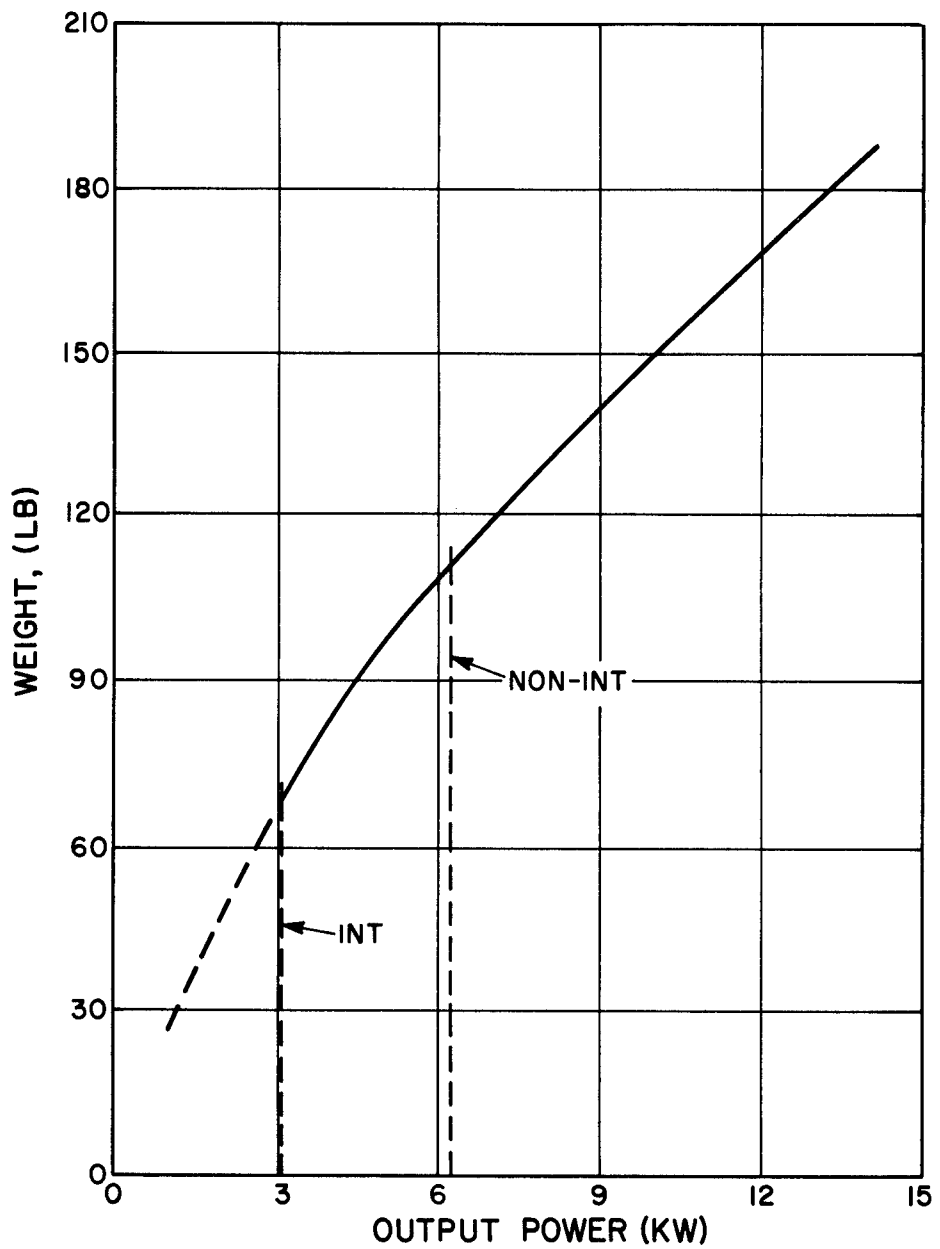


Figure 7-11. Mercury-Rankine System Structure Weight Vs. Output Power
(From PIC-SOL 209/4, Figure 39)

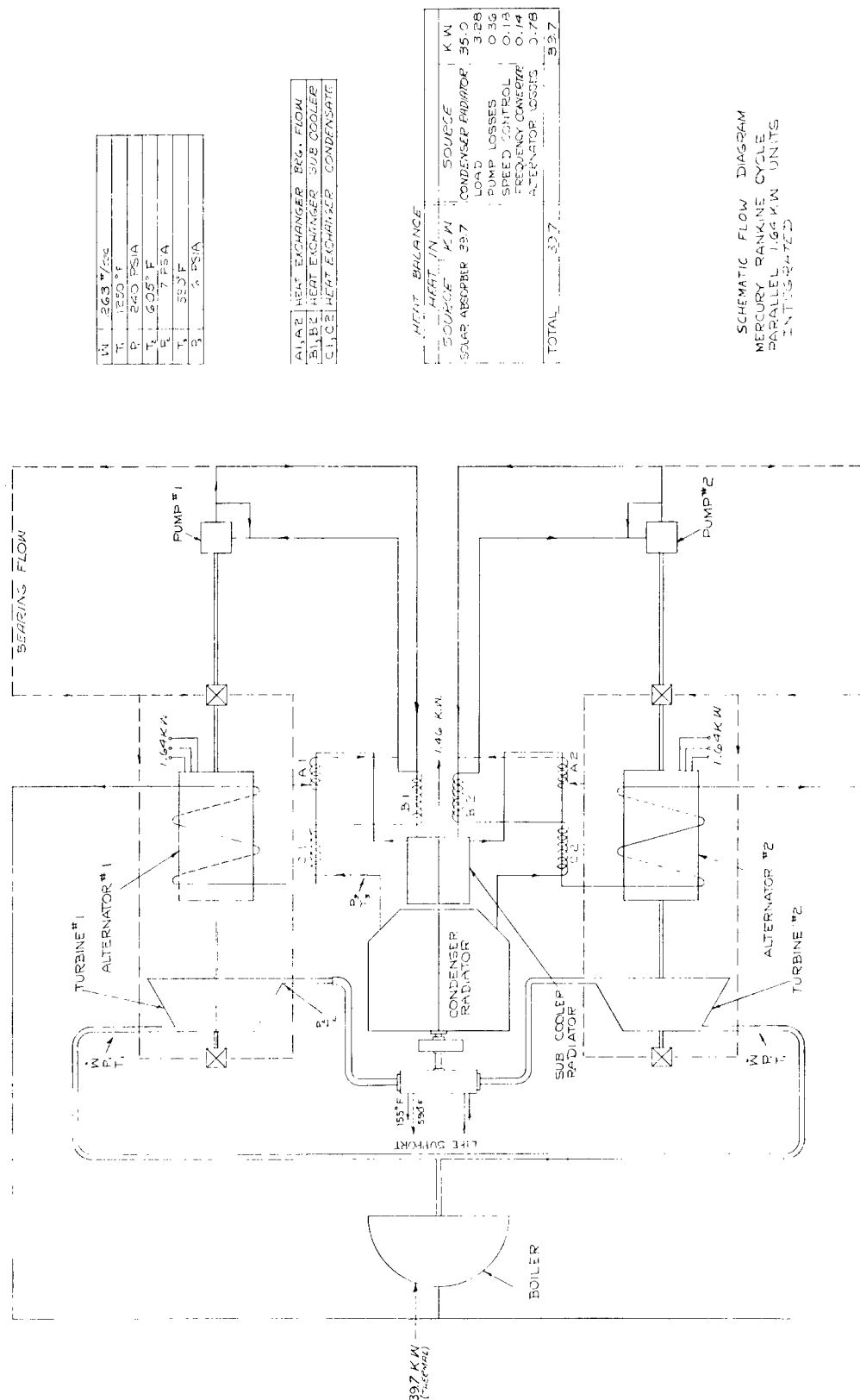


Figure 7-12. Schematic Flow Diagram-Mercury Rankine Cycle Parallel Integrated 1.64 KW Units

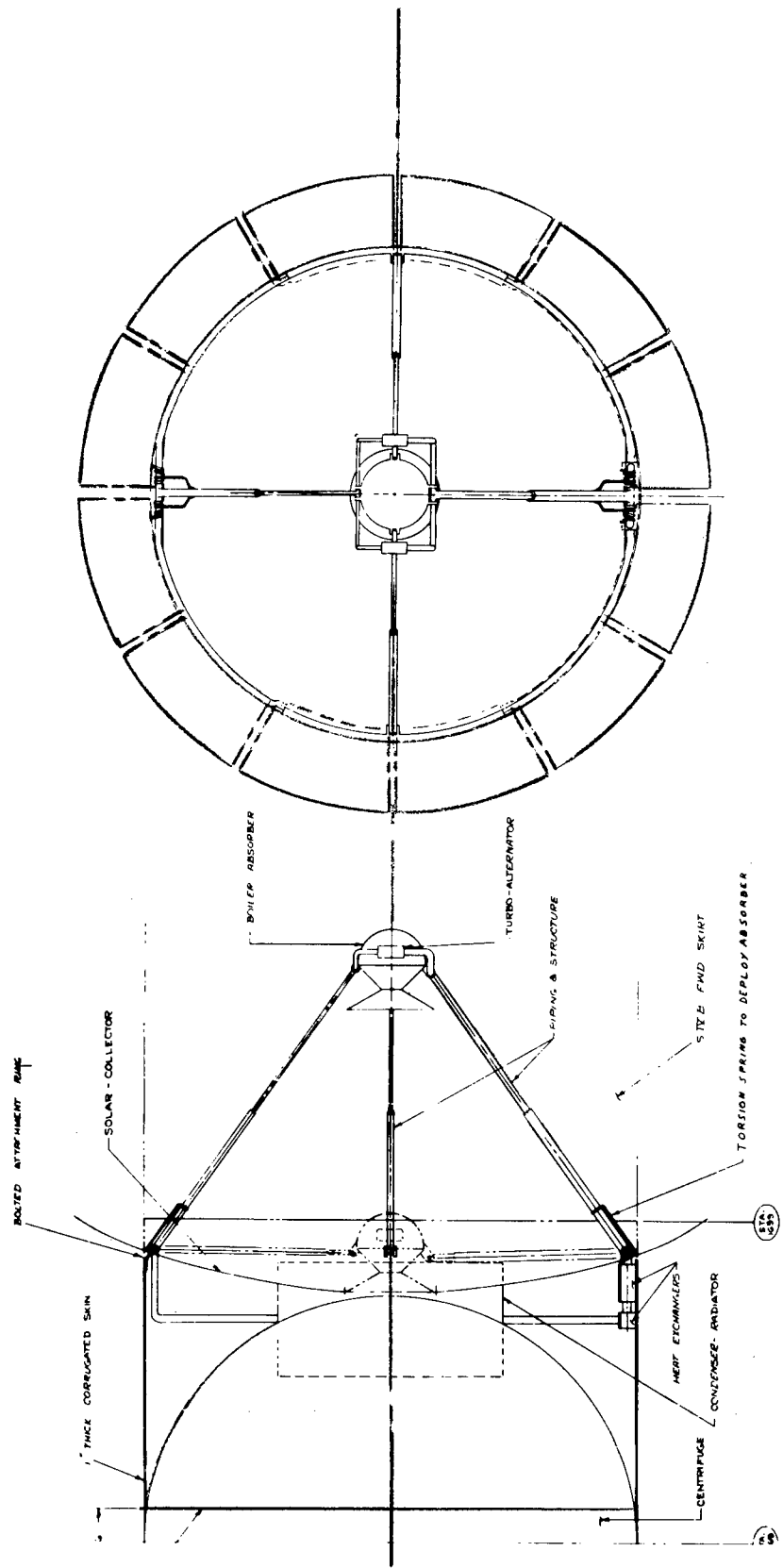


Figure 7-13. Power System Component Layout-Solar Mercury Rankine

using the reduced load requirements as a starting point. Size reductions effected by scaling down of the components were, of course, modified by efficiency losses. The magnitude of these losses was determined by the use of efficiency vs. load relationships derived from Sunflower or other referenced data.

TABLE 7-2. MERCURY RANKINE SYSTEM POWER REQUIREMENTS

Non-Integrated L. S.	4.566 KW
Other electrical power	<u>1.674</u>
TOTAL	6.240 KW
Integrated L. S.	1.601
Other	<u>1.674</u>
TOTAL	3.275 KW
Power system output	
(2) parallel units at 1.64 KW each	

7.3.3 POWER SYSTEM COMPONENT PERFORMANCE

7.3.3.1 Turboalternator

When account is taken of the reduced load requirement, the combined turboalternator efficiency drops from 42.1 to 34.4 percent, while the component weight is reduced 12 pounds from 60 to 48 pounds. It is of interest to note that if, instead of two (2) 1.64 KW units operating in parallel, one 3.28 KW unit and one 3.28 KW unit as a stand-by are used, an additional net weight saving of 178 pounds is indicated for the integrated system.

7.3.3.2 Condenser Radiator

Thermal integration of the Mercury Rankine system allows all life support endothermic requirements to be met by waste heat from the turbine exhaust which is available at 605° F. The integrated radiator, therefore, is reduced in size by two factors. First, the total heat rejected by the cycle is reduced from 51.7 KW to 35.0 KW due to the smaller electrical output requirement of the system, and second, an additional 3.48 KW is removed from the exhaust to serve the life support requirement. The integrated radiator, then is sized to dissipate 31.52 KW for a weight of 79 lb., a reduction of 39 percent.

7.3.3.3 Boiler Absorber

The integrated absorber design is identical, except for size, to the non-integrated equipment. The reduction in power required from 60.0 KW to 39.7 KW nets a weight saving in this unit of 31 percent.

7.3.3.4 Collector

The reduced power required by the integrated system allows the collector to be reduced in diameter from 34.15 to 27.8 feet, with an attendant weight saving of 34 percent.

The required collector is larger in diameter than the vehicle by about 6 feet. For an actual design, a petaline construction would be dictated, incurring some weight and efficiency penalty, due to the additional structure and erection mechanism needed.

By using a single 3.28 KW turbo-alternator with a stand-by unit, the efficiency improvements allow the collector diameter to be reduced to 24.2 feet. This reduction is not sufficient to allow the collector to be stored in the vehicle as one piece. Sizing the collector to fit into the vehicle would limit the useable power output to 1.75 KW for parallel units and 2.59 KW for redundant single units. Neither would be sufficient to serve the electrical requirements of 3.28 KW for the integrated station, although either would provide the endothermic heating needs of the life support system.

7.3.3.5 Speed Control and Auxiliary Equipment

Weights and sizes for this equipment were obtained by extrapolation of Sunflower data. (See Figures 7-8, 7-9, 7-10 and 7-11.)

7.4 INTEGRATED SYSTEM PARAMETERS

7.4.1 WEIGHT

The total weight of the system, as designed, is 1940 lbs. The two major components of weight are in the battery and the solar collector. The 600 lb. storage battery weight is dictated by the requirement to handle a 9 KW peak load for one hour per day. The alternative, to size the system to deliver the additional 3 KW continuously and eliminate the battery, results in a net saving of 32 lb.

The other large weight contribution (606 lb.) is made by the solar collector, presently estimated to weigh 1 lb. per square foot. The use of a lightweight collector, at 1/2 to 1/4 lb. per square foot, would effect a substantial system weight reduction.

7.4.2 VOLUME

Although the collector performance is based on a single piece reflector, it is recognized that the Mercury-Rankine collector will need to be folded in order to fit within the 260-inch diameter vehicle.

The stowed volume is calculated to be approximately 1025 cubic feet excluding life support equipment and heat exchangers.

7.4.3 AREA

One attribute which makes apparent the relatively low combined efficiency of the Rankine cycle is the design of the solar collector. The projected area required to collect the

necessary heat for the cycle is 606 square feet. This necessitates the use of a collector having a petaline design, as the one piece mirror diameter would exceed the vehicle diameter by 6.2 feet.

The radiators have been designed to be integral with the vehicle honeycomb skin and they pre-empt 100 square feet near the aft end of the cabin.

7.4.4 CREW HAZARDS

Since a solar heat source is used, there is no radiation risk or high temperature fluids in the crew area. The working fluid for the thermodynamic cycle, mercury liquid and vapor, is toxic and does constitute a potential hazard. However, it is never brought inside the crew area, so that the probabilities of contamination are small.

The 60,000 rpm speed of the alternator and turbine results in blade tip speeds in excess of 2000 feet per second. Structural failure could result in high velocity fragments in the vicinity of the crew.

7.4.5 LAUNCH, START AND RE-START

Due to the possibility of damage to bearing surfaces, it would be desirable to cage the rotor of the turboalternator during launch. Starting has been demonstrated on the Sunflower system using auxiliary equipment. It is assumed that capability for start and restart in flight configuration could be included within the allocated starting auxiliary weight penalty. The Sunflower system demonstrated startup by activation of the jet pump, presumably from an outside source of pressurized Hg liquid.

7.4.6 MAINTENANCE REQUIREMENTS

The system is designed for one year operation, with no planned maintenance required. Should a failure occur in either turboalternator or pump, automatically operated valves would bypass the failed unit and emergency power would be provided by the remaining functioning unit.

Suitable thermal control shutters or scattering lenses would reduce the energy fed to the absorber, so as to prevent radiator overloading.

7.4.7 COMPLEXITY AND RELIABILITY

Reliability has been a prime concern in the development of the Sunflower system. The following features are incorporated:

1. Completely hermetic sealed system
2. Internal seals are not required due to the use of a single fluid for all thermal and lubrication functions.
3. A single, rotating assembly, rather than separately packaged turbine, generator and pump.
4. The use of hydrodynamic bearings completely supported on a fluid film.

7.4.8 CONTROL REQUIREMENT

Speed control is accomplished by a variable dissipative load. It is simple and reliable.

Temperature control of the absorber has not been fully developed and may require additional weight and complexity.

7.4.9 DEVELOPMENT REQUIRED

The basic concept of the Rankine cycle has been demonstrated by TRW in the Sunflower Study. Some further work on zero "g" condensing is required. The problem of sealing fluid joints after deployment has not been developed. Absorber thermal control could pose a difficult problem.

7.4.10 SCHEDULE COMPATIBILITY

Since Sunflower development is reasonably advanced, risk and uncertainty is not high for meeting future schedules. However, zero "g" condensing problem may be a major concern.

7.4.11 STATION INTEGRATION

No special problems or restraints are imposed by the choice of a Rankine power cycle.

7.4.12 OPERATIONAL RESTRAINTS

Solar collector requires an accurate vehicle attitude control.

7.4.13 ADAPTABILITY

Complete system design is required for each load requirement. Since speed, and hence frequency of output is controlled by load, the band of scaling for load is extremely narrow.

7.5 REFERENCES

1. Picking, J. W. and Southan, D. L., "Sunflower Status Review," Proceedings of the Solar Dynamic Systems Symposium, PIC-SOL 209/4, September 24-25, 1963.
2. "Sunflower Status and Applications Considerations," Thompson Ramo Wooldridge Electromechanical Division, Cleveland, Ohio, TRW Bulletin 311-MRD-3.
3. Potter, P.J., "Power Plant Theory and Design," 2nd Edition, 1959.

SECTION 8.

PHOTOVOLTAIC POWER SYSTEM ANALYSIS

8.1 INTRODUCTION

A solar cell and battery power system has been selected for comparison with the various dynamic power conversion systems. The photovoltaic system is the logical standard of comparison as it is the only system suitable for this application that can be based upon the performance of flight proven equipment. The development of this system for this study application should involve little risk in cost and schedule areas. A conservative approach will be taken in order to provide a high degree of confidence that design performance can be achieved. Since thermal integration, in the sense used in this study, cannot be accomplished only one system design is necessary.

8.1.1 GENERAL DESCRIPTION OF SOLAR ARRAY

The solar array proposed for this study will use N/P silicon solar cells which are 11 percent efficient at 85° F to air mass zero solar radiation. A 2x2 cm size cell with an active area of 3.8 cm² will be assumed. A recent solar cell vendor survey resulted in the conclusion that a cell efficiency of 10.5 percent was reasonable under the ground rules that a system be available for flight within two years. (See reference 1). For a launch date in the 1969-71 period, an efficiency of 11 percent is considered to be a reasonable extrapolation.

The following loss factors have been assumed:

a. Soldering and manufacturing processes	0.97
b. Cover glass and filter attenuation	0.92
c. Micrometeorite erosion, ultraviolet degradation, and random cell failures	0.95
d. Lumped measurement uncertainties	0.96
e. Temperature degradation, relative output at 85° F	-0.26% per degree F

Previous analysis indicates, for N/P solar cells with a 6-mil cover glass, negligible radiation damage in 260 n. m. orbits with inclination up to 60 degrees for periods as long as 5 years. The seasonal variation in the solar constant, which is usually included as a loss factor, has been omitted for consistency with solar dynamic systems analysis.

The temperature of the solar cells, with blue-red filters optimized for use with N/P solar cells, is estimated at 124° F, using average values of albedo and earth radiation flux, and typical vehicle reflection and radiation heating values.

Using a solar constant of 130 watts/ft², the resultant power output is given by:

$$130 (0.11) (0.97) (0.92) (0.95) (0.96) \left[1 - 0.0026 (124 - 85) \right] = 10.45 \text{ watts/ft}^2 \text{ of active cell area}$$

The gross area of the solar panel will depend on the type of cell arrangement, panel construction, etc. A packing factor of 0.90 has been assumed as being typical of that attainable with reasonable effort. The packing factor is defined as the ratio

of the net active solar cell area to the gross area of the solar cell panel and is composed of a module packing factor of 0.99 and a module area-to-panel area ratio of 0.91.

The unit area weight of solar cell modules with 6 mil glass covers is tabulated in Table 8-1.

TABLE 8-1. MODULE UNIT AREA WEIGHT (with .006 inch glass)
LB/FT² OF ACTIVE CELL AREA

Solar Cells (Ref 3)(Avg. thickness - .0125 in.)	0.28
Glass-to-Cell Adhesive plus Wire & Solder	0.05
Cell-to-Substrate Adhesive	0.07
Electrical Insulation	- *
Substrate	0.33
Paint	0.027
Terminals	0.02
Diodes	0.003
End Members	- *
Glass	0.069
TOTAL	0.764

*Included in Weight of Substrate

Reference 2 reports panel weights ranging from 1.19 to 1.63 lb/ft² for fixed solar panels of smaller sized (1kw or less). Based on studies made in connection with other programs of solar panels in the size range considered here, a weight of 1.164 lb/ft² of active cell area will be used. This is composed of 0.764 lb/ft² of active cell area for the modules and 0.40 lb/ft² of active cell area for the frame (including hinges and springs).

8.1.2 GENERAL DESCRIPTION OF BATTERY

The batteries will consist of nickel-cadmium cells, charged using a two-step charge method. When operating a nickel-cadmium battery through a large number of charge-discharge cycles, an excess number of ampere-hours must be placed into the battery during the charge cycles in order to fully recharge the battery and prevent a deterioration in battery performance. At the charging rates to be considered for this application, the required overcharge amounts to 25 percent. During the overcharge period, the current must be limited, since the oxygen recombination rate is limited, and because, in overcharge, all the energy placed into the battery is converted into heat, which must be removed. The maximum usable overcharge rate is considered to be the 6-hour rate (that rate which would return all the current to the battery in 6 hours).

The two-step constant-current charging method charges the batteries at a high constant current until the capacity previously removed has been replaced. During the overcharge period, the rate is lowered to the 6-hour rate so that heat and gas generation rates are

acceptable. This method requires an increase in the size of the solar array, but results in a large reduction in size of the battery required.

The two-step charge method requires some means to determine when 100 percent of the capacity has been returned to the battery. The battery charge control will include an ampere-hour meter to determine when full capacity has been returned to the battery. The specific energy density for nickel-cadmium batteries in the cell sizes to be utilized for this application is estimated to be 11 watt-hours/lb. This weight will include the cells, internal connections, case, mounting brackets, and connectors.

8.2 DESCRIPTION OF SYSTEM AND DESIGN

Figure 8-1 shows the block diagram for the photovoltaic power system necessary to supply the electrical power output which is consistent with the other non-integrated dynamic systems. The solar array and battery are modularized units although shown as only single units in the diagram. In order to provide power with voltage regulation equivalent to the dynamic systems, a voltage regulator has been included in the system.

8.2.1 SOLAR ARRAY SIZING

The solar array size, for constant current battery charging with a continuous power requirement is given by:

$$P_{SA} = \frac{1}{Z} P_C + \frac{T_D}{\eta_e T_L} P_C$$

where:

P_{SA} = solar array power

P_C = average power requirement

Z = product of loss factors:

η_{AD} (array diodes)

η_H (Harnesses)

η_e = total power efficiency through battery, includes Z plus:

η_{BCR} (battery charge regulator)

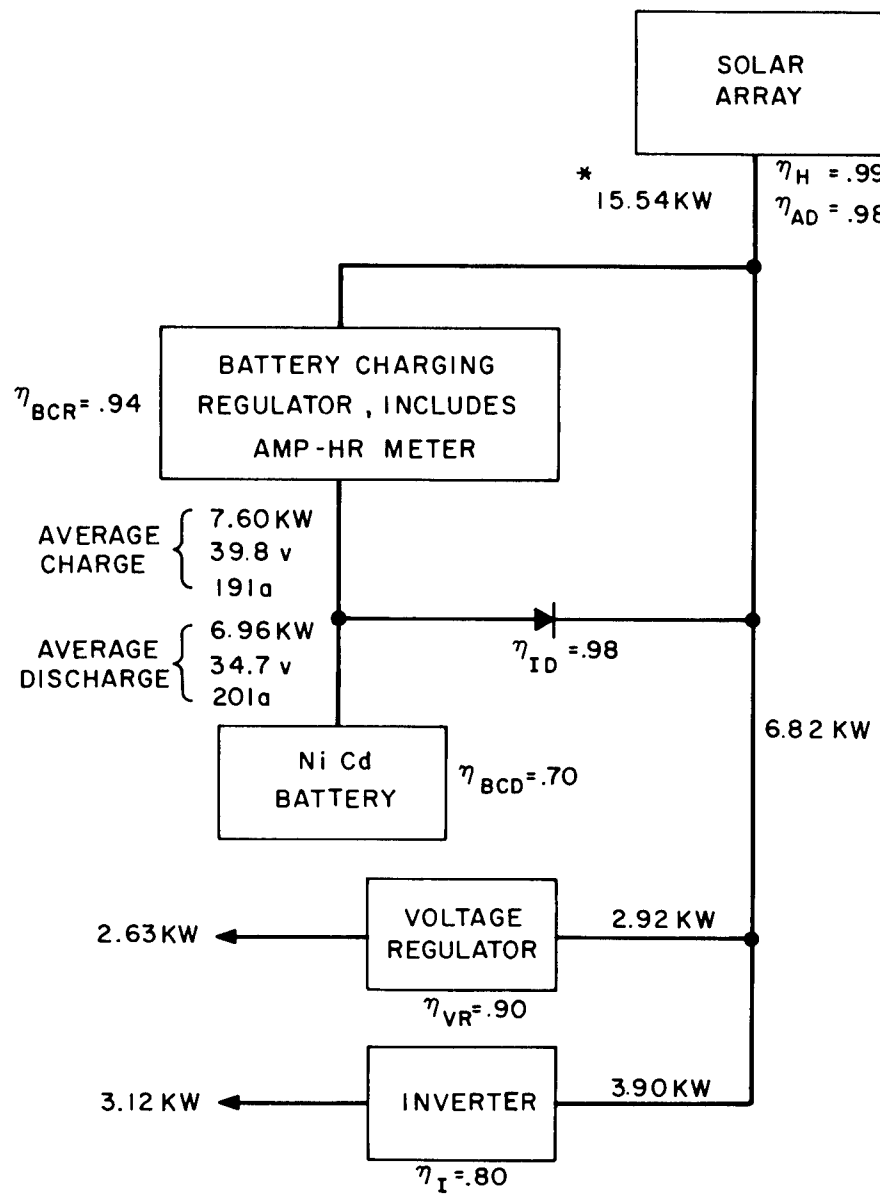
η_{BCD} (battery charge-discharge efficiency on a power basis including overcharge requirement)

η_{ID} (battery isolation diode)

T_D = orbit dark time

T_L = orbit light time

The design guide lines state that peak power is 9.0 KW for no more than 1 hour out of 24.



* NOTE:

THIS DIAGRAM IS FOR THE NOMINAL OPERATING CONDITION EXCEPT THAT THE SOLAR ARRAY SIZE ACCOUNTS FOR THE PEAK LOAD REQUIREMENT.
WITHOUT THE PEAK LOAD THE SOLAR ARRAY SIZE WOULD BE 15.16 KW

Figure 8-1. Photovoltaic System Block Diagram

With this power profile, P_C is 6.99 KW.

Referring to Figure 8-1, the loss coefficients are:

$$Z = (.98)(.99) = .97$$

$$\eta_e = (.97)(.94)(.70)(.98) = .625$$

For a 250 n. m. Circular Orbit

$$T_D = 36 \text{ minutes (maximum)}$$

$$T_L = 58 \text{ minutes (minimum)}$$

Therefore:

$$P_{SA} = \frac{1}{Z} P_C + \frac{T_D}{\eta_e T_L} P_C$$

$$P_{SA} = \frac{1}{.97} P_C + \frac{36}{(.625)(58)} P_C$$

$$P_{SA} = 1.03 P_C + 0.994 P_C$$

When a two-step battery charge is used, the battery charging term $\frac{T_D}{\eta_e T_L} P_C$ must be increased by the factor $\frac{1}{UF}$, where UF is defined as the ratio of the time average power from the portion of the solar array required for battery charging to the maximum power provided for battery charging.

To determine UF, consider the relationships shown in Figure 8-2.

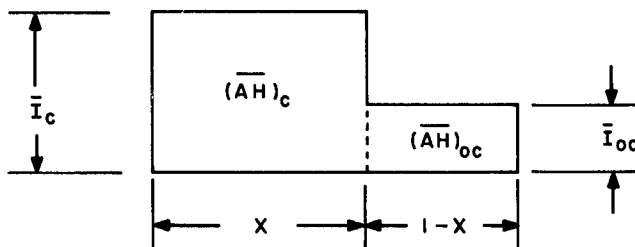


Figure 8-2. Two Step Battery Charging Cycle

Where:

- \bar{I}_C = Normalized charge current
- $= \frac{1}{CR}$
- CR = Charge rate in hours
- \bar{I}_{OC} = Normalized overcharge current
- = $1/6$ (for this application)
- $(\bar{AH})_C$ = Normalized ampere-hr charge
- $(\bar{AH})_{OC}$ = Normalized ampere-hr overcharge
- = $.25 (\bar{AH})_C$ (for this application)
- X = Fraction of light period required to return full charge to the battery

Therefore:

$$\begin{aligned}\bar{x}\bar{I}_C &= 4(1-X)\bar{I}_{OC} \\ \bar{x}\bar{I}_C &= 4(1-X)\left(\frac{1}{6}\right) \\ X &= \frac{1}{1 + \frac{3}{2}\bar{I}_C}\end{aligned}$$

and

$$UF = \frac{\bar{I}_C X + .25 \bar{I}_C X}{\bar{I}_C}$$

$$UF = 1.25X$$

Using a three-hour rate as the maximum charging rate:

$$\begin{aligned}\bar{I}_C &= \frac{1}{3} \\ X &= \frac{1}{1 + \left(\frac{3}{2}\right)\left(\frac{1}{3}\right)} = \frac{1}{1.5} = .667 \\ \frac{1}{UF} &= \frac{1}{1.25 (.667)} = 1.20 \\ \left(P_{SA}\right)_{2\text{-step}} &= 1.03 P_C + 0.994 \left(\frac{1}{UF}\right) P_C \\ &= 1.03 (.99) + 0.994 (1.20) (6.99) \\ &= 15.54 \text{ KW}\end{aligned}$$

The active solar cell area required is:

$$\text{Active Area} = \frac{15,540}{10.45} = 1490 \text{ ft}^2$$

The gross panel area required is:

$$\text{Gross Area} = \frac{1490}{.90} = 1655 \text{ ft}^2$$

The panel weight associated with this active area is:

$$\text{Weight} = 1490 (1.25) = 1860 \text{ lb.}$$

8.2.2 BATTERY SIZING

The battery is sized by the limitations on charging rate. The battery charging current is given by:

$$I_c = \frac{1}{V_c} \left(\frac{1}{U_F} \right) \frac{T_D}{\eta_{BCD} \eta_{ID} T_L} P_c$$

Where:

V_c = Average battery charge voltage
 η_{BCD} = Battery charge-discharge efficiency
 η_{ID} = Battery isolation diode efficiency

The voltage drop through an efficiency-designed switching diode regulator will be approximately 1 volt, and there will be about 0.6 volt drop through the battery blocking diode. At an end-of-discharge voltage of 1.1 volts per cell, 27 cells will be required.* The battery will use 28 cells (one additional for voltage margin). The following voltage range will result:

	CELL	BATTERY
Average discharge voltage	1.24 v	34.7 v
Average charge voltage	1.42 v	39.8 v
End-of-discharge voltage	1.1 v	30.8 v

These values are for batteries operating in the temperature range 60°F to 90°F.

*This end-of-discharge voltage is based on long term cycling tests conducted by General Electric Co-MSD. For a new cell the end-of-discharge voltage is approximately 1.2 volts.

Using the loss factors from Figure 8-1.

$$\frac{I}{C} = \left(\frac{1}{39.8} \right) (120) \frac{36(6,990)}{(.70)(.98)(58)}$$

$$\frac{I}{C} = 191 \text{ amp}$$

The battery capacity, in ampere-hours, is:

$$(AH)_C = (CR)(I_C)$$

$$(AH)_C = (3)(191) = 573 \text{ ampere-hours}$$

The battery energy capacity, in watt-hours, is:

$$(573)(34.7) = 19,900 \text{ watt-hrs.}$$

The battery weight is:

$$\frac{19,900}{11} = 1810 \text{ lbs.}$$

The depth-of-discharge for the case when the peak load does not occur during a dark period is $\frac{(6,820)}{(5,820)} \left(\frac{35}{60} \right) = .23$. The depth-of-discharge for the case when the peak load occurs during a dark period is $\frac{(573)(30.8)}{(573)(30.8)} \left(\frac{36}{60} \right) = .36$.

This is the worst condition. Since the maximum peak load occurs only once every 24 hours, the depth-of-discharge will exceed .23 only once every 24 hours and it will reach .36 only if the start of the peak load period coincides with the beginning of the dark period. A limited amount of data are available on the long time cycling life of nickel cadmium batteries. On the basis of Reference 4 information, 8,800 cycles at .23 depth of discharge and 5,500 cycles at .36 depth of discharge are considered reasonable battery lives for this study. Since all of the discharge cycles are not to .36, there should be no re-supply requirement for the one year mission (5,600 cycles).

8.2.3 POWER CONDITIONING EQUIPMENT

The following power conditioning equipment will be required in the photovoltaic system:

a. Voltage Regulator

This unit will utilize pulse-width modulation techniques and have an efficiency of 90 percent, a specific weight of 15 lb/kw, and provide ± 0.5 volt regulation of the output voltage.

b. Battery Charge Regulator

This unit will be a pulse-width modulated switch, but output filtering will not be required, since the battery itself acts as a large filter. Efficiency as high as 94 percent has been achieved by General Electric Company-MSD in flight-qualified hardware and a specific weight of 4 lb/KW is estimated.

c. Ampere-Hour Meter

This is required to sense the state-of-charge of the battery, and to control the battery charge current reference for the battery charge regulator. A weight of 5 pounds is estimated for this unit.

8.2.4 POWER SUPPLY HARNESS

A harness is required to collect the power from the solar array and distribute it within the power system. A specific weight for this harness, based on the flight hardware for the Advent Communication Satellite and other programs, is 13 lb/KW of solar array power.

8.2.5 POWER SYSTEM WEIGHT BREAKDOWN

Table 8-2 shows a tabulation of photovoltaic power supply weights along with other pertinent design parameters.

TABLE 8-2. DATA SUMMARY

Number of sections in power supply	4
Solar cell	N/P
Efficiency at 85°F, (air mass zero)	11.0%
Cover glass thickness	0.006 in.
Array weight per unit active area	1.164 lb/ft ²
Battery capacity per section	143 amp-hr
Battery type	Nickel-Cadmium
Solar array power per section	3,890 watts
Array power output per unit active cell area	10.45 w/ft ²
Net active cell area per section	373 ft ²
Gross solar array area per section	414 ft ²
Number of solar cells	365,000
TOTAL ARRAY WEIGHT	1,738 lbs
TOTAL BATTERY WEIGHT	1,810 lbs
Power conditioning equipment	75 lbs
Power supply harness	200 lbs
Battery cooling system	30 lbs
Additional structure (including panel tie-downs, structure to support array, deployment mechanism, structural support for batteries)	470 lbs
TOTAL POWER SUPPLY WEIGHT	4,323 lbs.

8.2.6 BATTERY COOLING

Heat is generated by the battery during all three phases of the cycle, (i.e., charge, overcharge, and discharge). The total heat generation can be estimated as follows:

During Charge

$$\begin{aligned} & (\text{number of cells}) (\text{Avg charge voltage} - \text{open circuit voltage}) \\ & (\text{charging current}) = (28) (1.42 - 1.34) (191) \\ & \quad = (28) (0.08) (191) \\ & \quad = 428 \text{ watts} \end{aligned}$$

During Overcharge

$$\begin{aligned} & (\text{number of cells}) (\text{Avg charge voltage}) \\ & (\text{overcharge current}) = (28) (1.42) \left(\frac{573}{6} \right) \\ & \quad = 3800 \text{ watts} \end{aligned}$$

During Discharge

$$\begin{aligned} & (\text{number of cells}) (\text{open circuit voltage} - \text{Avg discharge voltage}) (\text{discharge current}) \\ & = (28) (1.34 - 1.24) (201) \\ & \quad = 563 \text{ watts} \end{aligned}$$

If this is averaged over the entire charge, overcharge, and discharge cycle, the heat rejection rate is 1175 watts. Experience has shown that temperature has a strong effect on battery life. Therefore, the battery temperature will be maintained at 75°F by mounting the battery on a heat sink which is allowed to radiate to space through a temperature control shutter system.

8.3 DISCUSSION OF POWER SYSTEM

8.3.1 SOLAR PANEL CONSTRUCTION

The photovoltaic power system is divided into four independent sections. Each section is composed of 13 panels of solar cells arranged on a foldable platform as shown in Figure 8-3. There are twelve full size panels (11 modules) and one half size panel (11 half-modules) in each section.

8.3.2 PACKAGED POWER SYSTEM VOLUME

When stowed in the launch configuration, the solar platforms and associated deployment mechanism occupy a volume of 812 ft³. The battery volume is estimated as 11.6 ft³ based on a density of 156 lb/ft³. This includes the cells, internal connections, case, mounting brackets, and connectors. The volume of the power conditioning equipment is estimated as 2.4 ft³. Therefore, the total power system stowed volume is approximately 830 ft³.

8.3.3 AREA

The area of the vehicle surface which is required for the radiation cooling of the batteries has been estimated as 60 ft² based on a shutter effective emittance of 0.8, an

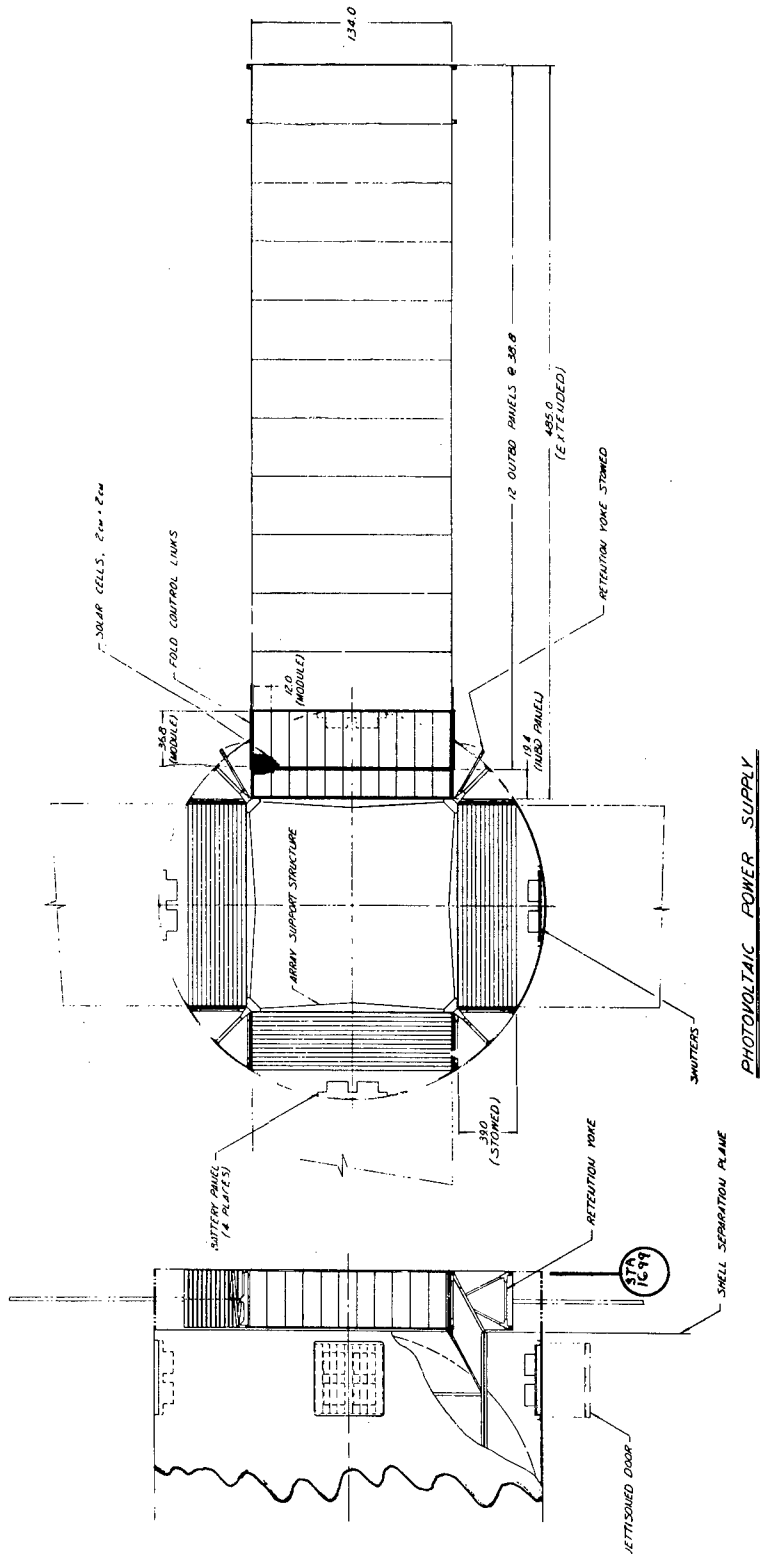


Figure 8-3. System Layout for Photovoltaic Power System

effective space sink temperature of 400°R, and an effective radiating temperature of 60°F. The deployed area of the solar array is 1655 ft².

8.3.4 ARRAY STOWAGE AND DEPLOYMENT

The array structure consists of a series of module mounting frames interconnected by hinges to permit folding for stowage during vehicle powered flight (see Figure 8-3). The method of stowage and deployment is similar to that used on the Pegasus Satellite.

Each frame consists of light sheet metal rectangular box sections which sustain the uniformly-distributed module loading. This loading is transferred frame-to-frame through hinge pins to the array support structure.

The array is maintained in the folded configuration by retention yokes which are fastened between the array support structure and the outermost array frame. Adjustment is provided in the yoke assemblies to permit preloading of the module frames against one another and against the array support structure.

Deployment is accomplished as follows:

1. Squib initiated separation bolts attaching the outer panel to the retention yokes are fired, freeing the folded array from the support structure. The yokes swing clear.
2. Torsion springs on the panel hinge pins power the panels to planar configuration, panel motion being constrained by the fold control links.
3. Residual spring torque maintains the array in the deployed position.

8.4 REFERENCES

1. MOL Electric Power Subsystem Study, Task C, Final Technical Documentary Report (U), Volume 1. Contract No. AF04(695)-639. AFSSD Report No. SSSD-TR-64-219. 15 October 1964. Prepared by Spacecraft Department, General Electric Company.
2. Cherry, W. R., "Solar Cells and the Applications Engineer" Astronautics and Aerospace Engineering, Vol I, No. 4, May 1963.
3. Solar Cell Specification Guide, RCA Direct Energy Conversion Department, July 1964.
4. Francis, Howard T., Space Battery Handbook, NASA Contract NASw-401, Armour Research Foundation, 10 West 35th Street, Chicago 16, Illinois, April 15, 1963.

APPENDIX A

ANALYSIS OF PEAK LOAD EFFECTS

A.1 SUMMARY AND CONCLUSIONS

In the design guidelines, the peak power requirement is stated as 9.0 KW_e for no more than a total of one hour in any twenty-four hour period, with the time between peak demands assumed to be at least five times the duration of the peak load. This requirement will be met by the storage of electrical energy in secondary Nickel-Cadmium batteries, with the result that an additional 0.24 KW_e will be required from the power system to charge the batteries.

A.2 DISCUSSION AND BACKGROUND INFORMATION

As originally defined, the peak power requirement was stated as follows: "The system is also designed to provide for peak power requirements of 150 percent of rated load (9KW) for as long as one hour per day". This statement is subject to several interpretations. It might be assumed that for one hour each day, the power requirement is 9 KW, giving the peak load a duty cycle of approximately 4 percent. If so, the peak load may occur at 24 hour intervals or it may occur at random during the 24 hour earth day with the result that back-to-back load periods could cause a two hour peak load period. Neither of these possibilities is considered likely since power profiles usually have peak requirements more or less randomly distributed as to the time of occurrence, duration, and magnitude. Peaks are caused by telemetry transmitters coming on when the satellite is within range of a tracking station; by programmed intermittent loads; by station keeping requirements such as attitude control and orbit maintenance demands; by startup requirements; and by faults in equipment. The combination of these requirements is not likely to result in a predictable periodic peak power requirement. Thus it was more realistic to restate the peak load requirements. The means of providing the peak load requirement was also investigated.

A.3 ANALYSIS

There are at least four methods of providing peak power requirements:

- a. Size the system for 9 KW, operate at 9 KW continuously and use a dissipative control for the difference between the load and 9 KW.
- b. Use an auxiliary battery storage system to take care of the peak requirements.
- c. Operate the dynamic systems over a range of power outputs using thermal energy storage to accomodate the changes in thermal requirements.
- d. Have a unit on standby and start it to take care of the peak requirements.

In analyzing these possibilities two do not appear feasible. Method (a) is impractical in that 50% excess capacity 96% of the time imposes too severe a penalty unless a standby system is required for reliability. Some means should be found to use the excess power, and the load then becomes 9 KW which is not intended in the study. Method (d) is impractical in that the time required to start a standby unit appears to be too long to accommodate the random and rapid transients that will surely occur. This scheme works if the peak loads occur for significant periods of time on a relatively regular basis. Thus two possibilities remain to be investigated.

Secondary batteries provide a convenient method for supplying peak loads and are particularly useful for short transients in that their response time can be very short. In this application the battery will have to provide an extreme of 3 KW-hrs. in a twenty-four hour period and there will be at least 23 hours for recharge. A depth of discharge of 50% can be tolerated under these conditions so that 6 KW-hours of battery capacity are required. At 10 watt-hours per pound the weight penalty is 600 pounds. A low rate of charge will replace the energy removed, i.e., 50 percent of the battery capacity in 23 hours or a 46 hour rate. At least 100% overcharge will be required under these conditions or at least a 23 hour charging rate. For this rate the power system must provide 6/25 or .24KW on a continuous basis (taking into account the extra power system capability during the peak load period). Since there will surely be auxiliary batteries on board for startup, extreme emergencies, etc., it is likely the battery package on board can serve a dual function so that the weight penalty may be shared with other requirements.

APPENDIX B

SOLAR COLLECTOR DESIGN

B.1 INTRODUCTION

The heat energy for the solar dynamic power systems considered in this study (Solar Mercury Rankine, Solar Stirling and Solar Brayton) is supplied by a solar collector/absorber combination. In order to size the solar collector for each of these power systems, it was necessary to generate mirror/aperture performance data. Mirror/aperture data provided by NASA-Lewis were used to establish the basic mirror characteristics and performance was calculated for the range of variables expected to be encountered in the study. Some additional background information is included in this Appendix which lists the characteristics used in this study. The performance is considered to be that which can be achieved with single piece mirrors and the ground rules of this study.

B.2 DESIGN VALUES

For this study the following design values have been specified:

$$\text{Mirror rim angle} = 55^{\circ}$$

$$\text{Reflectivity} = .90$$

$$\text{Weight per unit of projected area} = 1 \text{ lb}/\text{ft}^2 \text{ (equivalent to } .935 \text{ lb } / \text{ft}^2 \text{ of surface area).}$$

Performance was given for a mirror 30 feet in diameter. For study purposes it was assumed that mirror characteristics are not a function of size. Accurate orientation with respect to the sun (a time average misorientation of 0.1° or 6 minutes based on the absolute value of the orientation error) was assumed. Mirror performance is tabulated in Table B-1 for a number of conditions. Inspection of the data shows that the mirror performance in the range of interest for each system does not change significantly with temperature and orientation so linear interpolation of the available data was sufficiently accurate for study purposes. Table B-2 is a tabulation of selected aperture diameters for various cavity temperatures and 6% of the mirror area shadowed.

B.3 BACKGROUND AND ANALYSIS

The purpose of the mirror is, of course, to reflect the sun's rays to a focus where they can be admitted to a cavity and absorbed in its walls, so the energy can be utilized to heat a working fluid to the required temperature. Nomenclature for the parabolic mirror/aperture system is given in Figure B-1.

Equations relating mirror parameters

$$X = y^2/4F \quad (\text{Equation of Surface}) \quad (1)$$

$$\frac{D_c}{F} = \frac{4 \sin \phi_r}{1 + \cos \phi_r} \quad (2)$$

$$\frac{R_r}{D_c} = \frac{1}{2 \sin \phi_r} \quad (3)$$

$$\frac{R_r}{F} = 1 + \frac{1}{16} \left(\frac{D_c}{F} \right)^2 \quad (4)$$

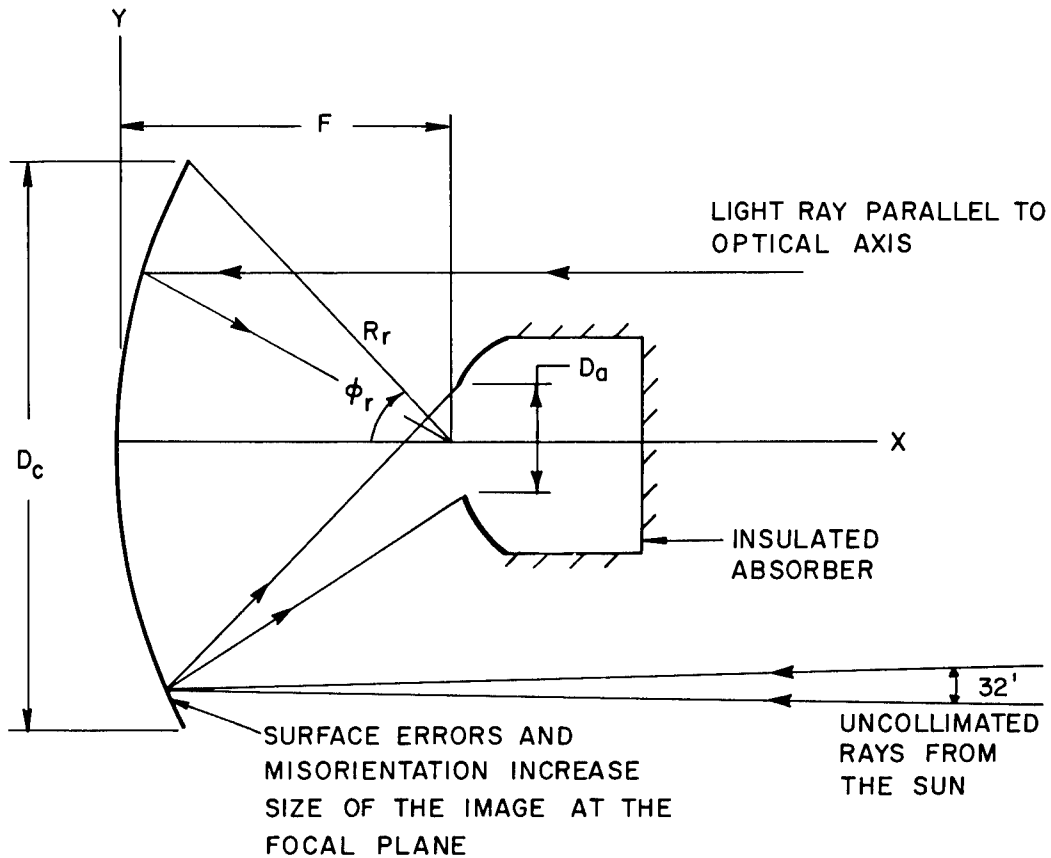


Figure B-1. Mirror/Aperture Nomenclature

In selecting an aperture diameter for a mirror a first consideration is the relation between the size of the aperture and the amount of solar power that passes through the opening. The sun is not a point source so that each element of the mirror surface reflects a cone of light rather than a single ray. The thermal power distribution across the surface of the sun is not uniform so the distribution of power in the cone of light is not uniform. Misorientation of the complete mirror and surface irregularities in the mirror further distort the location and distribution of power. Finally the mirror is not a perfect reflector so that less energy is reflected than is incident upon the mirror. Expressing in equations:

$$\begin{aligned} \text{Total Thermal Power Intercepted by Mirror (TTP)} &= \text{Solar Constant} \times \text{Area} \quad (5) \\ (\text{TTP}) &= 130\left(\frac{\pi}{4}D_c^2\right) \text{ Watt} \end{aligned}$$

To determine the Gross Power through the Aperture, the Total Thermal Power is multiplied by the reflectivity of the mirror surface (.90 is being used for this study), the fraction of the reflected power that passes through the aperture which is a function of aperture diameter, misorientation and surface accuracy, and the fraction of the surface area not shadowed by the receiver and other structure.

$$(GPA) = (TTP) (\eta_R) (\eta_c) (\eta_s) \quad (6)$$

η_R = reflectivity of mirror surface (.90)

η_c = aperture collection efficiency (a function of aperture diameter, misorientation, and surface accuracy)

η_s = fraction of total area not shadowed.

The product η_R and η_c , denoted as Gross Mirror Efficiency, represents the basic performance of the mirror and is plotted in Figure B-2, as derived from the data provided by NASA-Lewis.

The Gross Power through the Aperture is not all available for use because of losses from the absorber. It is convenient to consider them in two parts-- one being the reradiation and reflection back through the aperture and the other being the remaining losses (the largest of which is the loss through the insulated absorber walls). The re-radiation plus reflection loss is nearly proportional to aperture area and enters into the selection of aperture size. The remaining losses are charged to the absorber and are not a part of the mirror/aperture problem as defined here.

The absorber cavity is assumed to radiate as a black body from the aperture. This assumption is the usual one and test results on General Electric Company programs for solar thermionic systems have shown that the black body assumption is a good approximation for the re-radiation plus reflection loss. With this assumption the losses from the aperture are given by

$$\text{Aperture Loss} = (RR) = \left(\frac{\pi}{4}\right) \sigma T^4 (D_a)^2 \quad (7)$$

σ = Stefan Boltzman Constant

T = Absolute Temperature

Subtracting the Aperture Loss from the Gross Power through the Aperture, Equation (6) gives the Net Power through the Aperture.

$$\begin{aligned} \text{Net Power through the Aperture} &= (NPA) = (GPA) - (RR) \\ &= (TTP) \eta_R \eta_c \eta_s - \sigma T^4 \frac{\pi}{4} (D_a)^2 \end{aligned} \quad (8)$$

Dividing Equation (8) through by (TTP) and denoting the quotient as the Overall Collection Efficiency,

$$\begin{aligned} \text{Overall Collection Efficiency} &= (OCE) = \frac{(NPA)}{(TTP)} \\ &= \eta_s \eta_R \eta_c - \frac{\sigma T^4 D_a^2}{130 D_c^2} \end{aligned}$$

Using the Gross Mirror Efficiency (GME) plotted in Figure B-2 (OCE), can be evaluated as a function of D_a/D_c with shadow area and cavity temperature as parameters to determine the optimum aperture size. This data is tabulated in Table B-1.

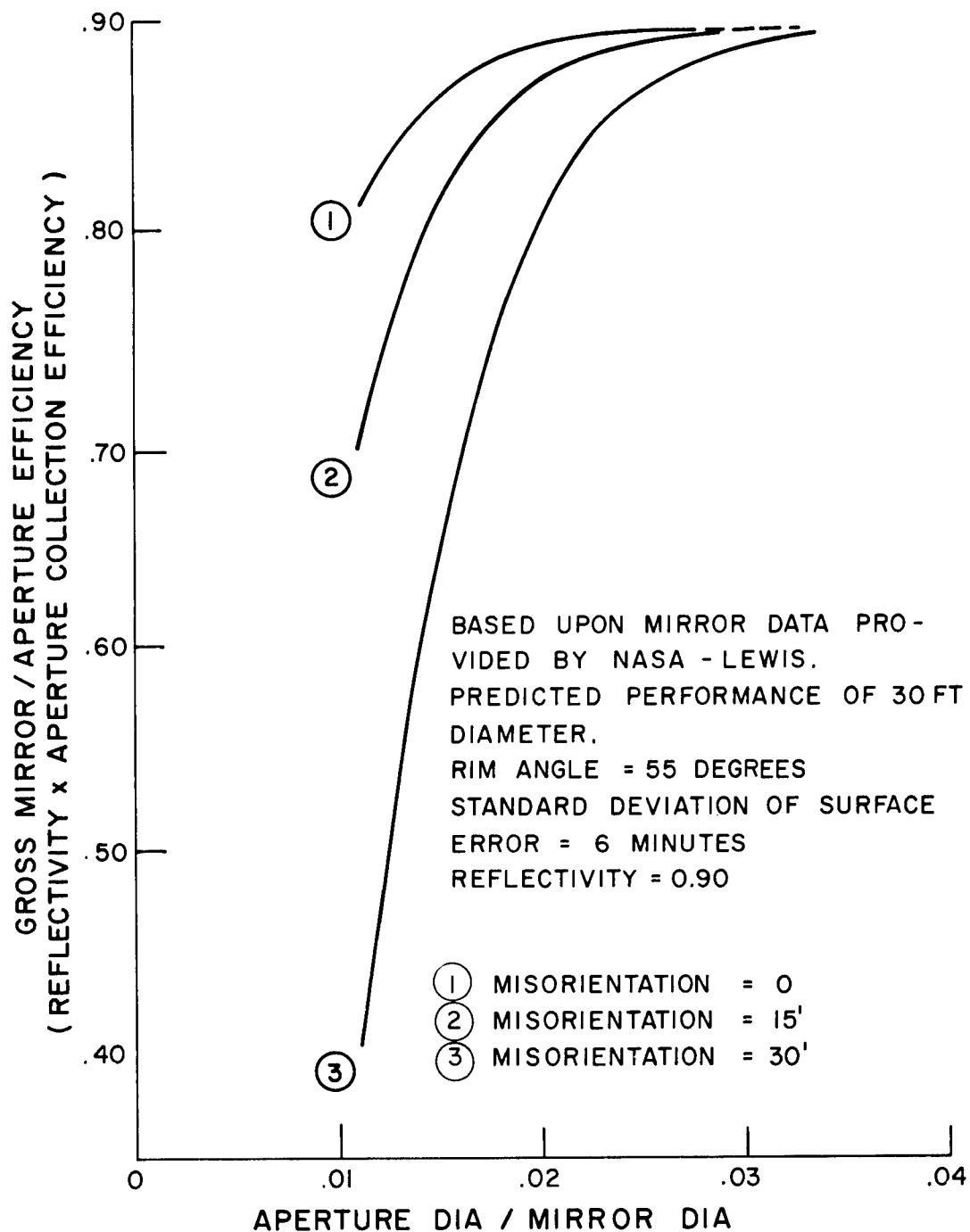


Figure B-2. Performance of Solar Collector and Absorber

TABLE B-1. OVERALL COLLECTION EFFICIENCY (OCE) OF
MIRROR APERTURE ASSEMBLY SHADOW AREA - 6%

D_a^*	D_a/D_c	T = 0°R			T = 1710°R**			T = 1760°R			T = 1810°R			
		Misorientation	0	15'	30'	0	15'	30'	0	15'	30'	0	15'	30'
4.0	.0111	.762	.654	.374	.758	.650	.370	.757	.650	.370	.757	.649	.369	
4.5	.0125	.788	.709	.475	.783	.704	.470	.783	.703	.469	.782	.703	.469	
5.0	.0139	.805	.746	.556	.799	.740	.550	.798	.739	.550	.797	.738	.548	
5.5	.0153	.816	.771	.622	.808	.763	.614	.807	.760	.613	.806	.761	.612	
6.0	.0167	.822	.791	.673	.813	.782	.664	.812	.781	.663	.811	.780	.662	
6.5	.0181	.829	.807	.713	.818	.796	.702	.817	.794	.700	.815	.793	.699	
7.0	.0194	.832	.816	.744	.820	.804	.732	.819	.803	.731	.817	.801	.729	
7.5	.0208	.834	.824	.771	.820	.810	.757	.819	.808	.755	.816	.806	.753	
8.0	.0222	.835	.826	.790	.819	.811	.774	.817	.808	.771	.814	.806	.770	
8.5	.0236													
9.0	.0250													
9.5	.0264													
10.0	.0278													
10.5	.0292													
11.0	.0306													
11.5	.0319													
12.0	.0333													

D_a/D_c	T = 2010°R			T = 2060°R			T = 2110°R						
	Misorientation	0	15'	30'	0	15'	Misorientation	0	15'	30'			
.0111	.754	.646	.366	.753	.646	.366	.753	.645	.365				
.0125	.778	.699	.465	.778	.698	.464	.776	.697	.463				
.0139	.793	.734	.544	.792	.733	.543	.791	.732	.542				
.0153	.801	.756	.607	.800	.755	.604	.780	.753	.604				
.0167	.805	.774	.656	.803	.772	.654	.801	.770	.652				
.0181	.808	.786	.692	.806	.784	.690	.804	.782	.688				
.0194	.808	.793	.721	.806	.790	.719	.804	.788	.716				
.0208	.807	.797	.744	.804	.794	.741	.801	.791	.738				
.0222	.804	.795	.759	.801	.792	.756	.798	.789	.753				
.0236	.800	.794	.765	.798	.791	.762	.793	.787	.758				
.0250	.796	.791	.770	.794	.787	.766	.787	.783	.762				
.0264	.791	.789	.772	.789	.785	.768	.782	.780	.763				
.0278	.787	.786	.744	.785	.781	.769	.776	.775	.763				
.0292													
.0306													
.0319													
.0333													

*Aperture diameter in inches for

a 30 ft. collector

** From curves provided by NASA-Lewis.

NOTE: underlined values are maximum values.

TABLE S-2. TABULATION OF OVERALL COLLECTION EFFICIENCY (OCE) FOR SELECTED APERTURE DIAMETERS

Note: Aperture dimensions are based upon a thirty foot diameter mirror.

Performance is tabulated as Aperture Diameter in Inches. The first two OCE

rows for each temperature list the optimum aperture diameter and the corresponding OCE. The second two rows are the selected aperture diameter and the corresponding OCE.

CAVITY TEMPERATURE	6% Shadow Factor Misorientation		
	0'	15'	30'
1710R (1250F)	<u>7.5"</u>	<u>8.0"</u>	<u>11.0"</u>
	.820	.811	.800
	<u>8.5"</u>	<u>8.5"</u>	<u>8.5"</u>
	.819	.810	.782
1760R (1300F)	<u>7.0"</u>	<u>8.5"</u>	<u>11.0"</u>
	.819	.809	.796
	<u>8.5"</u>	<u>8.5"</u>	<u>8.5"</u>
	.816	.809	.780
1810R (1350F)	<u>7.0"</u>	<u>8.5"</u>	<u>11.0"</u>
	.817	.806	.792
	<u>8.5"</u>	<u>8.5"</u>	<u>8.5"</u>
	.812	.806	.777
2010R (1550F)	<u>7.0"</u>	<u>7.5"</u>	<u>10.0"</u>
	.809	.797	.774
	<u>7.5"</u>	<u>7.5"</u>	<u>7.5"</u>
	.807	.797	.744
2060R (1600F)	<u>7.0"</u>	<u>7.5"</u>	<u>10.0"</u>
	.806	.795	.769
	<u>7.5"</u>	<u>7.5"</u>	<u>7.5"</u>
	.804	.795	.741
2110R (1650F)	<u>6.5"</u>	<u>7.5"</u>	<u>10.0"</u>
	.804	.791	.763
	<u>7.5"</u>	<u>7.5"</u>	<u>7.5"</u>
	.801	.791	.738

APPENDIX C

RADIATOR, ABSORBER AND HEAT EXCHANGER DESIGN

C.1 RADIATOR DESIGN

C.1.1 BASIC DESIGN CRITERIA

Two basic design criteria have been established for all of the radiator designs developed in this study:

1. Micrometeoroid Damage -

a. Micrometeoroid Particle Flux

$$N(M) = \alpha M^{-\beta}$$

where $N(M)$ = number of particles impacting per unit area per unit time of mass M and larger

$$\alpha = 5.3 \times 10^{-11} \text{ particles/ft}^2 \cdot \text{day} \text{ (Ref 1)}$$

$$\beta = 1.34$$

b. Lifetime Considerations

Probability of survival = 0.99

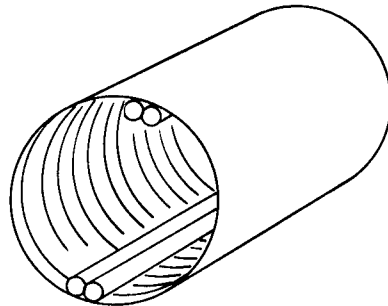
Life = 1 year at above probability level.

2. Effective Sink Temperature = 400°R (Per direction from NASA-Lewis)

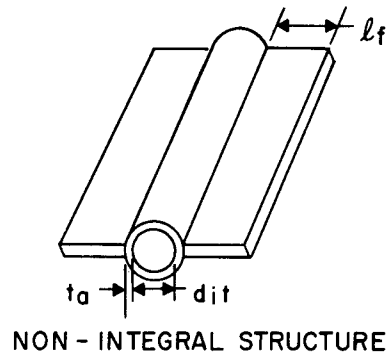
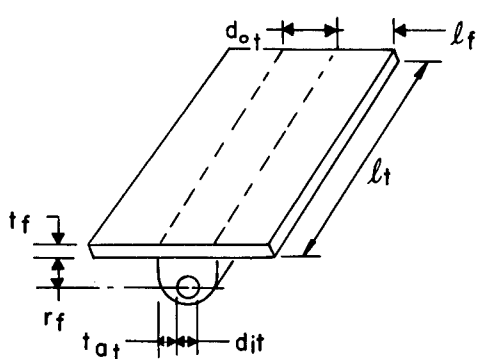
NOTE: The effective sink temperature is of particular significance only for the low temperature radiator designs.

C.1.2 CONFIGURATION

The basic radiator configuration analyzed is shown below:



Two tube configurations were analyzed:



INTEGRAL STRUCTURE

The major advantage to the arrangement shown for the integral structure is in the fact that the fin provides a significant portion of the tube armor. This effect will be discussed more fully in the analytical description.

The heat balance on a radiator tube element is as follows:

$$Q_{\text{net}} = F_{t-s} \epsilon \sigma (T_{t_{\text{eff}}}^4 - T_s^4) d_{ot} \ell_t + 4F_{f-s} \eta_f \epsilon \sigma (T_{t_{\text{eff}}}^4 - T_s^4) \quad (1.1)$$

where F = configuration factor

d = tube diameter

ℓ = tube length

Q_{net} = net heat rate

T = absolute temperature

ϵ = emittance

η_f = fin efficiency

Subscripts:

t = tube

f = fin

s = sink

eff = effective

Since the radiator is basically a light weight structure in terms of heat capacity, the radiator size was determined by the steady state accommodation of peak heat load.

The effective fin root temperature ($T_{t_{\text{eff}}}$) is derived as follows:

For an increment of tube length we can write:

$$-W C_p d(T_b) = \pi d_{ot} \epsilon \sigma T_t^4 dx \quad (1.2)$$

where W = weight flow rate

C_p = specific heat of fluid

T_b = fluid bulk temperature

T_t = fin root temperature

T_b can be expressed in terms of T_t as follows:

$$T_b = T_t + \left(\frac{d_{ot} \epsilon \sigma}{h d_{it}} \right) T_t^4 = T_t + K_1 T_t^4$$

so

$$d(T_b) = (1 + 4 K_1 T_t^3) dT_t$$

and

$$-W C_p (1 + 4 K_1 T_t^3) dT_t = \pi d_{ot} \epsilon \sigma T_t^4 dx = K_2 W C_p T_t^4 dx$$

Integrating:

$$\frac{1}{3} \left[\frac{1}{T_{to}^3} - \frac{1}{T_{ti}^3} \right] - 4K_1 \ln \left(\frac{T_{to}}{T_{ti}} \right) = K_2 \ell_t$$

where: o = outlet condition

i = inlet condition

The above expression can be rewritten as:

$$\frac{1}{3} \left[\frac{1}{T_{to}^3} - \frac{1}{T_{ti}^3} \right] \approx K_2 \ell_t \quad (1.3)$$

Equation (1.3) is equivalent to assuming that the film drop is essentially constant, in which case

$$W C_p (T_{bi} - T_{bo}) \approx W C_p (T_{ti} - T_{to}) \approx \pi d_{ot} \epsilon \sigma T_{t_{eff}}^4 \ell_t$$

so

$$T_{t_{eff}}^4 = \frac{3 T_{ti}^3 T_{to}^3}{T_{ti}^2 + T_{ti} T_{to} + T_{to}^2} \quad (1.4)$$

where $T_{t_{eff}}$ = effective radiator tube temperature

A derivation of fin efficiency is provided in references 2 and 3.

To obtain the temperature drop at the inlet and outlet of the radiator in order to calculate the fin temperature from the bulk temperature we make use of the following expression:

$$\Delta T_j = \left[\frac{Q_{net}}{h \pi d_{it} \ell_t} + \frac{Q_{net}}{2\pi \ell_t k} \ln \left(\frac{d_{it} + 2 t_{at}}{d_{it}} \right) \right] \left[\frac{T_{tj}^4 - T_s^4}{T_{t_{eff}}^4 - T_s^4} \right] \quad (1.5)$$

where k = tube material thermal conductivity
 j denotes either inlet or outlet condition
 h = film coefficient

Specifying all of the radiator parameters excepting tube length (ℓ_t) equation 1.1 can be solved to yield the tube length required.

The work done by Loeffler, Ref. 4, provides the basis for determining the required tube armor thickness. The design criteria to be used is derived in the aforementioned references.

$$t_a = 1.75 \gamma \left(\frac{\rho_m}{\rho_a} \right)^\phi \left(\frac{v}{c} \right)^\theta \left(\frac{6}{\pi \rho_m} \right)^{\frac{1}{3}} \left[\frac{\alpha A_v t}{-\ell_n P_o} \right]^{\frac{1}{3\beta}} \left(\frac{2}{3\eta \theta \beta + 2} \right)^{\frac{1}{3\beta}}$$

where A_v = vulnerable area

P_o = probability of radiator not being punctured

v = average meteoroid particle velocity

c = velocity of sound in armor material

ρ_m = meteoroid average density

ρ_a = armor density

t = mission duration time

$\alpha = 5.30 \times 10^{-11}$

$\theta = 2/3$

$\beta = 1.34$

$\phi = 1/2$

The quantity r_f is simply: $r_f = \frac{d_{it}}{2} + t_a - t_f$

The derivation of the quantity t_{at} is provided in reference 5.

C.1.3 OPTIMIZATION PROCEDURE

To design a radiator all of the specified parameters are individually varied by specified increments using a digital computer until a minimum weight system is obtained. The parameters commonly chosen to be optimized are:

1. Number of tubes
2. Tube inside diameter
3. Fin thickness
4. Temperature drop through radiator

C.1.4 RESULTS

Tables C-1 through C-5 summarize the computer analyses made for the cycles. Tables C-1 and C-2 present the characteristics of the Brayton cycle radiator. This radiator employs Argon as the heat transfer medium. The term integral or non-integral structure refers to whether or not the radiator is integral with the MORL vehicle. In the case of the integral structure the reported weight does not include the weight associated with the structural requirements of the MORL shell. Tables C-3 and C-4 give the design data for the Stirling cycle radiator. Table C-5 gives a summary for the Rankine cycle radiator. In all the cases the headers were sized so as to keep the pressure drop in the headers to less than 10 percent of the tube pressure drop.

Nomenclature

Q_r	=	heat radiated	NT	=	no. of tubes
T	=	fluid temperature	d_{it}	=	tube I. D.
ΔP	=	pressure drop	r_f	=	see Table C-1.
NP	=	no. of passes	t_a	=	see Table C-1.
WGT	=	radiator weight	t_{at}	=	see Table C-1.
H	=	header length			
LT	=	tube length			
TF	=	fin thickness			

TABLE C-1. BRAYTON CYCLE - INTEGRAL RADIATOR STRUCTURE

Q_r	T _{in}	T _{out}	ΔT	ΔP	NP	WGT 1bs.	Area ft ²	H ft.	LT ft.	TF in.	NT in.	d _{it} in.	r _f in.	t _a in.	t _{at} in.
KW	°F	°F	°F	psi											
16	366	76	290	.1	4	1013	610	10.2	14.6	.058	36	1.07	.798	.321	.101
12						711	418	7.7	13.3	.052		.98	.742	.304	.101
8						419	276	6.5	10.4	.049	↓	.81	.630	.274	.088
16				.2		871	518	8.2	15.5	.055	36	.97	.742	.314	.103
12					↓	595	398	7.7	12.7	.049	↓	.84	.662	.294	.099
8					↓	354	261	6.4	10.0	.043	↓	.70	.571	.264	.093
16				.3		835	497	6.2	18.75	.055	24	1.07	.786	.300	.105
12					↓	562	379	5.6	16.71	.049	↓	.95	.711	.285	.095
8					↓	327	261	5.1	12.63	.040	↓	.78	.607	.256	.094
16						1141	593	10.7	13.5	.061	48	1.05	.799	.335	.105
12						779	444	9.6	11.3	.055	↓	.91	.711	.311	.101
8						469	306	7.2	10.4	.049	36	.88	.668	.279	.091
16				.2		988	635	10.5	14.8	.049	36	1.04	.790	.319	.119
12					↓	675	427	8.0	13.1	.052	↓	.92	.704	.298	.098
8					↓	399	285	6.9	10.1	.046	↓	.76	.604	.270	.091
16				.3		895	559	8.9	15.4	.052	36	.96	.742	.314	.109
12					↓	615	415	7.9	12.9	.049	↓	.84	.663	.292	.100
8					↓	360	276	6.8	9.9	.043	↓	.69	.566	.264	.093

TABLE C-1. BRAYTON CYCLE - INTEGRAL RADIATOR STRUCTURE (Cont'd.)

Q_r	T_{in}	T_{out}	ΔT	ΔP	NP	WGT lbs.	Area ft ²	H ft.	LT ft.	TF in.	NT in.	d_{lt} in.	r_f in.	t_a in.	t_{at} in.
KW	°F	°F	°F	psi											
16	415	76	339	.23	4	765	485	8	14.9	.052	36	.88	.694	.306	.103
12						540	360	7	12.7	.049	36	.79	.633	.286	.096
8						340	230	6	9.5	.040	24	.67	.548	.253	.092
16						660	455	8	14.6	--	36	--	--	--	--
12						450	340	7	12.2	.043	36	.66	.563	.276	.101
8						262	225	6	9.3	.040	36	.54	.478	.248	.088
16						593	432	7.5	14.4	.046	36	.69	.589	.290	.105
12						405	325	6.6	12.1	.046	36	.60	.527	.270	.097
8						241	220	6.0	9.1	.037	36	.50	.456	.243	.092

TABLE C-2. BRAYTON CYCLE - NON-INTEGRAL RADIATOR STRUCTURE

Q_r	T_{in}	T_{out}	ΔT	ΔP	NP	WGT	Area	H	LT	TF	NT	d_{it}	r_f	t_a	t_{at}
KW	$^{\circ}F$	$^{\circ}F$	$^{\circ}F$	psi	lbs.	ft ²	ft.	ft.	in.	in.	in.	in.	in.	in.	in.
24	416	76	340	.32	4	1441	536	11.5	11.2	.034	48	1.025		.393	
20							1145	452	10.9	9.97	.031	48	.941	N/A	.377
16							866	367	10.3	8.55	.031	48	.848		.356
12	376	76	300	.2		685	295	7.9	8.99	.028	36	.965	N/A	.339	N/A
10						548	251	7.6	7.92	.028	36	.89		.324	

TABLE C-3. STIRLING CYCLE - INTEGRAL RADIATOR STRUCTURE

Q_r	T_{in}	T_{out}	ΔT	ΔP	NP	WGT	Area	H	LT	TF	NT	d_{it}	r_f	t_a	t_{at}
KW	$^{\circ}F$	$^{\circ}F$	$^{\circ}F$	psi	lbs.	ft ²	ft.	ft.	in.	in.	in.	in.	in.	in.	in.
25	155	135	20	13.5	2	510	691	9.0	38.3	.030	20	.235	.349	.262	.125
					13.7	504	680	9.5	35.5	.030	22	.223	.343	.262	.125
					13.7	500	671	10.0	33.5	.030	24	.214	.340	.262	.126
20		13.5	387	526	7.0	37.5	.029	18	.223	.332	.250	.119			
		13.1	382	543	7.5	36.1	.028	18	.223	.332	.248	.120			
		13.3	377	535	8.0	33.3	.028	20	.210	.326	.248	.121			
15		13.3	267	404	5.5	36.6	.026	14	.220	.315	.231	.112			
		11.9	266	419	6.0	34.8	.026	14	.223	.314	.228	.110			
15															

TABLE C-4. STIRLING CYCLE - NON-INTEGRAL STRUCTURE

TABLE C-5. RANKINE CYCLE - INTEGRAL RADIATOR STRUCTURE

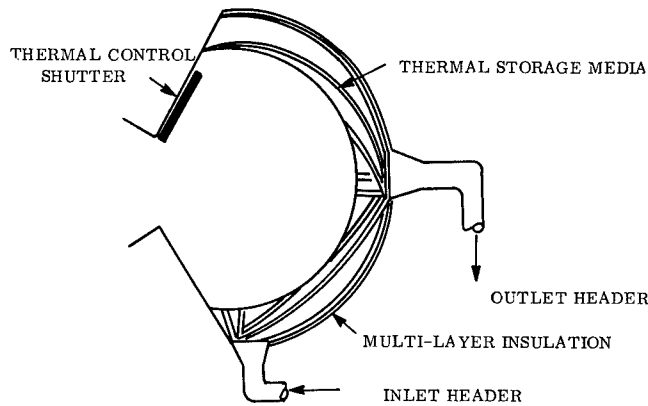
Q_r	T_{in}	T_{out}	ΔT	ΔP	NP	WGT	Area	H	LT	TF	NT	d_{it}^*	r_f	t_a	t_{at}
KW	$^{\circ}F$	$^{\circ}F$	$^{\circ}F$	psi		lbs.	ft ²	ft.	ft.	in.	in.	in.	in.	in.	in.
50	605	605	0	21.9	2	118	148	3	24.6	.021	12		.326	.126	.10
40					13.7	93	118			.021	12		.319	.119	.10
30						69	88			.021	12		.311	.111	.10

*Tapered from .58 inch (inlet) to .224 inch (outlet)

C. 2 ABSORBER DESIGN

C. 2.1 CONFIGURATION

The configuration assumed for all of the solar absorbers analyzed is shown below.



The tubes carrying the primary heat transfer fluid are wrapped inside of a hemispherical shell forming the absorber surface of the cavity receiver. During the insolated portion of the orbit, sunlight focused in the cavity is used directly in providing the heat requirements to the primary fluid. The heat required during the eclipse portion of the orbit is stored as latent heat of fusion. During eclipse an insulated door closes the cavity opening and the primary fluid draws its heat from the solidifying thermal storage media. The assumed thermal properties of the heat storage materials are summarized below.

Material	Thermal Conductivity Btu /hr-ft-°F	Latent Heat of Fusion Btu/lb.	Density at Melting Temp. lb./ft ³
Lithium Hydride	2.5	1125	41.0 (1256°F)
Lithium Fluoride	1.5	450	111.5 (1550°F)

C. 2.2 ANALYTICAL MODEL

The rate of heat transfer into the primary fluid is:

$$Q = N_t UA \Delta T_{lmtd} \quad (2.1)$$

where A = effective heat transfer area per tube

ΔT_{lmtd} = log mean temperature difference

$$= \frac{\Delta T_i - \Delta T_o}{\ln \Delta T_i / \Delta T_o}$$

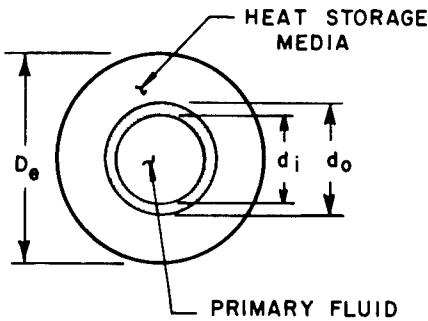
ΔT_i = temperature difference at tube inlet

ΔT_o = temperature difference at tube outlet

N_t = number of tubes

U = overall film coefficient

Each tube is considered to have an effective cylindrical element of heat storage material surrounding it.



Using this assumption the overall conductance is taken as:

$$UA = \left(\frac{1}{\pi h d_i l} + \frac{\ln D_e / d_o}{2\pi k_2 l} \right)^{-1} \quad (2.2)$$

where h = film coefficient

k_2 = thermal conductivity of heat storage material

l = length

For turbulent flow, the film coefficient was obtained from either of two relations:

Liquid metals - $\frac{hd_i}{k_1} = 0.625 (N_{Re} \cdot (N_{Pr})^{0.4})$

Gases - $\frac{hd_i}{k_1} = 0.23 (N_{Re})^{0.8} (N_{Pr})^{0.4}$

Where N_{Re} and N_{Pr} are the Reynolds and Prandtl numbers, respectively. Combining equations 2.1 and 2.2 the length per tube can be calculated

$$l = \frac{Q \left(\frac{1}{h d_i} + \frac{\ln D_e / d_o}{2k_2} \right)}{N_t \pi \Delta T \cdot \text{lmtd}} \quad (2.3)$$

Two simplifying assumptions have been made: the transient movement of the interface between the liquid and solid portion of heat storage material has been neglected since the limiting condition is when the heat storage material has almost completely solidified (Ref. 6) and the thermal resistance of the heat storage material is based on the full equivalent thickness of the material (Ref. 7).

The minimum heat storage volume required is

$$V = \frac{Q \cdot T_s}{\lambda \rho_m}$$

where Q = heat removal rate

T_s = shadow time (36 minutes maximum)

λ = latent heat of fusion

ρ_m = density of heat storage material

The effective diameter of the heat storage material is taken as:

$$D_e = \sqrt{\frac{4V}{\pi \ell N_t} + d_o^2}$$

so equation (2.3) can be written as:

$$\ell = \frac{Q \left(\frac{1}{h_{di}} + \frac{\left[\frac{4V}{\pi \ell N_t} + d_o^2 \right]^{1/2}}{2k_2} / d_o \right)}{N_t \pi \Delta T_{lmtd}} \quad (2.4)$$

$$= f(\ell, d_i)$$

This equation has been solved iteratively for ℓ for a given d_i and a fixed tube wall thickness.

C. 2.3 OPTIMIZATION PROCEDURE

The major design requirement for the absorber is minimum weight. Four items were accounted for in optimizing the weight estimate: (1) Primary fluid piping weight; (2) Primary fluid weight; (3) Heat storage material shell; (4) Primary fluid pump work weight penalty. These were determined as follows:

Primary Fluid Piping Weight (Wpt)

$$W_{pt} = N_t \rho_{pt} \frac{\pi (d_o^2 - d_i^2) \ell}{4} \quad (2.5)$$

where ρ_{pt} = density of primary tubing

Primary Fluid Weight (Wpf)

$$W_{pf} = N_t \rho_{pf} \frac{\pi d_i^2 \ell}{4} \quad (2.6)$$

where ρ_{pf} = density of primary fluid

Heat Storage Material Shell

For a set upper limit on the maximum heat flux (q), the inner cavity radius is simply

$$R_i = \sqrt{\frac{Q}{2\pi q}} \quad (2.7)$$

The outer radius of the shell, in terms of the equivalent diameter

D_e is:

$$R_o = \sqrt[3]{\frac{3}{8} N_t \ell D_e^2 + R_i^3} \quad (2.8)$$

The shell weight is then:

$$W_{si} = \rho_{si} 2\pi R_i^2 t_{si} \quad \text{inside shell} \quad (2.9a)$$

$$W_{so} = \rho_{so} 2\pi R_o^2 t_{so} \quad \text{outside shell} \quad (2.9b)$$

where s_o = outside shell

s_i = inside shell

t = wall thickness

Primary Fluid Pump Work

A general expression for the pressure drop experienced by a compressible fluid can be derived as follows:

The momentum equation may be written as:

$$-\frac{dp}{g_c d A^2} = \frac{2f \rho v^2}{g_c d A^2} + \frac{\rho v dv}{g_c} \quad (2.10)$$

where A = flow area

d = tube inside diameter

f = Fanning friction factor

Δp = pressure drop

v = velocity

dx = incremental length along tube

W = weight flow rate

g_c = gravitational constant

From the continuity equation we can write

$$\rho v = W/A \quad (2.11)$$

resulting in

$$-\frac{dp}{g_c} = \frac{2f}{d} \frac{p}{\rho} \left(\frac{W}{A} \right)^2 dx + \frac{W}{A g_c} pdv$$

If we assume the perfect gas law $p = \rho RT$, then the above equation can be integrated, noting that $dv = (\frac{W}{A}) d(\frac{1}{\rho})$ to give:

$$\frac{1}{2} (\rho_1^2 - \rho_0^2) = \frac{2f}{d g_c} \left(\frac{W}{A} \right)^2 R T \ell + \left(\frac{W}{A} \right)^2 \frac{\int_{\rho_1}^{\rho_0} p d(\frac{1}{\rho})}{g_c} \quad (2.12)$$

Integrating the last term by parts and setting $\bar{\rho} = 1/2 (\rho_1 + \rho_0)$

we obtain:

$$\Delta p = \frac{1}{g_c \bar{\rho}} \left(\frac{W}{A} \right)^2 \left[\frac{2f \ell}{d} + \frac{T_o - T_i}{T} + \ln \frac{P_i}{P_o} \right] \quad (2.13)$$

where the bar denotes an average condition

o = outlet condition

i = inlet condition

The friction factor for turbulent flow is taken as the smooth pipe relation.

$$f = \frac{0.023}{(NRe) 0.2} \quad (2.14)$$

The ideal pumping power required to circulate the primary fluid through the absorber is simply the change in enthalpy across the pump. For an adiabatic compression, and small pressure drop, the pump work is:

$$P = \frac{W \Delta P}{\rho_i} \quad (2.15)$$

The pump work weight penalty is then:

$$W_{pp} = \frac{K_p P}{\eta_p \eta_m} \quad (2.16)$$

where K_p = lb/kw of electrical power

η_m = motor efficiency

η_p = pump efficiency

The value of K_p taken for each of the systems studied is given below:

Cycle	K_p (kw)
Solar Stirling	125
Solar Brayton	125
Solar Rankine	110

The total system weight (W_s) optimized is:

$$W_s = W_{pt} + W_{pf} + W_{si} + W_{so} + W_{pp} \quad (2.17)$$

C. 2. 4 DESIGN RESULTS

C. 2. 4. 1 General

Only two of the three cycles studied, the Stirling cycle and the Brayton cycle, were analyzed since sufficient information was available from previous studies on the Rankine cycle.

C. 2. 4. 2 Brayton Cycle (See Figures C-1 through C-10)

The basic design requirements are given below:

$$T_{inlet} = 996^{\circ}\text{F}$$

$$T_{outlet} = 1490^{\circ}\text{F}$$

$$\Delta P \text{ allowable} = .68 \text{ psi}$$

Heat Storage Material - Lithium Fluoride

Figures C-9 and C-10 essentially summarize all of the preceding figures giving all of the design characteristics of the selected design. Figures C-1 and C-2 give the absorber frictional pressure drop versus the tube inner diameter. The number of tubes was restricted to a maximum of 35 in order to avoid operating the absorber in the transition flow regime. Fifteen percent of the total pressure drop was taken as entrance and exit losses. Figures C-4 through C-6 give the component weight versus the tube inner diameter. The component weight includes the weight of the shell, tubing and gas inventory.

Figure C-7 gives the tube inner diameter versus the number of tubes for a fixed total pressure drop. Figure C-8 gives the component weight versus the number of tubes for a fixed total pressure drop.

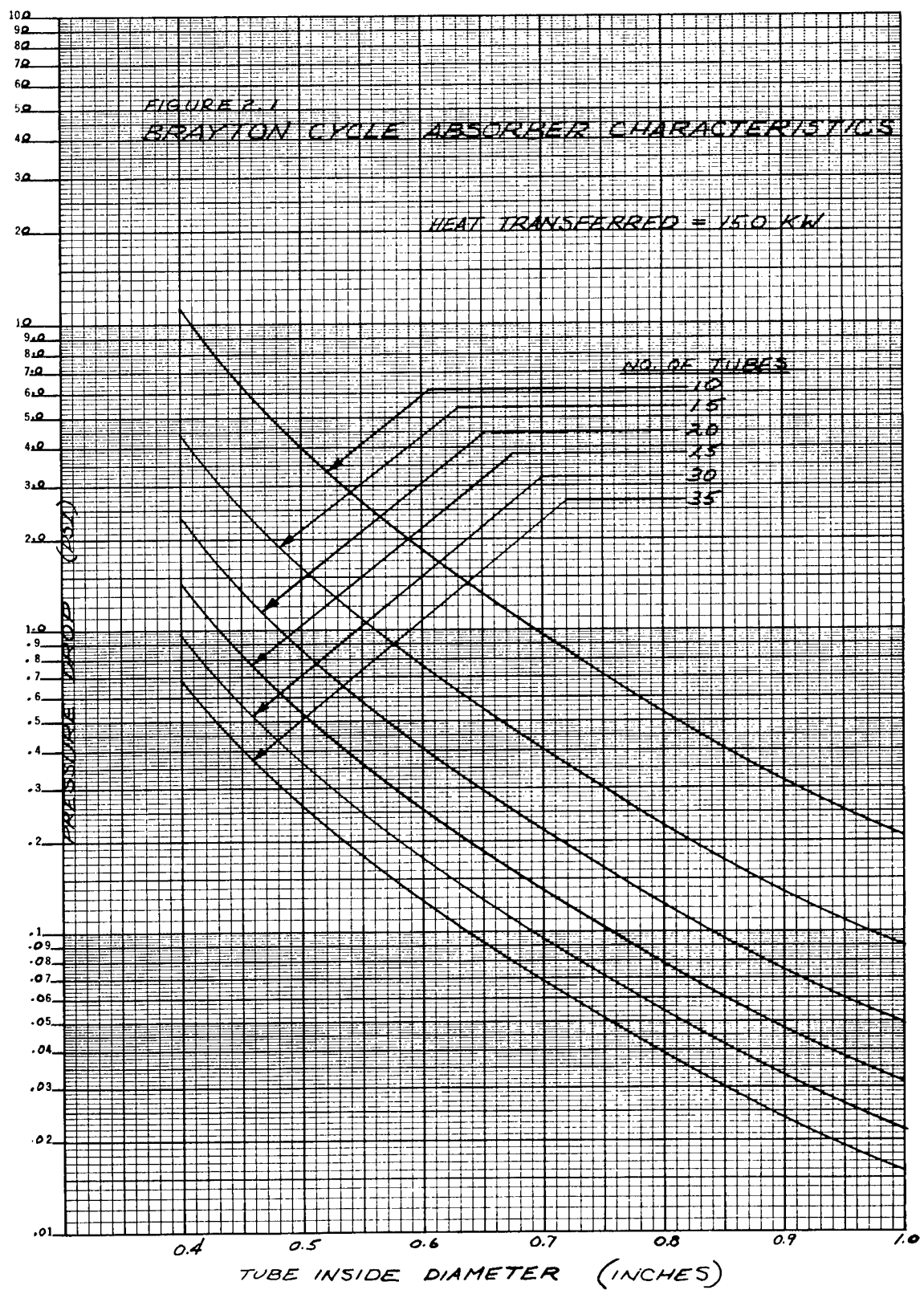


Figure C-1. Pressure Drop Vs. Tube ID (Heat transferred = 15.0 KW)

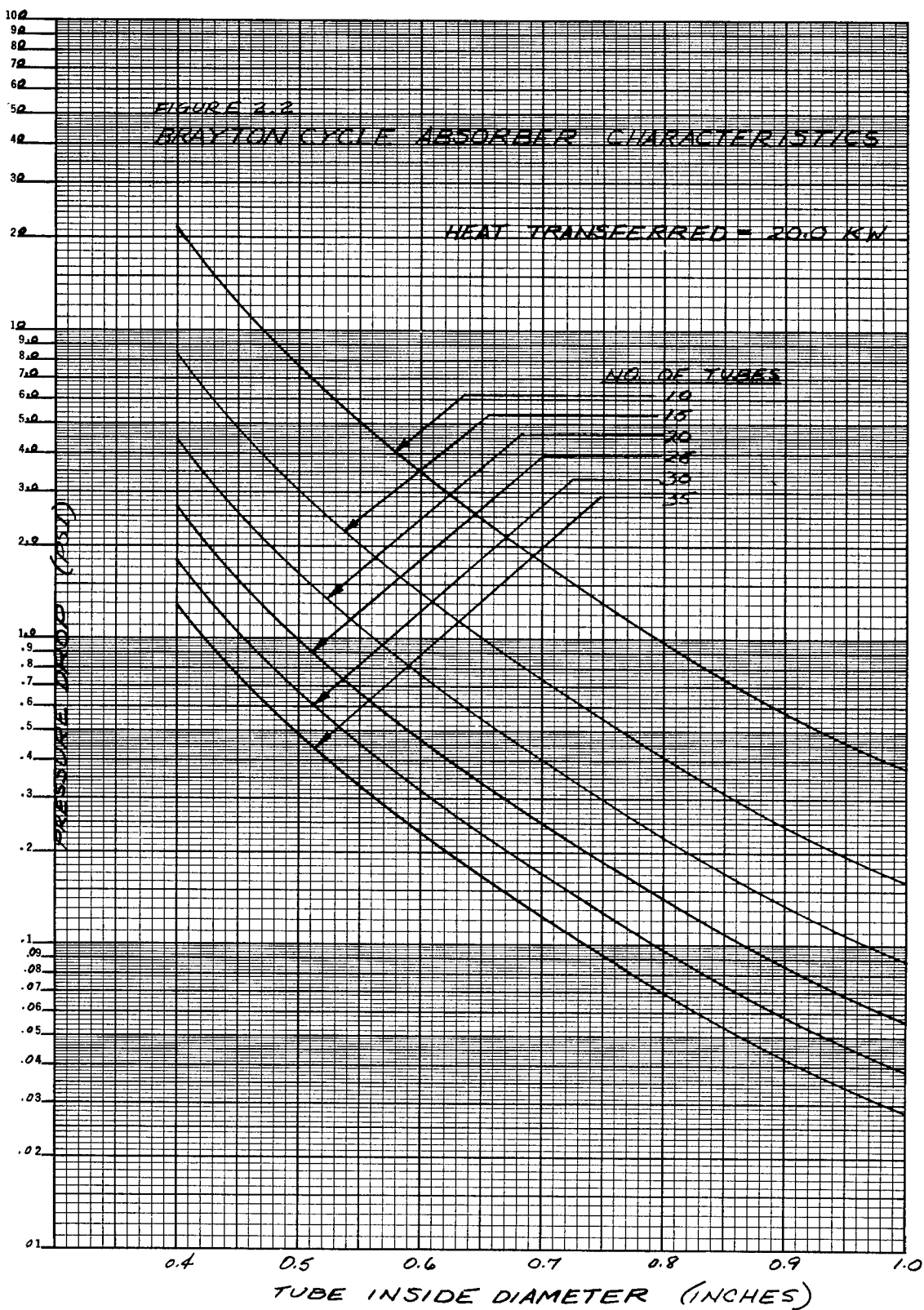


Figure C-2. Pressure Drop Vs. Tube ID (Heat transferred = 20.0 KW)

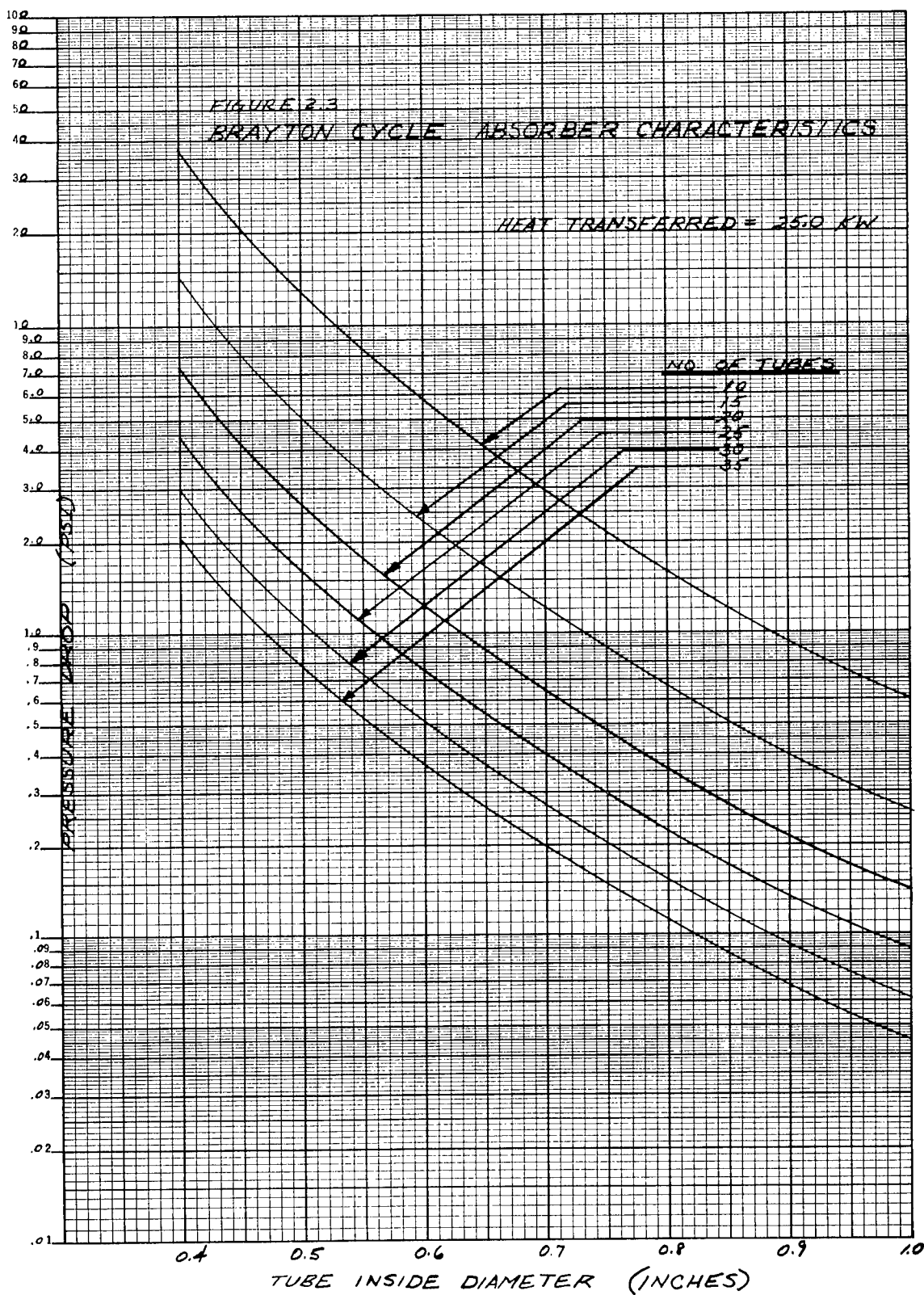


Figure C-3. Pressure Drop Vs. Tube ID (Heat transferred = 25.0 KW)

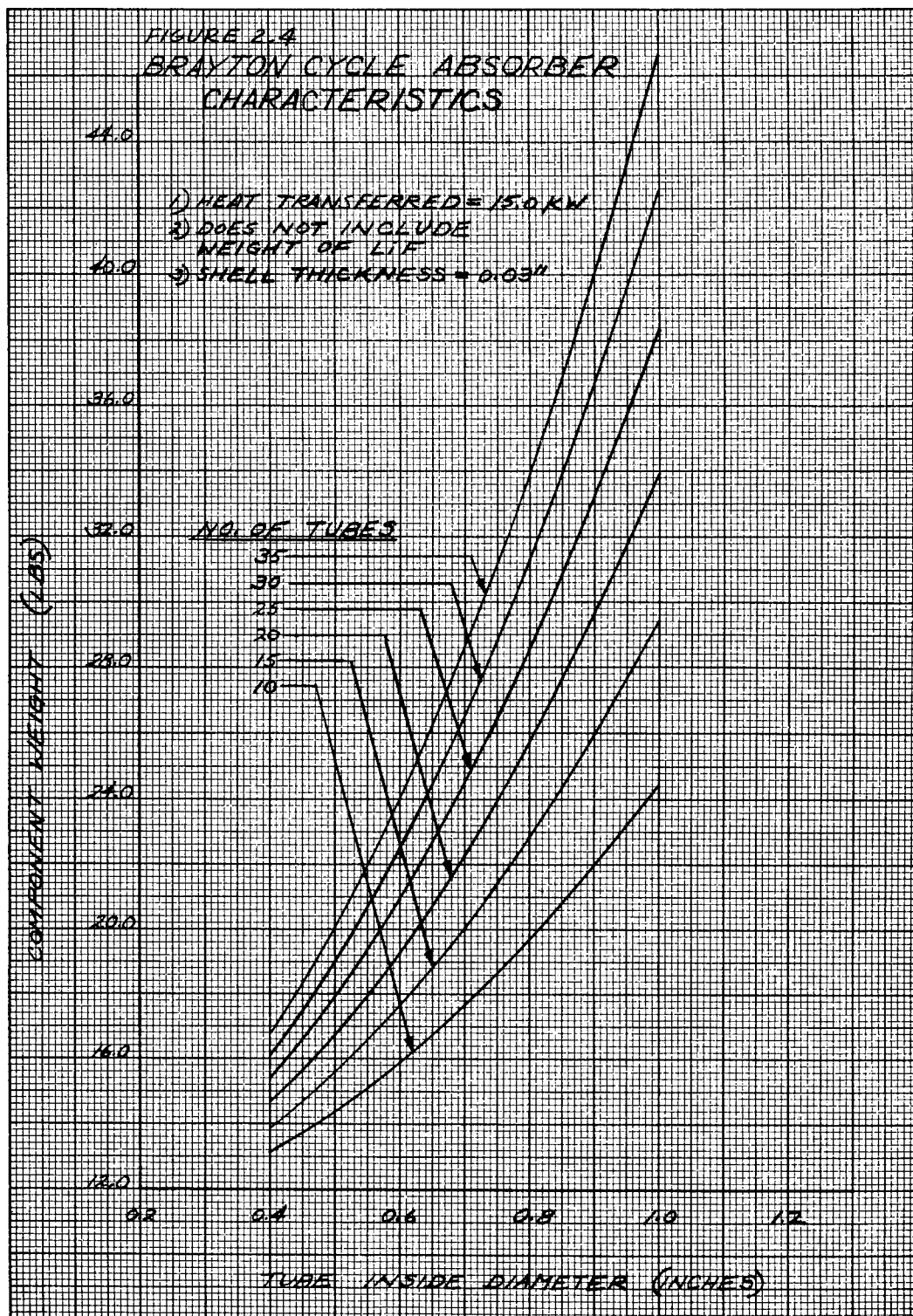
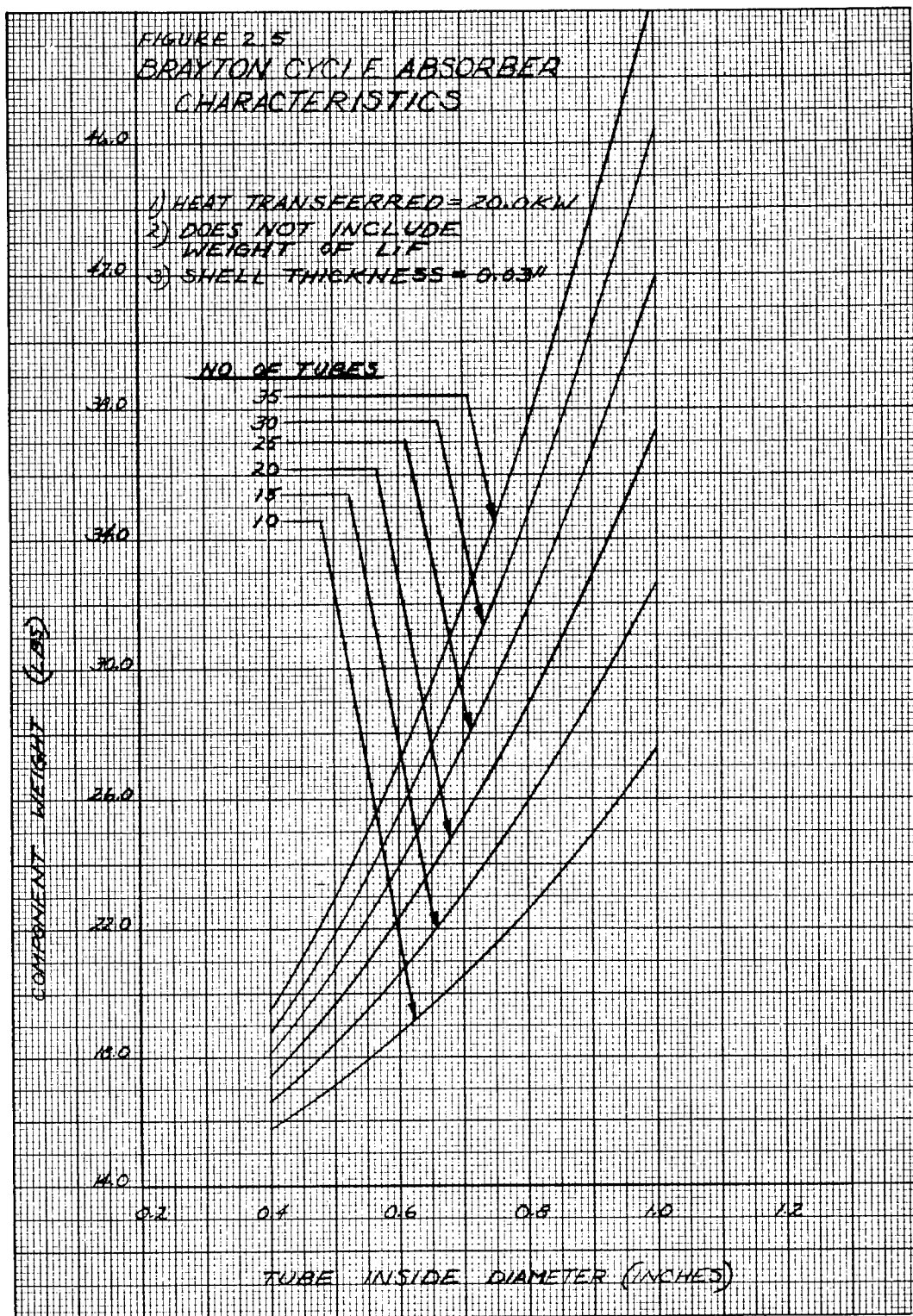


Figure C-4. Component Weight Vs. Tube ID (Heat transferred = 15.0 KW)



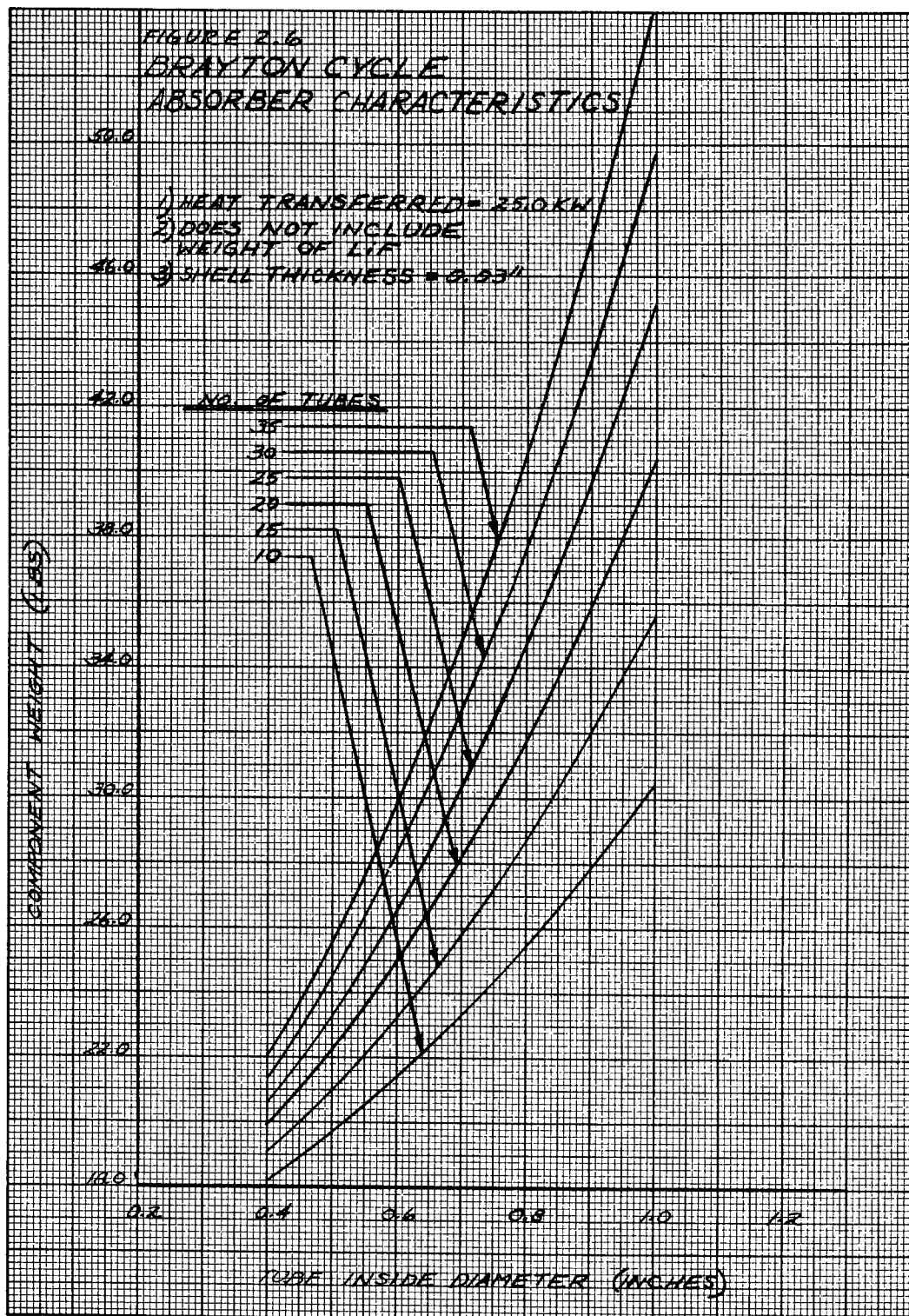


Figure C-6. Component Weight Vs. Tube ID (Heat transferred = 25.0 KW)

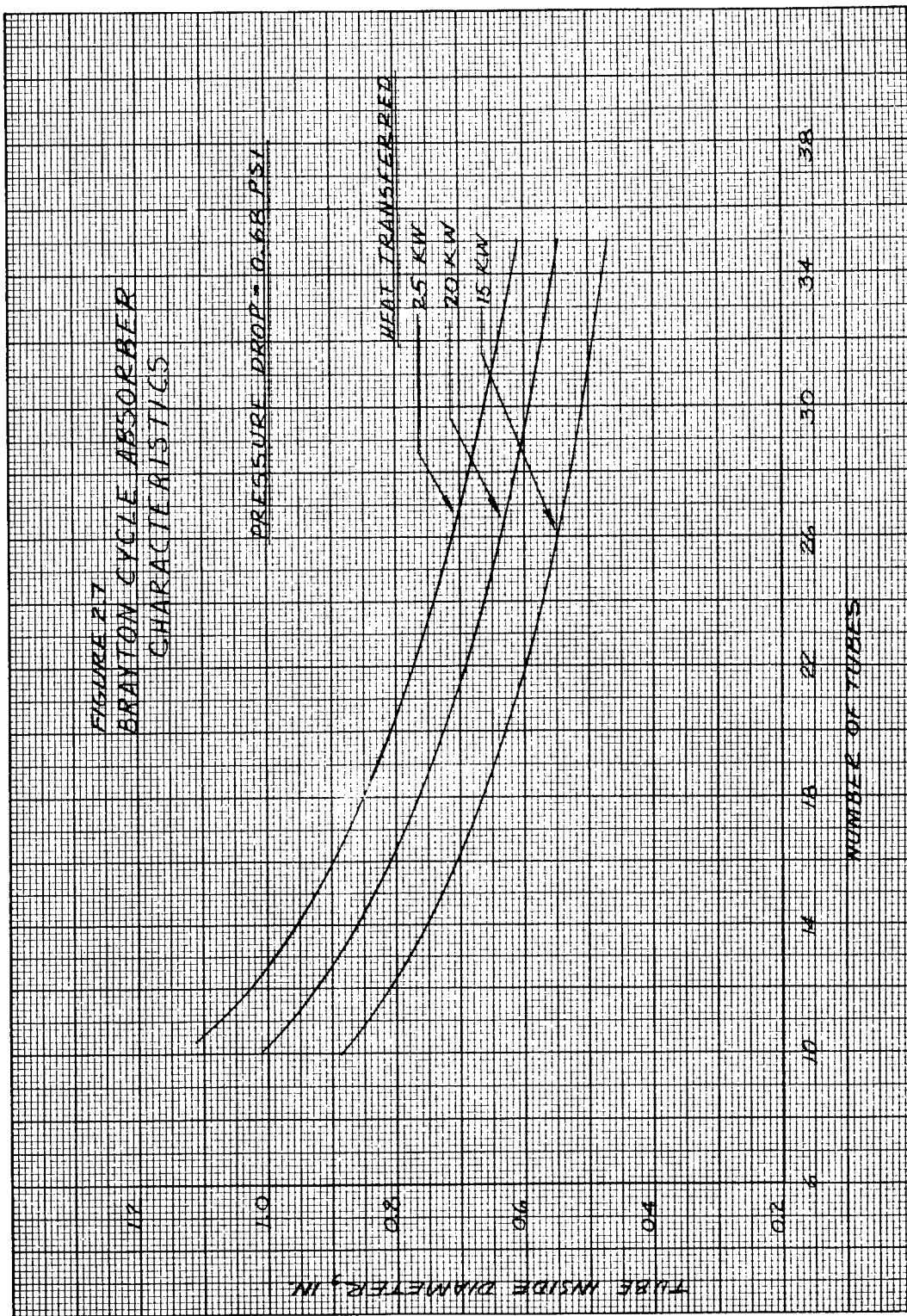


Figure C-7. Tube ID Vs. Number of Tubes

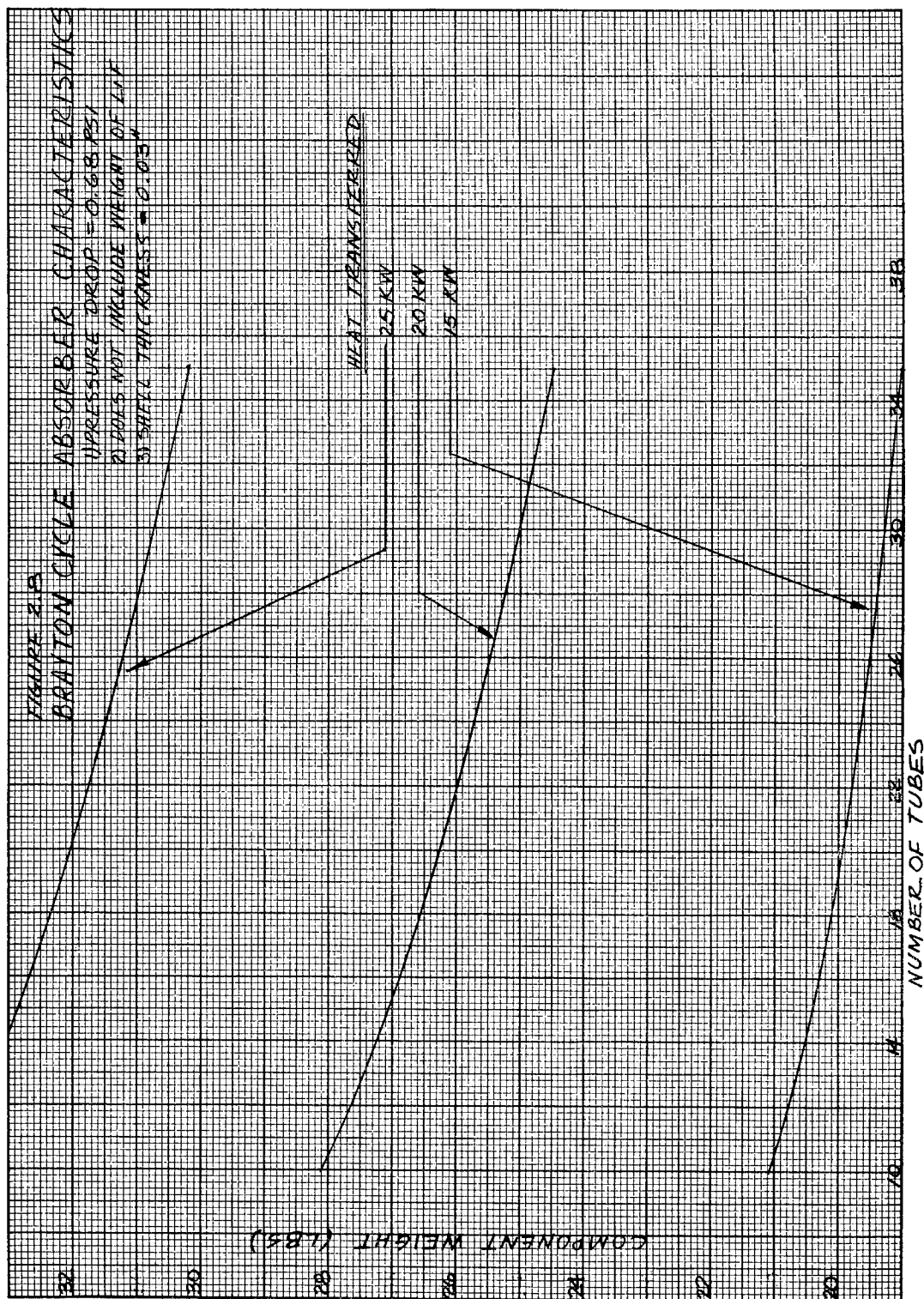


Figure C-8. Component Weight Vs. Number of Tubes

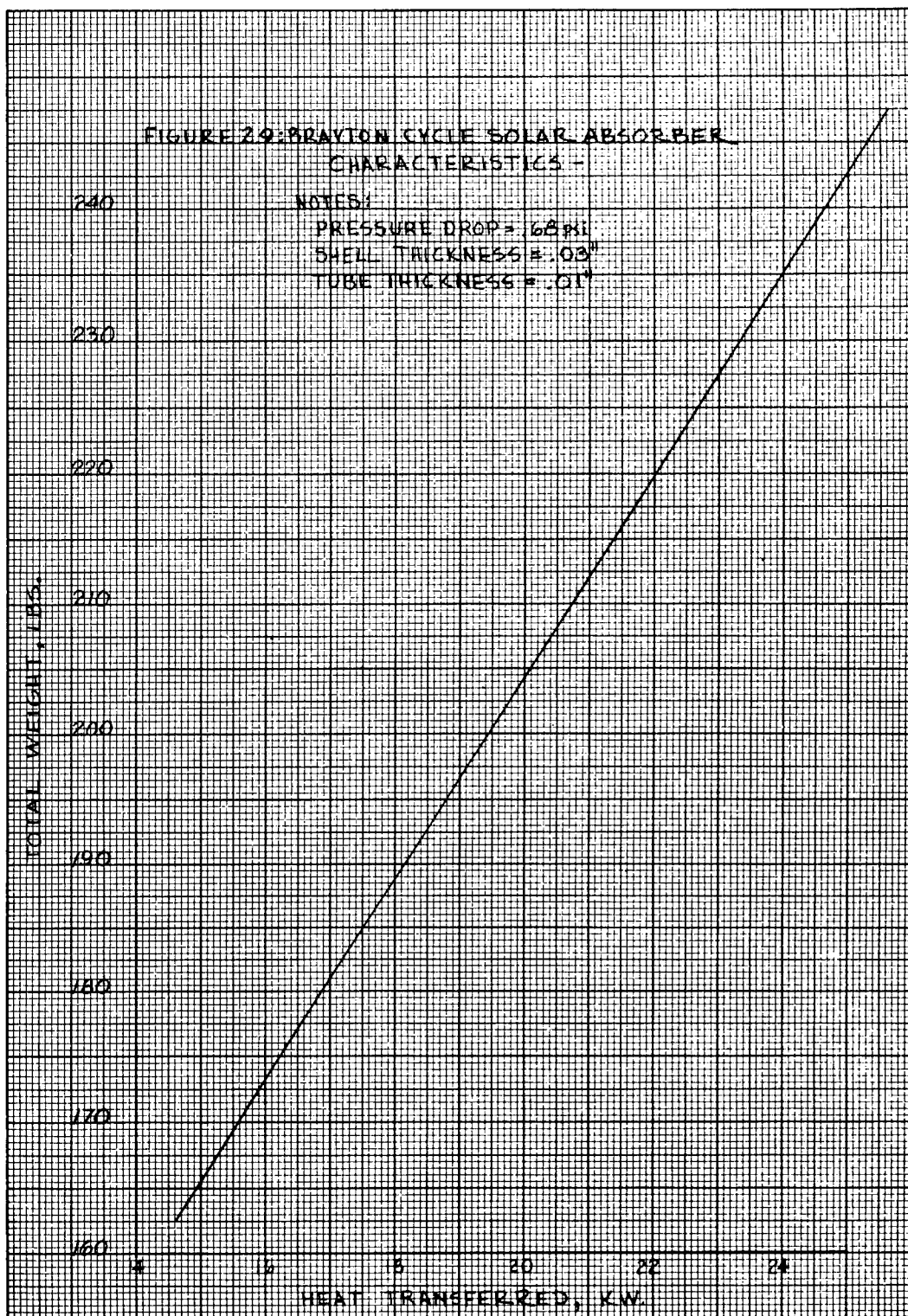


Figure C-9. Total Weight Vs. Heat Transferred

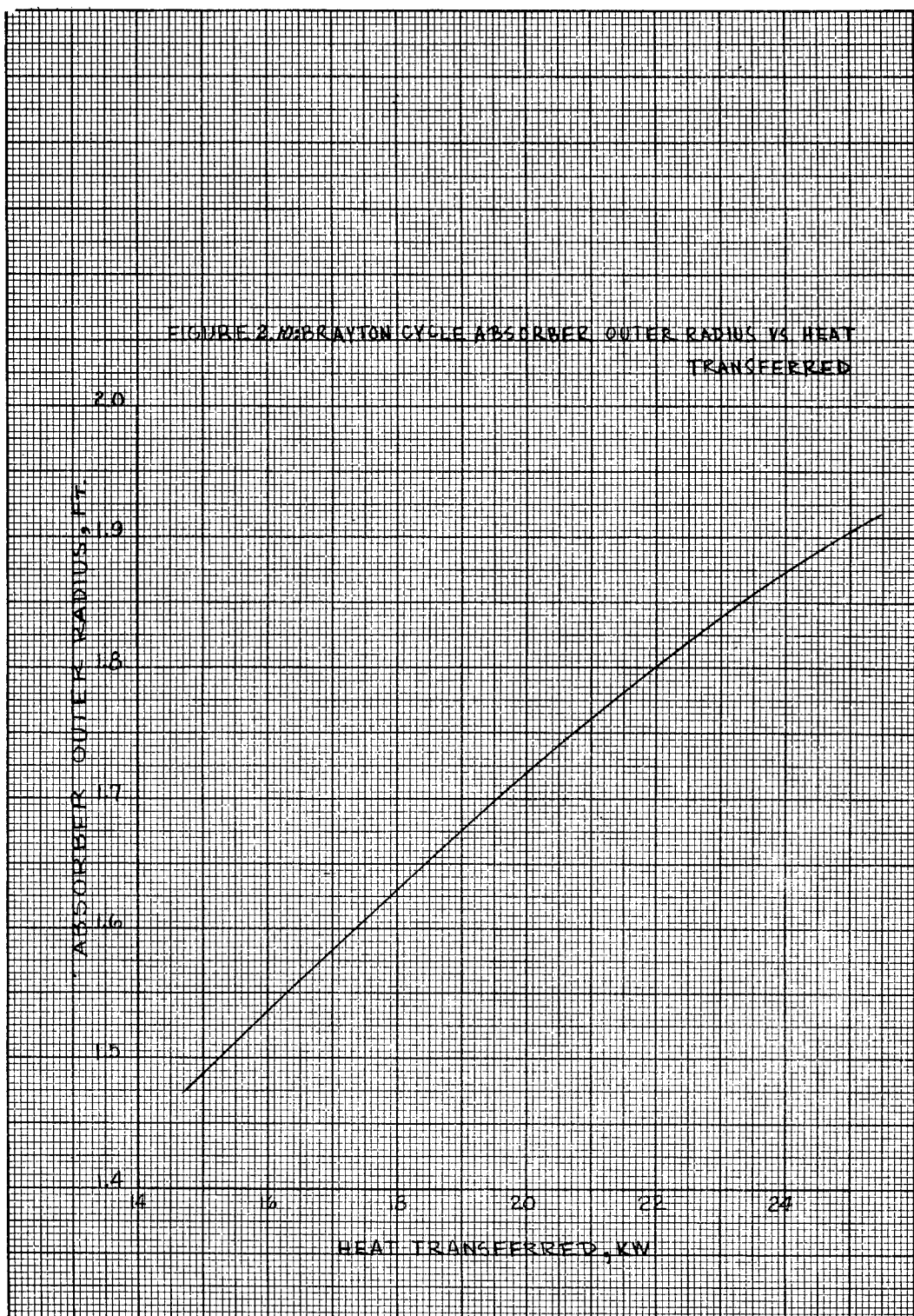


Figure C-10. Absorber Outer Radius Vs. Heat Transferred

C. 2. 4. 3 Stirling Cycle

The specified design requirements are summarized below:

$$T_{\text{inlet}} = 1220^{\circ}\text{F}$$

$$T_{\text{outlet}} = 1250^{\circ}\text{F}$$

Heat Storage Material = Lithium Hydride

Figures C-11 and C-12 summarize the design characteristics of the Stirling cycle solar absorber. Figures C-13 through C-18 give the detailed design curves on which the above curves were based.

C. 2. 5 INSULATION DESIGN

The heat loss through the insulation assembly on the absorber is:

$$Q_i = \frac{k_{\text{eff}} A_i}{t} (T_i - T_o) = \epsilon_o A_i \sigma T_o^4 \quad (2.18)$$

where A_i = insulation area

k_{eff} = effective thermal conductivity of super insulation

t = insulation thickness

T_i = inside surface temperature of insulation

T_o = outside surface temperature of insulation

ϵ_o = emittance of outer surface of insulation assembly = 0.1

σ = Boltzmann's constant

Figure C-19 shows characteristics of super insulation. The optimum weight is determined from the following expression:

$$W_s = \rho_i A_i t + P_q Q_i$$

where ρ_i = insulation density - 17 lb/ft³

P_q = heat loss weight penalty (includes only the weight of the solar collector plus the absorber)

Q_i = heat loss through insulation

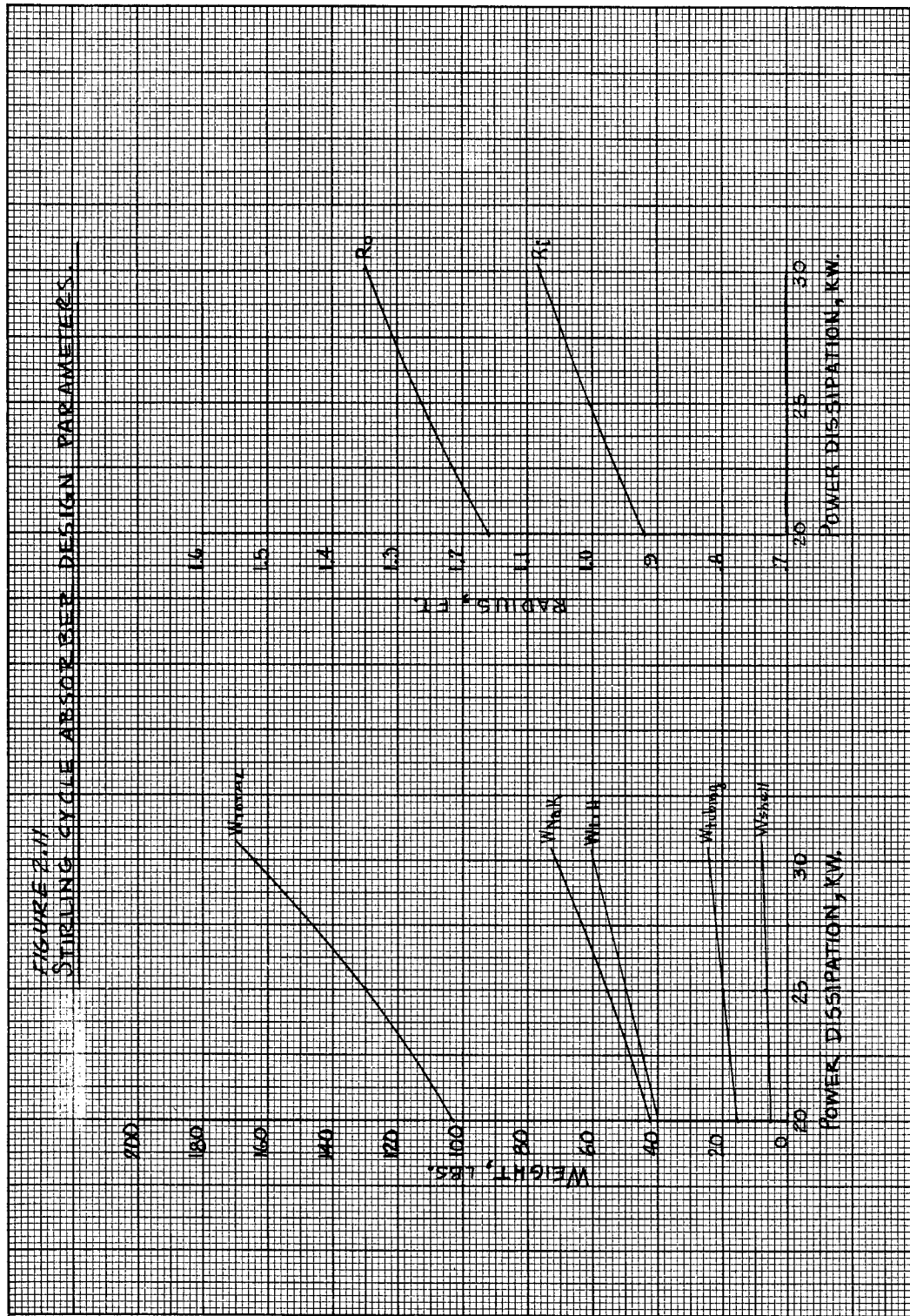


Figure C-11. Weight and Radius Vs. Power Dissipation in KW

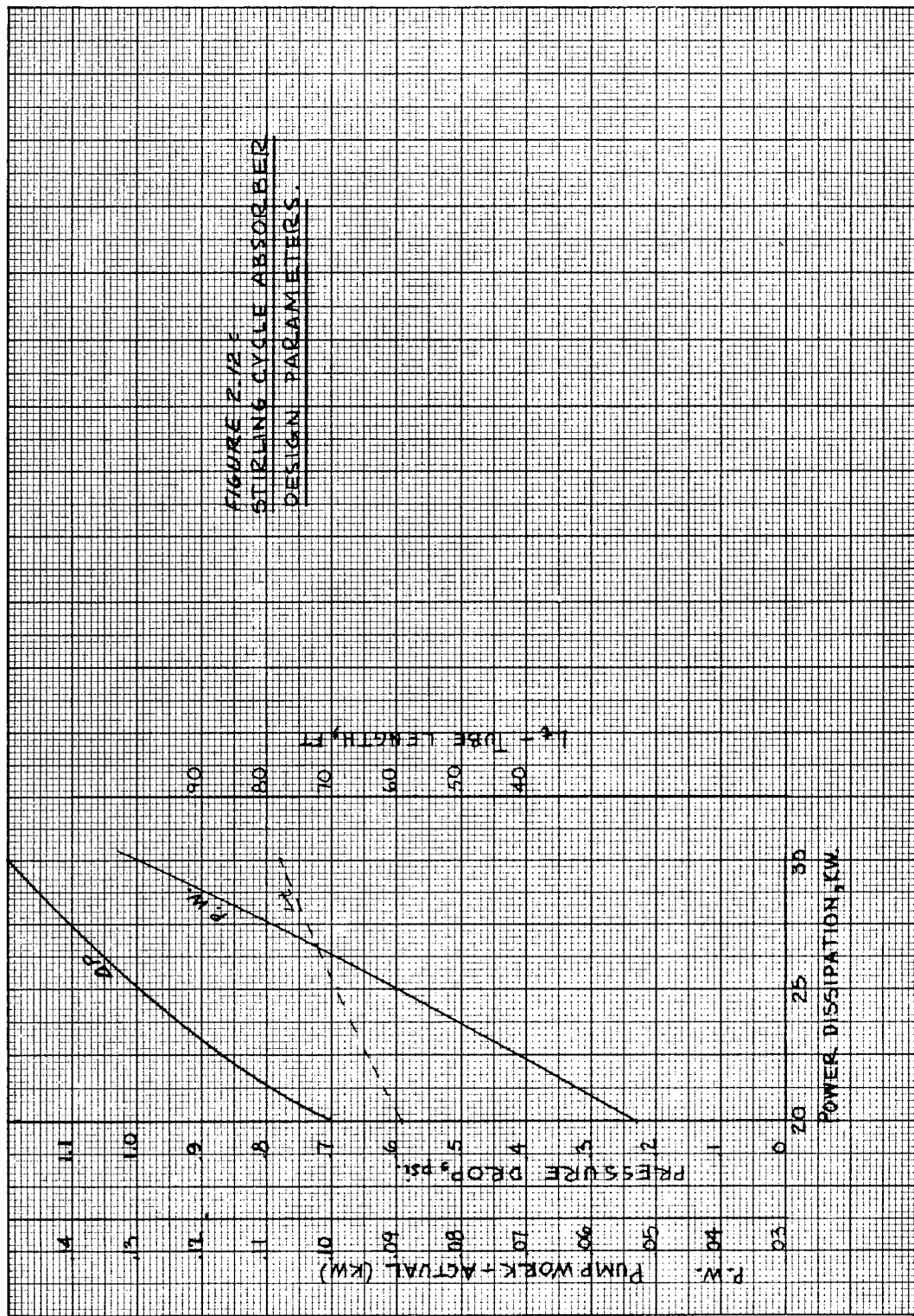


Figure C-12. Actual Pump Work Vs. Power Dissipation in KW

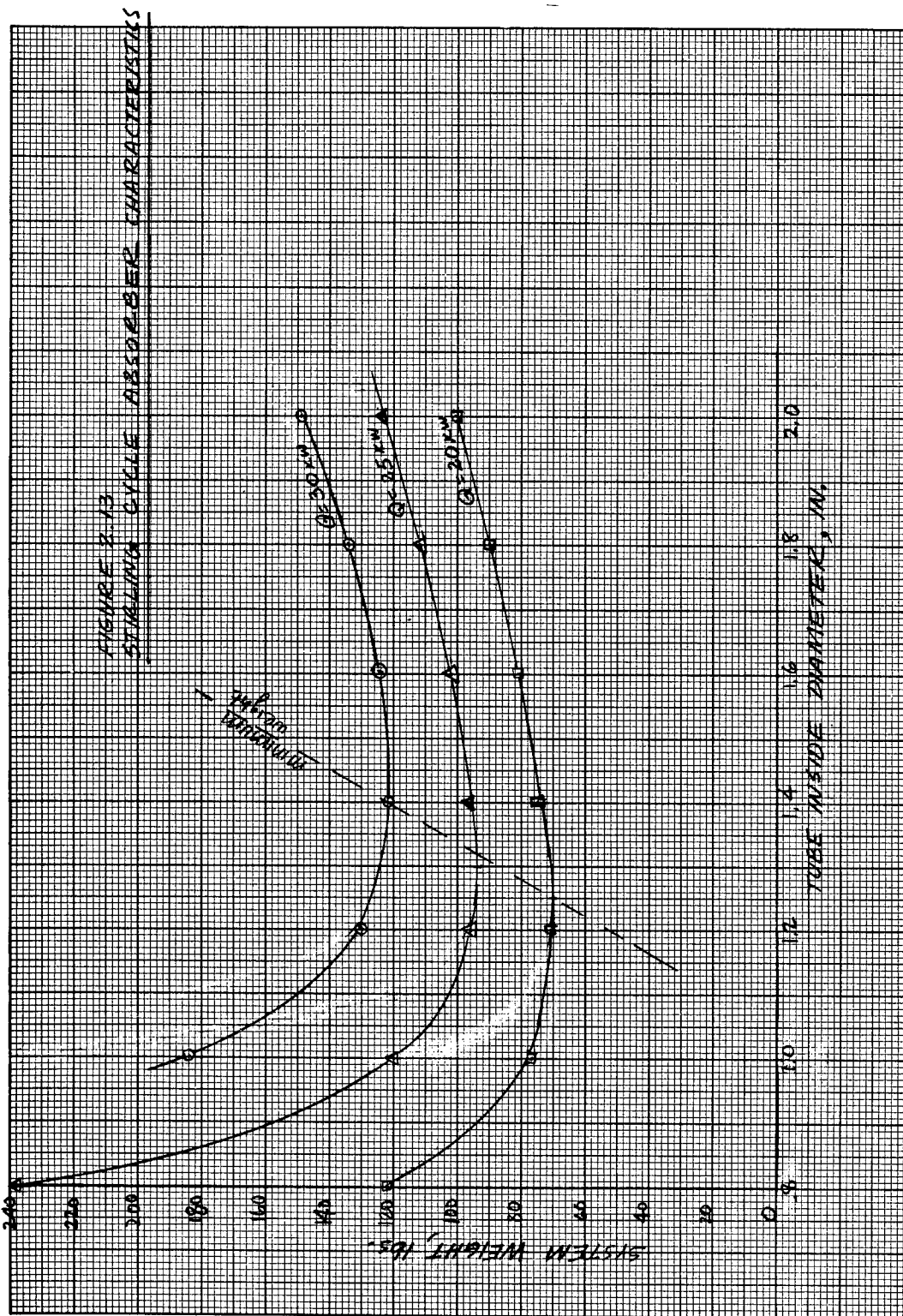


Figure C-13. System Weight Vs. Tube ID

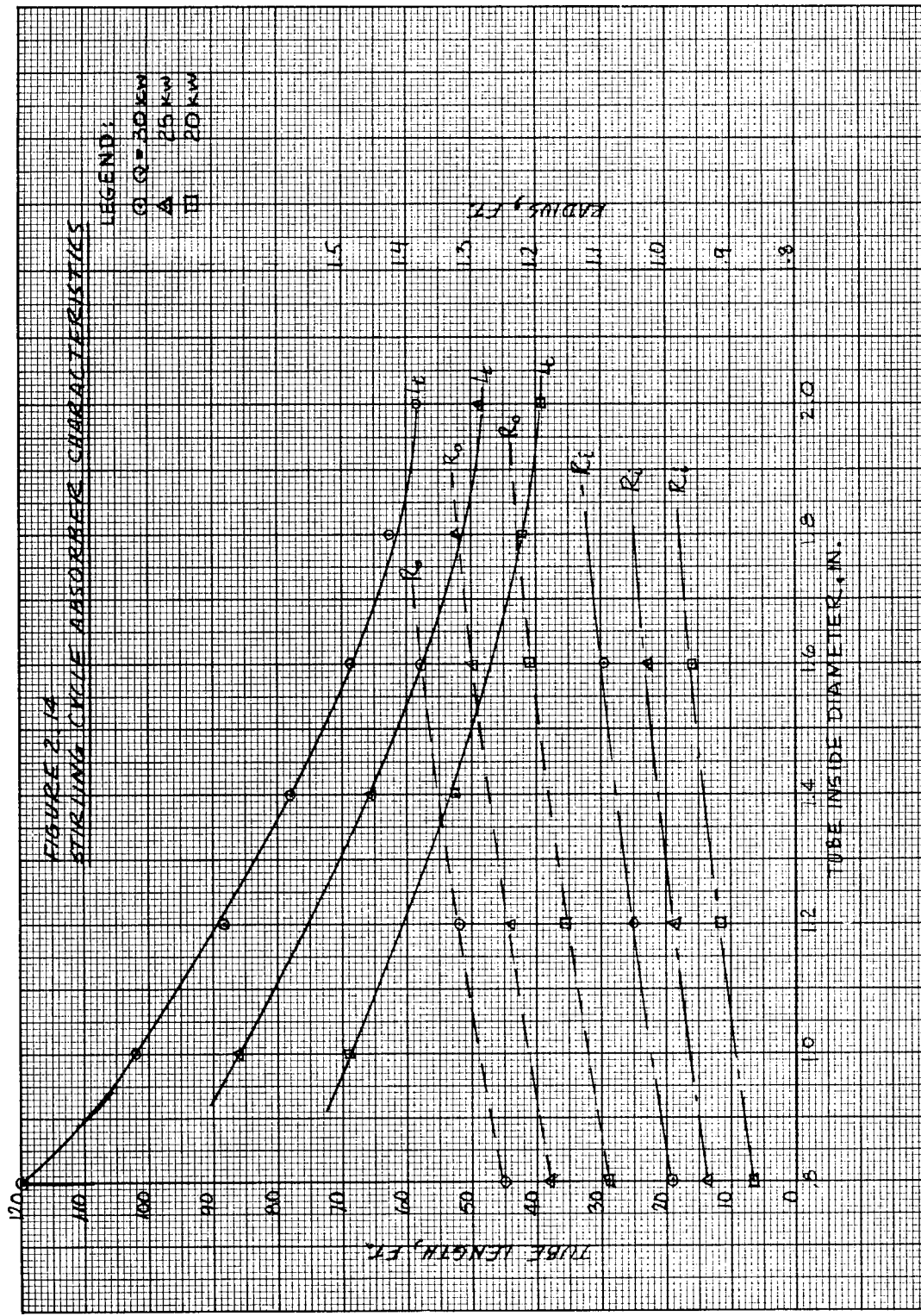


Figure C-14. Tube Lengths Vs. Tube ID

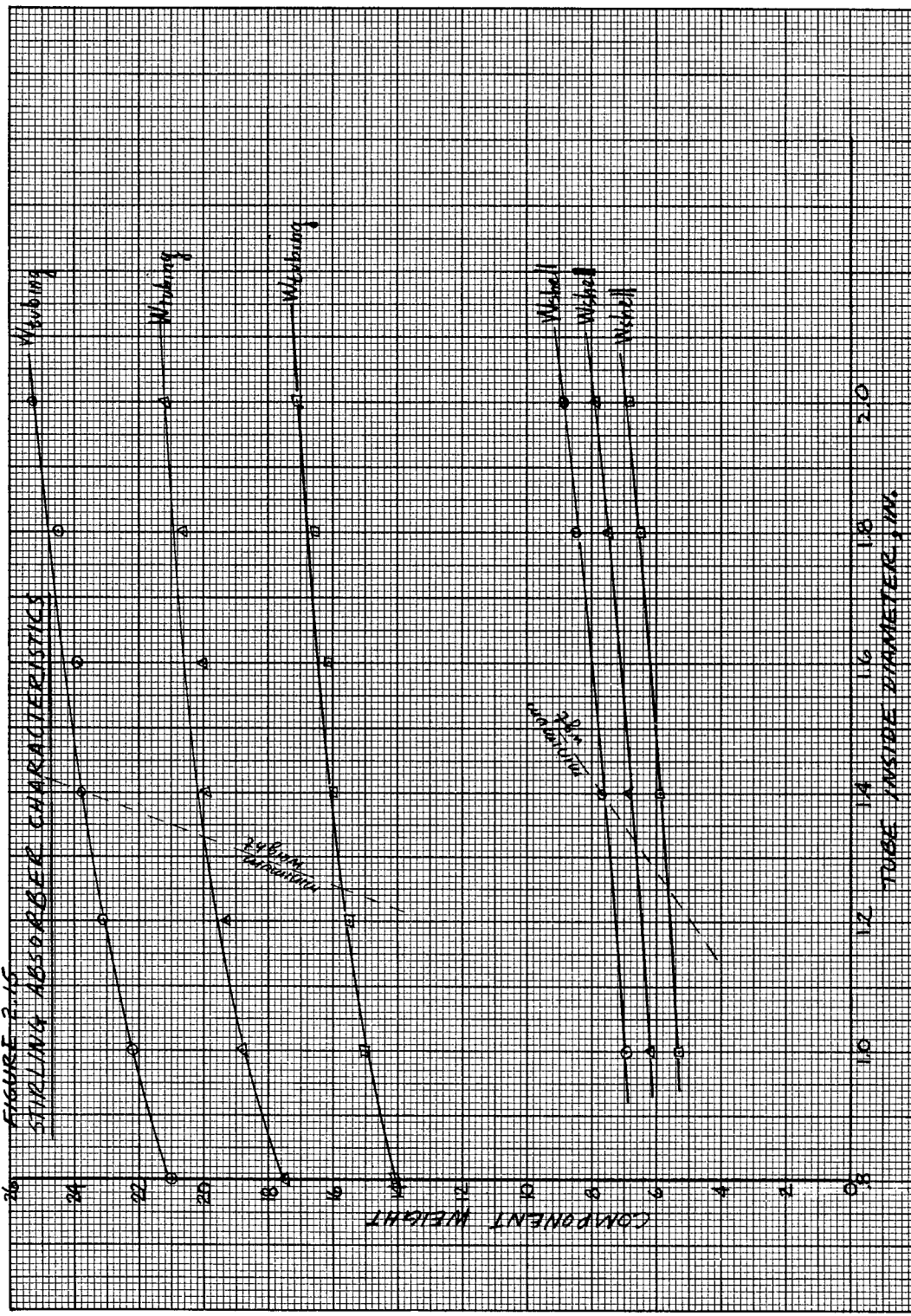


Figure C-15. Component Weight Vs. Tube ID (W_{tubing})

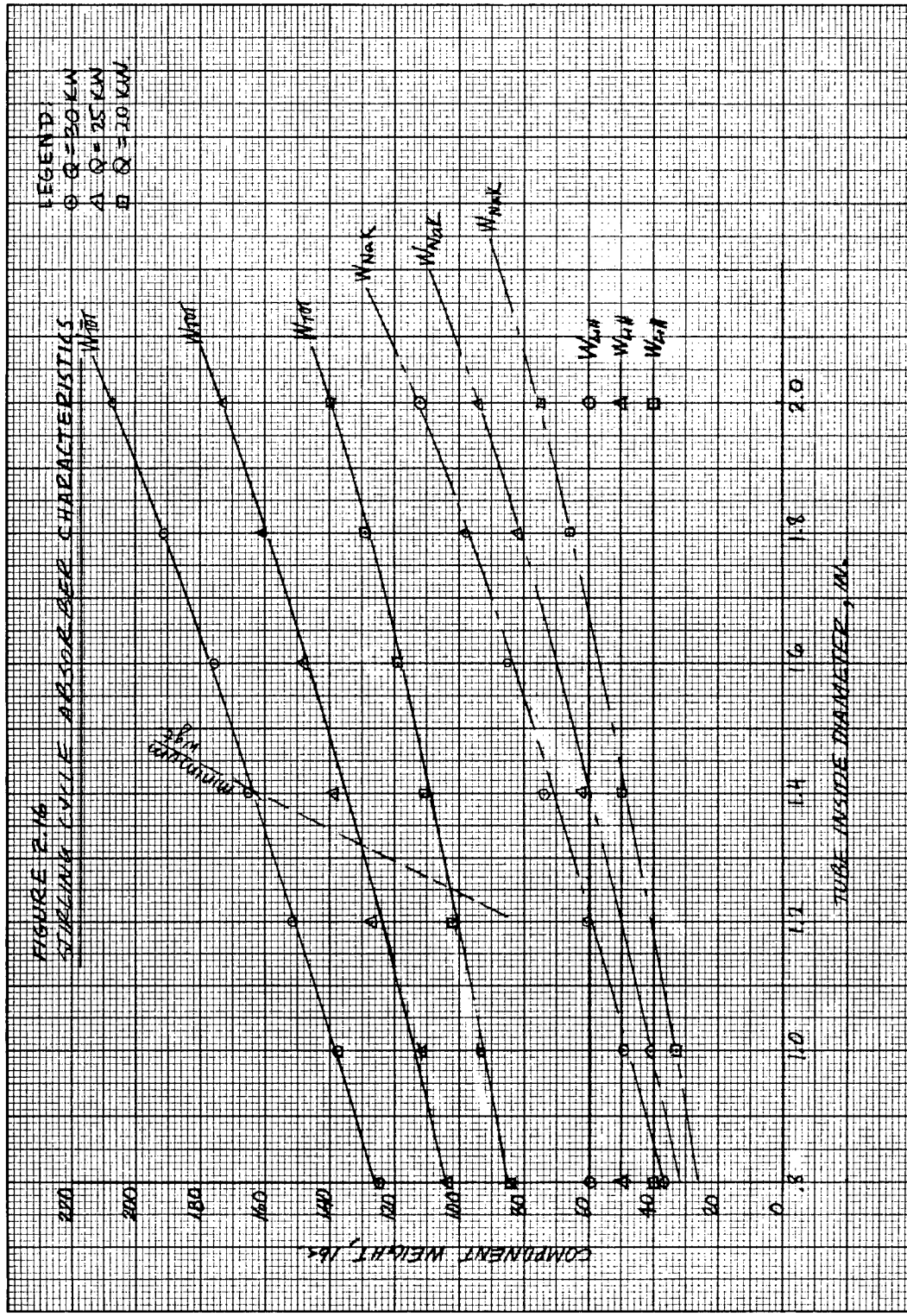


Figure C-16. Component Weight Vs. Tube ID (W_{NaK})

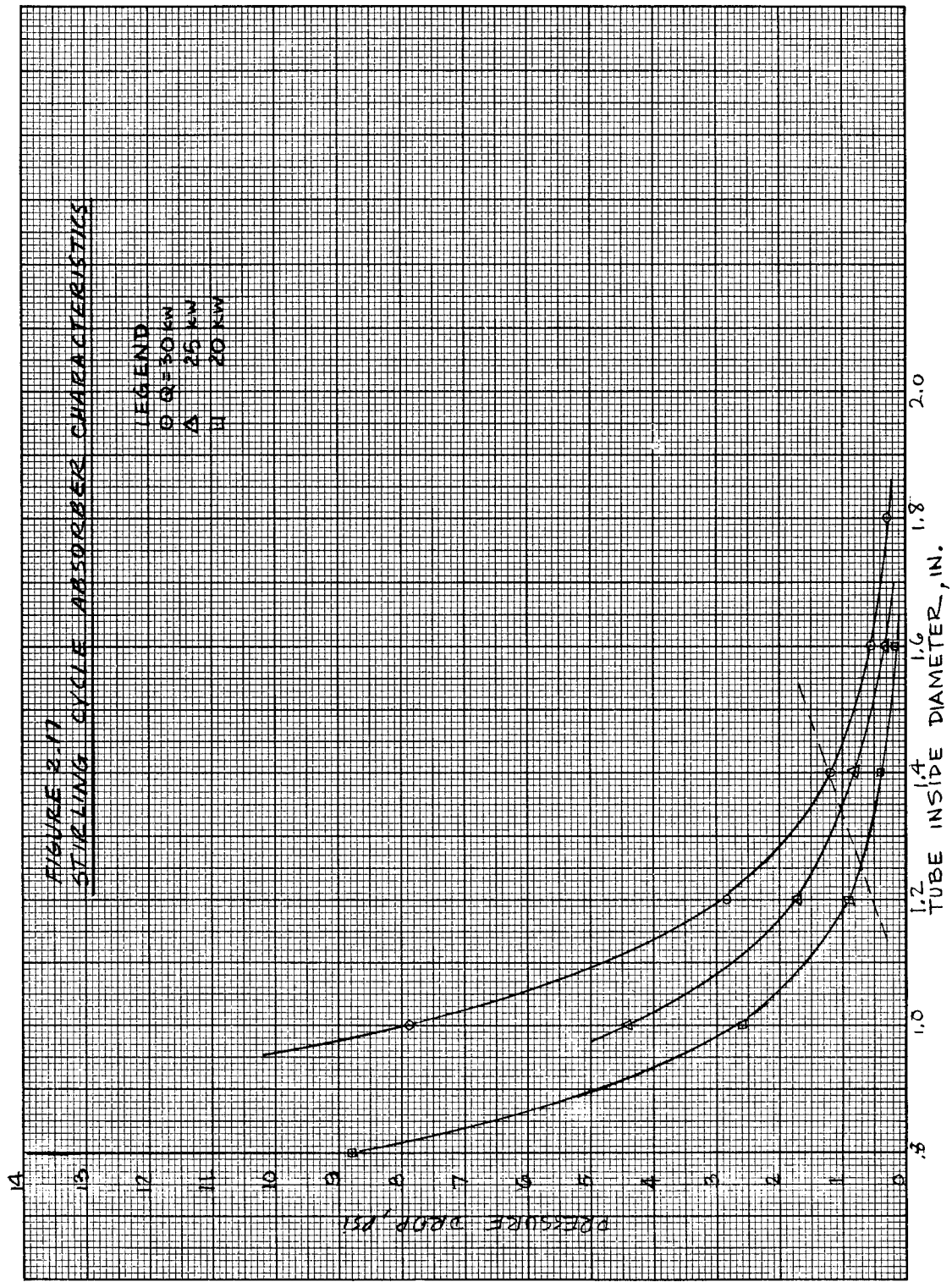


Figure C-17. Pressure Drop Vs. Tube ID

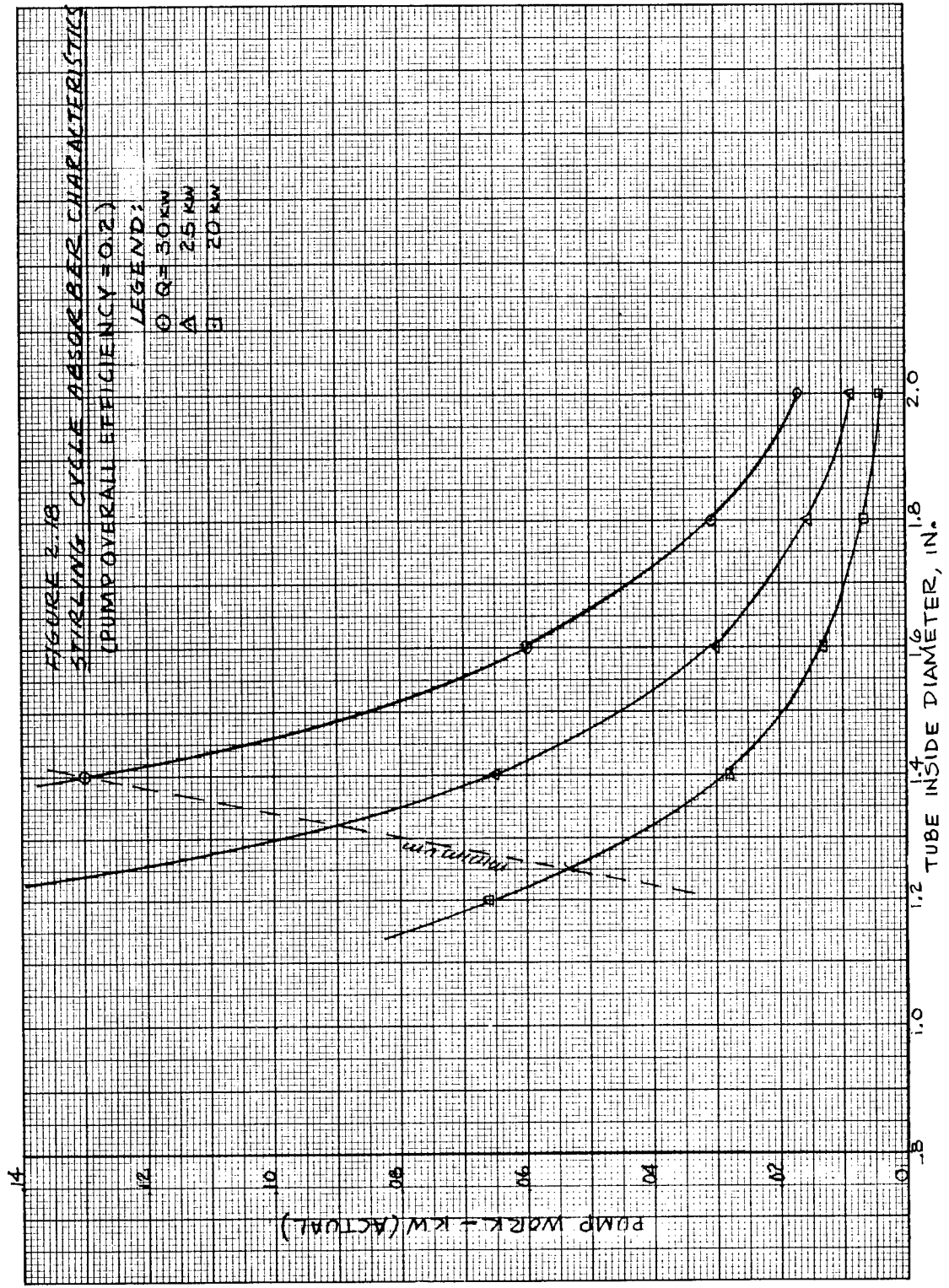


Figure C-18. Pump Work Vs. Tube ID

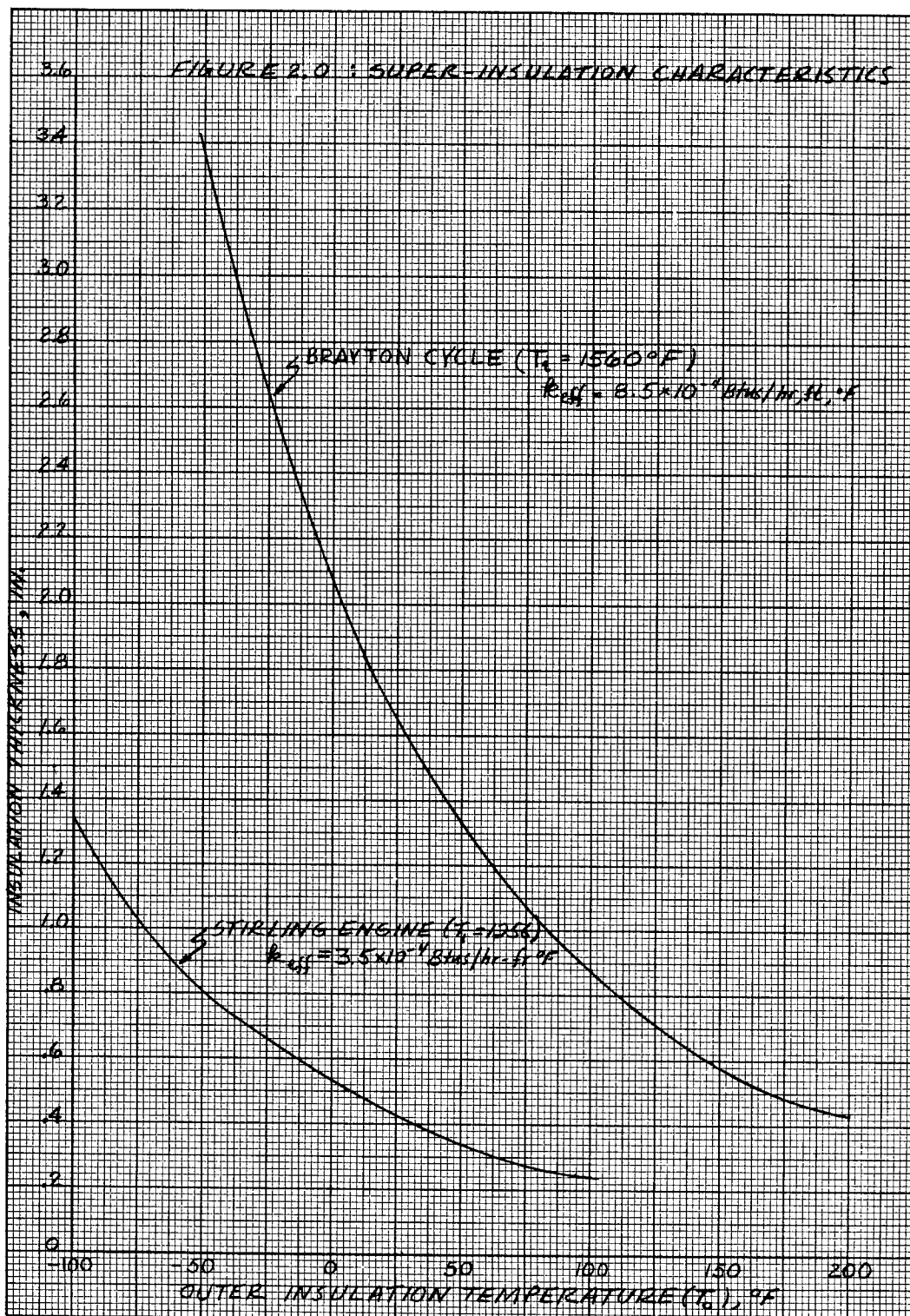
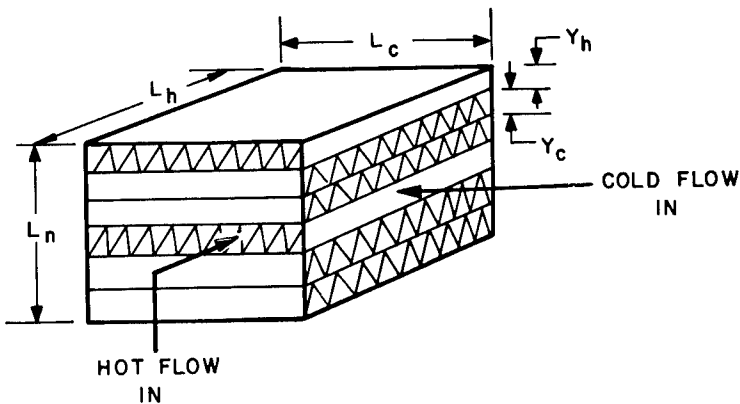


Figure C-19. Super-Insulation Characteristics: Insulation Thickness Vs. Outer Insulation Temperature

C. 3 HEAT EXCHANGER DESIGN

C. 3.1 CROSS FLOW HEAT EXCHANGER

The configuration for a typical cross flow heat exchanger is shown below



Nomenclature

A	= free flow area
A_f	= face area between plates i.e. free flow area plus fin blockage
A_i	= heat transfer area
C_p	= specific heat at constant pressure
f	= Fanning friction factor
F	= f/j
g_c	= Gravitational constant
h	= convective film coefficient
j	= Colburn modulus
L	= flow length
ΔP_f	= frictional pressure loss
Pr	= Prandtl number
Q	= heat transferred
Re	= Reynolds number
r	= hydraulic radius
$\Delta \bar{T}$	= effective mean temperature difference
U	= overall film coefficient
W	= weight flow rate
X	= number of fins per inch
α	= $Pr^{2/3}/C_p$
β	= A/A_f
ρ	= average density
K	= number of fluid passages
η	= efficiency

Subscripts:

- h = hot side
- c = cold side
- f = fin
- o = overall
- t = total

The frictional pressure drop through the core can be calculated as follows:

$$\Delta P_f = \frac{fL}{2r} \frac{W^2}{A^2 \rho g_c} \quad (3.1)$$

noting that $r = \frac{AL}{A_i}$ by definition, then

$$\frac{L}{r} = \frac{\Delta P}{f \frac{W^2}{2A^2 \rho g_c}} \quad (3.2)$$

The Colburn modulus is,

$$j = \frac{hA_i \alpha}{W} = \frac{rh A_i^\alpha}{WL}$$

so,

$$\frac{L}{r} = \frac{\alpha h A_i}{j W} \quad (3.3)$$

Equating equations 3.2 and 3.3,

$$A = \sqrt{\frac{\alpha}{2 \rho g_c} F \frac{W h A_i}{\Delta P_f}} \quad (3.4)$$

Equation 3.4 is referred to as the "impossibility" equation since it gives the possible values that satisfy the flow area and heat transfer area constraints.

The overall film coefficient is defined as follows:

$$UA_i = \frac{1}{\frac{1}{\eta_h (hA_i)_h} + \frac{1}{\eta_c (hA_i)_c}} \quad (3.5)$$

Rearranging

$$UA_i = \frac{\eta_h (hA_i)_h}{1 + \frac{\eta_h (hA_i)_h}{\eta_c (hA_i)_c}} = \frac{\eta_c (hA_i)_c}{1 + \frac{\eta_c (hA_i)_c}{\eta_h (hA_i)_h}} \quad (3.6)$$

Defining

$$\phi = \frac{\eta_h (hA_i)_h}{\eta_c (hA_i)_c}$$

$$(hA_i)_h = \left(\frac{1 + \phi}{\eta_h} \right) UA_i \quad (3.7)$$

and

$$(hA_i)_c = \frac{1 + 1/\phi}{\eta_c} UA_i \quad (3.8)$$

where

$$UA_i = Q/\Delta \bar{T}$$

$\Delta \bar{T}$ = effective temperature difference between the hot and cold streams.

The value of $\Delta \bar{T}$ can be determined from reference 8. Equation 3.4 can now be expressed as:

$$A_h = \sqrt{\frac{\alpha_h}{2 \rho_h g_c} F_h \frac{W_h UA_i (1 + \phi)}{\eta_h \Delta P_{fh}}} \quad (3.9a)$$

$$A_c = \sqrt{\frac{\alpha_c}{2 \rho_c g_c} F_c \frac{W_c UA_i (1 + 1/\phi)}{\eta_c \Delta P_{fc}}} \quad (3.9b)$$

If we define

$$L_{nh} = K_h y_h = A_{fh}/L_c \quad (3.10a)$$

$$L_{nc} = K_c y_c = A_{fc}/L_h \quad (3.10b)$$

$$\delta = L_{nh}/L_{nc}$$

Then

$$L_h = \frac{A_c (1 + \delta)}{\beta_c L_n} \quad (3.11)$$

and

$$L_c = \frac{A_n (1 + 1/\delta)}{\beta_n L_n} \quad (3.12)$$

where

$$L_n = L_{nh} + L_{nc}$$

An examination of the characteristics of typical heat exchanger cores shows that f/j is only a weak function of Reynold's number. This allows the following design procedure to be followed, having already selected specific core designs:

1. Assume values of ϕ , η_c , η_h , ΔP_{fc} , ΔP_{fh} , F_n , F_c
2. From equations (3.9a) and (3.9b) calculate A_h and A_c

3. Reynold's number for both sides can now be computed

$$R_{e_h} = \frac{4W_h r_h}{A_n \nu_h}$$

$$R_{e_c} = \frac{4 W_c r_h}{A_c \nu_c}$$

where ν = kinematic viscosity

A new value of F_h and F_c can now be calculated and the proper flow areas computed.

4. L_h and L_c can be calculated from equations 3.11 and 3.12 assuming a value of L_n and
 5. The number of hot and cold passages can be calculated with equations 3.10 as follows:

$$K_h = \frac{A_h}{Y_h \beta_h L_c}$$

$$K_c = \frac{A_c}{Y_c \beta_c L_h}$$

From this the assumed fin efficiency η_h , η_c can be checked. The effective fin height for the hot and cold sides are respectively:

$$y_{h_{\text{eff}}} = \frac{y_h K_h}{2 K_c} = \bar{y}_h \quad (3.13a)$$

$$y_{c_{\text{eff}}} = \frac{y_c K_c}{2 K_h} = \bar{y}_c \quad (3.13b)$$

The overall efficiency can be determined from the relation (Ref. 9):

$$\eta_h = 1 - \left(\frac{A_{\text{fin - cold}}}{A_{i-c}} \right) \left[1 - \frac{\tanh \bar{y}_h \sqrt{\frac{2 h_c}{k_{fc} t_{fc}}}}{\bar{y}_h \sqrt{\frac{2 h_c}{k_{fc} t_{fc}}}} \right] \quad (3.14a)$$

$$\eta_c = 1 - \left(\frac{A_{\text{fin - hot}}}{A_i - h} \right) \left[1 - \frac{\tanh \bar{y}_c \sqrt{\frac{2 h_h}{k_{fh} t_{fh}}}}{\bar{y}_c \sqrt{\frac{2 h_c}{k_{fh} t_{fh}}}} \right] \quad (3.14b)$$

where A_{fin} = fin area

$$A_{\text{fin-cold}} = 2 K_h L_c L_h X_h y_h$$

$$A_{\text{fin-hot}} = 2 K_c L_c L_h X_h y_h$$

t_f = fin thickness

h = convective film coefficient

The core weight plus fluid inventory can be calculated as follows:

$$W_{\text{core}} = L_{nh} L_h L_c (1 - \beta_n) \rho_{cm} + L_{nc} L_h L_c (1 - \beta_c) \rho_{cm} + L_{nh} L_h L_c \beta_h \rho_h \\ + L_{nc} L_h L_c \beta_c \rho_c \quad (3.15)$$

where ρ_{cm} = density of core metal

ρ_c = density of cold side fluid

ρ_h = density of hot side fluid

The Brayton cycle heat exchanger design was selected on the basis of providing a reasonable physical design, i.e. header configuration, without necessarily optimizing weight. The reason is that extremely awkward header designs result from the condition of minimum weight. The core volume (V) is:

$$V = L_n L_h L_c \\ = \frac{UA_i (2 + \delta + 1/\delta) \sqrt{2 + \phi + 1/\phi}}{2 g_c L_n \sqrt{\rho_c \rho_n \beta_c \beta_h}} \sqrt{\frac{\alpha_h \alpha_c F_c F_n W_c W_h}{\Delta P_{fh} \Delta P_{fc} \eta_c \eta_h}} \quad (3.16)$$

It is seen that the condition of a minimum volume is $\delta = 1$, $\phi = 1$.

From equations 3.11 and 3.12, setting $\delta = 1$, $\phi = 1$.

$$\frac{L_h}{L_c} \approx \sqrt{\frac{\alpha_h F_h W_h \Delta P_c \rho_c}{\alpha_c F_c W_c \Delta P_h \rho_h}} \quad (3.17)$$

Noting the large difference in density between the gas and liquid stream, setting $\delta = 1$ and $\phi = 1$ results in a very large ratio of L_h to L_c

For the Brayton systems the total life support heat requirements are supplied at 400°F to a Therminol FR-1 loop. This loop in turn supplies the low temperature (150°F) heat requirements by means of a counterflow heat exchanger to a 30% ethylene glycol loop.

The basic specification for the argon-Therminol heat exchanger are as follows:

Argon Side

$T_{in} = 415^{\circ}\text{F}$

$W = 947 \text{ hr.}$

$T_{out} = 293^{\circ}\text{F}$

max ΔP allowable = .3 psia

$Q = 14,364 \text{ BTUs/hr.}$

Therminol FR-1

$T_{in} = 278^{\circ}\text{F}$

$W = 368 \text{ lbs/hr.}$

$T_{out} = 400^{\circ}\text{F}$

ΔP allowable = not specified

Core Characteristics

Argon - 10.27T - .544/.544 - 2.5 (S) - .01 (A1) (Ref 10)

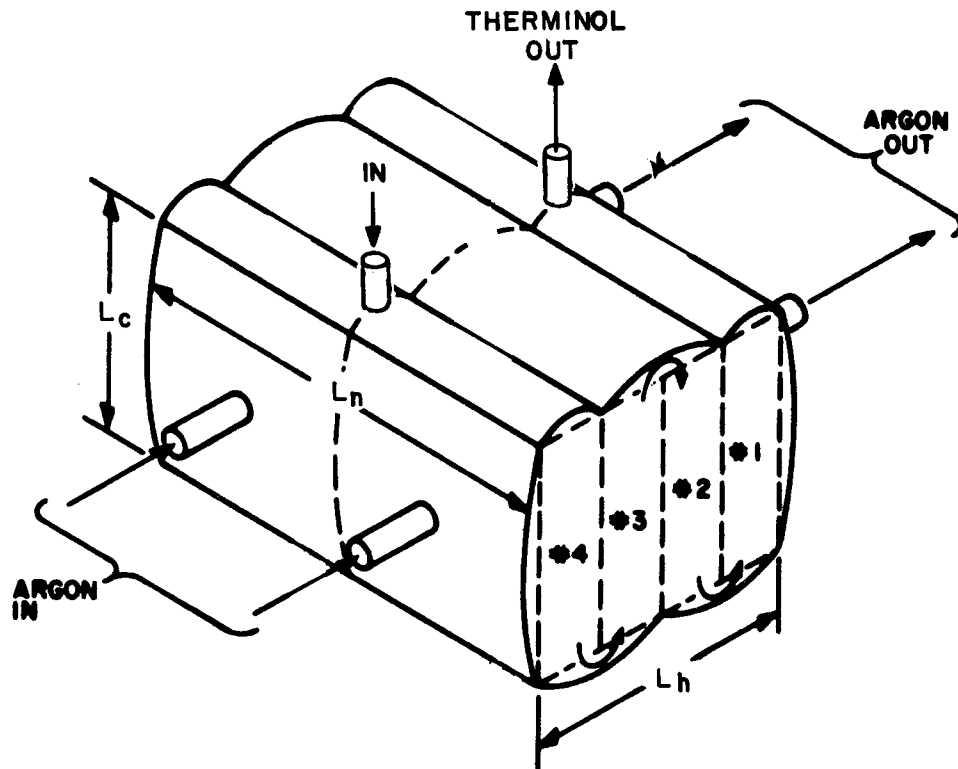
Therminol - 17T - .125 - 1.58 - .006 (A1) (Ref 11)

The summary of the core characteristics are summarized below:

<u>Code</u>	<u>Fins Per in.</u>	<u>Configuration</u>	<u>Plate Spacing in.</u>	<u>Hydraulic Radius in.</u>	<u>β</u>	<u>Material</u>
10.27T-.544/.544 2.5(S) - 0.1 (A1)	10.27	Triangular - 2.5 inch strip	.544 inch	.0387 inch	.863	A1
17T-.125-1.5(S) - .006 (A1)	17	Triangular - 1.5inch strip	.125 inch	.0176 inch	.887	A1

Plots of the friction factor (f) and Colburn modulus j versus Reynolds number are provided in Figure C-20.

In light of the extremely high effectiveness requirements called for, the following configuration was chosen:



In order to achieve a reasonable physical design in terms of header design and uniform flow distribution, the quantities δ and ϕ were set at 3 and 0.1 respectively. From Reference 8, the one pass number of transfer units $\frac{UA}{(WC_p)_{\min}}$ was determined to be 8.2

which gives a value of $UA = 965 \text{ BTU/hr.}^{\circ}\text{F}$. Figure C-21 gives a plot of heat exchanger

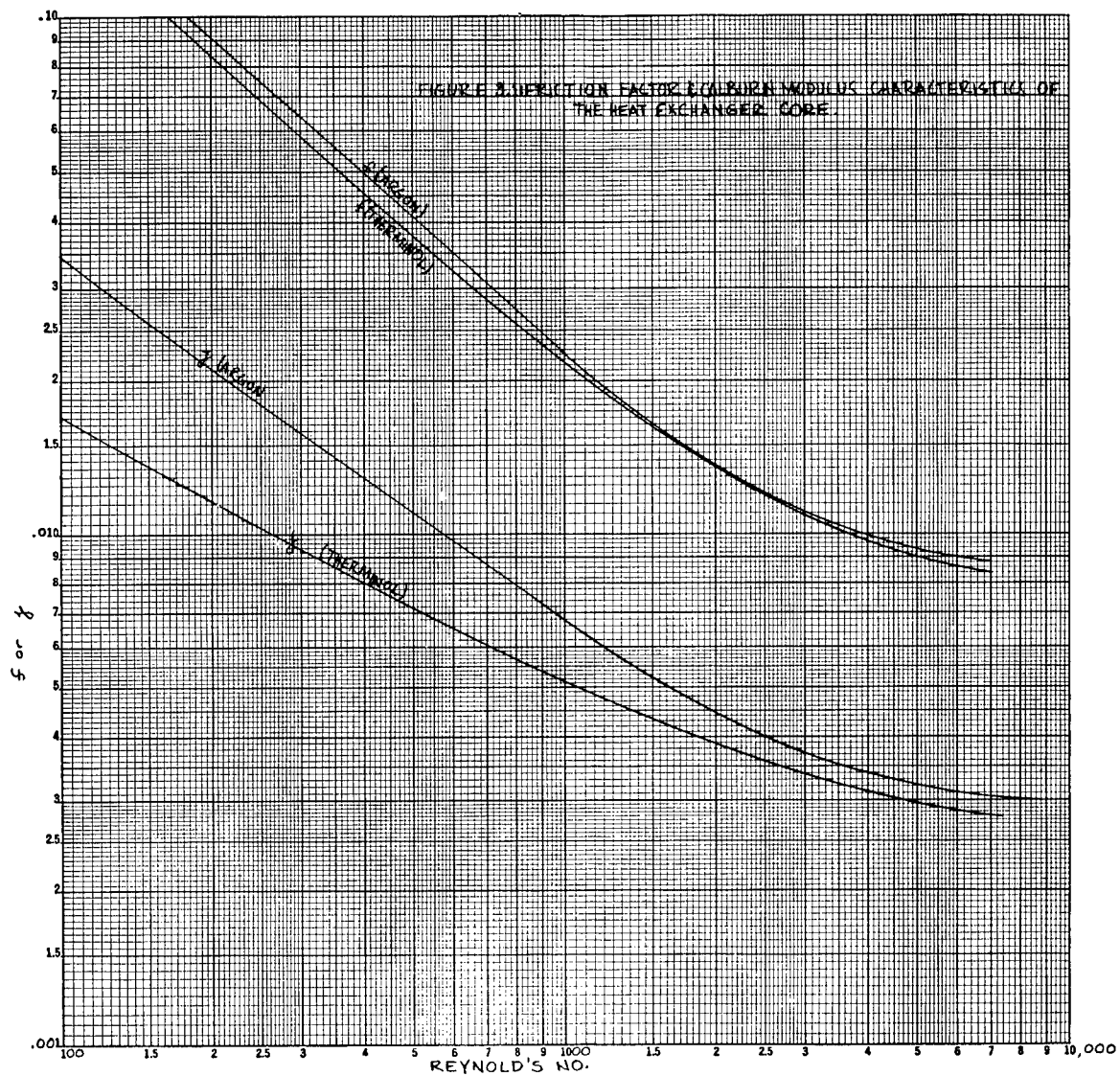


Figure C-20. Friction Factor and Colburn Modulus Characteristics of the Heat Exchanger Core

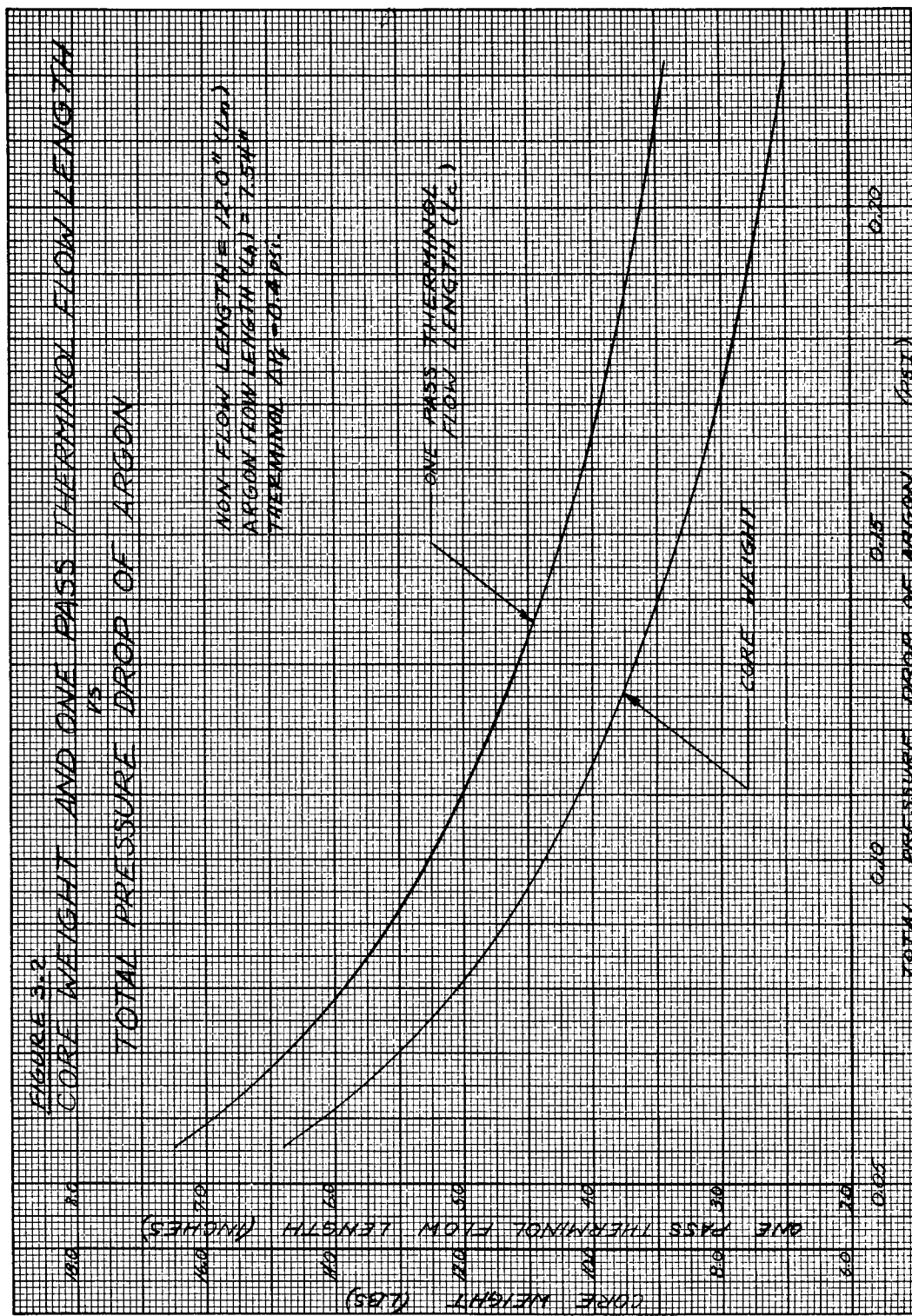


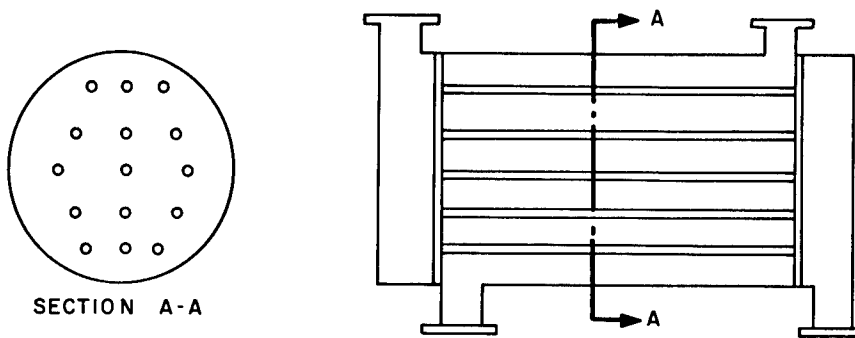
Figure C-21. Core Weight and One-Pass Thermol Flow Length Vs. Total Pressure Drop of Argon

core weight versus argon side pressure drop. Figure C-22 gives a plot of the total heat exchanger weight versus the argon pressure drop. In estimating the pressure losses, it was assumed that 10% of the allowable pressure loss was accounted for in entrance for exit effects.

C.3.2 COUNTERFLOW HEAT EXCHANGERS

C.3.2.1 Method of Analysis

The selected configuration is shown below:



For a pure cross flow heat the heat transfer can be written as:

$$Q = N_t U A \Delta T_{LMTD} = N_t U_{\pi} d_i \ell \Delta T_{LMTD} \quad (3.18)$$

where

$$\Delta T_{LMTD} = \frac{\Delta T_i - \Delta T_o}{\ln \Delta T_i / \Delta T_o}$$

$\Delta T_i, \Delta T_o$ = inlet and outlet temperature differences respectively

also

$$U = \frac{1}{\frac{1}{h_c} + \frac{1}{h_h}} = \frac{h_c h_h}{h_c + h_h} \quad (3.19)$$

so that the required heat exchanger tube length is simply:

$$\ell = \frac{Q (h_c + h_h)}{h_c h_h N_t \pi d_i \Delta T_{LMTD}} \quad (3.20)$$

Equation (3.20) was used as required in designing heat exchangers for the study.

C.4 REFERENCES

1. Whipple, F. L., "On Meteoroids and Penetration", paper presented at the Interplanetary Mission Conference, January, 1963.
2. Mackay, D. B., Bacha, C. P., "Space Radiator Analysis and Design" ASD Technical Report 61-30, October, 1961.
3. Leiblein, S., "Analysis of Temperature Distribution and Radiant Heat Transfer Along a Rectangular Fin of Constant Thickness," NASA TN D-196, November, 1959.

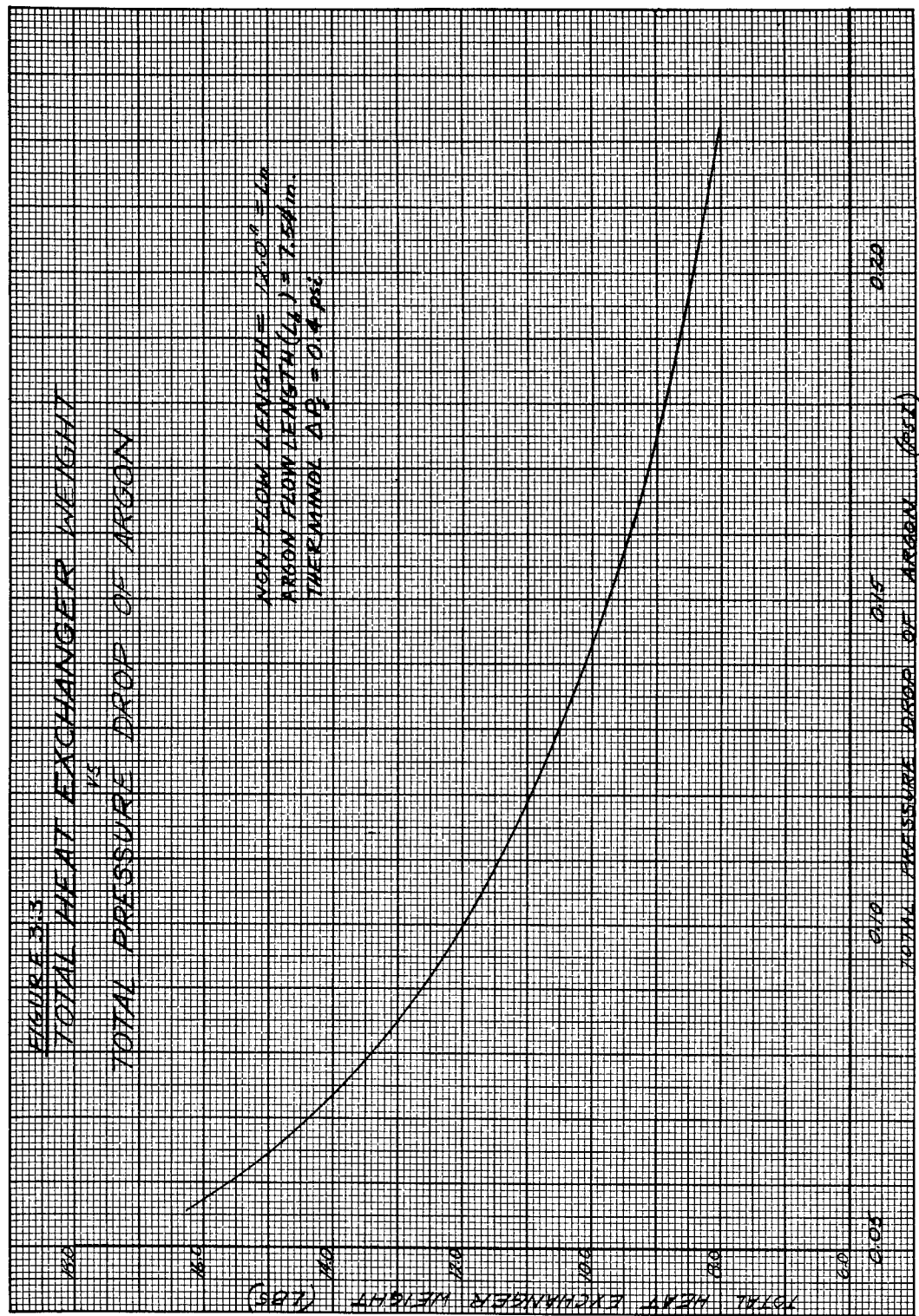


Figure C-22. Total Heat Exchanger Weight Vs. Total Pressure Drop of Argon

4. Loeffler, I. J. et al, "Meteoroid Protection for Space Radiators", ARS Paper No. 2543 of September, 1962 as revised by May 23, 1963 Addendum.
5. Hagen, K. et al, "Radiator Design and Development for Space Nuclear Power Plants", G.E. Technical Information Series 64SD224A, February, 1964 (External disclosure requires General Electric Co. Approval).
6. Lubarsky, B., Kaufman, S. J., "Review of Experimental Investigations of Liquid Metal Heat Transfer", NACA TR 1270, 1956.
7. McAdams, Wm., "Heat Transmission", 3rd ed. McGraw Hill, N. Y., 1954, p. 219.
8. Stevens, R. A., Fernandez, J. and Woolf, J. R. "Mean Temperature Difference in One, Two and Three Pass Cross Flow Heat Exchangers", Trans, ASME, Vol. 79, 1957 - pp 287 - 297.
9. McAdams, Wm, "Heat Transmission" 3rd ed., McGraw Hill, N. Y., p 268, 1954.
10. Mason, J. L., "Plate Fin 5 - A Design Procedure for Compact Heat Exchangers" - ASD-TDR-62-559, Oct. 1963.
11. Briggs, D. L., London, A. L., "The Heat Transfer and Flow Friction Characteristics of Five Offset Rectangular and Six Plain Triangular Plate-Fin Heat Transfer Surfaces", Proc. 1961-1962 Heat Transfer Conference, American Soc. of Mech. Engineers, p 122-134.

APPENDIX D. CABIN PRESSURIZATION

The work statement for this study contract specified that waste energy from the power systems could also be considered for use in pressurizing the cabin. This is assumed to be for normal pressurization as well as emergency pressurization. Since, in an emergency, the requirement would be to re-establish cabin pressure in a minimum time, that premise will be made.

D.1 POWER AVAILABLE FOR EMERGENCY PRESSURIZATION

The following mode of operation of the Life Support System under emergency conditions is expected. The emergency operation being considered will occur if the cabin pressure is totally lost, during which period the astronauts must have time to don their space suits, locate the problem area, repair it, and return the cabin to normal pressure. During this emergency operation period, Life Support System equipment can be shut down to provide maximum power from the Life Support System to aid in converting stored liquid oxygen and nitrogen to gases at the required cabin temperature and pressure. The systems which can be shut down will be discussed in the following sections.

D.1.1 OXYGEN RECOVERY SYSTEM

Two modes of operations are envisioned for the oxygen recovery system under emergency conditions. During the first phase of the emergency, i.e., locating and repairing the leaking area, the oxygen recovery system would be disconnected from the ECS air duct and connected into the emergency packs supporting the astronauts. This would provide a closed loop system for both respiration and space suit cooling requirements. The operation of the system would be limited to the removal of the CO₂ produced.

The collected CO₂ would be dumped to the cabin at the assumed near vacuum conditions. Make-up oxygen would be provided by the emergency supply.

During the second phase of the emergency, the men would subsist on an open loop system, dumping the exhaled gases to the cabin. All power would be diverted from the oxygen recovery system to the cabin repressurization task.

The available power for repressurization would then be:

a. Integrated system

Electrical = 1,440 watts

Waste Heat 7,548 BTU/HR. at 600°F = 2,210 Watts
9,908 BTU/Hr. at 400°F = 2,900 Watts

b. Non-integrated system

Electrical = 3,256 Watts

D.1.2 URINE WATER RECOVERY

The urine water recovery equipment should be continued in operation during both phases of emergency to maintain the water storage level intact, avoiding accumulating excess urine and overloading the system when the emergency is over, and avoiding the possibility of difficulties in restarting due to the components reaching temperatures other than

those required for optimum operation. Power available for repressurization for either integrated or non-integrated system is zero.

D.1.3 SOLID WASTE MANAGEMENT

The equipment for solid waste management cannot be used by space suited men and would therefore be shut down after the end of the last cleaning cycle.

Power available for repressurization

- a. Integrated System
 - Electrical = 7 watts
 - Waste Heat = 1050 BTU/HR. = 293 Watts
- b. Non-integrated System
 - Electrical = 327 Watts

D.1.4 WASTE WATER RECOVERY

Waste water process equipment would be turned off as soon as the waste water tank is emptied, assuming that no peak power requirement exists while the process is still taking place. This is a non-essential process for short time duration, therefore all the process power can be used for repressurization.

- a. Integrated System
 - Electrical Power = 7 watts
 - Waste Heat = 1500 BTU/HR. = 342 Watts
- b. Non-integrated
 - Electrical = 449 Watts

D.1.5 FOOD MANAGEMENT

Food preparation equipment should be left in operation during an emergency situation so that the men may use some hot beverages or even some bite size solid food from squeeze bags. The power required is a minimum and the men may take the advantage of some comfort during and after a period of distress.

It is possible, and the feasibility has already been investigated, to modify the present - day space suit design so that the suited astronaut can accept some food and beverages through an appropriately designed receptacle in the face shell.

D.1.6 CONCLUSION

POWER AVAILABLE FROM LSS FOR EMERGENCY REPRESSURIZATION

	Integrated	Non-Integrated
	Electrical	Electrical
A. Oxygen Recovery	1,440	2,210*
B. Urine Water	---	---
C. Solid Waste	7	293
D. Waste Water	7	342
E. Food Management	---	---
	<u>1,454 W</u>	<u>2,845 W*</u>
TOTAL		<u>1,454 W</u>
		<u>4,299 W*</u>
		4,032 W

* This quantity must be increased by approximately 690 W (2360 BTU/HR.) for the Brayton Cycle, see Reference 4 of Section 4.8.

D.2 CABIN PRESSURIZATION, NON-INTEGRATED SYSTEMS

Since the emphasis of this study is on the advantages to be realized from thermal integration, only a minimum effort will be applied in determining the time to repressurize the non-integrated systems cabin. Although in paragraph D.1.6 the power available from the Life Support System by shutting down some of the processes is totaled, the study ground rules specified that the minimum power to be provided by the electrical power system was to be 1.4 KW. The operating components comprising this minimum load were not specified, but it is assumed that the load would consist of minimum Life Support equipment and certain other station keeping processes. Rather than speculate what those processes would be, for this analysis it will be assumed that enough equipment is shut down to meet the 1.4 KW minimum power requirements necessary to keep the space station operating. With an electrical generating capability of 6.24 KW, the difference, or 4.84 KW will be assumed to be available for repressurization.

The cabin volume is assumed to be 2/3 of a 258-inch sphere (allowing one inch for wall thickness from a nominal diameter of 260 inches), or 3470 cubic feet. The total amount of oxygen required to refill the cabin atmosphere to the specified partial pressure of 160 mm Hg (3.1 psia) and at 77°F is 60.3 lbs. The amount of nitrogen required at 6.9 psia for a cabin total pressure of 10 psia is 117.5 lbs. The amount of heat required is:

Latent heat:

$$\begin{aligned} Q_{O_2} &= 60.3 \text{ LB.} \times 91.5 \text{ BTU/LB.} = 5,520 \text{ BTU} \\ Q_{N_2} &= 117.5 \text{ LB.} \times 85.5 \text{ BTU/LB.} = 10,050 \text{ BTU} \\ \text{Total Latent Heat} &= 15,570 \text{ BTU} \end{aligned}$$

Sensible heat: $Q = WC_p \Delta T$

$$\begin{aligned} \text{for } O_2, C_p \text{ av.} &= .223 \text{ BTU/LB.}^{\circ}\text{F}, & \Delta T = 72^{\circ}\text{F} - (-297^{\circ}\text{F}) = 369^{\circ}\text{F} \\ \text{for } N_2, C_p \text{ av.} &= .256 \text{ BTU/LB.}^{\circ}\text{F} & \Delta T = 72^{\circ}\text{F} - (-320^{\circ}\text{F}) = 392^{\circ}\text{F} \\ Q_{O_2} &= 60.3 \times .223 \times 369 & = 4,950 \\ Q_{N_2} &= 117.5 \times .256 \times 392 & = 11,800 \\ \text{Total sensible heat} & & = 16,750 \text{ BTU} \end{aligned}$$

The total energy requirement is 32,320 BTU.

For the Non-Integrated system:

$$\frac{\text{Energy required} = 32,320 \text{ BTU}}{3,413 \text{ BTU/KW HR}} = 9.48 \text{ KW HR}$$

Assuming ideal heat transfer, no losses and neglecting practical problems of heat exchanger design, the pressurization time is:

$$\frac{9.48 \text{ KW HR}}{4.84 \text{ KW}} = 1.9 \text{ Hours}$$

It is assumed that electric heaters would be used to vaporize the cryogenic oxygen and nitrogen in the storage containers, and electric heaters in the Life Support System used to warm the gas to 72°F.

D.3 CABIN PRESSURIZATION, INTEGRATED SYSTEMS

As was the requirement for the non-integrated systems, the minimum electrical power requirement was defined to be 1.4 KW. Definition of the equipment which would be shut down to reduce the station electrical load to this value is lacking. It has been shown that Life Support system processes can be shut down in an emergency to require significantly reduced power requirements. The Integrated Life Support system electrical requirements, for all sub-systems operating, is 1,601 watts. With some systems shut down, this requirement is reduced to 147 watts electrical power. Considering that there is still the defined emergency power requirement of 1.4 KW, and lacking definition of what constitutes this load, it will be assumed, in spite of the fact it has been shown that additional power can be made available from the Life Support System, that 1.4 KW is the minimum power to be supplied.

A study ground rule was that the integrated electric power system would be reduced by the amount of energy supplied to the Life Support System from waste thermal energy. The resulting size of the electrical generating equipment was 3.275 KW. Subtracting 1.4 KW leaves 1.875 KW electrical power available for pressurization. 2.845 KW thermal energy is available from the shut down life support processes. It will be assumed that the electrical power is used to vaporize cryogenically stored oxygen and nitrogen, and the available waste thermal energy from the Life Support System used to warm the gas to 72° F.

$$\underline{15,570 \text{ BTU Latent heat}} = 4.56 \text{ KW HR}$$

$$3,413 \text{ BTU/KW HR}$$

$$\underline{4.56 \text{ KW HR}} = 2.43 \text{ Hours to vaporize the oxygen and nitrogen}$$

$$1.875 \text{ KW}$$

Assuming this is the time available and required to warm the gas to +72 F:

$$\underline{16,750 \text{ BTU Sensible Heat}} = 4.91 \text{ KW HR}$$

$$3,413 \text{ BTU/KW HR}$$

$$\underline{4.91 \text{ KW HR}} = 2.02 \text{ KW power required}$$

$$2.43 \text{ HR}$$

Since 2.845 KW thermal energy is available from the shut down Life Support System Processes, the time to vaporize the cryogenic oxygen and nitrogen is the limiting factor. This approach, however, does not utilize all available waste energy.

Total energy available is the electrical power which exceeds the station minimum requirement, the thermal energy available from shut down Life Support System Processes, and power system waste energy being radiated to space through the radiators. If all this energy could be effectively used, and again neglecting losses and practical design problems, the cabin pressurization could be accomplished in 0.72 hours.

$$\underline{9.48 \text{ KW HR}} = 0.72 \text{ Hours}$$

$$1.85 + 2.845 + 8.35^* \text{ KW}$$

* Heat rejected by the Isotope Brayton Integrated System radiator
(Table 6-18)

To use all the energy in this manner would require that both electrical and thermal energy would be used to vaporize cryogenic oxygen and nitrogen. The difficulties of design of heat exchangers, heating coils, and other accessory equipment to make this possible, is recognized, but will be neglected for purposes of this comparison.

It will be assumed that energy from the power system, which would otherwise be radiated to space in the radiators, can be transferred to the water-glycol loop of the Integrated Life Support System.

$$\text{Total energy available} = 1.875 + 2.845 + 8.35 = 13.07 \text{ KW}$$

This is the total energy which must be transferred to the water-glycol loop in 0.72 hours.

$$13.07 \text{ KW in } 0.72 \text{ hours} = 18.15 \text{ KW HR} \\ = 61,946 \text{ BTU/HR.}$$

From Life Support Section 4.8.1 the water-glycol flow rate is 1 gpm or 463 Lbs./Hr, $c_p = 0.9 \text{ BTU/LB/}^{\circ}\text{F}$, $T_1=155^{\circ}\text{F}$.

$$\Delta T = \frac{Q}{W C_p} = \frac{61,946 \text{ BTU/HR}}{463 \text{ LB/HR} \times .9 \text{ BTU/LB } ^{\circ}\text{F}}$$

$$\Delta T = 149 \text{ F} \\ T_2 = 155^{\circ}\text{F} - 149^{\circ}\text{F} = 6^{\circ}\text{F}$$

This is well above the freezing point of the water-glycol mixture used in the loop. Therefore it appears reasonable to assume that with proper heat exchanger design, heat could be transferred to the water-glycol and then to the cold gas.

A comparison of cabin pressurization times is provided in Table D-1.

TABLE D-1. CABIN PRESSURIZATION TIMES

<u>Cabin Pressurization</u>	<u>Time</u>
Using electrical power from non-integrated electrical system	1.9 hours
Using electrical power from integrated systems and thermal energy from the life support system	2.43 hours
Using electrical power from integrated systems, thermal energy from the life support system and all available waste heat	0.72 hours

The real and practical problems of heat exchanger design for two phase flow, valving, controls, and electrically heating the cryogenic storage tanks have been neglected for this comparison. In addition, a bypass loop would be required in the power systems to bypass the radiator while emergency pressurization is being accomplished. The final time required would be longer than the 0.72 hours shown above, but it should be significantly shorter than the 1.9 hours required for the non-integrated system.